NASA Contractor Report 4128

Aerofoil Testing in a Self-Streamlining Flexible Walled Wind Tunnel

Mark Charles Lewis

GRANT NSG-7172
MAY 1988

NASA

NASA Contractor Report 4128

Aerofoil Testing in a Self-Streamlining Flexible Walled Wind Tunnel

Mark Charles Lewis
University of Southampton
Hampshire, England

Prepared for
Langley Research Center
under Grant NSG-7172

National Aeronautics
and Space Administration

Scientific and Technical
Information Division

1988

CONTENTS

UNIVERSITY OF SOUTHAMPTON

ABSTRACT

FACULTY OF ENGINEERING AND APPLIED SCIENCE

DEPARTMENT OF AERONAUTICS AND ASTRONAUTICS

Doctor of Philosophy

AEROFOIL TESTING IN A SELF-STREAMLINING FLEXIBLE WALLED WIND TUNNEL

by Mark Charles Lewis

Two-dimensional self-streamlining flexible walled test sections eliminate, as far as experimentally possible, the top and bottom wall interference effects in transonic aerofoil testing. The test section sidewalls are rigid, while the impervious top and bottom walls are flexible and contoured to streamline shapes by a system of jacks, without reference to the aerofoil model. The concept of wall contouring to eliminate or minimise test section boundary interference in two-dimensional testing was first demonstrated by the National Physical Laboratory (NPL) in England during the early 1940's. The transonic streamlining strategy proposed, developed and used by NPL has been compared with several modern strategies. The NPL strategy has proved to be surprisingly good at providing a wall interference-free test environment, giving model performance indistinguishable from that obtained when using the modern strategies over a wide range of test conditions. In all previous investigations the achievement of wall streamlining in flexible walled test sections has been limited to test conditions up to those which result in the model's shock just extending to a streamlined wall. This work, however, has also successfully demonstrated the feasibility of two-dimensional wall streamlining at test conditions where both model shocks have reached and penetrated through their respective flexible walls. Appropriate streamlining procedures have been established and are uncomplicated, enabling flexible walled test sections to easily cope with these high transonic flows.

ACKNOWLEDGEMENTS

The author is most grateful to his supervisor, Dr. M.J. Goodyer,† for his encouragement, advice and assistance throughout the course of this work.

The work was funded by NASA under Grant NSG-7172 and by the British Science and Engineering Research Council.

† Reader in Experimental Aerodynamics, Department of Aeronautics and Astronautics, University of Southampton, England.

1. INTRODUCTION

The need for improved test environments for wind tunnel model tests has long been apparent from disparities between tunnel and flight data. At some transonic test regimes the magnitude of the uncertainties in wind tunnel data can render any analysis of the test meaningless. A variety of reasons may be put forward for the uncertainties, however the two main factors† limiting the application of transonic tunnel data of existing commercial facilities to full-scale flight conditions are recognised to be inadequate Reynolds number simulation and test section boundary interference. The *' Reynolds number gap '* has been closed recently with the introduction of cryogenic wind tunnels; the National Transonic Facility (NTF) at NASA Langley Research Center being the most notable example.

The undesirable effects of test section boundary interference have long been recognised as a problem in wind tunnel testing. A post test analysis of measured data and application of corrections is often unsatisfactory[1-3], particularly for the most interesting and challenging regimes of modern aeronautics, namely those of transonic flight and those of V/STOL. The basic concept of applying corrections to tunnel data is deceptive, because the test section boundary interference effects are not distributed uniformly over the model. However, in the most severe cases, the test section flow past the model is distorted to such an extent that the application of corrections becomes impossible. In principle, wall boundary effects can be minimised by testing smaller models in larger test sections, but reduction of model size reduces test accuracy and Reynolds number, whereas the alternative of increasing the test section dimensions substantially increases the facility cost and power consumption.

This state of the art has led to the attractive concept of an adaptive walled test section, in which wall boundary interference is either eliminated or significantly reduced by actively adapting the flow near the boundaries of the test section to match that of a free flowfield. In most cases adaptive test

---

† Other factors include support interference, model deformation, flow non-uniformities and propulsive effects.

sections are *'self-streamlining'* in that the process of matching the shape of the test section flowfield to the free flowfield (a process referred to as streamlining) is made by reference to the test section alone, independent of any knowledge of the model or the flow around the model. The streamlining process is usually iterative, involving successive approximations of the test section flowfield shape to that of the free flowfield. Each iteration requires numerous test section measurements and theoretical calculations to check whether interference-free flow conditions have been reached and to determine any necessary adjustments to the shape of the test section flowfield. In this way, the best features of experiment and theory are combined in an attempt to eliminate test section boundary interference.

Two distinctly different adaptive wall testing techniques have evolved. The two adaptive techniques are schematically illustrated on Figure 1.1. One is a development of the existing ventilated wall technique, employing the new feature of controlled distribution of ventilation along the test section walls. The test section flow near the walls is adapted to match that region of the free flowfield by controlled out-flow and in-flow through the ventilated walls. Local flow control may be achieved either by dividing the plenum chamber into a number of segments or by providing a means for the local variation of wall porosity. The other adaptive wall technique, employing solid impervious but flexible walls, adapts the test section flowfield by wall contouring. The latter technique removes the need for test section ventilation and offers the possibility of overcoming the many difficulties inherent in the operation of ventilated test sections. It is the adaptive flexible wall technique which is considered in this thesis.

The idea of using active control of the test section flowfield by *'accommodating'* walls to eliminate or minimise wall interference is not new[4-6]. The first documented wind tunnel employing a test section with adaptive walls was constructed in England by the National Physical Laboratory (NPL) during the late 1930's. NPL established an experimental procedure for the streamlining of adaptive walls that is followed today, namely that the adjustments of the walls are based on the measurement of two independent flow variables at or near the test section walls. The flow near the model need not be computed, measured, or even considered. In the case of the flexible wall technique, first developed at NPL, the measured flow variables become

the wall static pressure (responding to the streamwise component of the disturbance velocity) and the local wall position (determining the flow angle).

Ideally, the adaptive test section should provide three-dimensional control of the test flowfield, in the case of flexible walls the test section would constitute some form of a deformable elastic streamtube.† The control of three-dimensional flexible walled test sections is mechanically complex†† and therefore initial research into the flexible wall technique has largely concentrated on two-dimensional control of the test flowfield. The test section design then simplifies to one with rigid sidewalls supporting flexible top and bottom walls having single curvature. In two-dimensional testing the aerofoil model is mounted between the rigid sidewalls and contouring the top and bottom walls can, in principle, eliminate wall boundary interference effects at the model.

The claim for the realisation of two-dimensional interference-free flow requires some qualification. It relates only to the effects of top and bottom walls, and here one has to recognise that because of normal experimental and theoretical errors there will be residual interferences present, although they would normally be small.

The flexible wall technique will not magically solve all of the other problems which can cause anomalous experimental results. As with all wind tunnel tests, there is an interference induced by the finite length of the test section and in two-dimensional testing there may also be sidewall interference effects. Also, due to practical considerations control over the test flowfield can only be achieved at a finite number of positions (i.e. jack positions).

---

† Research into the flexible wall technique at DFVLR (Germany) has largely concentrated on the development of a three-dimensional test section comprising of a large deformable rubber tube.

†† The eight flexible walls of the three-dimensional test section at the Technical University of Berlin (Germany) are controlled by seventy-eight jacks.

1.1 Past Two-Dimensional Flexible Wall Research at Southampton

The flexible wall research programme at the University of Southampton has its origins in an attempt in 1971 by a group of researchers at NASA Langley Research Center to increase the attraction of Magnetic Suspension and Balance Systems (MSBS) for transonic wind tunnel testing. One of the restricting features of such testing was the requirement for a plenum chamber, which forced the suspension electro-magnets far away from the model and thus increased their capital and running costs. A solution proposed by Goodyer† was the flexible wall technique where the walls of the test section are adjusted to follow streamlines in order to simulate infinite flow conditions and thereby remove the need for a plenum chamber. Hence the electro-magnets could be closer to the model and therefore smaller, resulting in reduced capital and running costs of the tunnel. Therefore, the design of a low speed test section was begun at Southampton in 1972 by Goodyer with the intention of investigating the flexible wall technique.

The resulting low speed tunnel, called the Self-Streamlining Wind Tunnel (SSWT 1), was first used to demonstrate the simulation of infinite flow around two-dimensional models[7,8]. A substantial body of low speed streamlined-wall data was gathered[9-11], particularly on an aerofoil model of NACA 0012-64 section. However, it quickly became apparent that flexible walled test sections offered several advantages over conventional test sections (see Section 4 for details).

Also, during 1975, a small flexible walled test section was designed, constructed and operated by Wolf to investigate the simulation of two-dimensional cascade flow in a single turbine blade[12]. The findings were inconclusive due to the absence of reference data.

At an early stage it was realised that the development of a transonic testing facility employing a flexible walled test section would be advantageous. Design of such a facility commenced in 1975 and was

---

† A proposal was placed on record and witnessed in the invention declarations *' Transonic Test-Section Design '* and *' Self Adapted Flexible Test Section Walls '* by M.J. Goodyer in July 1972 retained for reference at NASA Langley Research Center.

commissioned in 1978, the facility is now referred to as the Transonic Self-Streamlining Wind Tunnel (TSWT). Tunnel operation was limited until 1979 when a semi-manual operating system became operational[13]. Subsequent development of the operating procedure and the installation of closed loop computer control significantly reduced the time associated with the streamlining process, thereby rendering the manually operated tunnel (SSWT 1) redundant. The TSWT has been used extensively during 1979-84 to test three aerofoil models (of NACA 0012-64, supercritical NPL 9510 and CAST 7 sections), particularly at the high Mach number range[14-17]. The tests have proved (up to high subsonic reference speeds) the notion that adjusting the top and bottom walls to unloaded streamlines allows the simulation of infinite flow around two-dimensional models. In addition, the secondary advantages of the flexible wall technique, in terms of increased Reynolds number, reduced power requirements and improved flow quality have also been demonstrated.

1.2 Principal Objectives of Author's Research

1.2.1 Wall Streamlining of a Choked Test Section

Validation data[14-17] from the TSWT has demonstrated the principle of two-dimensional wall streamlining at test conditions up to those which result in the model's shock just extending to a streamlined wall.

The prime objective of the author's research was to demonstrate the principle of wall streamlining in the TSWT at test conditions where the shocks of the model may extend *'through'* a streamlined wall and intrude into the imaginary flowfields.† At such conditions, in a flexible walled test section, the channels over and under the model may both be choked. The achievement of wall streamlining infers, in principle, that the top and bottom wall interference effects at the model are eliminated.

1.2.2 Evaluation of Several Wall Adjustment Strategies

The wall adjustment strategy is a fundamental component of the self-streamlining concept. The aim of any strategy is to adjust the flexible

† See Section 3.1 for definition of imaginary flowfields.

walls to follow the shapes of streamlines within an acceptable number of streamlining iterations.†

A secondary objective of the author's research was the assessment of several transonic wall adjustment strategies in the TSWT, including a detailed evaluation of the strategy proposed, developed and used by the National Physical Laboratory in England during the early 1940's.

† Satisfactory streamlines are only achieved after a number of streamlining iterations. One streamlining iteration comprises of setting walls to known shapes, measuring wall pressures, assessing the quality of wall streamlining and computing new wall contours.

2. REVIEW OF TWO-DIMENSIONAL ADAPTIVE WALL RESEARCH

2.1 Early Flexible Walled Test Section Development at NPL†

In the 1930's the technology to deal with test section boundary interference developed in three major directions. In one direction, the *'classical'* theory predicting boundary interference corrections was systematically expanded to include more realistic aircraft and test section configurations. The second direction (which during the 1930's appears to have only been considered for low speed testing) was the application of the notion of ventilation as a means of minimising wall interference. This followed the observation of opposite signs of the corrections applied to open test sections and closed test sections. The third direction was related to a pressing practical problem; namely choking in high speed wind tunnels. During the 1930's the term high speed meant velocities approaching that of sound. Choking is the result of massive blockage-induced wall interference and was a real barrier to the advancement of test speeds and therefore, to the understanding of transonic flows.

2.1.1 6 x 3 NPL Tunnel

In 1937 Bailey and Wood[18] of the National Physical Laboratory (NPL) reported that the effect of modifying the longitudinal profile of a test section, to compensate for the presence of the model, was to raise the speed at which choking occurred. Adjustments to the test section, 15.24cm (6 inches) x 7.62cm (3 inches) in cross-section and 15.24cm (6 inches) in length, were made by the insertion of liners.

As the profile of the 6 x 3 NPL Tunnel varied for each test condition Bailey and Wood suggested the use of adjustable flexible walls on the sides of the test section parallel to the axis of the two-dimensional model. This is thought to be the first reference relating to the use of adaptive walls in wind tunnel test sections. Bailey and Wood further postulated that the flexible walls could be given such a profile that free flowfield conditions could be

† NPL - National Physical Laboratory, Teddington, Middlesex, England.

simulated; at the time they believed, incorrectly, that such a profile was one that gave constant static pressure, equal to the reference value, along the centrelines of the flexible walls.

2.1.2 5 x 2 NPL Tunnel

In order to determine the feasibility of using flexible walls the 6 x 3 NPL Tunnel was modified. The test section of the modified tunnel (5 x 2 NPL Tunnel) was 12.70cm (5 inches) x 5.08cm (2 inches) in cross-section, the narrower walls being flexible along their length of 22.86cm (9 inches). A schematic layout of the test section is shown on Figure 2.1. Each flexible wall, manufactured from spring steel plate, was adjusted by six micrometer screws spaced at 3.81cm (1.5 inches) intervals. The author believes the 5 x 2 NPL Tunnel to be the first documented wind tunnel employing a test section with adaptive walls.† Investigations were carried out in three major areas: the reduction of interference between tunnel and model; the control of tunnel speed by a downstream contraction; and into the length of test section necessary for satisfactory upstream and downstream conditions to be reached. The test data, reported by Bailey and Wood[4] in 1938, demonstrated the elimination of wake blockage in two-dimensional tests up to a reference Mach number of 0.89. Thus, Bailey and Wood appear to have been the originators of the concept of adaptive walled test sections, and were first to apply the method successfully in transonic testing.

2.1.3 20 x 8 NPL Tunnel

Utilising the valuable experience gained with the 5 x 2 NPL Tunnel the High-speed Rectangular Tunnel (20 x 8 NPL Tunnel) was designed in 1937 and given its initial run in May 1941[20]. The tunnel operated with stagnation conditions of ambient pressure and temperature and initially had an open circuit but in June 1945 a return leg was fitted. The induced-flow was driven by compressed air through an injector (of similar design to that employed in the TSWT) downstream of the test section.

---

† The 5 x 2 NPL Tunnel was still in operational service at the University of Southampton in 1957.[19]

The test section was of rectangular shape, a nominal 44.45cm (17.5 inches) x 20.32cm (8 inches) in cross-section, the narrower walls being impervious and flexible along their entire length of 1.23m (48.5 inches). A schematic layout of the test section is shown on Figure 2.2. The flexible walls were made from 0.51mm (0.02 inches) spring steel and were adjusted in single curvature by nineteen screw micrometers on each wall, the last two downstream micrometers on each wall controlling an adjustable throat, as shown on Figure 2.2. Hence, the streamlined portion of the test section effectively extended from the first to the seventeenth micrometer, giving 95.76cm (37.7 inches) of streamlined length, on each wall. In the vicinity of the model micrometers were spaced at 3.81cm (1.5 inches) intervals, whilst upstream and downstream of the model micrometer spacing increased to 7.62cm (3 inches). Static pressures were measured on the centrelines of the flexible walls, via 0.51mm (0.02 inches) diameter tapppings and multitube manometers, at all micrometer positions and at a few points in the vicinity of the downstream throat. The tunnel reference speed was deduced from the static pressure measured on one of the flexible walls 21.59cm (8.5 inches) ahead of the leading edge of the standard 12.70cm (5 inches) chord model, as shown on Figure 2.2. The 50.80cm (20 inches) sidewalls, rigid and parallel, were provided with glass windows which supported the model and enabled flow visualisation near the model.

The flexible walls were contoured to follow streamlined shapes according to a strategy suggested by Lock and Beavan[5] (for details of the strategy see Section 6.3), which utilised only the tunnel reference flow conditions and the available *'wall data'*.† Thus, the 20 x 8 NPL was the first truly self-streamlining wind tunnel and employed the most advanced flexible walled test section developed by NPL.

The tunnel remained in service for about fifteen years and enabled valuable investigations into wall boundary interference at compressible speeds.[20,5,21] During the investigations the highest attained reference speed was Mach 0.955 with an empty test section and Mach 0.94 with a model installed in the test section. The tunnel was also run empty at a low

† *'Wall data'* consists of wall geometry and static pressure distributions along the centrelines of the flexible walls.

supersonic speed (Mach 1.15) by adjusting the flexible walls to form a convergent-divergent nozzle. Lock and Beavan concluded that for two-dimensional tests reliable wall interference-free data from the tunnel could be obtained for reference speeds up to about Mach 0.85; only when a model shock had just extended to one of the flexible walls of the test section were the tunnel results invalidated. They also concluded that a model of 12.70cm (5 inches) chord (representing a nominal test section height to chord ratio of 3.5) was about as large as should be used, and in this case lift could be estimated from the static pressures measured on the streamlined walls.

2.1.4 NPL 4ft No.2 Tunnel

At one stage NPL proposed to construct a wind tunnel with a flexible walled test section of 3.66m (12ft) x 1.83m (6ft) in cross-section and 14.63m (48ft) in length. It was thought necessary that the scheme be put to the test on a larger scale than the existing 20 x 8 NPL Tunnel to aid the design of the two-dimensional test section of the proposed tunnel. This led to the installation of adaptive flexible walls, 1.22m (4ft) wide and 3.96m (13ft) long, in the NPL 4ft No.2 Tunnel. A schematic layout of the test section is shown on Figure 2.3. The test section was not self-streamlining because in this case the flexible walls were contoured, by twelve jacks on each wall, to follow calculated streamline shapes.[22] In 1944 Preston et al.[23] reported that wall interference-free conditions had been established in the tunnel and that no operational difficulties existed with large scale flexible walled test sections. Furthermore, they suggested that wall jacks driven by electric motors should be considered as a possible means to reduce the time and labour associated with wall adjustment. This scheme is used in the majority of all modern flexible walled test sections. However, the proposed large scale NPL flexible walled wind tunnel was never constructed.

2.1.5 Proposed 18 x 14 NPL Tunnel

In 1946 NPL proposed to construct a new high speed wind tunnel of closed circuit design with a test section of 45.72cm (18 inches) x 35.56cm (14 inches) in cross-section. The narrower walls were to have been adjustable with a range of movement adequate for both the reduction of wall interference at subsonic speeds, and the formation of a diffuser for supersonic

operation. Although the design of the proposed tunnel appears to have been completed[21] construction was never commenced.

2.1.6 Demise of Flexible Walled Test Sections

Research into flexible walled test sections at NPL was initially driven by the need to relieve test section choking; the most severe consequence of wall boundary interference. Parallel research efforts which explored, in turn, several other approaches to obtaining high speed interference-free test data (including drop tests, the transonic bump, the profile flow method, and small models on aircraft wings), finally settled on test sections with ventilation. The ventilated wall-geometry (developed initially for low speed testing) alleviated the choking problem and reduced the effects of wall interference without unacceptable power losses. The ventilated test sections proved more practical in operation by eliminating the long wall setting times associated with the iterative streamlining process without the aid of a modern computer. Hence, research into adaptive flexible walled test sections at NPL ceased† and ventilated test sections became universally accepted for transonic testing. Some ventilated test sections of 1940/50 vintage are still in use. However, in moving to the ventilated design at least two features of tunnel testing deteriorated; tunnel drive power increased and flow quality was reduced. The ventilated walls were *'passive'* in the sense that there was no overt control of the flow through the walls. Ventilated wall geometry significantly reduced the level of test section boundary interference, but not to negligible magnitudes especially at transonic conditions.

2.2 Revival of Adaptive Test Sections

In the early 1970's the demand for higher quality test data on more sophisticated aerodynamic configurations, such as highly complex manoeuvering vehicles and large commercial transport aircraft, exposed the limitations of existing transonic testing facilities. The effects of Reynolds number and wall boundary interference were recognised as unknown

† It should be noted that in 1945 a 9ft high speed wind tunnel employing a flexible walled test section was discovered in West Germany (at Ottobrunn, near Münich). The only documentation relating to the tunnel detected by the author may be found in References 24-26.

quantities, the latter being of particular concern within the limitations of transonic testing. In addition, the development of supercritical aerofoils for transonic cruise caused a re-assessment of conventional procedures for two-dimensional aerofoil testing. The absence of a rational interference assessment method for test sections with conventional ventilation (due to the non-linear nature of the transonic flow equations, the complex wall geometries and the ill-defined boundary conditions which they produce) further complicated the situation. The recognition of these uncertainties in transonic wind tunnel testing led to the general concept of self-adapting test sections. The notion occurred to numerous researchers during the early 1970's,[8] in particular Sears, Ferri and Baronti[27], Goodyer, Rubbert and Chevallier, who realised that adaptive test sections were feasible with the aid of on-line computers that could continually monitor the tunnel flow and control the adjustment of the walls.

2.3 Review of Recent Two-Dimensional Adaptive Wall Research

Since the early 1970's several research organisations have worked on many concepts to develop a system which fulfils the adaptive wall promise; a wall boundary interference-free testing environment. Concept demonstrations which have been completed to date have largely concentrated on two-dimensional testing. However, much of the groundwork for three-dimensional applications has been completed and experimental efforts are under way at several organisations, but are beyond the scope of this thesis. Details of all documented adaptive test sections since 1970 are summarised in Tables 1.1-1.3.

In the following (Sections 2.3.1-2.3.3), the work of organisations which have made major contributions to the development of the two-dimensional adaptive wall technique since the early 1970's is briefly outlined in an attempt to present the current state of the art. The variations in test section hardware and the different techniques used for the measurement of the two independent flow variables necessary to govern the streamlining process (as discussed in Sections 1 and 3.3) are also illustrated. It should be noted that the review is not exhaustive; a comprehensive annotated bibliography on all adaptive wall research has been compiled by Tuttle and Mineck,[28] whilst an

excellent and concise review of the state of the art has been given by Ganzer.[29]

2.3.1 The Ventilated Technique

2.3.1.1 Calspan Corporation

The 1ft Self-Correcting Wind Tunnel (see Table 1.1 for test section details) at the Calspan Corporation, U.S.A.[30,31] was probably the first wind tunnel facility employing an adaptive test section of ventilated design. The project was initiated in 1973 by the work of Sears.[32] The test section plenum was segmented, the top and bottom plenums were divided into ten and eight segments respectively. Active control of the flow through the top and bottom perforated walls was achieved by the application of pressure or suction to the plenum segments.

The two independent flow variables necessary for wall adaptation were measured on a control surface near each perforated wall by static pipes and flow angle probes. Two static pipes provided approximately forty pressure readings at each control surface, whilst there was only one flow angle probe for each plenum segment. The non-intrusive technique of volumetric measurement of flow through the walls proved unsuccessful in determining flow angle.[30]

The principle of two-dimensional wall adaptation was demonstrated, initially at Mach numbers up to 0.725 and up to 4.0^{o} angle of incidence with a 6% solid blockage model,[33,34] and later with supercritical flow at the control surfaces and perforated walls for a Mach number of 0.9 and up to 4.0^{o} angle of incidence with a 4% solid blockage model.[35] However, the small number of flow angle probes per wall were found to be inadequate to define the variation of the normal velocity component, and under some conditions the probes produced weak shock waves. In an attempt to overcome these problems a new static pipe, known as the *'Calspan pipe'*,[36] was devised to measure both the static pressure and its gradient normal to the control surface. Erickson et al.,[37] however, concluded that a finer wall control in the vicinity of the model was desirable, especially at conditions which resulted in

supercritical flow at the walls, as complete wall interference-free flow conditions had not been achieved.

2.3.1.2 Arnold Engineering Development Center

Adaptive wall investigations at the Calspan Corporation led to more detailed two-dimensional studies at the Arnold Engineering Development Center (AEDC) during the period from 1976 to 1979.[38-40] The main objective of the studies was to determine the most suitable control of wall ventilation for adaptive test sections, with a view to future application to three-dimensional flowfields.

Several wall configurations were investigated. The experiments employed a two-dimensional model with a NACA-0012 aerofoil section of 15.24cm (6 inches) chord, which represented a 6% solid blockage in the 30.48cm (1ft) square test section (see Table 1.1 for further details of the 1ft Tunnel). Static pressure and flow angle were measured on control surfaces near the two ventilated walls of the test section. The static pressure distribution was obtained with a static pipe, whilst the flow angle was obtained with individual miniature aerodynamic probes mounted from the walls in the early experiments and, in later experiments, with aerodynamic probes that were traversed longitudinally along the upper and lower control surfaces.

The control of flow through the walls was found to result in a significant reduction in two-dimensional wall interference even when supercritical flow regions had extended to the test section walls, but complete interference-free flow conditions were not achieved. Variable porosity walls in conjunction with plenum pressure control were considered the most suitable configuration for the control of wall ventilation. The two-dimensional investigations provided the foundation necessary for extending the development of ventilated adaptive test sections to three-dimensional flowfields, which is the aim of present investigations in the 1T Tunnel (see Table 1.3 for test section details) at AEDC.[41-43]

2.3.1.3 NASA Ames Research Center

Adaptive wall research at NASA Ames Research Center (Ames) has concentrated on two-dimensional test sections employing slotted wall configurations with plenum pressure control (except the HRC-2 Tunnel[44]:- see Table 1.2 for test section details). A feature of the research was that non-intrusive flow measurement techniques were used, since intrusive flow measurements can introduce inaccuracies.

Initial investigations were carried out in the Indraft Tunnel (see Table 1.1 for test section details) using a 15.24cm (6 inches) chord model of NACA 0012 aerofoil section. Laser-Doppler Velocimetry (LDV) was used to measure the vertical component of the flow at two different control levels above and below the model, as suggested by Davis.[45] The measured velocities were used to compute from linear flow theory the wall interference and the required changes in the vertical component to produce wall interference-free flow conditions.[46] The plenum pressure changes necessary to achieve the desired vertical component distribution were determined by means of a measured influence coefficient matrix. Convergence to wall interference-free flow conditions was demonstrated, as long as the regions of supercritical flow generated by the model remained below the two control levels nearest the ventilated walls.[47] The wall adaptation process was slow because of the inadequacies of the adjustment strategy and the methods of flow measurement. The entire data acquisition sequence of one tunnel run took approximately ten minutes of which eight minutes were spent on acquiring and reducing laser data.

Present two-dimensional adaptive wall research at Ames is aimed at obtaining wall interference-free flow conditions at free-stream Mach numbers close to unity in the 25 x 11 Tunnel (see Table 1.1 for test section details). Two methods for the assessment of wall interference are being compared: one component flow measurements at two control levels, and two component flow measurements at one control level. The measurements are obtained either by using intrusive instrumentation, such as pitch probes and hot wires or by a complex LDV system. At present published work shows a sparsity of aerodynamic data with the test section adapted for wall interference-free

flow. Bodapati and Celik,[48] however, have concluded that the use of the LDV system is not only complex but at present requires excessive testing run-time.

A new two-dimensional adaptive test section[49] for the 2ft Transonic Wind Tunnel at Ames is nearing completion (see Table 1.1 for details of the new test section). The flow through the slotted walls will be controlled by sixty-four slide valves, whilst the LDV system involves a fast computer controlled traverse system of mirrors which will significantly reduce tunnel run-time associated with LDV data acquisition. Operation of the new test section is expected soon.

2.3.2 The Flexible Wall Technique

2.3.2.1 University of Southampton

The work at the University of Southampton on flexible walled test sections was initiated in 1972 by Goodyer. The demonstration of wall interference-free flow, achieved by wall contouring in a low speed tunnel[7-9] (see Table 1.2 for details of test section:- SSWT 1), was particularly impressive because of the large solid blockage of the models; a NACA 0012-64 aerofoil of 10% blockage that gave a nominal test section height to model chord ratio of 1.1 and two circular cylinders of 25% and 30% blockage.

Based on the experience gained with the SSWT 1 and detailed analytical work[9,50] a new flexible walled test section was designed, constructed and inserted into an existing transonic wind tunnel at the University of Southampton (see Table 1.2 and Section 5 for further details of the test section and wind tunnel:- TSWT). The TSWT has been used extensively to develop the flexible wall technique, particularly at the high Mach number range. The achievement of two-dimensional wall interference-free flow has been demonstrated[14,16,17] at conditions up to those which result in the model's shock just extending to a streamlined wall, which usually occurs at around Mach 0.85. Recent work has been aimed at streamlining the flexible walls at conditions where the test section is fully choked. This work forms a major part of this thesis.

The old low speed test section (SSWT 1) has recently been modified to allow wall streamlining around swept wings (see Table 1.2 for details of the

modified test section:- SSWT 2). Initial tests using an untapered wing of NACA 0012-64 section, swept at 40.0°, have proved to be highly promising.[51] Further tests are planned in the near future.

2.3.2.2 ONERA/CERT

Adaptive wall research at ONERA was initiated during the early 1970's and experimental investigations were first carried out in the two-dimensional flexible walled test section of the S4 LCh Tunnel (see Table 1.2 for test section details). Chevallier[52,53] reported that tests had demonstrated rapid convergence to wall interference-free flow conditions for reference Mach numbers up to about 0.85.

Experience gained with the S4 LCh Tunnel led to the ONERA/CERT T2 Tunnel[54] (see Table 1.2 for test section details). The tunnel can be operated at stagnation pressures up to 5 bars and at cryogenic conditions. Cryogenic operation began in 1981, although the automated flexible walled test section has been in operation at normal temperatures for some time.[55] In the case of cryogenic operation the model has to be cooled outside the test section since tunnel run-time is only thirty to sixty seconds. Tunnel operation requires sophisticated procedures to be followed for the correct determination of the actual angle of incidence and the actual reference Mach number. However two-dimensional wall interference-free flow conditions have been obtained at cryogenic temperatures,[56,57] but for all the reported tests the flow at the contoured walls was subsonic.

2.3.2.3 Technical University of Berlin

Initial adaptive wall research at the Technical University of Berlin (TUB) used a two-dimensional flexible walled test section (see Table 1.2 for test section details:- TUB 1). Investigations employing a NACA 0012 and a CAST 7 aerofoil model were made at transonic speeds, but for all reported tests[58,59] the flow at the contoured walls remained subsonic. Although the minimisation of wall interference was demonstrated, rather large truncation effects were experienced. In an attempt to reduce these effects the length of the test section has been extended from 69cm (27.17 inches) to 99cm (38.98 inches). Further tests with two and three-dimensional models are

planned in the modified test section (see Table 1.2 for test section details:- TUB 2).

2.3.2.4 NASA Langley Research Center

A two-dimensional flexible walled test section has been installed in the 0.3-m Transonic Cryogenic Tunnel (TCT)[60] at NASA Langley Research Center. The design of the test section[61] (see Table 1.2 for test section details) was based on the research carried out at the University of Southampton.† The integration of an adaptive test section with a continuous flow cryogenic wind tunnel is unique and will allow full-scale Reynolds number matching to be linked with an improved testing environment. The available test Reynolds number per foot of over 100 million far exceeds the capabilities of any current adaptive wall facility. The strategy[62] governing the streamlining (wall adaptation) process, proposed,[63,50] developed,[11,64] and proven[13,14,16,17,65] at the University of Southampton, limits the achievement of wall interference-free flow to conditions which result in the supercritical flow regions just extending to a streamlined wall. Tunnel calibration is complete and two-dimensional model tests aimed at identifying the limits of the test envelope and improving operational procedures have commenced.

2.3.3 Capabilities of Current Adaptive Test Sections

The advantages of the two-dimensional adaptive wall technique (as discussed in Sections 1, 3.1 and 4) are well established and the technique is ready for employment in production test facilities at conditions where the flow at the adapted walls remains subsonic. Wall adaptation at conditions which result in supercritical flow at the walls has been demonstrated in adaptive test sections of ventilated design, but the degree of local flow control at the walls necessary to obtain wall interference-free flow conditions is still in question. Prior to data presented in this thesis, the principle of wall streamlining at such conditions had not been demonstrated in flexible walled test sections.

---

† Under NASA grant NSG-7172

2.4 Three-Dimensional Model Tests in Test Sections with Two Flexible Walls

Three-dimensional control of the test flowfield requires mechanically complex test sections,[58,66,67] in which flow visualisation and optical measurement techniques (such as Laser-Doppler velocimetry) are often impossible. Hence, attention has turned recently to extending the coverage of theoretical and experimental work associated with utilising two-dimensional flexible walled test sections for three-dimensional model testing. With just two of the walls deformable and these only in single curvature the wall interference cannot be totally eliminated because the streamtube represented by the four walls will be loaded. However, in principle, wall interference effects at the test section centreline can be eliminated. It is anticipated that the remaining wall interference will be of a correctable level and will certainly be less than for conventional test sections.

Initial investigations at the Technical University of Berlin[68] and in the ONERA/CERT T2 Tunnel[69] employing three-dimensional models and utilising a two-dimensional wall adjustment strategy[70], proposed by Wedemeyer and Lamarche, have demonstrated that the residual wall interference can be assessed and is correctable. Further experimental evidence, reported by Harney,[71,72] concluded that it is difficult to justify the additional complexity of flexible sidewalls at the expense of reduced or no flow visualisation. A numerical study by Smith[73] showed similar results.

Further investigations are necessary before a clear judgement can be made, but the evidence so far suggests that two-dimensional wall adjustment is a very promising technique for three-dimensional model tests up to transonic speeds. Development of the technique continues at several research organisations including the University of Southampton, details of which are beyond the scope of this thesis.

2.5 Supersonic Testing in Two-Dimensional Adaptive Test Sections

At present the documented research relating to the development of the adaptive wall technique at low supersonic speeds is limited. It is anticipated that a test section with ventilated walls and local control of wall porosity will provide an improved test environment compared with ventilated

test sections of constant wall porosity. The properties of flexible walled test sections at supersonic speeds are largely unknown. A theoretical study by Ganzer et al.[68] demonstrated that the required wall contours exhibit greater gradients than at subsonic speeds but they appear to be feasible, as also suggested by Goodyer (see Section 3.1). The experimental demonstration of test section boundary interference-free flow conditions is awaited.

3. THE ADAPTIVE FLEXIBLE WALL TECHNIQUE

3.1 Principle of Wall Streamlining

If the walls of a test section could be adapted to follow any one of the infinite number of streamtubes that exist around a model in a free flowfield, then the test section boundary interference on the model would be eliminated provided that the streamtube was infinitely long. At this condition the walls of the test section can be considered simply as substitutes for streamtube surfaces (neglecting, for simplicity, the wall boundary layer). In practice, the streamtube shape varies with reference Mach number, model shape and incidence, therefore the walls of a non-ventilated test section need to be flexible.

In the case of a two-dimensional model in an infinite flowfield as shown on Figure 3.1, the streamtube can be regarded as bounded (above and below) by a pair of streamlines. Therefore, only two of the test section walls need be contoured, and then only in single curvature. The wall boundary interference effects at the model are eliminated when the two flexible walls follow any two streamlines (one above and one below the model), at which condition the walls are termed *'streamlined'*. As also shown on Figure 3.1 the flowfield can be divided into three portions:-

1) An imaginary portion extending to infinity above the test section - I1.

2) A real portion within the test section - R.

3) An imaginary portion extending to infinity below the test section - I2.

If a wall is to be considered as a substitute for a streamline, then the properties of a streamline must be applicable to the wall. A streamline cannot sustain forces, the pressures on both sides of the streamline must be equal; there may be a pressure gradient across the streamline but not a pressure jump. This is the streamlining criterion used to determine whether the wall shape corresponds to that of a streamline in an infinite flowfield.

Hence when the walls are streamlined, there will be no pressure imbalance across the two boundaries between the real and imaginary flowfields (i.e. the wall loading is zero).

The full advantages of the adaptive flexible wall technique are realised when the flexible walls are positioned close to the model (as discussed in Section 4.1). Thus at high subsonic speeds the shocks from the model extend to the walls and beyond into the imaginary flowfields surrounding the test section. However, even at these conditions, the principle of wall streamlining is still applicable; top and bottom wall boundary interference effects on the model are eliminated when the flexible walls exhibit zero wall loading and therefore are correctly streamlined. One feature assured by the proper adjustment of the flexible walls to zero wall loading is that none of the shock waves produced by the model would be reflected in any way from the walls. One requirement of zero wall loading, at such conditions, is that the patches of supercritical flow in the real and imaginary flowfields are closely matched, as illustrated on Figure 3.2. The flexible wall itself supports the pressure rise across the shock, therefore the change of flow direction which might otherwise occur with a conventional ventilated test section is prevented in a flexible walled test section.

For supersonic testing, yet to be investigated in the TSWT, it is anticipated that the initial portion of the test section would be used to form a convergent-divergent nozzle. There will be a need to cancel the bow shock reflections and initial work by Goodyer (summarised on Figure 3.3) suggests that this may well be possible in the TSWT by wall contouring.

3.2 Measures of Wall Streamlining Quality

It must be recognised that zero wall loading is a practical impossibility† and therefore some measures of acceptable levels of loading, or their consequences, must be established. One measure of wall streamlining quality is determined from the wall loadings given by the differences between

† Test section truncation effects, lack of wall control between jacks, experimental and computational errors contribute to the impossibility of zero wall loading.

the static pressures measured at the flexible walls inside the test section and imaginary static pressures on the outside of the walls. The imaginary (external) pressures are derived during computations of the imaginary flowfields which extend outwards from each flexible wall to infinity. The imaginary flowfields are treated analytically independent of each other, but have common values of free-stream properties far upstream. The contour which is used as the boundary of the imaginary flowfields is not the physical shape of the wall, but an effective shape, called the effective aerodynamic wall contour. These effective aerodynamic contours allow for the displacement thickness of the flexible wall boundary layers.

Provided that the effective aerodynamic contour does not penetrate the wake or boundary layer of the model an inviscid solution to the imaginary flowfields is possible and proper. It follows that the imaginary flowfields will be less complex than the real flowfield close to the model, and the accuracy of the imaginary flowfield computations will be more reliable than theoretical estimates of model performance, whatever the current state of the art. An accurate prediction of the external wall pressures given by the imaginary flowfield computations is necessary for the correct determination of wall streamlining quality.

Wall loading is evidence of wall interference; if the real (test section) and imaginary pressures (or corresponding velocities) differ at any point along a wall then the wall shape is not that of a streamline in the infinite flowfield. In practice, the loading will be finite as the flexible walls can only be positioned within some tolerance band set by experimental and theoretical features of the system. As a matter of policy the flexible walls of the TSWT are contoured to eliminate as far as is feasible the top and bottom wall loadings.

The difference in pressure across a wall has been introduced as one measure of the quality of wall streamlining. At a point along a wall the apparent pressure difference, having in general a true component but also an erroneous component because of measurement and computational errors, is converted into a pressure difference coefficient and used as a measure of the local wall loading. Coefficient values are available at each jack position, but the practice has long been adopted of evaluating an average value for each

wall, given the symbol E. Formally, E is the average of the modulus of the set of pressure difference coefficients determined at each jack along a wall. Experience[13,65] has shown that for the TSWT satisfactory streamlines exist when the value of E is less than 0.01 on both walls.

When streamlined the flexible walls are unloaded, but the streamlined portion of the test section is necessarily finite. It can be assumed that the truncation of the test section length leads to loading beyond each end of the test section, even when the walls are streamlined. However, by using a suitably long test section with the model mounted symmetrically in the streamlined portion, the effects of the loading at the two ends of the test section largely cancel each other.[50]

After each streamlining iteration the residual interference effects at the model due to the remaining wall loading are calculated using linearised theory,[13] providing more measures of the quality of wall streamlining. For convenience the interference effects are expressed in terms of:-

1) Induced angle of incidence at the aerofoil leading edge.

2) Induced camber.

3) Streamwise velocity error at the quarter chord point of the aerofoil expressed as an error in pressure coefficient.

Past experience[13,65] has shown that when the walls are streamlined ($E < 0.01$ on both walls), none of the three components of the residual interference alone induces an error in C_L greater than about 0.008. Typically this limit in C_L results from maximum residual interference effects of:-

$$\alpha = 0.015^{\circ}$$

$$\text{Camber} = 0.07^{\circ}$$

$$C_p = 0.007$$

3.3 Principles of Flexible Walled Test Section Operation

The wall streamlining process must be free from dependence on any assumption about the nature of the flow over and in the vicinity of the model. This requirement is based on the argument that if such flows could be calculated, or otherwise determined with confidence, there would be no need for the wind tunnel test.

Hence, the only information necessary for the streamlining of two-dimensional adaptive test sections is the tunnel reference flow conditions and the wall data. Wall data is obtained by the measurement of two independent flow variables on control surfaces at or near the test section walls. The variables may be perturbation velocities, flow deflection angles or static pressures. The important fact is that the test section itself, influenced by the flow disturbances generated by the model, provides all information necessary for wall streamlining, hence the use of the descriptive phrases *'self-streamlining'* or *'self-adapting'*. No knowledge about the model or the flow in the vicinity of the model is required. In the case of flexible walled test sections the control surfaces are the flexible walls and the measured flow variables become the flow deflection angle (which can be obtained from the wall geometry) and the static pressure, therefore the wall data is inherently easy to obtain. This is not the case with adaptive test sections of ventilated design (as previously indicated in Section 2.3.1).

In practice, wall streamlining is achieved by means of wall adjustments in iterative steps (streamlining iterations); the general operating procedure is shown on Figure 3.4. In this example, it is assumed that the walls are to be re-streamlined after a small change in the test conditions of model incidence and/or reference Mach number. The streamlining cycle† starts with the measurement of tunnel pressures, from which a new pair of wall contours are computed. Wall loading and the resulting residual interferences are assessed as an indication of the quality of wall streamlining (see Section 3.2 for details). If the wall streamlining criterion is not satisfied, then the walls are adjusted to the new contours and the process is repeated until the walls

† A streamlining cycle consists of a series of iterations bringing the walls to satisfactory streamlines.

are satisfactorily streamlined, at which stage the streamlining cycle is complete and the model pressures are recorded.

4. DISTINCTIVE FEATURES OF FLEXIBLE WALLED TEST SECTIONS

4.1 Advantages Over Conventional Test Sections

In addition to the elimination (as far as experimentally possible) of top and bottom wall interference effects, the two-dimensional flexible walled test section offers the following advantages over test sections of conventional design:-

4.1.1 Higher Reynolds Number

The elimination of wall interference allows the reduction of test section height, or conversely, the model size may be increased. Both actions reduce the ratio of test section height to model chord (h/c). The reduction of h/c for a given test section flow area and model aspect ratio leads to improved Reynolds number capability.

The desire to bring the flexible walls as close as possible to the model is limited by several practical and aerodynamic limitations.[7,8] The most notable limitation is that mixing of the wake or boundary layer of the model with the flexible wall boundary layer invalidates the underlying assumptions of wall streamlining.

4.1.2 Reduced Power Requirements

A reduction of tunnel drive power is an important alternative to increased Reynolds number capability. The reduction of test section size coupled with the elimination of test section ventilation can lead to significantly reduced tunnel power requirements. The overall power reduction brought about by the use of flexible walled test sections may exceed 80% for some transonic test regimes.[8]

4.1.3 Improved Flow Quality

Test section flow quality is recognised as an important characteristic in unsteady and transonic aerodynamics. However, existing transonic wind tunnels employ ventilated test sections which produce high levels of turbulence and noise, generating largely unknown interference effects.

Flexible walled test sections remove the need for ventilation. The test section walls are impervious and smooth, leading to improved test section flow quality.

Test section flow quality is also dependent on secondary flows. In two-dimensional testing the magnitude of secondary flow effects presumably increase with test section height and reduce with increasing model aspect ratio. Wall streamlining allows the use of shallower test sections and/or larger models since wall interference is eliminated. When the test section height is small the cross-sectional shape of the flow channels over and under the model becomes slit-like. In these circumstances, it may be argued that the flow becomes highly two-dimensional, with any secondary flow effects tending to be limited to the tips of the model. This may not be the case with test sections of conventional height.

4.1.4 Available Wall Data

A prerequisite of the streamlining process is the measurement of *'wall data'* (as previously noted in Sections 1 and 3.3). The wall data, which consists of the geometries of the flexible walls and static pressure distributions along their centrelines, also allows the wall interference effects at the model to be quantified[13] at any stage of the streamlining process. Therefore, as a means of reducing the streamlining run-time overhead there remains the option of terminating the streamlining process before the walls have been set to the best possible streamlines, and then to apply conventional corrections (of modest level) to the model data. When considering the application of model corrections it should be noted that the recent progress in boundary interference-assessment methods[74-82] has been achieved by the realisation that measured boundary conditions are more reliable than those obtained from wall modelling.[83,84] The nature of the streamlining process demands that the boundary conditions are routinely measured in flexible walled test sections, which is often not the case in test sections of conventional design.

The wall data, in principle, also contains information on lift, pitching moment, model wake displacement thickness and model aerodynamic shape. In practice, only lift[85] and model wake displacement thickness[11] have been satisfactorily estimated from wall data obtained in the TSWT. Inadequate resolution of wall measurements prevents the satisfactory assessment of the

other quantities. The displacement thickness of the model wake is available from the movement apart of the flexible walls downstream of the model after wall streamlining (this point is discussed in greater detail in Section 10). Lift can be extracted from the corresponding forces on the flexible walls together with vertical components of momentum at the test section ends.

It can, therefore, be argued that flexible walled test sections routinely provide more reliable boundary information than conventional transonic test sections, leading to the realisation of the correctable interference wind tunnel, postulated by Kemp.[86]

4.1.5 Test Mode Versatility

Flexible walled test sections offer the possibility of simulating many two-dimensional flows.[7,11] Careful design of the test section can allow six test modes of operation. The test modes are as follows:-

4.1.5.1 Closed Tunnel Mode

The closed tunnel mode is the mode of operation of many low speed and supersonic wind tunnels of unventilated design, where the test section walls are straight and generate the flowfield of an infinite array of images. The straight dividing streamlines between these images and the model coincide with the test section walls, and therefore the wall streamlining criterion for a flexible walled test section is simply that the walls follow *'straight'* contours, as shown on Figure 4.1a. The flexible walls are adjusted to straight contours experimentally by setting up a condition of constant static pressure, equal to the reference value, along the centreline of each wall with the test section empty.† In this way the walls diverge to allow for the growth of the boundary layer displacement thickness along the test section.

4.1.5.2 Open Jet Mode

The wall streamlining criterion for the simulation of open jet test conditions, is satisfied when the flexible walls are contoured to give constant pressure, equal to the free-stream ambient value, along the centreline of each

† Contours derived in this way are usually described as aerodynamically straight (see Section 8.1 for further details).

wall with a model installed in the test section,† as shown on Figure 4.1b. The setting of such contours was one step in the wall streamlining procedure used by Lock and Beavan[5] of the National Physical Laboratory in the 1940's (see Section 6.3 for further details).

4.1.5.3 Infinite Flowfield Mode

The infinite flowfield mode of operation is the most widely used in commercial two-dimensional wind tunnel testing. As described in Section 3.2, the wall streamlining criterion is satisfied when the flexible walls are contoured to eliminate inequalities between static pressures measured at the walls inside the test section, and external wall pressures derived during computations of the imaginary flowfields. For lifting or non-symmetrical models the two flexible walls are required to follow different shapes, as shown on Figure 4.1c.

4.1.5.4 Ground Effect Mode

In the ground effect mode, the flow to be generated in the test section is a portion of that about a pair of models, one being the mirror image of the other. The flexible walls bound the real flowfield which contains one of the models, as shown on Figure 4.1d. One wall represents the line of symmetry between the real and imaginary models and the other follows any convenient streamline along the other side of the real model. The wall streamlining criterion is satisfied when the *'ground'* wall is set straight as for the closed tunnel mode, while the other wall is contoured to satisfy the infinite flowfield criterion.

4.1.5.5 Cascade Mode

In the cascade mode of operation, the flexible walled test section simulates a portion of the flow about an infinite cascade of aerofoils. The test section bounds a single aerofoil with the walls contoured to streamlines between the aerofoils, as shown on Figure 4.1e. As the flowfield between each aerofoil is identical, the walls may follow identical streamlines above

† Contours derived in this way are usually described as constant pressure contours.

and below a single aerofoil in the cascade. A simple wall streamlining criterion is that the measured static pressures along the flexible walls should be equal when the walls are spaced one aerofoil pitch apart in the plane of the cascade[12] (i.e. pressures at A, B and C are respectively equal to pressures at A', B' and C'). Turbine and compressor cascades may be simulated, in principle, around one model by re-streamlining the walls for different cascade planes (pressure matching angles).

4.1.5.6 Steady Pitching Mode

In a flexible walled test section it is possible to simulate different steady pitching rates with a stationary model, in order to assess the associated changes in model force and pitching moment coefficients.[87] The procedure first involves wall streamlining for an infinite flowfield, then some curvature of the tunnel centreline is introduced. The walls are adjusted in accordance with local changes of the centreline position from straight to curved, as shown on Figure 4.1f. Different pitching rates are simulated by varying the magnitude of centreline curvature. The walls, while not perfect†, may be assumed to be approximately streamlined for steady pitching.

4.2 Disadvantages Compared with Conventional Test Sections

4.2.1 Operational Aspects

The flexible walled test section moves towards interference-free boundaries in a series of iterations which may be regarded as non-productive in terms of providing interference-free data on the model. The number of iterations required to streamline the flexible walls is a function of:-

1) The rate of convergence of the wall adjustment strategy which predicts any necessary wall movement.

2) The magnitude of the change in test conditions between streamlining cycles.

---

† Steady pitching investigations at Southampton[87] did not attempt to produce the change of flow velocity with test section height necessary for the full simulation of steady pitching.

Much research has been aimed at minimising the streamlining run-time overhead by developing complex wall adjustment strategies and fast automated wall setting systems. However, the number of necessary streamlining iterations may be significantly reduced by careful design of the test programme, based on the general rules that in two-dimensional testing changes in wall contour with test conditions are small in the case of a Mach sweep and, of course, are small if the change of angle of incidence is small. The test programme is usually initiated from straight contours, but the walls need never be, and usually are not, re-set to straight during a test programme. Furthermore, it should be noted that as additional means of reducing tunnel run-time associated with wall streamlining there remain the following options not explored so far:-

1) Compromise in the quality of wall streamlining coupled with the application of modest corrections to the model data.

2) Initiating the streamlining cycle from wall contours previously computed to follow *'near'* streamlines.

4.2.2 Increased Complexity

A practical self-streamlining test section demands automatic control of wall shape to ensure efficient and economical use of wind tunnel run-time.

Any future dynamic testing in flexible walled test sections will demand wall control systems of even greater complexity, so that the flexible walls will be able to follow the dynamic mode. Such wall control systems may prove to be impractical. However, if the walls are streamlined at the mid-position of the dynamic mode then the wall interference may prove to be negligible and will certainly be less than for a conventional test section of the same proportions.

4.3 Advantages Over Ventilated Adaptive Test Sections

Adaptive ventilated wind tunnels locally control the flow through the test section walls, which necessitates the use of complex test section hardware and advanced flow instrumentation for the measurement of flow angularity (as illustrated in Section 2.3.1). In flexible walled test sections the

need for ventilation is removed, hence reduced tunnel drive power, and the required measurements of wall static pressure and wall position are relatively simple to make. Therefore, in practice, the operation of flexible walled test sections is less complex than the operation of adaptive test sections employing ventilation.

5. DESCRIPTION OF TRANSONIC SELF-STREAMLINING WIND TUNNEL

5.1 Wind Tunnel Layout

A schematic layout of the wind tunnel[88] is shown on Figure 5.1. The tunnel has a closed circuit with stagnation conditions of ambient pressure and temperature. The induced-flow is driven by dried compressed air through an injector downstream of the test section, as shown on Figure 5.2. Mach number in the tunnel may be varied continuously from low subsonic to low supersonic by adjustments to inducing air pressure and test section wall contours.

Tunnel run-time varies from near infinity at low speeds to a maximum of about two minutes at high speeds. Inducing air pressure control is handled by a pneumatic Fisher control valve system which allows the rapid setting up of reference Mach number, and provides good stabilisation of Mach number despite the falling compressed air reservoir pressure experienced during a high speed run.

There are a series of screens mounted in the settling chamber upstream of the contraction for flow smoothing. The tunnel cross-section at the screens is 91.44cm (36 inches) square, therefore with the test section at its nominal 15.24cm (6 inches) depth and width the contraction ratio is 36:1. In the return leg of the tunnel circuit there is an air exhaust to maintain ambient conditions and for safety reasons there are two blow-off vents.

5.2 Flexible Walled Test Section

5.2.1 Layout

A schematic layout of the TSWT test section is shown on Figure 5.2. The layout represents what is regarded as a near optimum design of a flexible walled test section.

The test section is 15.24cm (6 inches) square in cross-section at the upstream end, with parallel rigid non-porous sidewalls throughout. The impervious top and bottom flexible walls, 1.12m (44 inches) in length, are anchored at their upstream ends to the fixed contraction and adjusted in single

curvature by twenty motor-driven screw jacks on each wall. Wall shape is monitored at all jack positions. The 20th and last downstream jack of each wall controls the free ends of the flexible wall in a sliding joint coupled to a variable diffuser. Hence, the streamlined portion of the test section effectively extends from jack 1 to jack 19, giving 96.52cm (38 inches) of streamlined length, on each wall.

The flexible walls are made from woven man-made fibre (Terylene) laminate. Presumably, they deform between jacks to contours dictated by their structural properties rather than following streamlines. Since the wall pressure loading and the streamline curvature both peak near the model, jacks are pitched closer together in this region than elsewhere. There are eight closely grouped jacks per wall near the model with a spacing of 2.54cm (1 inch), whilst upstream and downstream of the model the jack spacing increases to 7.62cm (3 inches) maximum, as shown on Figure 5.2 and by the picture on Figure 5.3 which shows the model mounted in the test section with one sidewall removed. The flexible walls are 5.08mm (0.2 inches) thick at their ends, with a central portion de-laminated to a thickness of 2.54mm (0.1 inches) coinciding with the closely grouped jacks.

The wall jacks are housed in the test section *'backbones'* which support the heavy sidewall plates. The chambers formed between the backbones and flexible walls are vented to the test section at the variable diffuser, as a means of minimising wall pressure loading. There is a clearance of approximately 0.76mm (0.03 inches) between the flexible walls and the rigid sidewalls to allow free movement. The gap is closed with a rubber seal bonded to the flexible walls to prevent in-flow and out-flow of air around the walls.

The two-dimensional model is mounted horizontally on glass windows integral with the rigid sidewalls, as shown by the picture on Figure 5.3. This arrangement allows the use of several flow visualisation techniques, such as schlieren photography. There is no provision for sidewall boundary layer control. The quarter chord point of the model is arranged to translate vertically with the change in angle of incidence to minimise wall curvature and help centralise the model between the walls in the presence of changing up and downwash.

As shown on Figures 5.2 and 5.3 a pitot rake is positioned on each flexible wall between jacks 19 and 20 to search for a potential flow core between the model wake and flexible wall boundary layers. Mixing of the model wake and wall boundary layer invalidates the underlying assumptions of wall streamlining.

The pressure data used in predicting the contours for two-dimensional interference-free flow comprises merely of the static pressure distributions along the flexible walls, and the tunnel reference Mach number. Static pressures are measured on the centreline (and other stations) of both flexible walls at all jack positions, except at the last downstream jack of each wall (i.e. jacks 20). The tunnel reference Mach number is determined from a reference static pressure measured on the centre of one sidewall in the plane of the flexible wall anchor points (as shown on Figure 5.2) and the reference total pressure measured just downstream of the screens in the settling chamber. The length of the test section has been chosen[50] so that the disturbance induced by the model in the streamwise component of flow is negligible at the reference static point. Furthermore, by mounting the model symmetrically in the streamlined portion of the test section the effects of induced upwash at both ends of the test section largely cancel each other[50]. It is argued that these features, coupled with the streamlining of the flexible walls, eliminate any need to apply corrections to the test data to account for top and bottom wall interference or length truncation.

5.2.2 Jack Layout

Each wall jack communicates with the computer to allow the following:-

1) Transmission of wall position data.

2) Transmission of wall static pressure data.

3) Change of wall position.

Each jack is driven through a worm reduction gear by a stepper motor (SLO-SYN M051-DW601) allowing easy digital control by the TSWT computer. One motor step corresponds to 15.0^{o} of motor shaft rotation, whilst one motor shaft revolution corresponds to a wall movement of 0.036mm (0.0014 inches).

Maximum motor power is achieved at a step rate of approximately 200Hz resulting in a wall increment of 0.30mm (0.012 inches) per second. A single jack is designed to have power sufficient to contour the flexible wall but insufficient to damage the wall. The stepper motors of adjacent jacks are mounted on alternate sides of the test section.

A linear potentiometer (Sakae 20 LP 30) provides simple analogue information on the wall position. The potentiometer monitors the movement of a connecting bar which is directly coupled to the flexible wall.

The maximum travel of a jack is 2.54cm (1 inch), the movement being limited by the maximum stroke of the linear potentiometers. This monitored range of travel can be set anywhere within 5.08cm (2 inches) of available mechanical travel. The wall setting accuracy is estimated to be 0.127mm (0.005 inches).

5.2.3 Pressure Data Acquisition System

The pressure data acquisition system samples tunnel and model static pressures; a Scanivalve system converts pressures to analogue signals for computer sampling.

The TSWT is fitted with a Scanivalve module system consisting of a solenoid drive coupled to four 48 port scanner modules and an encoder, enabling rapid sampling of 192 inputs. The minimum number of pressure inputs for the two-dimensional tests under discussion was 84, comprising 38 wall static pressures, tunnel reference static and stagnation pressures and 44 model pressures.

One transducer is rated at 103.4 kN/m^2 (15 p.s.i.) maximum differential pressure, while the others are rated at 17.2 kN/m^2 (2.5 p.s.i.). The 15 p.s.i. transducer, which is referenced to atmosphere, monitors the reference static pressure every sixth port during the 48 port scan and is arranged to sample large suction pressures on the model, as well as the reference total pressure. All 2.5 p.s.i. transducers are referenced to the tunnel reference static pressure and sample all other pressures (mainly wall and model static pressures).

Signal levels from the transducers are significantly lower than the ±5 volt range of the analogue to digital converter. Therefore, signal conditioning was required and simple operational amplifiers were used. To minimise the effects of long term drift in the outputs of the amplifiers zero readings were taken from the transducers before each tunnel run.

During a tunnel run a dwell time of at least 80 milli-seconds at each Scanivalve port was used to allow for stabilisation of pressures and transducer rise-time. Each recorded transducer signal was an average of fifteen samples taken at a rate of 1KHz. An automatically controlled 48 port scan took about eight seconds.

5.3 The Model

The model used throughout this investigation was a NACA 0012-64 aerofoil of 15.24cm (6 inches) span and 10.16cm (4 inches) chord (see Tables 2.1 and 2.2 for further details of the model). The resulting ratio of test section height to model chord of 1.5 is much lower than normal for conventional two-dimensional testing. The same model had been used for the majority of all previous two-dimensional model tests in the tunnel[14,15,65] and is constructed from stainless steel.

Each surface of the model has twenty-two static pressure tappings with five tappings grouped within the first 10% of the chord and the remainder spaced at approximately 5% chord intervals, as shown in Table 2.2. The tappings on the lower surface are positioned along a chord line 9.52cm (3.75 inches) from one sidewall. The tappings on the upper surface are positioned along a chord line 5.71cm (2.25 inches) from the same sidewall. Hence, the sets of upper and lower tappings are displaced spanwise by 3.81cm (1.5 inches) symmetrically about the mid-span.

A grit transition band, approximately 2.54mm (0.1 inches) wide, was applied to the upper and lower surfaces centered at the 5% chord position.[89] Under some test conditions (M_∞ greater than about 0.7) the concentration of grit could be seen by schlieren pictures to produce weak shock waves near the leading edge. The weak shock waves affected the detailed shape of the pressure suction peak near the transition band.

No attempt was made to accurately align the model zero angular reference with the test section flow and therefore, the quoted angles of model incidence are merely nominal. However, care was taken in measuring the changes in angle of incidence which are estimated to be accurate to 0.1^{o}.

5.4 TSWT Control System

The main functions of the on-line computer control system of the TSWT are to:-

1) Streamline the flexible walls.

2) Acquire test data from the model.

The control system consists of two control loops, one for Scanivalve control and one for wall contour control, as illustrated by the control system outline shown on Figure 5.4.

5.4.1 Hardware

The nucleus of the control system is a dedicated mini-computer which communicates with the tunnel through its peripheral devices using digital and analogue signals. The control system hardware performs three main functions:-

1) Wall movement.

2) Wall and model pressure measurement.

3) Wall position sensing.

The wall movement function involves controlling (via digital lines) the forty stepper motors. Power pulses are transmitted to the 3-phase motors for a pre-determined and variable time interval. The wall has then moved one increment, giving between 0.05mm (0.002 inches) and 1.22mm (0.048 inches) of wall movement at each jack position. The sequence is repeated until the two walls are correctly contoured, which typically takes about ten seconds.

In addition to the computer control of wall position there is available to the user the option of a *'manual'* control system. This system allows each jack to be individually selected and adjusted to a known position.

The wall and model pressure measurement function involves operating the Scanivalve system. The Scanivalve begins its 48 port scan from a known starting point, and dwells at each port to allow averaged transducer signals to be recorded by the computer. The encoder indicates to the computer that each step of the scan has occurred.

The wall position sensing function involves the computer sampling the output from each of the forty linear potentiometers. All of these signals are, in principle, continually available for computer sampling. However, as the potentiometer outputs are not electrically isolated from the jack motor control system, due to noise they cannot be usefully monitored when the flexible walls are moving.

The operation of the control system was monitored from a command VDU console, with provision for the tunnel operator to display test data on the console in real time. A hard copy on a line-printer and/or on a Tektronix 4662 plotter could be obtained subsequent to the tunnel run. The TSWT control system hardware is shown in the picture on Figure 5.5.

5.4.2 Software

Computer software for the on-line control of the TSWT uses a versatile modular architecture.[64] The main program comprises a collection of sub-programs which combine to control the tunnel and output real time results, or to provide a more detailed re-analysis of previously acquired data.

The software, written in FORTRAN IV language, is linked to a system library, a FORTRAN library and a Real Time System Library (RTSL) to access peripheral control subroutines. Where possible, standard FORTRAN IV has been used but some commands are peculiar to the DEC system used. These commands can be grouped into analogue to digital sampling commands (ADC and RTS), programmable clock commands (SETR and LWAIT) and digital input and output commands (IPEEK and IPOKE).

The versatility of the control software, due to the modular architecture, has allowed the generation of computer programs for particular tasks such as:-

1) Aerodynamically straight† wall streamlining.

2) Prediction of the imaginary flowfields by several computational methods.

3) Wall streamlining according to several wall adjustment strategies.

Also, numerous utility computer programs have been developed to assist with the operation of the TSWT. The tasks of such programs include the following:-

1) Set both walls to specified contours together or individually.

2) Modification of wall contour records.

3) Display current position of flexible walls.

4) Display wind-on wall movement†† during a tunnel run.

5) Data file handling.

In addition, computer programs have been written to command the Tektronix plotter to display tunnel and model data.

5.4.3 Safety features

The hardware and software of the control system include many safety features to guard against possible system failure which may result in physical damage to the test section.

---

† See Section 8.1 for definition of aerodynamically straight.

†† See Section 5.6.3 for definition of wind-on wall movement.

The hardware safety features include:-

1) Wall adjustments are made by a series of small increments of movement, thus the failure of a motor to move will not overstrain the wall.

2) Flexible walls are strong enough to withstand the full stall force of a single jack motor.

3) An electronic guard against accidental jack operation at system switch-on.

The software safety features include:-

1) Jack position is sampled before and after each increment of wall movement, as a check on proper movement.

2) Displacement of the first jack on each wall is limited to prevent damage to the wall anchor point.

5.5 Tunnel Operation

A streamlining cycle consists of the following stages:-

1) The model is set to the required angle of incidence.

2) The flexible walls are set to starting contours.

3) The control software is initiated. The tunnel stagnation temperature (measured by a thermocouple in the settling chamber), ambient pressure and test reference conditions are manually entered into the computer by the tunnel operator.

4) The tunnel air is turned on and the reference Mach number is stabilised by adjustments to inducing air pressure.

5) The Scanivalve system is operated and tunnel and model pressures are recorded by the computer.

6) The computer reduces raw pressure data allowing analysis of the data in order to generate a new set of wall contours.

7) The computer assesses the quality of wall streamlining.

8) If the streamlining criterion has not been satisfied the walls are adjusted to the new wall contours (computed in stage 6). Then stages 5 to 8 are repeated until the walls are correctly streamlined.

9) A summary of tunnel and model test data is displayed on the command VDU console and line-printer.

In practice, the tunnel drive air was turned on and off between each streamlining iteration as a means of minimising air consumption. During high speed runs (M_∞ greater than about 0.8) a dwell time (of 10 minutes maximum) between streamlining iterations was required in order to allow recovery of reservoir air pressure.

5.6 Recent Modifications to the TSWT Facility

5.6.1 Computer

The original computer dedicated to the TSWT was a DEC PDP 11/34 running a single job operating system (DEC RT-11 V.4). The 16 bit processor was capable of addressing 32K words of real memory (plus 32K words of virtual memory), but of this only 22K words of real memory was available for a user's program. This memory capacity was dependent on the size of the operating system. The present TSWT control program requires up to 31K words of real memory, therefore to run the control software on the PDP 11/34 the technique of overlaying was required, so that only a small portion of the software is stored in the real memory at any instant during execution. The overlaying technique reduced the control program's memory requirement from 31K words to 17.9K words.

The need to reduce TSWT TSP code run-times (see Section 7 for details of the code) and the desire for increased memory available to a user's program led to the PDP 11/34 processor being updated to a PDP 11/84 and the

installation of a multi-user operating system (TSX Plus). These updates, plus the installation of extra disc storage, enables the facility to simultaneously accommodate up to thirty-two users, each accessing 32K words of real memory, whilst typical TSWT TSP code run-times were reduced by a factor of four. However, at present the TSX Plus operating system does not support the necessary peripherals to allow tunnel operation, hence the control software can only be run on the PDP 11/84 under a regenerated version of the single job operating system. This system limits the real memory available to the user's program to 16.9K words, therefore the technique of overlaying is still required to run the TSWT control program.

5.6.2 Flexible walls

The pushrods of jacks 1 to 19 were attached to the original flexible walls by thin metal flexures and wall stiffener ribs. The ribs were screwed and bonded to the wall and each supported three wall static pressure tappings. One tap was on the wall centreline (Orifice 2) and one 5.08cm (2 inches) on either side of the centreline (Orifices 1 and 3). The metal flexures were designed to accommodate varying local wall slopes and allow *'pull-up'* due to wall curvature. The free length of the flexures was 6.35mm (0.25 inches).

The original flexible walls were in operational use for over six years by which time signs of wear had become obvious, therefore new flexible walls were installed. The new walls feature five static pressure tappings per jack position. One tap is on the wall centreline (Orifice 3), and two 5.08cm (2 inches) and 2.54cm (1 inch) on either side of the centreline (Orifices 1, 5, 2 and 4). The increased number of pressure tappings is aimed at improving the three-dimensional research capability of the tunnel.

The new walls have an improved jack/wall link mechanism to eliminate some weaknesses which had become apparent in the metal flexures previously used to link the jack push rods to the wall stiffener ribs. The weaknesses included occasional flexure buckling and cracking plus a limited amount of slipping of the flexure end-fixings. Since wall position is measured by monitoring connecting bar movement, which is directly coupled to the jack push rods, any uncontrolled free play between the push rods and the flexible walls is most undesirable. The design of the jack/wall mechanism now in use with the new walls is shown on Figure 5.6. The swinging links perform the

same function as the old metal flexures but provide a more permanent jack/wall attachment. Operation of the new jack/wall link mechanism is clearly demonstrated by the picture shown on Figure 5.3.

5.6.3 Wind-on wall movement

The TSWT wall streamlining procedure relies on the position of the flexible walls remaining unchanged between the wind-on and wind-off stages of the streamlining process. However, during some model tests[90] using the original flexible walls, wind-on deflections (at jack positions) of up to 0.38mm (0.015 inches) were experienced compared with their wind-off positions. The wall movement was almost always towards the tunnel axis indicating a greater plenum chamber pressure than test section pressure. If ignored, the wind-on wall deflections of such a magnitude are likely to have a significant effect on the quality of wall streamlining. Thus, the TSWT control software now routinely measures and records the wind-on wall deflections during each streamlining iteration. However, the improved jack/wall link mechanism of the new flexible walls has reduced the wind-on wall deflections to negligible magnitudes.

6. DESCRIPTION OF THE WALL ADJUSTMENT STRATEGIES EVALUATED

The wall adjustment strategy (WAS) is a fundamental component of the self-streamlining concept. A rapid convergence of the walls to streamlines depends on the adequacy of the strategy governing the streamlining process. Thus, the evaluation of several strategies has formed a major element of the research covered by this thesis.

The object of all the strategies under evaluation is to bring the flexible walls to streamlined shapes in order to eliminate top and bottom wall interference. The flexible walled test section itself, influenced by the flow disturbances generated by the model, provides all the data required by the strategies (as discussed in Sections 1 and 3.3).

The requirement that the strategy should be free from dependence on any assumption about the flow in the vicinity of the model necessitates the iterative nature of the streamlining process. A one-step strategy which does not invoke any knowledge of the aerodynamic behaviour of the model would require the behaviour not to change with wall shape, whereas the whole adaptive wall concept arises because model behaviour is not predictable and is dependent on test section boundary conditions (i.e. wall shape).

6.1 Predictive Wall Adjustment Strategy

Following the realisation that the simple Imbalance wall adjustment strategy (see Section 8.3 for details of the strategy) for contouring the flexible walls of two-dimensional test sections to streamlined contours was too slow for practical use,[7] Judd proposed,[50,63] developed and placed in service[9] the Predictive wall adjustment strategy (WAS 1). During the following years the strategy was further refined[11,64] and extensively used and proved up to transonic speeds.[13,14,16,17,90,91]

The strategy reduced by 75% or more the number of iterations required to bring the flexible walls to satisfactory contours, and therefore the tunnel run-time attributable to the streamlining process was significantly reduced. It has been demonstrated that the strategy works well in

two-dimensional testing at any set of conditions up to those which result in the model's shock just extending to a streamlined wall (usually this would be the suction surface shock just extending to the nearest wall).

The strategy was first implemented in 1976 in work with a low speed flexible walled test section (SSWT 1) and is still used for routine two-dimensional testing in the TSWT. More recently the strategy has been embodied in the software which controls the flexible walls of the test section insert of the 0.3-m Transonic Cryogenic Tunnel[60,61] at NASA Langley Research Center.

The strategy requires the wall shape and the velocity distributions along both sides of each flexible wall to be known. The real side velocity distributions are derived from measurements of static pressures along the insides of the walls, while the velocities on the outside of the walls, generated by the imaginary flowfields, are obtained by computation. The strategy utilises this wall information in predicting new wall contours which will reduce the wall loading present during the current run† and thereby reduce top and bottom wall interference effects at the model, whilst simultaneously providing the imaginary side velocity distributions over the new wall contours. Therefore, if the present wall contour has been derived by using the strategy the required imaginary side velocity distributions are available.

The underlying principles and theory which form the basis of the strategy are briefly outlined in Appendix A. A more detailed account including the presentation of software which embodies the procedures of the strategy can be found in Reference 62.

6.1.1 Operational Requirements

The strategy can only be initiated from wall contours where the imaginary side velocity distributions are known. Thus, to avoid the need for imaginary flowfield computations for a starting case it has become practice to

† The word *'run'* is used here in the context of data gathering; a run is a period during which all pressures (and perhaps other data) are being gathered.

initiate the streamlining cycle from aerodynamically straight contours, so that the imaginary side velocity distributions are known.

i.e. $V_{(x)}$ = imaginary side velocity at position x

= U_∞ = Constant

The linearised compressible theory of the strategy limits its operational use to conditions up to those which result in the velocity distributions along both sides of each flexible wall just remaining subsonic. Therefore, in tests aimed at wall streamlining at high reference Mach numbers, it is necessary to first run a test at a reference Mach number below that which chokes the test section with the walls straight. The first wall movements predicted by the strategy have a profound effect on the test section flow, and for most conventional tests the streamlining cycle is usually able to proceed at the required reference Mach number after the first iteration.

The imaginary flowfield computations (which are an inherent part of the strategy) assume that the changes in wall boundary layer displacement thickness (δ^*), due to the presence of the model, are negligible.† The underlying aerodynamic theory of the strategy does not allow any other assumption to be easily made in this respect. However, such an assumption is usually valid for routine two-dimensional testing (as discussed in Section 9.5).

With a correctly designed test programme (as discussed in Section 4.2.1) the strategy has allowed wall streamlining to be achieved within two or three iterations. Analysis of both walls takes about 3 seconds on the DEC PDP 11/84 computer.

6.2 Exact Wall Adjustment Strategy

Following the successful demonstration of the Predictive strategy up to transonic speeds, Judd proposed[92] and developed[93] the Exact wall adjustment strategy (WAS 2). The aim was to eliminate some of the

---

† See Section 9.1 for reasons why the imaginary flowfield computations may be required to account for the changes of δ^* along the flexible walls.

mathematical approximations present in the Predictive strategy in order to further reduce the number of iterations required to adjust the flexible walls of two-dimensional test sections to streamlined contours. The strategy requires the wall shape and the real side velocity distributions of both flexible walls to be known, and utilises this information in predicting new wall contours of reduced, ideally zero, wall loading. The equations derived by Judd which form the basis of the strategy are presented in Appendix B. The approximations still present in the strategy include:-

1) The use of linearised flow theory.

2) Compressibility is incorporated in the form of the Prandtl-Glauert factor (β).

3) No account is taken of the dependence of model behaviour on wall shape.

Experience with the Predictive strategy in the TSWT has shown that the effects of 1) and 2) are not large for reference Mach numbers not too close to unity. However, as with the Predictive strategy, the linearised flow theory limits the application of the strategy up to conditions which result in the flow at the walls just remaining subcritical. As already stated the effect of 3) would probably result in one or more iterations. However, as the strategy does account for the aerodynamic coupling of the walls and also includes some major second order effects (such as wall slope†), it was anticipated that the strategy would offer the strong possibility of reducing wall adjustments associated with a streamlining cycle governed by the Predictive strategy. The validity of the strategy, within the above mentioned limits, was confirmed by an exact analytic test case.[93]

6.2.1 Operational Requirements

The strategy can be initiated from any wall contour of known shape. Unlike the Predictive strategy the streamlining cycle does not have to start from aerodynamically straight contours or contours previously derived by the

† As described in Appendix A the underlying principles and theory of the Predictive strategy applies only to a single flat flexible wall.

strategy. This fact has important implications on the design of the test programme.

The imaginary side velocity distributions are computed according to Equation B.2 of Appendix B (in the following this computational method is denoted by IMAG 2). The form of Equation B.2 permits variations in δ^* to be easily incorporated in the imaginary flowfield computations. However, in routine two-dimensional testing such an allowance is not usually required (see Section 9.5 for further details).

At present the Exact strategy requires about 6 seconds of computer run-time with the DEC PDP 11/84 computer.

6.2.2 Summary of Initial Operational Experience

The strategy was first implemented in the TSWT by Norman[94] in 1983 and this initial evaluation of the strategy revealed the following problems:-

1) Unexpected wall shapes at both ends of the test section.

2) Slow convergence of the walls to satisfactory contours.

3) Difficulty in satisfying the existing wall streamlining criterion ($E < 0.01$ on both walls).

It was, therefore, concluded that the strategy did not warrant further development. However, errors relating to the programming of the equations and to the installation of the strategy into the TSWT control software have recently been discovered by the author which has renewed interest in the strategy.†

6.3 NPL Wall Adjustment Strategy

The transonic strategy proposed, developed and used by NPL[5,21,25,95-98] in the 1940's for wall streamlining involved determining, experimentally, the wall contours that gave constant static pressure (hence

† The author's experience with the strategy is reported in Section 10.

constant Mach number) equal to the reference value along the centrelines of the flexible walls. These contours were derived with the model installed in the test section and for the purposes of this thesis are described as *'constant pressure'* contours. Such contours simulate open jet conditions and therefore still induce wall interference effects at the model. For wall streamlining, the flexible walls were then positioned to shapes between the constant pressure contours and the previously derived aerodynamically straight contours.

The strategy was based on conclusions from a series of theoretical calculations of inviscid incompressible flows around simple two-dimensional models.[5,21] In this theoretical work the blockage of the model was represented by a single doublet, the wake behind the model by a single source, and any lift by a point vortex. It was found that the streamlined contours were everywhere roughly half-way between the constant pressure and aerodynamically straight contours.

The above described wall adjustment strategy employing a half-way setting factor (NPL 1 WAS) was used to streamline the flexible walls of the 20 x 8 NPL Tunnel[20,5,21,91] (see Section 2.1.3 for tunnel details). Difficulty was experienced in the 20 x 8 NPL Tunnel in obtaining wall contours that gave constant static pressures, equal to the reference value, on both walls when lift was present. Consequently, NPL adopted the practice of adjusting the flexible walls to contours that gave constant static pressures along the centrelines of the walls, but with the pressures differing on the two sides of the test section, the value of the difference depending on the magnitude of the lift present. The contours were derived experimentally by employing what we now term the Imbalance strategy (see Section 8.3 for details of the strategy), as were the aerodynamically straight contours.

The above mentioned NPL practice was not required when deriving constant pressure contours in the TSWT, as contours exhibiting constant static pressures equal to the reference value on both walls could be attained without difficulty. The problems experienced in deriving constant pressure contours in the 20 x 8 NPL Tunnel may have been due to the reference pressure orifice being influenced by the disturbance caused by the lifting model, as the orifice was situated only 21.59cm (8.5 inches) ahead of the leading edge of the standard 12.70cm (5 inches) chord model. The fact that the reference orifice

was located on one flexible wall further complicated the matter, since the orifice would be influenced by the disturbance caused by wall movement.

Lock and Beavan[5] suggested that the NPL strategy employing a setting factor of six-tenths towards the constant pressure contour (NPL 2 WAS) would be more *'nearly correct'* in the vicinity of the model than the original half-way setting factor. Presumably, in an attempt to account for the approximate definition of constant pressure contours derived in the 20 x 8 NPL Tunnel they also suggested an additional calculated wall movement based on the estimated lift coefficient of the model. As far as the author is aware no tests utilising the new setting factor of six-tenths (NPL 2 WAS) or the extra wall movement to streamline the flexible walls of the 20 x 8 NPL Tunnel have ever been published.

The value of the setting factor between the constant pressure and aerodynamically straight contours may well be test section dependent. However, the two setting factors suggested by NPL were expected to be sufficiently accurate for most test sections,[96] therefore only these setting factors were used during the present evaluation of the NPL strategy in the TSWT. The additional wall movement suggested by Lock and Beavan was not applied as contours exhibiting constant static pressures equal to the reference value on both walls were easily attained in the TSWT.

6.4 Notation of Wall Adjustment Strategies

The wall adjustment strategies (and their variations) under evaluation in this thesis are denoted by the following:-

1) WAS 1 - Predictive strategy proposed by Judd and used in routine two-dimensional testing in the TSWT.

2) WAS 1A - WAS 1 strategy but with the external velocity distributions computed by the TSWT TSP code.†

† See Section 7 for details of the TSWT TSP code.

3) WAS 1B - WAS 1 strategy but with the external velocity distributions computed according to IMAG 2†.

4) WAS 2 - Exact strategy proposed by Judd to reduce the number of streamlining iterations (external velocity distributions computed according to IMAG 2).

5) WAS 2A - WAS 2 strategy but with the external velocity distributions computed by the TSWT TSP code.

6) NPL 1 WAS - NPL strategy used in two-dimensional testing in the 20 x 8 NPL Tunnel during the 1940's.

7) NPL 2 WAS - Modification of NPL strategy suggested by NPL.

† IMAG 2:- Imaginary flowfield computations according to Equation B.2 of Appendix B.

7. PREDICTION OF MIXED FLOW IN THE IMAGINARY FLOWFIELDS

The nature of the imaginary flowfield computations embodied in the WAS 1 strategy limits the operational Mach number of the TSWT† (as already stated in Section 6.1). At higher speeds supercritical flow extends *'through'* the flexible walls when they are not straight, invalidating the linearised theory used to compute the imaginary flowfields. To permit the extension of two-dimensional testing to higher transonic speeds (where the channels over and under the model can both be choked) a major new development was necessary. This was the provision of a code to solve the mixed flows now in the imaginary flowfields. It was anticipated that there would be a considerable computational time penalty associated with the increased complexity of a suitable code.

7.1 Past Attempts

7.1.1 Time Marching Code

In 1980 Mason[99] adapted a code (developed by Spurr[100] and capable in principle of introducing supercritical flow) in an attempt to compute the imaginary flowfields at high subsonic reference speeds. The code, originally designed to compute two-dimensional transonic flow in turbomachinery, employed a time marching finite area method developed by Denton.[101] Due to the problems encountered in the practical application of the code†† and in the accuracy of shock placement, the time marching method proved to be unsuitable for the needs of the TSWT.

---

† The same limitation applies to the WAS 2 strategy.

†† The code could not be run on the TSWT computer and often exceeded the CPU time limit for a single job when run on the ICL 2970 computer at Southampton.

7.1.2 Streamline Curvature Code

Extensive attempts by the author to modify an existing (locally written) compressible subsonic streamline curvature code in order to compute the mixed flow of the imaginary flowfields failed.

7.2 RAE Transonic Small Perturbation Code

7.2.1 Background

At high subsonic speeds the two-dimensional inviscid flows of the imaginary flowfields are often characterised by the presence of adjacent regions of subsonic and supersonic flow, which are described by elliptic and hyperbolic equations respectively. Hence the mathematical description of such flows requires the solution of mixed equations, but as the problem is non-linear there are no analytical solutions. However, recent advances in digital computers have allowed numerical solutions to be obtained.

The breakthrough in practical computation of inviscid transonic flow came with the application of finite-difference techniques. Two basic approaches have evolved; time dependent techniques[102,103] and relaxation methods.[104-107] The former approach requires lengthy computation; Magnus and Yoshihara[108] quote a typical computing time of over two hours on a CDC 6400 computer.

Relaxation methods were first developed by Emmons[109-111] in the 1940s but were reformulated for transonic flow computation in the early 1970s by Murman and Cole[104] and by Krupp.[105] The majority of methods developed so far are based on the transonic small perturbation (TSP) equation, although the full potential (FP) equation has also been solved.[106] However, it has been shown[105,112,113] that solutions of the TSP equation can be obtained which do not differ appreciably from the corresponding solutions of the FP equation.[114] Furthermore, the computational demands of solving the TSP equation are more realistic than solving the FP equation. Krupp[108] quotes a TSP computing time of about thirty minutes on an IBM 360/44 computer. On a faster machine (CDC 6600) the same calculation took only four minutes.

Following discussions a code was offered by RAE Farnborough (in which the TSP equation is solved by the employment of finite-difference schemes and relaxation), which appeared to offer real promise in computing the mixed flows of the imaginary flowfields and thereby extend the operational test envelope of the TSWT. The code (RAE TSP code)[112] was originally designed to predict two-dimensional irrotational flow past lifting aerofoils in free air at transonic speeds. RAE Farnborough (RAE) has used the code as a convenient and versatile tool for basic design† and to investigate test section boundary interference.[113]

In the following (Sections 7.2 and 7.3) the code is first briefly outlined and then its adaptation to the purposes of the TSWT is detailed.

7.2.2 Governing Equation and Boundary Conditions

7.2.2.1 Transonic Small Perturbation Equation

The TSP equation

$$\left[K - (\gamma - 1)\Phi_x\right]\Phi_{xx} + \Phi_{z'z'} = 0 \qquad (7.1)$$

approximates the exact equation for isentropic irrotational two-dimensional flow about an aerofoil when:-

1) Perturbations from reference conditions are small.

2) Reference Mach number (M_∞) is close to unity.

The aerofoil is assumed to be thin [ratio of thickness to chord (δ) $\ll$ 1] and at a small angle of incidence (α).

In Equation (7.1):-

γ = Ratio of specific heats

† The RAE TSP code was used extensively in the design of the Airbus wing geometry.

ϕ = Scaled perturbation potential given by $\Phi = x + \delta^{2/3} M_\infty^{-2/3} \phi$

where Φ = Velocity potential

x = Co-ordinate in reference direction, scaled with respect to aerofoil chord

z' = Stretched co-ordinate given by $z' = (M_\infty^2 \delta)^{1/3} z$

where z = Co-ordinate normal to reference direction, scaled with respect to aerofoil chord

K = Similarity parameter

It has been shown[112,113] that good agreement with solutions of the FP equation[114] can be obtained when the form of K is taken as

$$K = \frac{1 - M_\infty^2}{\delta^{2/3} M_\infty^r} \qquad (7.2)$$

where $r = 1$

The velocity components (u,w), scaled with respect to the reference speed (U_∞), respectively parallel and normal to the reference direction are given by[113]:-

$$u = 1 + \left[\delta / M_\infty\right]^{2/3} \phi x$$

$$w = \delta \phi_{z'}$$

7.2.2.2 Aerofoil Boundary Conditions

The exact tangency flow condition at the aerofoil surface may be approximated by[112]:-

$$\phi_{z'} = f' - \frac{a}{\delta} \tag{7.3}$$

where

f' = slope of aerofoil surface relative to chord line, divided by δ.

7.2.2.3 Kutta Condition

A solution for ϕ will, for a lifting aerofoil, contain a discontinuity along a slit taken to be running from the trailing edge (assumed to lie on the x axis) along $z = 0$ to $x = +\infty$. The Kutta condition implies finite velocities at the trailing edge (and of course elsewhere) and in the absence of viscous wake velocities can be assumed to be continuous across $z = 0$. Hence, the Kutta condition may be taken as:-

$$\phi_x(z = +0) = \phi_x(z = -0) \quad \text{on the discontinuity}$$

7.2.2.4 Far-Field Boundary Conditions

The boundary condition on ϕ at infinity depends upon the lift generated by the aerofoil (or the circulation around the aerofoil) and therefore is not known in advance. However, the far-field boundary condition may be written by[112]:-

x	=	$+\infty, z' < 0$	ϕ	=	0
z'	=	$-\infty$	ϕ	=	$P/4$
x	=	$-\infty$	ϕ	=	$P/2$
z'	=	$+\infty$	ϕ	=	$3P/4$
x	=	$+\infty, z' > 0$	ϕ	=	P

The normalised circulation (P) is determined as part of the solution to Equation (7.1) and is given by[112]:-

$$P = \Delta\phi\,(x = +\infty)$$

Applying the Kutta condition gives:-

$$P = \Delta\phi \quad \text{at the trailing edge}$$

7.2.3 Outline of Numerical Method

The RAE method for the numerical solution of the TSP equation involves three major steps. The first step is to transform the co-ordinate system so that the infinite flowfield (x, z') becomes a finite flowfield (X, Z). A uniform rectangular finite-difference mesh is specified for the computing plane which enables the far-field boundary conditions to be easily specified and applied.

The second step is to introduce finite-difference approximations so that an algebraic, rather than a differential, equation is to be satisfied at each mesh point in the computing plane. The derivatives in the Z direction are replaced by central-difference approximations and the derivatives in the X direction by central-difference approximations when the flow is subsonic (elliptic equation) and backward-difference approximations when the flow is supersonic (hyperbolic equation).

The final step is the solution of the set of algebraic equations by successive over-relaxation on lines of constant X, starting at $X = -1$ and sweeping through computing plane regions 1,2,3 and 4 to $X = +1$ (the computing plane regions of the RAE TSP code are defined on Figure 7.1a). Values of ϕ not on the current line of constant X are needed for the finite-difference approximation and when values for the current sweep are unknown values from the previous sweep are used. Relaxation is applied after the values of ϕ along a line of constant X have been calculated. The convergence rate of the over-relaxation process is improved by adding an increment to ϕ, at the end of each sweep, for all interior points of the computing plane. The amount added is proportional to the change in the value of ϕ at infinity.

The whole process is first followed on a coarse mesh of 41 points in the X direction and 21 points in the Z direction, starting with conditions of undisturbed flow. Then the mesh is refined to 81 x 41 points and the solution of the coarse mesh computation is used as a first approximation to ϕ for the fine mesh computation. A few hundred fine mesh iterations are normally needed to reach a converged solution.

7.2.4 Transformation to Finite Computing Plane

As already stated the RAE numerical method involves transforming the infinite plane (x, z') into a finite square plane (X, Z) and the superposition of a uniform rectangular computing mesh on the transformed plane.

The X transformation is defined by:-

Term

$$X_{(x)} = \left(1 - A_1\right)\left[A_2 x e^{-(A_3 x)^2} + \left(1 - e^{-(A_5 x)^2}\right)\frac{2}{\sqrt{\pi}}\int_0^{A_4 x} e^{-t^2}\,dt\right] \quad \text{(A)}$$

$$+ \frac{2A_1}{\pi}\tan^{-1}\left[A_6\left(x + A_7\right)\right] \quad \text{(B)} \qquad (7.4)$$

where $A_1, A_2, A_3, A_4, A_5, A_6$ and A_7 are transformation parameters chosen to give the required distribution of points in the infinite plane (x, z'). The form of Equation (7.4) is such that as $x \rightarrow \pm\infty, X \rightarrow \pm 1$ and $\partial X/\partial x \neq 0$ for $|x| < \infty$.

The Z transformation is defined by:-

$$Z_{(z')} = \frac{2}{\pi}\tan^{-1}\left(\frac{z'}{0.05}\right) \qquad (7.5)$$

Equal intervals in Z give rise to intervals in z' which increase monotonically with $|z'|$. The form of Equation (7.5) is such that as $z' \rightarrow \pm\infty$, $Z \rightarrow \pm 1$ and $\partial z/\partial z' \neq 0$ for $|z'| < \infty$.

Equations (7.4) and (7.5) define the RAE computing plane with $-1 \leq X \leq 1$ and $-1 \leq Z \leq 1$, as shown on Figure 7.1.

7.2.5 RAE TSP Case

The memory requirements of the RAE TSP code exceeded the maximum memory available to a user of the TSWT computer (then a DEC PDP 11/34). Therefore to run the RAE TSP code on the TSWT computer the technique of overlaying† was used, which necessitated extensive alterations in the layout of the code.

Comparisons of RAE TSP code results obtained at RAE on a CDC 6600 computer with those obtained at Southampton were made for a single test case (RAE test case:- RAE 2822 section ; $M_\infty = 0.725$; $\alpha = 2.62^O$). The change of computer hardware resulted in discrepancies in shock position and pressures at the foot of the shock, as illustrated by the results shown on Figure 7.2. The reasons for the discrepancies are at present unknown. However, as RAE have observed similar discrepancies between results obtained on a 64 bit and a 32 bit machine, the discrepancies shown on Figure 7.2 may be the inevitable result of using a 16 bit machine (TSWT computer) as opposed to a 64 bit machine (CDC 6600 computer at RAE). Employing double precision in the TSWT computations may reduce the discrepancies, but as memory requirements and run-times would be dramatically increased this option has not been pursued.

The similarity parameter (K) defined by Equation (7.2) (see Section 7.2.2.1) depends on the magnitude of the exponent (r) of M_∞ in the denominator. Albone et al.[112] have shown that small variations of r from the chosen value of unity have an appreciable effect on the solution in the vicinity of any shocks. Attempts to match the RAE TSP code results obtained at Southampton with those obtained at RAE by small variations in the value of r have suggested that a value of 0.96 may be more suitable at Southampton than the RAE chosen value of unity, as illustrated on Figure 7.3. Hence during all subsequent TSP computations at Southampton the value of r was taken to be 0.96.

---

† The technique of overlaying involves storing only a small portion of the code in memory at any one time during execution. The rest of the code is stored on disc and execution requires a continuous exchange of information between memory and disc which considerably reduces memory requirements but increases run-time.

Despite these early difficulties it was decided that adaptation of the RAE TSP code to the needs of the TSWT should proceed. Encouragement was gained from the fact that a converged solution was obtained for the RAE test case within a computational time of one hour, which was a vast improvement on the time marching code.†

7.3 Adaptation of RAE TSP Code to TSWT Applications

7.3.1 Application

The underlying theory of the RAE TSP code assumes that the flow is isentropic and irrotational, therefore any shocks should be weak. Also, the perturbations of the flow should be small and the reference Mach number should be close to unity. However, it has been shown[112,113] that RAE TSP code solutions for several aerofoil sections ($\delta \simeq 0.12$) compare favourably with those obtained by other computational methods, even when the perturbations were far from small and the reference Mach number was as low as 0.6. TSWT application of the code would provide a less severe test, as typical wall contours would be *'represented'* in the code by aerofoils of small thickness to chord ratios ($\delta \leq 0.02$). Hence, the RAE TSP code appeared to be more than adequate for the next proposed extension of TSWT operation where mixed flows with weak shocks intrude into the imaginary flowfields. The only limitations of the code (in relation to its application to the TSWT) were that in its present form it was confined to reference Mach numbers below unity and that computing run-times were relatively long. As it was intended to apply the code independently to each imaginary flowfield computing run-times of up to two hours per streamlining iteration were anticipated. Thus, adaptation of the RAE TSP code to the needs of the TSWT initially concentrated on reducing computing run-times. The resulting code is referred to as the TSWT TSP code.

† Section 7.1.1 discusses the time marching code.

7.3.2 Computing Plane Mesh

7.3.2.1 Mesh Regions

The RAE numerical method divides the computing plane into four regions, as shown on Figure 7.1a. However, for TSWT applications the aerofoil representing the wall contour is taken to be symmetrical and at zero incidence, hence without circulation. Therefore, the computing plane of the TSWT TSP code may be reduced to three regions with $-1 \leq X \leq 1$ and $0 \leq Z \leq 1$, as shown on Figure 7.1b. The subsequent reduction of computing mesh points (from 81 x 41 to 81 x 21 for the fine mesh) removed the need for the overlaying technique as memory requirements were reduced to approximately 15K words. Implementation of the new computing plane and other minor alterations reduced TSWT TSP code computing run-times (on a DEC PDP 11/34) from 10 seconds to 4 seconds per fine mesh iteration.

7.3.2.2 Mesh Concentration

The X transformation of the RAE TSP code is defined by Equation (7.4) (see Section 7.2.4). Term (A) produces a fairly uniform distribution of mesh points over the aerofoil chord in the x, z' plane together with a moderate fall off in the density of points in the near-field beyond the leading and trailing edges and a rapid fall-off in the far-field. Term (B) produces a high density of points near the leading edge where the gradients are greatest. The transformation parameters of Equation (7.4) chosen by RAE are:-

$$A_1 = 0.225 \quad A_2 = 1.4 \quad A_3 = 1.6 \quad A_4 = 0.75$$

$$A_5 = 2.0 \quad A_6 = 30.0 \quad A_7 = 0.603$$

For TSWT applications the accuracy in the prediction of shock location is of paramount importance,[99,65] whilst for typical wall contours the leading edge gradients are relatively small. Thus, the TSWT TSP code only employs Term (A) of Equation (7.4) in order to produce a near uniform mesh concentration in the x direction over the wall contour, thereby increasing the fine mesh concentration in the vicinity of the expected shock location from 40 to 49 points per wall chord. The wall chord is taken to be the chord of the aerofoil representing the wall contour in the TSP computations.

It should be noted that the wall chord will be approximately ten times greater than the chord of the model being tested. Thus a small error in shock location relative to chord in the TSP computation may become significant when compared to the actual shock of the model. This fact coupled with the fact that a shock in the TSP computation may be smeared over two or more mesh points led to the development of a new computing mesh.[90] The new mesh produces a variable mesh concentration in the x direction over the wall contour, but with a fine mesh concentration in the region of the expected shock location of 65 points per wall chord. The X transformation parameters of the new mesh are:-

$$A_1 = 0.225 \quad A_2 = 1.69 \quad A_3 = 2.1 \quad A_4 = 0.75$$

$$A_5 = 2.5$$

A natural cubic spline† code has been developed to interpolate the TSWT TSP code results at fine mesh points to convenient reference stations along the wall contour (i.e. jack positions).

7.3.3 Boundary Conditions

The condition of zero circulation of the TSWT TSP code removes the need to satisfy the Kutta condition and reduces the far-field boundary conditions to:-

$$x = \pm\infty \qquad \phi = 0$$

$$z' = +\infty \qquad \phi = 0$$

Furthermore, the RAE procedure of adding an increment to ϕ at the end of each computational sweep in order to increase convergence (as discussed in Section 7.2.3) becomes redundant, as the new boundary conditions specify that the amount added to ϕ should be zero.

† For a natural cubic spline the end conditions are specified by zero slope, which for normal TSWT applications is a valid approximation.

7.4 Initial Validation of TSWT TSP Code

7.4.1 TSWT Test Case

Development, refinement and initial validation[115] of the TSWT TSP code used existing data from an earlier run (Run 184)[65] of the TSWT at an appropriately high reference Mach number. At Run 184 conditions (0012-64 section (h/c = 1.5) at M_∞ = 0.8862 ; $\alpha \simeq 4.0^o$) the supercritical flow regions generated by the model had reached both flexible walls, but the WAS 1 strategy had declared the walls to be *'nearly'* streamlined (E_T = 0.0126; E_B = 0.0149). This was believed to be reasonable since there was fair agreement of model pressure distribution with reference data.[99,65] However, due to the limitations of the WAS 1 strategy (as discussed in Section 6.1) exact agreement between the experimental data (Run 184) and the results obtained from the TSWT TSP code was not anticipated. In particular, the code was not expected to predict the rise in Mach number just downstream of the shock exhibited by the top wall of Run 184, as shown on Figure 7.4. The rise was probably due to choking of the flow between the thickening model wake and the wall boundary layer. Initial validation was largely confined to the top wall as this was a more critical case than the bottom wall.

7.4.2 Relaxation Parameters

The rate of convergence to an acceptable solution is accelerated by adopting the standard numerical technique of successive line over-relaxation. The value of the relaxation parameter is varied according to whether the governing equation is hyperbolic or elliptic and whether coarse or fine mesh computations are being performed. During initial validation tests the relaxation parameters suggested by RAE[112] resulted in non-convergence. This problem was rectified by adjusting the relaxation parameters until values resulting in rapid convergence were obtained. These new relaxation parameters proved to be adequate for all subsequent TSWT TSP code computations.

	Relaxation Parameters	
	RAE TSP Code	TSWT TSP Code
Elliptic points (Coarse mesh)	1.5	1.5
Elliptic points (Fine mesh)	1.5-1.7	1.3
Hyperbolic points	0.9-1.0	0.7

Converged TSP solutions for the imaginary flowfields over the wall contours of Run 184 have been obtained for reference Mach numbers up to 0.95.[115] These TSWT TSP code computations have suggested a strong Mach number/iteration relationship.

7.4.3 Convergence Parameter

TSP computations are judged to be converged when the maximum change in ϕ at a computing point between consecutive iterations is considered suitably small; the value is known as the convergence parameter. During initial validation tests it became apparent that the convergence parameter suggested by RAE[112] was unnecessarily strict for TSWT applications. Hence, during all subsequent TSWT TSP code computations the convergence parameter was taken to be the value that for the TSWT test case (Run 184) produced results that were no more than $\pm 0.1\%$ different from results produced using the convergence parameter suggested by RAE. The new convergence parameter had the effect of reducing the number of fine mesh iterations by more than two thirds, thereby significantly reducing computing run-times.

	Convergence Parameter	
	RAE TSP Code	TSWT TSP Code
Coarse mesh	0.00025	0.0005
Fine mesh	0.00005	0.0001

7.4.4 Wall Representation

Wall contours are represented in the TSWT TSP code by symmetrical aerofoils at zero incidence. However, typical wall contours exhibit positive wall displacement at jack 20, as illustrated by the top wall contour shown on Figure 7.5. Hence, there is a need for a *'closure'* scheme in order to represent the wall contour as an aerofoil.

It has been shown[115,90] that wall contours may be adequately represented in the TSWT TSP code by several different schemes. The geometries of several wall representations (Schemes 1-5) which have been investigated are illustrated on Figure 7.5. As mesh concentration in the x direction decreases with an increase in wall chord it was decided to employ Scheme 5 in all TSWT TSP code computations. The scheme produces a fine mesh concentration in the region of the expected shock location of a mesh point every 1.72cm (0.68 inches).

The similarity parameter (K) defined in Equation (7.2) (see Section 7.2.2.1) depends, to some extent, on the magnitude of the thickness to chord ratio (δ).

For TSWT applications δ is given by:-

$$\delta = \frac{2\left[|y_{max}| + |y_{min}|\right]}{\text{Wall chord}} \tag{7.6}$$

where

y_{max} = Maximum positive wall displacement†

y_{min} = Maximum negative wall displacement

Wall chord = 1.12m (44 inches)
(Scheme 5)

Although variations in the value of K have an effect on the solution (as discussed in Section 7.2.5), for TSWT applications it has been found that solutions are relatively insensitive to variations in the value of δ. Therefore, the approximation of Equation (7.6) appears to be more than adequate for TSWT applications.

7.4.5 Validation Results

The TSWT test case did not allow confident validation of the TSWT TSP code, but it did enable valuable development and refinement of the code whilst confirming its potential for TSWT applications. The final structure of the code is illustrated by the flow diagram on Figure 7.6.

As anticipated and shown on Figure 7.4 agreement of the experimental data (Run 184) with the results obtained from the TSWT TSP code can only be described as fair. Encouragement, however, was gained from the following:-

1) Solutions obtained using several wall representation schemes did not differ appreciably, especially in the vicinity of the predicted shock position.

2) Consistent prediction of shock location downstream of the experimental position reinforces the view that the flexible walls of Run 184 are not fully streamlined.

† Wall displacements are referenced to the appropriate aerodynamically straight contour.

3) Reasonable agreement with results obtained by the time marching code.†

4) The iterative nature of the streamlining process demands that the run-times of the imaginary flowfield computations should be short. Current TSWT TSP code run-times of 3-6 minutes per flowfield for the present test section and computer (DEC PDP 11/84) are more than adequate for practical development testing.

7.5 TSP Comparisons with Other Computational Methods

7.5.1 10% Circular Arc Aerofoil

A 10% circular arc aerofoil at zero incidence represents a relatively severe test case for the TSWT TSP code, as the ratio of thickness to chord is usually around 1% for TSWT applications. However, results obtained from a New York University (NYU) code†† which solves the full potential equation 114 and those obtained from the TSWT TSP code for a 10% circular arc, show good agreement. As shown on Figure 7.7 the agreement is excellent when the flow is wholly subsonic, even when the reference Mach number is as low as 0.25. At the supercritical test condition (M_∞ = 0.84) there are discrepancies in the pressures at the regions just upstream and downstream of the shock, but there is excellent agreement in shock position. The results of this comparison gave confidence in the use of the TSWT TSP code to compute the imaginary flowfields of the TSWT over a wide range of reference conditions.

7.5.2 TSWT Wall Conditions

Further verification of the TSWT TSP code has included checks on the velocity distributions predicted by the code over the outside of actual TSWT wall contours against those derived by other computational methods. The nature of the latter methods limited the checks to conditions where the imaginary flowfields were wholly subsonic. The computational methods

---

† Section 7.1.1 discusses the time marching code.

†† The NYU code was developed by Garabedian and Korn. The NYU results presented in this thesis were produced by J.B. Adcock at NASA Langley Research Center.

available to the TSWT, apart from the TSWT TSP code, may be summarised as follows:-

1) IMAG 1

Imaginary flowfield computations embodied in the WAS 1 strategy (see Section 6.1 and Appendix A for details).

2) IMAG 2

Imaginary flowfield computations according to Equation B.2 (see Section 6.2 and Appendix B for details).

3) IMAG 3

A streamline curvature code, locally written in order to provide a source of inviscid compressible flow solutions for internal and external two-dimensional flowfields. The code's predictions for external flowfields of the imaginary type had been extensively checked against well established codes, such as the NYU code and the General Electric Streamline Curvature code used at NASA Langley Research Center.[116]

4) IMAG 4

A source-sink code, where the wall contours are represented by the appropriate source-sink distributions in a uniform flowfield. The code had been verified against exact two-dimensional potential flow streamlines.[7,11,117]

The TSWT TSP code checks employing the above computational methods were extensive, however the results of only three typical conditions are presented in this thesis. The three wall contours are those around the NACA 0012-64 model tested at the following conditions:-

Condition 1† - $M_\infty = 0.6025$; $\alpha \simeq 6.0^o$

(Figure 7.8a) Wall contours predicted by the WAS 1 strategy after running with straight walls.

Condition 2 - $M_\infty = 0.6998$; $\alpha \simeq 6.0^o$

(Figure 7.8b) Walls streamlined according to the WAS 1 strategy.

Condition 3 - $M_\infty = 0.7981$; $\alpha \simeq 6.0^o$

(Figure 7.8c) Wall streamlined according to the WAS 1 strategy.

In general, there is poor agreement between IMAG 1 results and those derived by the other computational methods, as shown on Figures 7.8a-7.8c. The magnitude of the discrepancies, which increase with reference Mach number and are particularly large on the bottom wall, indicate that the imaginary flowfield computations embodied in the WAS 1 strategy are unreliable. Since the change of wall shapes and the judgement of whether they are streamlined depends on such computations, the streamlining performance of the WAS 1 strategy must be in doubt (this point is discussed in greater detail in Section 10.6.1).

However, there is good agreement between the external Mach number distributions predicted by all the other computational methods, as shown on Figures 7.8a-7.8c. As expected, there are small discrepancies in the vicinity of peak Mach number on the top wall, particularly as the peak Mach number approaches unity. At all other stations along each wall contour the agreement is excellent.

The results of this work not only gave further confidence in the predictions of the TSWT TSP code, but also led to the conclusion that external velocity distributions computed by the IMAG 2 method are also reliable.

† IMAG 4 results are only presented for Condition 1.

7.6 Concluding Remarks

Validation tests have led to the conclusion that the imaginary velocity distributions computed by the TSWT TSP code are reliable not only at conditions where mixed flow intrudes into the imaginary flowfields, but also at conditions where the reference Mach number is as low as 0.4.

The only significant disadvantage associated with the TSWT TSP code when compared with other subsonic computational methods is run-time, but current run-times (of 3-6 minutes on the TSWT computer) are more than adequate for practical testing. However, modern production wind tunnel facilities usually employ computers of greater computational power than that available to the TSWT. For example, tests have indicated that the Modcomp computers of the 0.3-m Transonic Cryogenic Tunnel[60] at NASA Langley Research Center are about five times faster than the TSWT computer. Thus run-times of approximately 1 minute are expected for the present version of the TSWT TSP code on machines of similar performance to the Modcomp computer.

8. STREAMLINING THE WALLS OF AN EMPTY TEST SECTION

8.1 Aerodynamically Straight Contours

The iterative process of contouring the flexible walls towards streamlines depends on the magnitude of the flow disturbances caused by the model within the test section, and also on computations of the imaginary flowfields extending from the flexible walls out to infinity. Both depend on the displacement of the walls from straight. Therefore a prerequisite for streamlining the walls around a model is the determination of straight contours, at first sight a contradiction in terms which requires explanation. The aim of straight wall contours is to diverge the two flexible walls from geometrically straight, in order to absorb the growth of the displacement thickness of the boundary layers on all four walls of the empty test section. The diverging contours result in a constant indicated Mach number along the centrelines of the flexible walls of the empty test section, equal to the reference Mach number. Wall contours derived in this way are described as 'aerodynamically straight'.

The aerodynamically straight contours are functions of Reynolds number and Mach number. In the TSWT the two vary together because of the atmospheric stagnation conditions. Hence, the variation of aerodynamically straight wall contours is, in principle, a continuous function of reference Mach number. However, it has been found[15,118,119] that variations of straight contours are a rather weak function of reference Mach number and it is adequate to determine only a few sets of aerodynamically straight contours and to designate each set to a band of reference Mach number. The determination of aerodynamically straight contours in wind tunnels which have the provision for variable stagnation conditions would be a more complex procedure.† When streamlining the flexible walls around a model it has

† Calibration of the recently installed flexible walled test section of the NASA Langley 0.3-m Transonic Cryogenic Tunnel[60] has suggested that it is probably adequate to assume that the variation of aerodynmically straight contours is a function of reference Mach number only, despite the variable stagnation conditions.

become practice that wall displacements be referenced to the appropriate aerodynamically straight wall contours.

8.2 A Measure of the Quality of Aerodynamically Straight Streamlining

Inevitably, following the best efforts to establish contours which give nominally constant Mach number there will exist some experimental scatter. This can arise from a variety of sources such as the variation of reference Mach number during a tunnel run, backlash in the jack mechanism, the finite minimum increment in wall position provided by the jack, and the pressure transducer and A-D convertor which are measuring the wall pressures at the jacks. The sum of the effects of these errors gives an apparent scatter in wall Mach number.

In addition, there can be systematic errors such as would arise from errors in transducer calibrations and leaks or imperfections in the mechanical construction of the wall pressure tappings. Errors in indicated wall Mach number which arise from these sources tend to be masked by the action of wall streamlining; the jacks drive the walls to an incorrect position and fully compensate for the error (within the experimental limits discussed in the previous paragraph). Evidence of the existence of errors of this kind appears in the resulting wall contours which display an unexpected waviness. As the effect is systematic and present also when a model is under test it is felt that the consequences, in terms of the aerodynamic behaviour of the model, will be small provided that the waviness of the wall contour is small in relation to the total depth of the test section.

The quality of aerodynamically straight streamlining of one flexible wall is summarised by the standard deviation of the Mach number errors measured on the centreline of the wall at the first eighteen jack positions. The standard deviations of both walls may be weighted by the reference Mach number, and the quality of streamlining of a pair of walls is then summarised by the average weighted standard deviation (σ_{av}) given by:-

$$\sigma_{av} = \frac{\sigma_T + \sigma_B}{2 M_\infty}$$

where σ_T, σ_B are respectively the top and bottom wall standard deviations in measured Mach number from the reference value (M_∞).

8.3 Experimental Procedure

As a starting point the top and bottom flexible walls were manually adjusted to geometrically straight contours, parallel to each other and to the test section backbones. When run in this condition the Mach number distribution along the centrelines of the flexible walls are, of course, non-uniform. The magnitude of the effect is illustrated by the following example. At a reference Mach number of 0.63 the measured Mach number on the wall centreline at the downstream end of the test section rose to just over 0.7.

Aerodynamically straight contours were derived by adjusting the flexible walls according to an old strategy[7] (now referred to as the Imbalance strategy). This strategy uses the simple rule that in subsonic flow the Mach number at a point on the wall will be reduced by moving the wall locally away from the test section centreline, and vice-versa. The movement of a jack is made proportional to the difference between the local (wall centreline) and the reference Mach number. Wall adjustments were continued until the standard deviation values of the two walls were small and approximately equal. Employment of this strategy on geometrically straight walls resulted in satisfactory contours being achieved after not more than 10 aerodynamically straight streamlining iterations.† Once the first set of constant Mach number contours was found the number of iterations required to produce the next set at another reference Mach number was significantly reduced if the streamlining cycle was initiated from the previous aerodynamically straight contours (as opposed to the geometrically straight contours). The relationship between the wall increment (δy) and the desired change of local wall Mach number (δM) which was used varied from:-

† One aerodynamically straight streamlining iteration comprises of measuring the local Mach numbers at all jack positons on both walls, then moving all jacks in response to the local errors.

$\delta y/\delta M$ = 2.0 - 0.25cm (0.8 - 0.1 inches)

The value was reduced with Mach number error in an attempt to reduce the number of streamlining iterations required to produce satisfactory contours. However, if one value of $\delta y/\delta M$ is used then 1.0cm (0.4 inches) is recommended for the TSWT.

8.4 Aerodynamically Straight Results

The scope and quality of aerodynamically straight contours obtained using the original and the recently installed new flexible walls is summarised in Table 3, whilst the Mach number distributions along the centrelines of the flexible walls for each of the contours is shown on Figures 8.1 and 8.2. Wall displacements relative to geometrically straight of a typical aerodynamically straight contour (Contour D) are illustrated on Figure 8.3.

The highest reference Mach number at which aerodynamically straight contours were determined was 0.95, using the original flexible walls. The sensitivity of Mach number to flow area, coupled with the consequences of the poor condition of the original walls and the inherent weaknesses of the jack/wall flexure design (as discussed in Section 5.6.2), prevented streamlining at higher reference Mach numbers. A temporary reduction in the pressure of the dried air supply (from 300 to 150 p.s.i.) limited the determination of aerodynamically straight contours with the new walls to a reference Mach number of 0.8.

Inspection of the results presented in Table 3 reveals that the quality of aerodynamically straight contours obtained in the TSWT was significantly improved by the installation of the new flexible walls. It is possible that the new walls with their improved jack/wall link mechanism (see Section 5.6.2 for details) may allow satisfactory aerodynamically straight contours to be derived at speeds higher than Mach 0.95. However, as the variations of the contours are a rather weak function of Mach number (the function becoming increasingly weaker as Mach 1.0 is approached), it is anticipated that the new flexible walls will allow the determination of aerodynamically straight contours adequate for model tests up to a reference Mach number of unity. Tests aimed at defining such contours will commence once the pressure of the

dried air supply has been returned to its original level (300 p.s.i.). Furthermore, the jack/wall link mechanism now in use should significantly increase the operational life of the flexible walls in terms of the rate of deterioration of the standard deviation in wall Mach number.

The consequence of using one of the contours at a reference Mach number outside its designated band of validity is not serious, since the contours are such a weak function of reference Mach number. For example, Contour A (derived for Mach 0.3) when run at Mach 0.7 showed an average weighted standard deviation value of 0.0048, which compares quite well with the value of 0.0037 obtained with Contour E (derived for Mach 0.7).

As already stated, the wall divergence exhibited by aerodynamically straight contours absorbs the growth of displacement thickness of the boundary layer on all four walls of the empty test section. This is demonstrated on Figure 8.4, where discrepancies between total wall movement from geometrically straight and predicted values are small; the predicted values being four times the calculated growth of the boundary layer displacement thickness for one wall. The non-linear movement of the walls, as shown on Figures 8.3 and 8.4, can probably be attributed to wall imperfections (as discussed in Section 8.2).

The boundary layer displacement thickness was computed by the following two methods.

1) A numerical solution of the Von Karman momentum integral equation for a turbulent boundary layer (TSWT BL code).[7]

2) The RAE lag-entrainment method for the prediction of turbulent boundary layers in compressible flow (RAE BL code).†

As expected, similar boundary layer displacement thickness distributions were computed by either method for this simple case.

† See Section 9.4 for further details on the RAE lag-entrainment method.

8.5 Some Cautionary Notes

8.5.1 Off-Centre Performance of Aerodynamically Straight Contours

The original and new flexible walls both exhibit higher standard deviations in wall Mach number along off-centre pressure tappings rows than along the centreline (see Table 4).† The most likely reason is waviness in the flexible walls and, therefore, a monitoring device (designed to be bolted onto the side of the test section in place of the usual sidewall) to show defects in wall shape is presently being manufactured. When completed, investigations will commence aimed at identifying the reasons for the large variations in wall Mach number across the width of the test section.

8.5.2 Aerodynamically Straight Contours with Centreline Curvature

It is possible to derive aerodynamically straight contours that fulfil the standard deviation criteria but do not diverge symmetrically from geometrically straight. Figure 8.3 shows a wall contour derived by Neal†† that produces Mach number standard deviation values for the top and bottom walls of 0.0016 and 0.0012 respectively at a reference Mach number of 0.6, despite top wall displacements between jacks 2 and 9 being negative (that is, towards the tunnel centreline) with respect to geometrically straight. Although this contour does absorb the test section boundary layer displacement thickness, it should not be used as aerodynamically straight since the test section centreline is curved. The data on Figure 8.3 suggests a curvature of about 2.54mm (0.1 inches) over a 50.80cm (20 inches) length of test section. Approximating this to an arc it is easy to show that the curvature of the test section centreline will induce a camber angle of just over 0.1^{o} over the chord of a typical aerofoil model. Therefore, when determining aerodynamically straight contours it is recommended that wall displacements be carefully monitored to minimise this effect, otherwise there could be questions on the validity of later claims for the quality of

---

† It should be noted that the positions of the off-centre pressure tapping rows of the original and new flexible walls are different - see Section 5.6.2 for relative positions of pressure tapping rows.

†† Neal - Research Assistant, Department of Aeronautics and Astronautics, University of Southampton, England. (NASA Grant NSG 7172).

streamlining around a model because of uncertainty in the effects of induced camber and on angle of incidence. Such monitoring also serves to identify other faults such as leaking pressure tubes etc. (as discussed in Section 8.2).

9. PREDICTION OF BOUNDARY LAYER GROWTH ALONG THE FLEXIBLE WALLS

9.1 Effective Aerodynamic Wall Contour

The top and bottom wall contours felt by the flow around a two-dimensional model are the physical wall contours modified by the displacement thickness of the wall boundary layers (δ^*). By setting the flexible walls to aerodynamically straight contours an allowance is automatically made for the development of δ^* through the empty test section. It has become practice, therefore, that the geometrical wall contour is given by wall displacements referenced to the appropriate aerodynamically straight contour (as discussed in Section 8.1). However, in the presence of a model the flexible walls and sidewalls are subject to very different pressure fields, and consequently, there are pressure-induced changes in δ^* ($\Delta\delta^*$) on all four walls of the test section. The sidewalls experience the strongest pressure gradients and, therefore, the largest local changes in boundary layer thickness and perhaps even separations. In the TSWT, however, no attempt is made to eliminate or reduce any interference effects due to the changes in δ^* on the sidewalls.† Thus, in the general case with a contoured wall and a model present, the $\Delta\delta^*$ distributions of only the top and bottom walls are used as corrections to the geometrical wall contour, giving an effective aerodynamic wall contour. This contour forms the boundary of the imaginary flowfields and is the contour which must ultimately become a streamline.

Past experience has shown that for the sizes of models normally used in this tunnel and for reference speeds below about Mach 0.85 the changes in δ^* due to the pressure field of the model are small and that an allowance for the changes need not be made. Thus, in routine two-dimensional testing [14,16,17,90] the effective aerodynamic contour may be taken as the physical wall contour referenced to the appropriate aerodynamically straight contour. Previous investigations[99,65], however, have indicated that at conditions which result in a shock extending to a flexible wall, it is probably necessary to

† The probable consequences of ignoring the sidewall boundary layer effects are discussed in Section 11.4.2.1.

account for the growth in δ^* associated with the shock-boundary layer interaction.

9.2 Shock-Boundary Layer Interaction

The fluid in the inner part of the boundary layer, adjacent to the wall, has subsonic velocity and is unable to undergo the discontinuous change in pressure associated with a shock. Hence, when a shock impinges on a wall the boundary layer adjusts itself so that the pressure rise at the wall is continuous. One feature of the adjustment is the thickening of the boundary layer just downstream of the shock-wall impingement position. The shock-boundary layer interaction is usually a localised phenomenon, depending only on the properties of the initial boundary layer and of the local flowfield. If the overall pressure rise associated with the shock system is not too large (as is the case with systems experienced so far at the flexible walls of the TSWT[99,65]) the wall boundary layer is able to negotiate the interaction without separating. The streamwise extent of the interaction region is then typically two or three times the thickness of the undisturbed boundary layer.[120] Consequently, for small overall pressure rises, the shock pattern outside the boundary layer differs only very slightly from that which would occur in an inviscid flowfield. Thus, it was anticipated that shock-boundary layer interaction would pose no major practical problems when streamlining the flexible walls. However, under such conditions it was envisaged that it would probably be necessary for the effective aerodynamic contour to account for the changes in δ^* induced by the large pressure gradients associated with the shock-boundary layer interaction.

9.3 Past Investigations

Past investigations[99,65] have indicated that when a model shock impinges on a flexible wall it is probably necessary to account for the thickening of the wall boundary layer associated with the shock-boundary layer interaction. Run 184 data formed the basis of these investigations. At Run 184 conditions (0012-64 section ($h/c = 1.5$) at $M_\infty = 0.8862$; $\alpha \simeq 4.0^o$) the WAS 1 strategy (which assumes that the changes in δ^* are negligible) had declared the flexible walls to be *'nearly'* streamlined ($E_T = 0.0126$;

E_B = 0.0149), despite the existence of supercritical flow at both flexible walls. This was believed to be reasonable since there was fair agreement of model pressure distribution with the reference data.† The agreement was improved when a localised hollow was introduced into the top wall contour (Run 223). The hollow (wall movement away from the tunnel centreline) was intended to accommodate the wall boundary layer growth due to the shock-boundary layer interaction. However, the streamwise position and shape of the hollow did not correspond to the $\Delta\delta^*$ distribution†† predicted by the existing boundary layer method (TSWT BL code)[7], as illustrated on Figure 9.1. In fact the TSWT BL code, which solves the Von Karman momentum integral equation for a turbulent boundary, predicted negative $\Delta\delta^*$ values at the streamwise position of the hollow. Such values suggest that a bump (wall movement towards the tunnel centreline) should have been introduced into the top wall contour at this position. It was, therefore, also concluded that the TSWT BL code was probably inadequate for the prediction of wall boundary layer development at conditions which result in a shock impinging on a flexible wall. Thus, a prerequisite of wall streamlining at such conditions was to find a boundary layer method capable of coping with shock-boundary layer interactions.

9.4 Lag-Entrainment Method

The lag-entrainment method is an integral procedure, developed by RAE Farnborough in 1973, for the prediction of turbulent boundary layers and wakes in two-dimensional and axisymmetric, compressible adiabatic flows. It is believed[121] to be a significant improvement upon, and was developed as a replacement for, the version[122] of Head's entrainment method[123] which had been in use at RAE since 1967. The method takes account of longitudinal surface curvature and of the influence of the upstream flow history on the turbulent stresses. The computational procedure involves the integration of the momentum equation, the entrainment equation and an equation for the

† See Section 11.4.1 for details of the reference data.

†† The $\Delta\delta^*$ values correspond to the changes in wall boundary layer thickness induced by the pressure field due to the contoured wall and the presence of the model.

streamwise rate of change of entrainment coefficient. As the equations are predominantly algebraic, computation is very rapid.

It was anticipated that the prediction of boundary layer development along the flexible walls of the TSWT would be within the capabilities of the lag-entrainment method, even at conditions resulting in relatively strong shock-boundary layer interactions. Thus, it was envisaged that the lag-entrainment method would be more appropriate to the needs of high speed testing in the TSWT, than the existing boundary layer method (TSWT BL code).[7] Hence a code provided by RAE, which embodied the lag-entrainment method, was installed into the TSWT computer and successfully validated against test cases supplied by RAE. The code has been tailored to the needs of the TSWT and analysis of both flexible walls by the present version (RAE BL code) takes approximately 15 seconds on the TSWT computer (DEC PDP 11/84).

9.5 Typical Wall Boundary Layer Predictions

When the pressure gradients at the flexible walls are not excessive the $\Delta\delta^*$ distributions calculated by the existing boundary layer method (TSWT BL code) and lag-entrainment method (RAE BL code) are in reasonable agreement, as illustrated by the Run 235 data presented on Figure 9.2. At Run 235 conditions ($M_\infty = 0.8$; $\alpha \simeq 4.0^o$) the peak Mach number measured on the top and bottom flexible walls was 0.93 and 0.83 respectively, and the WAS 2A strategy had declared the walls to be streamlined (i.e. $E < 0.01$ on both walls). The calculated $\Delta\delta^*$ distributions for the bottom wall are in excellent agreement, whilst the top wall distributions exhibit small discrepancies downstream of the peak wall Mach number. However, when the streamlining strategy (WAS 2A) employed an effective aerodynamic contour which made use of the $\Delta\delta^*$ distributions (calculated by the RAE BL code) the effect on model performance at Run 235 conditions was negligible, as demonstrated by the excellent agreement of the model pressure distributions presented on Figure 9.3. This reinforces the long held view that in routine two-dimensional tests the effective aerodynamic contour may be taken as the physical wall shape referenced to the appropriate aerodynamically straight contour. Routine two-dimensional tests are defined as model tests at any set of

conditions up to those which result in the flow at both flexible walls just remaining subsonic.

9.6 Run 184 Wall Boundary Layer Predictions

The top wall $\Delta\delta^*$ distributions (due to the pressure field of the model) predicted by the existing boundary layer method (TSWT BL code) and the lag-entrainment method (RAE BL code) at Run 184 conditions ($M_\infty = 0.8862$; $\alpha \simeq 4.0^o$) are shown on Figure 9.1. For stations upstream of the shock-boundary layer interaction (which occurs near the position of maximum $\Delta\delta^*$) the distributions predicted by both codes are in good agreement. However, downstream and in the vicinity of the interaction significant discrepancies become apparent because, as expected, the RAE BL code predicted a greater recovery of the boundary layer thickness than the TSWT BL code. For example, the TSWT BL code predicted a δ^* increase of about 20% across the shock impinging on the top wall. The value predicted by the RAE BL code was in the region of 50%, whilst an approximate method proposed by Reshotko and Tucker[124] predicted a value of about 40%. The above-mentioned trends are also followed on the bottom wall at Run 184 conditions, as shown on Figure 9.4.

As already stated, the agreement of model pressure distribution with the reference data at Run 184 conditions was improved when a crude provision was made for the δ^* growth due to the shock-boundary layer interaction.[99,65] The crude provision consisted of introducing a localised hollow in the top wall contour (Run 223). However, it has been shown that the use of the hollow was not supported by the top wall $\Delta\delta^*$ distribution predicted by the TSWT BL code. This also applies to the $\Delta\delta^*$ distribution predicted by the RAE BL code, as illustrated on Figure 9.1. At the streamwise position of the hollow the RAE BL code predicted approximately zero change in δ^*, which suggests no need for any additional wall movement at this locatioin. Thus, on the basis of past investigations it may be supposed that the RAE BL code, as well as the TSWT BL code, is inadequate for calculating the δ^* growth due to shock-boundary layer interaction. However, it is the opinion of the author that the experimentally devised hollow not only accommodated the changes in δ^* due to the pressure field of the model, but also accounted for the limitations of the WAS 1 strategy (as discussed in Section 6.1). The fact that the reference

data may be unreliable at Run 184 conditions (as discussed later in Section 11.4) further complicates the situation. Thus it is possible, as originally anticipated, that the prediction of boundary layer development along the flexible walls of the TSWT over a wide range of conditions is within the capabilities of the RAE BL code. Further investigations (which do not form part of this thesis) are required to verify the code at conditions which result in shock-boundary layer interactions.

When the effective aerodynamic contour is adjusted to account for the predicted $\Delta\delta^*$ distributions at Run 184 conditions, the computed imaginary wall Mach numbers in the region just upstream of the shock-boundary layer interaction are raised, as illustrated on Figure 9.5. The imaginary Mach number distributions suggest that the thinning of δ^* due to the general pressure field prior to the shock-boundary layer interaction may well be more significant than any thickening of δ^* downstream of the interaction. Despite the discrepancies between the $\Delta\delta^*$ distributions predicted by the TSWT and RAE BL codes there is reasonable agreement between the corresponding imaginary wall Mach number distributions. This leads to the tentative conclusion that in the imaginary flowfield computations account must be taken of the effects of wall pressure gradients on δ^* when they are large, but the differences of opinion on the detailed variation of δ^* are relatively less important.

9.7 Concluding Remarks

The magnitude of δ^* growth due to shock-boundary layer interaction predicted by the RAE BL code was less than anticipated. The code, however, was considered to be a significant improvement upon the existing boundary layer method[7]. Therefore, in all subsequent tests where the effective aerodynamic contour attempted to account for the model-induced changes in δ^* the RAE BL code was employed.

10. EVALUATION OF WALL ADJUSTMENT STRATEGIES

10.1 Scope of Investigation

The evaluation of the wall adjustment strategies involved testing the model through a range of reference Mach numbers from 0.4 to 0.8 at four angles of incidence (nominally 0.5^{o}, 2.0^{o}, 4.0^{o} and 6.0^{o}). The investigation utilised the new flexible walls and generated a body of TSWT data comprising about one hundred and twenty streamlining cycles, which corresponds to nearly five hundred tunnel runs. The model chord Reynolds number of the tests, which varied with tunnel reference speed, was about 1.23 million at Mach 0.7. The test procedure involved, whenever possible, streamlining the walls according to all the wall adjustment strategies under evaluation (as detailed in Section 6.4) at each test condition. The *'streamlined'* data, except that obtained when employing the NPL strategy, is summarised in Tables 5.1-5.5. However, post-test analysis of the data has concentrated on determining the relative performances of the WAS 1, WAS 2 and NPL strategies.

One step in the NPL strategy is the determination of constant pressure wall contours (as discussed in Section 6.3). The maximum available jack movement of 2.54 cm (1 inch) limited the test range at which constant pressure contours could be obtained in the TSWT. However, the extent of the achieved test range (shown indirectly in Table 8) was considered great enough to provide an interesting and valid evaluation of the NPL strategy.

The severity of wall interference is a function of, amongst other things, the proximity of the walls to the model which can be expressed, for convenience, as a ratio of test section height to model chord. The ratio in the 20 x 8 NPL Tunnel was typically around 3.5, whereas in the TSWT it was 1.5, rendering the present investigation a more severe test of the effectiveness of the NPL strategy than the environment for which it was developed.

10.2 Test Programme

The test programme was designed to reduce uncertainties that might exist (due to different starting points of the streamlining process and variations in model incidence) when making comparisons between the several wall adjustment strategies, as opposed to minimising tunnel run-time. Thus, whenever possible, the streamlining cycle of each test condition was initiated from aerodynamically straight contours. When the test reference Mach number was greater than the aerodynamically straight choking value, the streamlined wall contours of the previous streamling cycle were used as the starting contours of the next cycle. Also, the model remained locked at one specific angle of incidence while the walls were streamlined through the Mach number band according to the various wall adjustment strategies under evaluation.

10.3 Effects of Moving from Straight† to Streamlined Walls

It is only possible to run with the walls set straight at subsonic and low transonic speeds when the model is present. At high transonic speeds ($M_\infty \geq 0.7$) the model chokes the straight walled test section preventing any changes in Mach number upstream of the model. Nevertheless, fourteen runs have been made with the walls set to aerodynamically straight contours, the *'straight wall'* data is summarised in Table 6.

The strong interference induced by straight walls can be inferred from the residual interferences presented in Table 6, but is also well illustrated in Table 7; a set of lift curve slopes for reference Mach numbers of 0.4, 0.5 and 0.6. Straight wall lift curve slopes are seen to be much greater than the corresponding streamlined slopes, the latter group being in rough agreement with each other. There is further information on straight wall interference in Table 8, which contains wall loadings (measured in terms of E) associated with straight walls and with walls streamlined according to the NPL strategies. The values of E are seen to be much reduced by both of the NPL strategies,

† The word *'straight'* refers to aerodynamically straight (not geometrically straight).

but neither strategy is consistently as good as the WAS 1 and WAS 2 strategies, which generally bring E below 0.01 on both walls.

The strength of interference which is possible with straight walls is best illustrated by the test condition of $M_\infty = 0.7$; $\alpha \simeq 4.0^\circ$. The effects on model pressure distribution of streamlining the walls according to the NPL strategies are shown on Figure 10.1. When the walls are set straight at this condition ($M_\infty = 0.7$; $\alpha \simeq 4.0^\circ$) there is a strong shock on the model's upper surface at about 55% chord. After streamlining alone (with no other change) the recompression shock is positioned at about 25% chord. This is associated with a reduction in the value of boundary layer pressure (form) drag coefficient which is another typical effect of streamlining at high Mach numbers. These effects of streamlining (by now very familiar to those working with transonic flexible walled test sections) are also illustrated in the corresponding schlieren pictures on Figure 10.2, where in the lower picture the walls have been streamlined according to the WAS 1 strategy but with essentially the same effect on the model behaviour as the NPL strategies (as confirmed on Figure 10.3).

The Mach number distributions along the centrelines of the flexible walls for aerodynamically straight and streamlined wall cases are shown on Figure 10.4. The strong interference induced by straight walls modifies the wall Mach number distribution around the model and can cause the model's shocks to be misplaced and modified in strength (as already has been shown), or can cause shocks to occur where they should not. In some severe cases this can lead to complete choking of the straight walled test section, although in the case presented on Figure 10.4 ($M_\infty = 0.7; \alpha \simeq 4.0^\circ$) such conditions were not quite reached. In this example, however, the channel over the upper surface of the model was choked with straight walls, as the shock on the upper surface of the model had reached the top wall giving a peak wall Mach number of approximately 1.05. Streamlining the walls (according to several strategies) reduced the peak Mach number on the top wall to around 0.8 for this test condition.

Another effect of wall streamlining is evident in the wall Mach numbers existing in the region downstream of the model. As has been seen from the earliest days, during the streamlining process the walls automatically

adapt to the blockage caused by the model's wake. In the case of straight walls the wall Mach number downstream of the model asymptotes to a value well above the reference value, as shown on Figure 10.4. This phenomenon was one which in 1937 led NPL to the use of liners[18] and then adaptive flexible walls in transonic two-dimensional testing.[4,20,5,21,22] When the walls are streamlined the wall Mach number downstream of the model is seen to return essentially to the reference value, as must be the case in simulating free flowfield conditions.

10.4 Streamlined Wall Contours

The effects of compressibility and model lift on streamlined wall contours (adopted by all the wall adjustment strategies) were to demand increased wall movement apart in the region of the model. When the model was generating lift the wall adjacent to the pressure surface (bottom wall) moved towards the model and an imprint of the model appeared in the wall shape, whilst the other wall (top wall) moved away from the model. Typical streamlined wall contours are shown on Figure 10.5 ($M_\infty = 0.7$; $\alpha \simeq 4.0^o$); wall displacements away from the test section centreline (with respect to aerodynamically straight) are considered positive. The complex curvature of the bottom wall demonstrates the need for close jack spacing in the vicinity of the model to maintain adequate wall setting accuracy along the entire length of the wall. Also noticeable on Figure 10.5 is the movement apart of the walls downstream of model to eliminate wake blockage (contours derived by the NPL strategy only partially alleviate wake blockage, but this point is discussed later), the effect being illustrated more clearly on Figure 10.6. It should be re-emphasised that the walls take up these streamlined contours quite automatically in response to measurements made only at the flexible walls.

Despite the fact that the flexible walls are relatively long, extending to about five chords upstream and downstream of the model, in some test cases the streamlined wall contours have noticeable slopes at the ends of the test section. This is an indication of the circulation-induced disturbance which led to the requirement of mounting the model symmetrically in the streamlined portion of the test section (as discussed in Section 5.2.1 and Reference 7).

In general, the streamlined wall contours adopted by the WAS 2 strategy exhibit wall displacements of greater magnitude than those adopted by the WAS 1 strategy, a good example ($M_\infty = 0.7$; $\alpha \simeq 4.0^o$) is that shown on Figure 10.5. The disparities between the contours may give the impression that the different walls must give different flow characteristics at the model. However, from the earliest days[50] it has been evident that it is possible for a wall to attach itself to, and then follow, any unloaded streamlining passing over or under the model and not disturb the model. Thus different wall contours can represent different but equally valid streamlines for a given test condition. The flexible walls are anchored at a fixed point upstream of the model, which suggests that a wall can only take one shape to be streamlined as only one streamline passes through the anchor point. In practice, however, when streamlined the wall follows the shape of a streamline that has been *'picked-up'* by the wall not at the fixed anchor point but rather at the first jack position, which is moveable. The shape of the streamline which is picked-up depends on the displacement of the first jack and therefore wall contours of different shape, within limits, may be termed streamlined for a given test condition. Analysis of model performance (see Section 10.5) demonstrates that such contours result in the same flow conditions around the model, despite the variations in wall loading just downstream of the anchor point between one streamlined wall contour and another. A typical example is the test condition of $M_\infty = 0.7$; $\alpha \simeq 4.0^o$ where model pressure distributions obtained with the walls set to streamlined contours of different shape are in fair agreement, as demonstrated by Figures 10.3 and 10.5.

When streamlined wall contours derived by the WAS 1 and WAS 2 strategies are analysed in terms of total wall movement (that is wall movement apart), then good agreement between the two strategies is found. A typical example ($M_\infty = 0.7$; $\alpha \simeq 4.0^o$) is shown on Figure 10.6, where both strategies move the walls outward downstream of the model by roughly the same amount, but generally to a greater extent than by the NPL strategies. It may, therefore, be concluded that the NPL strategies do not fully account for the model wake (Section 10.7.4 discusses this point in greater detail). Further inspection of Figure 10.6 reveals that the NPL strategies select contours which exhibit less total wall movement than the WAS 1 and WAS 2 strategies. The NPL strategy employing a setting factor of six-tenths (NPL 2 WAS)

appears, on the evidence of wall contours, to be more appropriate than the strategy employing a half-way setting factor (NPL 1 WAS).

10.5 Model Data with Streamlined Walls

Model pressure distributions were measured and recorded at every stage of the test programme, but only a few selected cases are reproduced in this thesis.† Force and moment coefficients were derived from the pressure distributions, hence the values of drag coefficient presented in Tables 5.1-5.5 only refer to boundary layer pressure (form) drag. Generally, form drag is only a small component of the total drag and quantitative comparisons of this component of drag are probably meaningless; therefore analysis of model performance has largely concentrated on pressure distributions and lift coefficients. The relevant streamlined model force data is summarised on Figures 10.7.1 and 10.7.2, which show the variation of normal force coefficient with reference Mach number for all the data sets ($\alpha \simeq 0.5^{o}$, 2.0^{o}, 4.0^{o} and 6.0^{o}). The lift curve slopes for reference Mach numbers of 0.4, 0.5 and 0.6, determined by the fitting of least square straight lines to the lift-incidence data, are summarised in Table 7.

In general, model data obtained when the walls were streamlined by the WAS 1 and WAS 2 strategies show excellent agreement (as shown on Figure 10.7.1), whilst the corresponding lift curve slopes agree to within 1% of each other. At the severe condition of $M_{\infty} = 0.8$; $\alpha \simeq 6.0^{o}$ the model's upper surface shock positions given by the WAS 1 and WAS 2 strategies agree to within 1.0% of chord, as illustrated by the pressure distributions shown on Figure 10.8. With pressure orifices positioned only at each 5% chord it is difficult to be more precise.

However, at some test conditions ($M_{\infty} = 0.8$; $\alpha \simeq 6.0^{o}$ and $M_{\infty} = 0.8$; $\alpha \simeq 4.0^{o}$) the WAS 1 strategy derived streamlined contours that resulted in slightly greater model lift than that obtained when utilising the other

† Reference 91 contains a detailed presentation of model data obtained when the flexible walls were streamlined according to the WAS 1, WAS 1A and NPL strategies.

strategies,† as illustrated by the corresponding C_N values shown on Figures 10.7.1 and 10.7.2. The increased lift may have been caused by the flow over the majority of the model's lower surface having slightly less velocity when the walls were streamlined by the WAS 1 strategy as opposed to the other strategies, as is evident by the model pressure distributions shown on Figure 10.8. In an attempt to explain these differences at this test condition ($M_\infty = 0.8$; $\alpha \simeq 6.0^o$), the imaginary velocities over the outside of the bottom wall were calculated by several computational methods and the results are shown on Figure 7.8c. Inspection of these imaginary velocities reveals that the reduced flow velocity over the lower surface of the model was probably due to erroneous imaginary flowfield computations embodied in the WAS 1 strategy, as first suggested during subsonic verification of the TSWT TSP code (see Section 7.5.2). Hence, for some test conditions, model data indicates that wall contours derived by the WAS 1 strategy may not be properly streamlined. This point is discussed further in Section 10.6.1.

Model data obtained when the walls were streamlined according to the NPL strategy generally compares very well with that obtained when employing the WAS 1 and WAS 2 strategies, especially for reference speeds up to Mach 0.7. For example, at the relatively severe test condition of $M_\infty = 0.7$; $\alpha \simeq 4.0^o$ there is reasonable agreement between the strategies in terms of the position of the model's upper surface shock, as illustrated by the pressure distributions shown on Figure 10.3. However, in general, comparison of model pressure distributions[91] reveals that the velocity of the flow around the model was slightly greater when the walls were streamlined according to the NPL strategy as opposed to the WAS 1 and WAS 2 strategies (this is just evident on Figure 10.3). As this was true to about the same extent (in terms of C_p) for the upper and lower surfaces of the model, the derived force coefficients and hence lift curve slopes show good agreement (see Figures 10.7.1 and 10.7.2 and Table 7 for the evidence). Hence, on the evidence of model data, wall streamlining according to the NPL strategy appears to result in near interference-free test conditions for speeds up to about Mach 0.7 for the present model in the particular test section configuration of the TSWT.

---

† The NPL strategy could not be used at such conditions. The WAS 1A, WAS 1B and WAS 2A strategies are defined in Section 6.4.

Breakdown of the NPL strategy is evident at some test conditions ($M_\infty = 0.8$; $\alpha \simeq 0.5^o$ and $M_\infty = 0.8$; $\alpha \simeq 2.0^o$), and is apparent in the model pressure distributions shown on Figure 10.9. In this case ($M_\infty = 0.8$; $\alpha \simeq 0.5^o$) the model shocks are stronger and misplaced with the NPL strategy, compared to those obtained when streamlining according to the WAS 1 and WAS 2 strategies. When the NPL strategy used a half-way setting factor (NPL 1 WAS) the test section was fully choked, as illustrated by the wall Mach number distributions shown on Figure 10.10. Also evident on Figure 10.10 is the inability of the NPL strategy to account properly for wake blockage; the whole region downstream of the model is at a Mach number appreciably above the reference value (this point is discussed further in Section 10.7.4). The effects of the breakdown of the NPL strategy (NPL 2 WAS) at $M_\infty = 0.8$; $\alpha \simeq 0.5^o$ are clearly demonstrated by the schlieren pictures shown on Figure 10.11. A consequence of the breakdown is reduced model lift, as illustrated by the relatively low C_N values obtained when using the NPL strategy at $M_\infty = 0.8$; $\alpha \simeq 0.5^o$ and $M_\infty = 0.8$; $\alpha \simeq 2.0^o$, as shown on Figure 10.7.1.

In tests in the 20 x 8 NPL Tunnel which used a model with an EC 1250 section of 12.7cm (5 inches) chord, breakdown of the NPL strategy (NPL 1 WAS) had not yet become evident at the test conditions of $M_\infty = 0.886$; $\alpha \simeq 0.0^o$ and $M_\infty = 0.827$; $\alpha \simeq 4.0^o$. That is to say at such conditions the model shocks had not reached the contoured walls. The relatively early breakdown of the strategy in the TSWT is evidence that the present evaluation is a more severe test of the effectiveness of the NPL strategy than the original NPL investigations. The limited scope of the TSWT investigation does not allow the boundary of the test regime within which the NPL strategy performs satisfactorily to be accurately defined.

10.6 Operational Experience

10.6.1 Streamlining Quality of WAS 1 Contours

A key component of the self-streamlining concept is the accurate prediction of the external velocity distributions, since the choice of wall shapes and the judgement of whether they are streamlined depend on the computed distributions. However, subsonic verification of the TSWT TSP code and some model data (see Sections 7.5.2 and 10.5 respectively) has indicated

that the velocity distributions given by the imaginary flowfield computations embodied in the WAS 1 strategy† may sometimes be unreliable. Therefore, the streamlining quality of wall contours adopted by the WAS 1 strategy was assessed. Wall streamlining quality is determined from wall loadings arising from differences between the test section and imaginary flowfields, and the parameter E has been introduced as a global measure of wall loading. Thus, wall loading values were calculated for each wall contour streamlined by the WAS 1 strategy, with the IMAG 2†† and TSWT TSP codes being used to verify the computations of the imaginary flowfields. The results of the assessment are presented in Table 9.

As expected the wall loadings calculated when employing the IMAG 2 and TSWT TSP codes are in good agreement with each other. Both codes predict that WAS 1 wall conditions satisfy the conventional wall streamlining criteria ($E > 0.01$ on both walls) only at the test conditions of $\alpha \simeq 0.5^{o}$ and 2.0^{o}. At $\alpha \simeq 4.0^{o}$ the WAS 1 contours exhibit a bottom wall loading of greater magnitude than 0.01, whilst at $\alpha \simeq 6.0^{o}$ both walls of the WAS 1 contours fail to satisfy the condition of $E > 0.01$. These results reinforce the opinion that the external velocity distributions computed by the WAS 1 strategy are unreliable. The lift generated by the model appears to be a factor limiting the test regime where the WAS 1 strategy may be considered adequate. Since the strategy controls the flexible walls of the 0.3-m Transonic Cryogenic Tunnel[60,61] at NASA Langley Research Center a more detailed investigation is highly recommended.

10.6.2 Convergence of the WAS 2 Strategy

The original form of the WAS 2 strategy resulted in the predictions of wall movement being somewhat exaggerated. Wall convergence was improved by scaling down the predicted wall movements by the empirically determined factor of approximately 0.7.

---

† These computations are denoted by IMAG 1.

†† The IMAG 2 code solves Equation B.2 of Appendix B and is used by the WAS 2 and WAS 1B strategies.

It was anticipated that the WAS 2 strategy would offer the possibility of wall streamlining within fewer iterations than necessary when utilising the WAS 1 strategy (as discussed in Section 6.2). In practice, however, the wall streamlining convergence rates of both strategies were approximately equal, as shown by the data presented in Table 10.

The uniqueness of model performance when employing the WAS 2 strategy has been demonstrated at reference Mach numbers up to 0.7. A good example is the test condition of $M_\infty = 0.7$; $\alpha \simeq 6.0^o$ where two values of C_L were obtained when the walls were streamlined from different start contours. One streamlining cycle (Run 285) was initiated from aerodynamically straight and required five iterations, whilst the other cycle (Run 280) was initiated from streamlined wall contours for $M_\infty = 0.6$; $\alpha \simeq 6.0^o$ and required only two iterations. For Run 285 C_L equals 0.6423 and for Run 280 C_L equals 0.6404, a difference of only 0.0019 or 0.3%, despite the use of different streamlining paths. The final streamlined wall contours of the two paths were almost identical, although this was not always the case.† The fact that Run 285 and 280 comprised of five and two iterations respectively is evidence that the severity of wall interference at the beginning of the streamlining cycle strongly influences the number of iterations in the cycle. This means that the test programme must be carefully designed if the number of iterations is to be minimised, as discussed in Section 4.2.1. The data also goes some way towards answering the question, sometimes raised, of whether an adaptive wall tunnel could in some way impose its own *'solution'* which was not a free-flowfield solution. The self-consistency of TSWT model data coupled with the agreement seen elsewhere between reference model data and adaptive wall data and the fact that unexpected streamlined-wall results are, in our experience, never seen combine to reduce the likelihood of non-unique solutions ever being experienced in two-dimensional testing.

It is interesting to observe how the walls move during a streamlining cycle governed by the WAS 2 strategy. The wall contours for each streamlining iteration of Run 285 ($M_\infty = 0.7$; $\alpha \simeq 6.0^o$) are shown on Figure 10.12. They demonstrate good wall streamlining convergence, despite severe

† For a given test condition different wall contours can represent different but equally valid streamlines, as discussed in Section 10.4.

wall interference (E_T and E_B equal to 0.1646 and 0.1101 respectively) at the beginning of the streamlining cycle and the relatively high reference Mach number. Inspection of Figure 10.12 reveals that the majority of all wall movement was accomplished after the first two or three iterations. The small magnitude of wall movement demanded by the remaining iterations was typical for streamlining cycles governed by the WAS 1 and WAS 2 strategies, particularly at reference speeds greater than Mach 0.6.

10.7 Further Notes on the NPL Strategy

10.7.1 Constant Pressure Wall Contours

The NPL strategy requires the experimental determination of constant pressure and aerodynamically straight contours, as noted in Section 6.3. The quality of constant pressure contours derived in the TSWT is summarised in Table 11 (σ_T, σ_B and σ_{av} are measures of streamlining quality), whilst the Mach number distributions along the centrelines of the walls for each of the contours are shown on Figures 10.13.1-10.13.3. The quality of the constant pressure contours does not match that achieved for aerodynamically straight contours, as can be seen by comparing the data presented in Tables 3 and 11. The Mach number distributions indicate that further wall adjustments, localised near the model, may have led to an improved definition of constant pressure contours. However, it was concluded that the present contours were defined satisfactorily. Confidence was gained by the fact that most contours (the exceptions are contours A.3 and B.3) satisfied the normal wall streamlining criteria ($E < 0.01$ on both walls) when the value of E was calculated by artificially setting the perturbations of the imaginary flowfields to zero. These artificial wall loading values (E^*) may be used as an alternative measure of the quality of constant pressure streamlining.

As with streamlined contours, the effects of increasing Mach number and model lift on constant pressure contours was to demand increased wall movement. Wall displacements (from geometrically straight) of a typical constant pressure contour ($M_\infty = 0.7$; $\alpha \simeq 4.0^o$) are shown on Figure 10.14. It is interesting to note that towards the downstream end of the test section the aerodynamically straight and constant pressure contours nearly coincide. That is to say that the discrepancy in total wall movement at jack nineteen

between the two contours was less than 0.15mm (0.006 inches). This implies that the thickness of the model wake was small, therefore it may be deduced that under the constant pressure conditions a shock induced separation of the model boundary had not occurred at this test condition ($M_\infty = 0.7$; $\alpha \simeq 4.0^o$). When the walls were streamlined according to the WAS 1 strategy the total outward movement of the walls at jack nineteen indicated a model wake displacement thickness of approximately 1.0mm (0.040 inches), as shown on Figure 10.6.

In experiments such as these where the reference Mach number is subsonic, the test section choking caused by the strong interference of straight walls is, by definition, overcome by contouring the walls to constant pressure contours. However, as the walls are far from streamlines† the model still suffers from wall interference effects. The magnitude of one interference effect present with straight and constant pressure wall contours may be seen in Table 7; a set of lift curve slopes. At each Mach number (0.4, 0.5 and 0.6) the slopes given by the streamlining strategies are in fair agreement with each other. With aerodynamically straight walls the slopes are high and conversely with constant pressure contours, with the magnitude of the errors increasing with Mach number. The opposite sign of the interference is of course an example of the phenomenon which led to the suggestion of ventilation as a means for reducing wall interference.

A further illustration of the existence of interferences with the walls set to constant pressure contours is illustrated by the data shown in Table 12. None of the contours satisfy the normal wall streamlining criteria ($E < 0.01$ on both walls) and, therefore, the resulting interference effects are larger than usually experienced when the walls are streamlined (see Section 3.2 for typical values of residual interference effects when the walls are streamlined). Typical effects on model pressure distribution of moving the walls from straight to constant pressure contours are illustrated on Figure 10.1; the over-correction is clear.

† Constant pressure contours simulate open-jet conditions.

10.7.2 Streamlining Quality of NPL Contours

In order to assess the streamlining quality of contours derived by the NPL strategy, wall loading values (expressed in terms of E) were calculated at each test condition, with the TSWT TSP code being used in the computations of the imaginary flowfields. The residual interference effects at the model due to any remaining wall loading were also calculated using linearised theory.

The results, presented in Tables 8 and 13, clearly illustrate that employment of the NPL strategy considerably reduces the level of wall loading from that present with straight walls. It is evident that a setting factor of six-tenths (NPL 2 WAS) is more appropriate than the half-way factor (NPL 1 WAS). Contours derived by the former setting factor nearly satisfy the normal streamlining criteria ($E < 0.01$ on both walls) for speeds up to about Mach 0.7. However, analysis of model performance suggests that the streamlining criteria may well be unnecessarily strict, especially up to Mach 0.7. It is also noticeable from the results presented in Tables 8 and 13 that wall loading and residual interferences increase with angle of incidence. Therefore the lift generated by the model may be a factor limiting the test regime where the NPL strategy could be considered applicable. Finally, the breakdown of the NPL strategy above Mach 0.7 is clearly illustrated in Table 8 by the excessive wall loading remaining after wall streamlining.

10.7.3 Convergence of Walls to NPL Contours

A prerequisite of setting wall contours according to the NPL strategy is the determination of constant pressure contours. Therefore, the rate of wall convergence to such contours determines the number of wall adjustments necessary during the NPL streamlining process. When employing the Imbalance strategy (see Section 8.3 for details of strategy) satisfactory constant pressure contours were reached only after many iterations; the extreme was the 17 iterations necessary to derive contour D.3 when the streamlining cycle was initiated from aerodynamically straight. Wall adjustments were continued until no further reduction in the value of σ_{av}† was experienced, the value typically lying in the band of 0.003 to 0.005. The

† See Section 8.2 for definition of σ_{av}.

relationship between the wall movement (δ_y) and the desired change of local wall Mach number (δM) which was used for all wall adjustments was $\delta_y/\delta M$ equal to 1.0cm (0.4 inches). The situation was improved by utilising the WAS 1 strategy but with the perturbations of the imaginary flowfields all the while artificially set to zero. However, convergence was still slow and wall streamlining according to the NPL strategy typically required 3 to 5 times as many iterations as the WAS 1 and WAS 2 strategies. This represents the only major operational disadvantage associated with the implementation of the NPL strategy. The WAS 1 and WAS 2 strategies have been developed to rapidly derive streamlined wall contours. Presumably a predictive strategy could be developed to derive constant pressure contours, but at present we cannot see any immediate need for this development.

10.7.4 Model Wake Approximation

As has been previously noted (see Section 10.3 and 10.4) properly streamlined walls automatically adapt to the blockage caused by the model wake. The wall Mach number some distance downstream of the model returns essentially to the reference value, as must be the case for the simulation of free flowfield conditions.

Constant pressure walls with a model present, and aerodynamically straight walls with no model both exhibit, by definition, constant Mach number (equal to the reference value) along the entire lengths of the walls. For constant pressure contours this requires outward wall movement (relative to aerodynamically straight) downstream of the model in order to eliminate the blockage caused by the model wake. The NPL strategy requires wall contours of less outward wall movement downstream of the model than contours giving constant pressure, thus raising the Mach number in this region above the reference value. Therefore the NPL strategy cannot totally eliminate model wake blockage. The problem is exaggerated at speeds where the effect of setting the walls to streamlined contours from constant pressure is to increase the strength of model shocks, because of the almost inevitable increase in the thickness of the wake.

In practice, however, for speeds up to Mach 0.7 the inadequate alleviation of wake blockage, caused by the approximate nature of the NPL strategy, appears to be of little consequence. The evidence is provided by

model data (as discussed in Section 10.5) and the measurement of wall Mach numbers downstream of the model which show them to be close to the reference value, as illustrated by the relatively severe test condition ($M_\infty = 0.7$; $\alpha \simeq 4.0^o$) shown on Figure 10.4. At Mach 0.8 where breakdown of the NPL strategy is evident, the downstream wall Mach numbers are appreciably higher than the reference value, as shown on Figure 10.10. At this speed the wake blockage approximation becomes more significant as the shock induced separation of the model boundary layer has led to increased wake thickness, as can be detected from the schlieren pictures shown on Figure 10.11.

In an attempt to indicate the magnitude of the effects on model performance of the inadequate alleviation of wake blockage, a *'wake pinch'* test was performed in the TSWT. For the test condition of $M_\infty = 0.8$; $\alpha \simeq 6.0^o$ model data obtained with walls streamlined according to the WAS 1 strategy was compared to that obtained with the walls set to a contour moved deliberately to cause wake blockage. The outward movement downstream of the model exhibited by the properly streamlined contour (CON 1) indicated a wake thickness of about 3.8mm (0.15 inches), whilst the high downstream wall Mach numbers ($\simeq 0.85$) associated with the other contour (CON 2) suggested significant wake blockage.† The expected effect of such blockage on the model was to increase the flow velocity near the trailing edge. However, comparison of the corresponding model pressure distributions (see Figure 10.15) reveals that no effect on model performance was detectable. It may, therefore, be tentatively concluded that the effects of the NPL wake approximation were insignificant for most test conditions of the present investigation.

10.7.5 Appropriate NPL Setting Factor for the TSWT

Analysis of streamlined wall contours has suggested that for the model and test section configuration of the present investigation a setting factor of seven-tenths towards the constant pressure contour would be more appropriate than the two setting factors suggested by NPL. An NPL strategy employing a factor of seven-tenths (NPL 3 WAS) derives wall contours that exhibit

† Further details on the wake pinch test are given in Reference 91.

approximately the same wall movement apart characteristics in the vicinity of the model as the WAS 1 and WAS strategies. However, it should be emphasised that disparities between the strategies (in terms of wall movement apart) still exist upstream and downstream of the model, as illustrated by the representative case ($M_\infty = 0.7$; $\alpha \simeq 4.0^o$) shown on Figure 10.6. Model tests with the flexible walls set according to the new strategy (NPL 3 WAS) are required in order to assess the streamlining performance of the strategy. It is anticipated that breakdown of the NPL strategy in the TSWT would be delayed by the employment of a setting factor of seven-tenths.

11. MODEL TESTS WITH MIXED FLOW IN THE IMAGINARY FLOWFIELDS

The aim of the tests detailed in this section was to demonstrate the principle of wall streamlining at test conditions where mixed flow and the attendant shocks have reached the streamlined walls and intruded into the imaginary flowfields. Hence, the TSWT TSP code (as detailed in Section 7) was used in all the imaginary flowfield computations associated with these tests.

11.1 Measures of Wall Streamlining Quality

The difference in pressure across a wall (i.e. wall loading) has previously been introduced as the most important measure of the quality of wall streamlining. Additional measures are provided by calculating the residual interference effects at the model due to any remaining wall loading. In the TSWT these effects are normally computed at every stage of the streamlining process. However, when supercritical flow has reached the flexible walls the linearised theory used in the residual interference computations is no longer appropriate. Thus, when testing at such conditions in the TSWT the residual interference effects are unknown and, therefore, the wall loading (expressed in terms of E) is the only available measure of wall streamlining quality.

11.2 Initial Tests

The initial model tests utilised the original flexible walls of the TSWT. During the tests the TSWT schlieren system was not available.

11.2.1 Scope of Tests

The tests were carried out in a reference Mach number band not before explored in two-dimensional flexible wall research, that is Mach 0.9 to 0.97, where at all times the flow channels over and under the model are choked. During the tests the model remained locked at a nominal angle of incidence of 4.0^{o}.

Contrary to fears expressed in some quarters that when the test section is fully choked control would be lost over the reference speed, no such difficulty was experienced. It should be noted that reference Mach numbers in this range are well beyond the reach of straight walls with this combination of model and test section. The technique developed to overcome this practical difficulty was as follows. With the model set at the desired angle of incidence the tunnel was run at a modest reference Mach number and the walls crudely streamlined. It was then found that the Mach number can be considerably increased because of the blockage relief accompanying the streamlining. The process of refinement in wall shape with attendant improvements in streamlining quality, followed by further increases in reference Mach number, allowed the wall shapes and the reference Mach number to converge as desired. Thus, as expected, the achievement of high subsonic reference speeds requires a few tunnel runs at Mach numbers below that ultimately required.

11.2.2 Quality of Wall Streamlining

The quality of wall streamlining achieved during the initial tests never reached the level where the walls are normally considered to be adequately streamlined ($E < 0.01$ on both walls), as demonstrated by the E_T, E_B and E_{av}† values shown in Table 14.1. The poor condition of the original flexible walls at this stage in their lives and the inherent weaknesses of the jack/wall flexure design (as discussed in Section 5.6.2), limited the attainable level of wall streamlining quality. Although localised differences between the real and imaginary flowfields still existed,[90] especially as the reference Mach number approached unity, the attained level of wall streamlining quality was considered to be highly encouraging.

11.2.3 0.9-0.94 Mach Number Band

In the 0.9-0.94 reference Mach number band the model shocks were locally normal to the flexible walls. The only significant discrepancies between the real and the imaginary wall Mach number distributions occurred in the vicinity of the shock-wall impingement positions,[90] as illustrated by the typical case ($M_\infty \simeq 0.9$; $\alpha \simeq 4.0^o$) shown on Figure 11.1.

† $E_{av} = (E_T + E_B)/2.0$

The best level of wall streamlining quality was achieved when the effective aerodynamic contour accounted for the changes in δ^* caused by the presence of the model,† as demonstrated by the results presented in Table 14.1.

11.2.4 0.95-0.97 Mach Number Band

In the 0.95-0.97 reference Mach number band the shocks on the upper and lower surfaces of the model had moved to the trailing edge,[90] and were likely to be oblique with respect to the flexible walls. When the walls are correctly streamlined (i.e. negligible wall loading) the model shocks will not be reflected in any way from the wall. This situation may not have been reached as significant wall loading still existed downstream of the shock-wall impingement positions, as illustrated by the real and imaginary wall Mach number distributions shown on Figure 11.2 ($M_\infty \simeq 0.95$; $\alpha \simeq 4.0^o$). However, the real Mach number distributions do not provide any supportive evidence regarding the reflection of model shocks. As the shock-wall impingement position on each flexible wall was downstream of both sidewall glass windows, any shock reflections could not have been observed even if the schlieren system had been in use. Limited shock reflections downstream of the model may be acceptable, since the effect on model performance might be small. Further tests aimed at quantifying the effects of such shock reflections on model performance are required.

11.2.5 Concluding Remarks

The initial model tests clearly demonstrated that, when supercritical flow has reached both flexible walls and extended with the attendant shocks into the imaginary flowfields, wall streamlining is feasible and that at such conditions the TSWT TSP code is a practical tool for the computation of the imaginary flowfields.

In the 0.95-0.97 Mach number band the peak Mach number on the top wall was greater than 1.4. At such conditions the strong pressure gradients associated with the shock-boundary layer interaction may induce separation of

† The RAE BL code was used to predict the changes in δ^* due to the model influences.

the wall boundary layer.[120] Since there is uncertainty as to the accuracy of the RAE BL code in such circumstances[121] it was concluded that further tests should initially concentrate on the 0.9-0.94 Mach number band. In this Mach number band the pressure gradients are unlikely to induce separation of a flexible wall boundary layer and the shock-wall interactions may be observed by use of the schlieren system.

It was anticipated that the jack/wall link mechanism of the new flexible walls (see Section 5.6.2 for details) would allow an improved level of wall streamlining quality to be obtained. Therefore, it was decided that further tests in the 0.9-0.94 Mach number band would only commence once the new flexible walls had been installed into the TSWT. It was planned that these tests would investigate the required standards of wall streamlining quality, with particular reference to the sensitivity of model performance to wall loadings localised around the shock-wall impingement positions.

11.3 Further Tests

These model tests utilised the new flexible walls of the TSWT and were aimed at providing additional data to that already gained during the initial tests detailed in Section 11.2. The TSWT schlieren system was available and used during the tests.

11.3.1 Scope of Tests

It was originally intended, for reasons previously discussed, that these tests would be carried out in the 0.9-0.94 Mach number band. However, due to an enforced temporary reduction in pressure of the dried air supply (from 300 to 150 p.s.i.) the tests were limited to a reference speed of below Mach 0.9. In fact, this Mach number could only be reached by the removal of the air filters situated in the air supply line just upstream of the tunnel injector box, which inevitably reduced the test section flow quality by introducing foreign particles to the tunnel circuit. Despite the limitation on reference Mach number a few test conditions which gave supercritical flow at the flexible walls and in the imaginary flowfields were obtained (see Table 14.2 for the

test conditions†). Hence, the tests provided further data demonstrating the principle of wall streamlining at conditions which result in a choked test condition.

11.3.2 Streamlining Performance

11.3.2.1 Quality of Wall Streamlining

As anticipated, the attainable level of wall streamlining quality was significantly improved by the installation of the new flexible walls. In fact, the usual wall streamlining criteria ($E < 0.01$ on both walls) was satisfied in the majority of cases, as demonstrated by the E_T, E_B and E_{av} values presented in Table 14.2.

The extent of supercritical flow at the flexible walls and in the imaginary flowfields for the test conditions of $M_\infty \simeq 0.89$; $\alpha \simeq 4.0^o$ and $M_\infty \simeq 0.87$; $\alpha \simeq 4.0^o$ is illustrated by the schlieren montages shown on Figures 11.3 and 11.4 respectively. In both cases, the supercritical flow regions of the real and imaginary flowfields are extremely well matched considering that wall data (wall position and static pressure) was only available at the jack stations, which in this region are spaced at 2.54cm (1 inch) intervals. The good match is also illustrated on Figures 11.5 and 11.6 ($M_\infty \simeq 0.89$; $\alpha \simeq 4.0^o$ and $M_\infty \simeq 0.87$; $\alpha \simeq 4.0^o$ respectively), where the real and imaginary wall Mach numbers near the model are scaled to the corresponding schlieren pictures. The flow direction on Figures 11.3 - 11.6 is right to left.

Differences between the real and imaginary flowfields still exist but they are small and confined to regions near the shock-wall impingement positions, as illustrated by the wall Mach number distributions shown on Figure 11.7 ($M_\infty \simeq 0.87$; $\alpha \simeq 4.0^o$). The wall Mach number some distance downstream of the model is seen to return approximately to the reference value, which indicates that the flexible walls have adapted to the blockage caused by the model wake. The wall displacements shown on Figure 11.8 suggest that at the typical test condition of $M_\infty \simeq 0.87$; $\alpha \simeq 4.0^o$ the displacement thickness of the model wake is about 5.1mm (0.2 inches). The

† At the test condition of $M_\infty \simeq 0.85$; $\alpha \simeq 4.0^o$ supercritical flow had extended into the imaginary flowfield of the top wall only.

large thickness was probably due to shock induced separation of the model boundary layer, hence the relatively low value of lift ($C_N \simeq 0.13$). The low level of lift at this test condition[65] ($M_\infty \simeq 0.87$; $\alpha \simeq 4.0^o$) may also be inferred from the near symmetrical shapes of the top and bottom wall contours shown on Figure 11.8.

11.3.2.2 Repeatability of Model Data

The repeatability of model data was investigated at the test condition of $M_\infty \simeq 0.89$; $\alpha \simeq 4.0^o$. Streamlined-wall model data was obtained from three different streamlining cycles (Runs 300, 305 and 306), all initiated from walls set to aerodynamically straight. Inspection of the model pressure distributions shown on Figure 11.9 reveals that the repeatability of model data at this test condition was excellent.

11.3.2.3 Required Level of Wall Streamlining Quality

The sensitivity of model performance to the quality of wall streamlining at the test condition of $M_\infty \simeq 0.89$; $\alpha \simeq 4.0^o$ is illustrated by the model pressure distributions shown on Figure 11.10. The rate of convergence of model pressure distribution with the fall of wall loading (expressed in terms of E_{av}) suggests that the quality of wall streamlining achieved with the new flexible walls may well be adequate for this test condition ($M_\infty \simeq 0.89$; $\alpha \simeq 4.0^o$). However, the quantity of data presently in hand is limited and, therefore, more experimental experience is required before being sure of the quality of wall streamlining needed to obtain wall interference-free model data at such conditions.

11.4 Comparisons of TSWT Model Data with Reference Data

11.4.1 NASA Reference Data

The NACA 0012-64 model had previously been tested in a slotted test section in the 19 inch x 6 inch transonic blowdown wind tunnel[125] at NASA Langley Research Center. The NASA tests provide model reference data with a ratio of test section height to model chord of 4.75 compared to about 1.5 in

the TSWT. The NASA data† has not been corrected for any test section boundary interference effects and covers a range of angles of incidence from 0^{o} to 16^{o} for test Mach numbers from 0.5 to 1.1. Most of the data is for a clean model, but additional tests with a transition band fitted to the model were made at 4^{o}, 8^{o}, 12^{o} and 16^{o} for each test Mach number. The data has been compiled into a reference data library on the TSWT computer in order to allow easy interpolation, thereby permitting routine comparison of model data at any given test condition. The interpolation process, however, is not always satisfactory for the transition-fixed data.

The Reynolds number of the reference data is higher than that of model tests in the TSWT. Model behaviour, in particular the positions of shocks, is sensitive to the state of the boundary layer, which for a clean model is strongly dependent on Reynolds number. Comparisons of TSWT data with reference data are therefore made with transition fixed, in an attempt to reduce the discrepancies caused by the differing Reynolds numbers. However, comparison is not straightforward because when model pressure distributions are compared, the model C_N's should be closely matched in order to remove uncertainty about the angle of incidence that exists in the two tunnels, and uncertainty over the magnitude of the correction which should be applied to the reference data.

When comparisons are made it should be noted that the condition of the model transition band used during the TSWT tests may have been different from that of the NASA tests, and secondly that recent work at NASA Langley Research Center[81] suggests that the reference data probably requires a Mach number correction. The magnitude of the suggested correction is small for subcritical flow but increases sharply as the Mach number is raised into the supercritical flow regime. This situation, combined with the usual difficulties of comparing model data from different wind tunnels, leads to the conclusion that the reference data can at best only be used as an approximate indication of model performance especially at high subsonic reference speeds.

† Unpublished work.

11.4.2 Model Data Comparisons

In an attempt to validate the principle of wall streamlining at conditions which result in supercritical flow at the flexible walls, the streamlined model data obtained at the test conditions shown in Table 14.2 has been compared with the NASA reference data. The best direct match before any interpolation is achieved at $M_\infty = 0.875$; $\alpha \simeq 4.0^o$ in the TSWT and $M_\infty = 0.864$; $\alpha \simeq 4.0^o$ for the reference data, as illustrated by the model pressure distributions shown on Figure 11.11. The most notable discrepancies are found in the position of the model's upper surface shock and in the pressure coefficient over the aft half of the upper surface. The extent of the discrepancies were increased when the reference data had been interpolated to $M_\infty = 0.875$; $\alpha \simeq 4.35^o$ in order to give a good match between the model C_N's, as illustrated on Figure 11.11.

As previously discussed there are many possible reasons for the lack of reasonable agreement between the TSWT and the reference data at high subsonic reference speeds. However, when model data comparisons are made the points raised in the following (Sections 11.4.2.1-11.4.2.2) should also be noted.

11.4.2.1 Sidewall Boundary Layer Effects

The influences of the boundary layers on the sidewalls of the test section have long been recognised to be important in two-dimensional testing.[126] Studies at ONERA[127] have indicated that the presence of sidewall boundary layers near the model can influence the test data even on the mid-span. The influences become particularly important for models of small aspect ratio (less than about 2.0) and for flows with shock waves.[128] Investigations[78] in the NASA Langley 0.3-m Transonic Cryogenic Tunnel[60] have suggested that at some supercritical conditions the sidewall boundary layer influences are probably greater than the influences due to any top and bottom wall interference.

The available correction methods[129-133] which attempt to account for the sidewall boundary layer influences are, at present, limited to attached boundary layers and use relatively simple flow models. For example, the Barnwell-Sewall method[132] ignores any three-dimensional effects on the

sidewall boundary layer and does not include the effect of model span. The method only strictly applies to narrow test sections, because it is assumed that the flow at each sidewall is strongly influenced by the other sidewall boundary layer. Despite these simplifications, investigations at NASA Langley Research Center[134,131] have shown that the Mach number correction suggested by the Barnwell-Sewall method was sufficient to approximately account for all the blockage effects caused by the changes in thickness of the sidewall boundary layers. The investigations also suggested that the method is valid up to transonic speeds provided that the sidewall boundary layer occupies a small enough fraction of the test section width to avoid substantial three-dimensional interaction with the model.

It may be argued that in adaptive wind tunnels the necessity to assess the extent of sidewall boundary layer influences is a matter of prime concern, as top and bottom wall interference effects are, in principle, eliminated when the walls are correctly streamlined. Such assessment in the TSWT is further complicated by the fact that the two sets of pressure tappings on the model are positioned on a chord line 1.90cm (0.75 inches) either side of the mid-span. In the TSWT, however, evidence of spanwise variations of flow velocity at the model might be expected to be apparent at the top and bottom walls, as they are close to the model. Hence, in an attempt to examine such variations some measurements of wall Mach number on the centreline and off-centreline positions (Orifice 3 and Orifice 1 respectively) have been made with the new flexible walls. Typical data is shown on Figure 11.12 ($M_\infty = 0.875$; $\alpha \simeq 4.0^o$), from which it may be tentatively concluded that any spanwise variations in the TSWT are small, even in the region of the model.

Despite the existence of several possible correction methods no assessment of the sidewall boundary layer influences has been made in the TSWT. Although wall streamlining may have a favourable effect on any blockage caused by the variations in thickness of the sidewall boundary layers, it is possible that at high subsonic speeds the sidewall boundary layer influences in the TSWT are significant. This comment probably applies to the reference data as well, but possibly to a different extent as the test section geometries of the TSWT and NASA tests differed somewhat. The uncertainties concerning the relative magnitudes of the sidewall boundary layer influences associated with the TSWT and reference data render the

validity of any comparisons even more dubious, especially at high subsonic reference speeds.

11.4.2.2 Model Transition Band Deterioration

During the TSWT tests aimed at streamlining the new flexible walls when the test section is choked, the transition band of the model suffered severe deterioration. This was probably due to the many foreign particles flowing around the tunnel circuit, an inevitable result of removing the air filters in the air supply line. The extent of the transition band deterioration is clearly visible on the pictures presented on Figure 11.13. The pictures show the condition of the model immediately after the tests.

The effect of transition band deterioration on model performance is well illustrated on Figure 11.14, where comparisons are made between model pressure distributions obtained when the walls were streamlined (according to the WAS 1A strategy) immediately before and after the tests during which the air filters were removed. At this test condition ($M_\infty = 0.8$; $\alpha \simeq 6.0^o$) the deterioration resulted in a downstream movement of the model's upper surface shock of about 15% of model chord. The direction of the movement is consistent with the discrepancies in model shock location experienced when comparing TSWT model data with the reference data.

11.4.3 Numerical Computations

Finding a reliable independent source of interference-free performance data for a model is a difficult task and such information is always open to question, as demonstrated by the many problems concerning the use of the NASA model data. Thus, in order to provide another independent source of model data it was decided to employ GRUMFOIL[135,136]; a two-dimensional full potential transonic code with viscous interaction. Although the GRUMFOIL code is not without problems of its own,[137,138] it was thought that at high subsonic reference speeds the code may provide the most reliable reference data available. However, initial GRUMFOIL computations† at the test conditions shown in Table 14.2 have

† The GRUMFOIL computations were carried out by A.V. Murthy at NASA Langley Research Center.

failed to converge to an acceptable level, rendering the results unusable. The lack of convergence is thought to be due to the fact that the Reynolds number of the TSWT tests ($\simeq$1.5 million) is considerably lower than normal for typical GRUMFOIL applications. Attempts to obtain usable model data from the GRUMFOIL code continue.

11.5 Shock-Boundary Layer Investigations

11.5.1 Background

Past investigations[99,65] attempted to alleviate the δ^* growth due to the shock-boundary layer interaction by locally modifying the wall contour. The action had a noticeable effect on the model pressure distribution. For example, at Run 184 conditions (M_∞ = 0.8862; $\alpha \simeq 4.0^o$) the localised hollow introduced into the top wall contour reduced the pressure coefficient over the aft half of the model's upper surface by 0.05, and moved the model's lower surface shock upstream by 5% chord.[65]

Recent work (see Section 9.6) has suggested that the thinning of δ^* (due to the general pressure field) prior to the shock-boundary layer interaction may well be more significant than any thickening of δ^* at the interaction. It was, therefore, concluded that at such conditions the effective aerodynamic contour should probably account for all the changes in δ^* induced by the pressure field of the model. Hence, there followed the need to predict $\Delta\delta^*$ distributions along the flexible walls. The lag-entrainment method (RAE BL code) was the preferred method.

11.5.2 Experimental Results

When the walls were adjusted to account for the predicted $\Delta\delta^*$ distributions the effect on model performance for a given level of streamlining quality was, in general, to move the model's upper surface shock upstream,[90] typically by about 5% of chord. The test condition of M_∞ = 0.8726; $\alpha \simeq 4.0^o$ was a notable exception among the data sets in hand. In this case the effect of the $\Delta\delta^*$ allowance was to move the upper surface shock downstream by about 2% chord. The movement is shown by the model pressure distributions presented on Figure 11.15. The limited quantity of data presently in hand does not allow any reliable conclusion to be drawn as to the

effect on model performance of making a $\Delta\delta^*$ allowance. The available evidence suggests that the effects may not be consistent. However, within this limitation the data has served to highlight the importance of using some form of $\Delta\delta^*$ allowance. The effects of making a $\Delta\delta^*$ allowance in the imaginary flowfield computations are significant, as clearly illustrated by the computations of imaginary wall Mach number shown on Figure 11.16 ($M_\infty = 0.8726$; $\alpha \simeq 4.0^o$). An allowance for $\Delta\delta^*$ is seen to change the wall loading parameter E by a factor of about 2. Further work (which does not form part of this thesis) is required to verify the $\Delta\delta^*$ allowance used during the present investigation.

11.6 Operational Experience

11.6.1 Experimental Technique

The experimental technique developed to streamline the flexible walls at test conditions which resulted in a choked test section made use of the WAS 1A and Imbalance strategies. Details of the strategies are given in Sections 6.4 and 8.3 respectively. The flexible walls were adjusted according to the WAS 1A strategy until no further reductions in the values of E_T and E_B were attained. The Imbalance strategy was then applied to a few individual jacks which exhibited unacceptable levels of local wall loading, these jacks usually being in the vicinity of the shock-wall impingement positions.

The WAS 1A strategy in its original form became less strongly convergent when supercritical flow reached the flexible walls. The tendency for the number of iterations per streamlining cycle to increase at such conditions was curbed by reducing the scaling factor† to 0.25 from the normal value of 0.7. The ratio of wall movement to the desired change of local Mach number ($\delta y/\delta M$) which was used with the Imbalance strategy was varied from 2.5 to 1.5mm (0.1-0.06 inches). The value being reduced as the local level of wall streamlining was improved.

The wall setting tolerance used in the wall control software was also reduced. A software tolerance of ±0.06mm (±0.0025 inches) was found to be

† See Appendix A for scaling factor details.

adequate for most tests, however testing with supercritical flow at the flexible walls was much improved by the use of a tolerance of ±0.025mm (±0.001 inches). The reason for this reduction was the increased sensitivity of the flow and, therefore, model performance to wall movement at such conditions.

Despite these modifications, the achievement of streamlined walls at reference speeds above Mach 0.85 required numerous streamlining iterations. For example, at the test condition of $M_\infty \simeq 0.89$; $\alpha \simeq 4.0^o$ 12 iterations were needed (8 governed by the WAS 1A strategy and 4 governed by the Imbalance strategy) when the streamlining cycle was initiated from walls set to aerodynamically straight. The desired reference Mach number was reached after the first 4 iterations. Further work is required in order to reduce the tunnel run-time associated with wall streamlining at high subsonic reference speeds.

11.6.2 Residual Wall Interference Assessment

The point has already been made that with a choked test section the wall loading is the only available measure of the quality of streamlining. The level of wall loading (expressed in terms of E) at which the walls can be judged to be providing interference-free flow is, at present, uncertain. An appropriate wall interference assessment/correction method is required, in order to provide additional measures of wall streamlining quality when the test section is choked.

The majority of present-day assessment/correction methods[139-141, 76,77] for two-dimensional flow assume the test section flow to be a superposition of a model induced flowfield, a wall induced flowfield, and the main oncoming flowfield. Consequently, these methods are restricted to subsonic flows although, in practice, they are usually sufficiently accurate in the low-transonic regime. However, the *'matching type'* of method[75,78,80] does not rely on the superposition principle and therefore can, in theory, be applied to any range of Mach number. The TWINTN4† code[78,80], which forms the basis of the matching type of method developed[81] for the NASA Langley

† The TWINTN4 code is a development of the TWINTAN code[75].

0.3-m Transonic Cryogenic Tunnel[60], employs the transonic small perturbation equation and, therefore, may be applicable with supercritical flow at the top and bottom walls of the test section.

The matching type of method requires pressure distributions to be measured on the model and on or near to the walls. From this pressure data, an effective inviscid model shape is computed by solving the *'inverse'* problem. The free-air pressure distribution of the effective shape is subsequently computed, iterating on Mach number and angle of incidence until the computed pressure distribution matches, within a specified error, the distribution originally measured on the model. The Mach number and angle of incidence of the free-air computation producing the match is the corrected test condition. If a match cannot be attained the case is judged to be uncorrectable.

An advantageous feature of the matching type of method, apart from the wide range of applicable Mach numbers, is that the usual assumption that the wall interference effects are uniformly distributed over the model is not made. However, the inverse computation is not attractive or even feasible for some complex models and the method requires much computational effort. For example, the TWINTN4 code requires 106K (octal) 60 bit words of storage and about 100 seconds of CPU time per pass on a CYBER 175 computer.[81] Such computational requirements are greater than that which can be accommodated on most computer systems used by present wind tunnel facilities.

It may, therefore, be concluded that the computations associated with the matching type of method are certainly not viable on the TSWT computer. Thus, the wall loading (expressed in terms of E) will remain as the only measure of wall streamlining available in the circumstances under discussion. This will probably be true even for tunnels with access to relatively large computational resources, as it is likely that computational times will prevent employment of the method at every stage of the streamlining process. Hence, in practice, the matching type of wall interference assessment/correction method may only be used as a post-test check on the quality of wall streamlining. In the interim, however, it would be useful for some organisation with access to the necessary computing power to gain experience

with supercritical walls streamlined to various levels of E, with the magnitudes of the residual interference effects monitored by a suitable code in order to more firmly establish the wall loadings which are satisfactory.

12. DISCUSSION OF FINDINGS

12.1 Evaluation of Wall Adjustment Strategies

The evaluation of several transonic wall adjustment strategies in the TSWT has formed a major element of this work. Such an evaluation is believed to be unique. The aim was to determine the relative performance of each strategy by assessing the viability of their use in flexible walled test sections, both in terms of test section operation and model performance.

12.1.1 NPL Strategy

The first documented wall adjustment strategy was proposed and developed by NPL in the early 1940's for use in their transonic self-streamlining flexible walled wind tunnel. The tunnel (20 x 8 NPL Tunnel) employed the strategy for about 15 years. The ratio of test section height to model chord in the 20 x 8 NPL Tunnel was typically around 3.5, whereas in the TSWT tests it was about 1.5. The TSWT was, therefore, a more severe test of the effectiveness of the NPL strategy than the environment for which it was developed. A constraint which existed at the time when the NPL strategy was being developed was that digital computers, which did exist, were available only for the most pressing national needs.

One step in the NPL strategy is the determination of constant pressure wall contours, which demands wall movements of greater magnitude than usually experienced when just contouring the flexible walls to free-flowfield streamlines. Therefore, for a given test condition the NPL strategy requires larger wall movements than the WAS 1 and WAS 2 strategies. This fact would have important implications on the configuration of a flexible walled test section designed to use the NPL strategy. In fact, the maximum jack movement of 2.54cm (1 inch) limited the test range within which constant pressure contours could be obtained in the TSWT.

An assessment of streamlining quality demonstrated that with the flexible walls adjusted according to the NPL strategy the wall interferences were significantly reduced from the levels present with straight walls. Despite the fact that wall contours predicted by the NPL strategy only

approximated to streamlines the resulting model performance, over a wide range of test conditions, compared favourably with that obtained when the walls were streamlined by the more modern strategies (i.e. WAS 1 and WAS 2 strategies). These model performance comparisons have indicated that the NPL strategy reduces wall interference effects at the model to levels which may be considered insignificant for test conditions up to $M_\infty = 0.7$; $\alpha \simeq 4.0^\circ$.

The test regime within which the NPL strategy performs satisfactorily appears to be limited. The strategy was observed to break down at the test conditions of $M_\infty = 0.8$; $\alpha \simeq 0.5^\circ$ and $M_\infty = 0.8$; $\alpha \simeq 2.0^\circ$. High values of model lift may well further restrict the applicable reference Mach number. Analysis of streamlined wall contours has suggested that for the model and test section configuration of the TSWT tests, an NPL strategy employing a setting factor of seven-tenths would be more appropriate than the two setting factors proposed by NPL. It is anticipated that employment of the seven-tenths setting factor would delay the breakdown of the NPL strategy in the TSWT, and thereby extend the applicable test regime.

The only significant disadvantage associated with the implementation of the NPL strategy (within its applicable test regime) was the number of wall adjustments necessary during the streamlining process, which are somewhat higher than the norm for modern strategies. This disadvantage might possibly be reduced following the development of a predictive strategy to derive constant pressure wall contours, but at present there does not appear to be any immediate need for this development. It may, therefore, be concluded that the only major development in the flexible wall testing technique since the 1940's (apart from the reduction of tunnel run-time attributable to the streamlining process) is the reduction of the ratio of test section height to model chord at which satisfactory streamlining may be achieved from approximately 3.5 to 1.5.

Recent library searches,[142,28] which have been extended by the author and others, have established beyond doubt that wall streamlining as a means of reducing test section boundary interference was not the new idea which some believed it to have been in the early 1970's. During the early 1940's and subsequently it was used extensively by NPL. Also a major German tunnel employing the principle of adjustable walls was constructed during the

same period. It is time for the wind tunnel community to cease the unfair practice of improperly accrediting the invention.

12.1.2 Modern Strategies

The rapid convergence of the flexible walls to streamlines has always been regarded as essential to the efficient use of flexible walled test sections. A rapid convergence depends on the adequacy of the wall adjustment strategy governing the streamlining process. The WAS 2 strategy eliminated some of the approximations present in the underlying theory of the WAS 1 strategy and, therefore, it was presumed that the WAS 2 strategy may further reduce the number of wall adjustments required to streamline the flexible walls. In practice, however, the wall streamlining rates of both strategies were approximately equal. This fact reflects the high efficiency of the WAS 1 strategy rather than any inadequacy of the WAS 2 strategy.

The WAS 2 strategy does offer several operational advantages over the WAS 1 strategy. The most notable advantage is that the strategy can be initiated from any wall contour of known shape, whereas the WAS 1 strategy must start from wall contours where the shape and the imaginary side velocity distributions are known. Thus, a streamlining cycle governed by the WAS 1 strategy is usually initiated from aerodynamically straight contours or contours previously derived by the strategy. Also, the imaginary flowfield computations of the WAS 1 strategy necessitate the assumption that the changes in δ^* due to the presence of the model are negligible, which is not a requirement in the case of the WAS 2 strategy. The increased operational flexibility offered by the WAS 2 strategy may prove to be an important characteristic in a commercial wind tunnel facility.

The operational benefits of the WAS 2 strategy stem from the fact that the strategy computes the imaginary flowfields of the present wall contour, whereas the imaginary side velocity distributions given by the WAS 1 strategy apply to the predicted wall contour. Thus, successful wall streamlining according to the WAS 1 strategy relies on the flexible walls being set correctly to the predicted position. Any error caused by inaccurate wall setting or pressure measurement is automatically carried forward to every subsequent streamlining iteration. Such compounding of any experimental error is not a feature of the WAS 2 strategy. However, the disadvantages and

the operational inflexibility inherent in the WAS 1 strategy can be overcome by replacing the imaginary flowfield computations embodied in the strategy with another computational method, so that the external velocity distributions given by the strategy apply to the present wall contour (i.e. WAS 1A and WAS 1B strategies).

The proper adjustment of the flexible walls to streamlines depends on the accurate prediction of the external velocity distributions. However, a verification exercise of the TSWT TSP code revealed that the imaginary flowfield computations which form part of the WAS 1 strategy may be unreliable in some circumstances. This view was reinforced during an assessment of the streamlining quality of wall contours derived by the WAS 1 strategy. Thus, despite the good agreement between model data obtained when the walls were streamlined by the WAS 1 and other strategies, the streamlining performance of the WAS 1 strategy is in doubt at some test conditions.

The lift generated by the model appears to be a factor limiting the test regime where the strategy can be considered to be more than adequate. Further investigations are required, but at present the evidence suggests that the imaginary flowfield computations of the WAS 1 strategy should be replaced by a more reliable computational method. As such an action can also have advantageous effects on the operational aspects of the strategy it is highly recommended.

In defence of the WAS 1 strategy it should be stated that it was the first predictive (now sometimes, but inappropriately, called one-step) strategy developed, and that in an environment when computing power was very restricted compared to present standards. In allowing flexible walls (for the first time) to converge rapidly to free-flowfield streamlines, and most times to good streamlines, it must be judged a major development. With the passage of time it has merely been overtaken by more refined methods.

12.2 Wall Streamlining of a Choked Test Section

12.2.1 Streamlining Performance

Probably the most important part of this work has been the successful demonstration in the TSWT of two-dimensional wall streamlining at test conditions where the model shocks have extended to the contoured walls and intruded into the imaginary flowfields. At such conditions, in a flexible walled test section, the flow channels over and under the aerofoil model are fully choked. The achievement of wall streamlining infers, in principle, the elimination of top and bottom wall interference effects at the model.

Contrary to fears expressed in some quarters that when the test section is fully choked control would be lost over the reference speed, no such difficulty was experienced. Once a modest level of wall streamlining quality was obtained for a given test condition, raising the inducing air pressure increased the reference speed by a small increment. Further streamlining iterations at the new speed were required to restore the quality of wall streamlining to its original level. Thus, the achievement of wall streamlining at high subsonic reference speeds requires many tunnel runs and features a double convergence. That is the simultaneous convergence of the reference Mach number to its intended value and the convergence of the walls to streamlines.

The present investigation was limited by a temporary reduction in pressure of the dried air supply and tunnel availability. Further tests are required before being sure of the quality of wall streamlining necessary to obtain negligible levels of wall interference at these high reference speeds. Unfortunately the situation was complicated by the fact that the available reference data was not ideal for comparison, since Reynolds numbers were not matched and test section boundary interferences were known to be present in the reference data at the relevant test conditions. However, some TSWT data suggests that the quality of wall streamlining achieved with the new flexible walls may well have produced *'near'* wall interference-free model data. One can argue that if the top and bottom walls are unloaded then they cannot be interfering. The wall data and codes employed suggest this to be the case.

These findings add further confidence to the use of flexible walled test sections but leave some residual doubt about the quality of model data obtained in the TSWT with a choked test section. The investigations, however, have clearly demonstrated the principle of wall streamlining at test conditions where the model shocks intrude into the imaginary flowfields, and have enabled appropriate procedures for wall streamlining at such conditions to be established. The procedures are relatively simple and clearly demonstrate that flexible walled test sections can cope with these flows.

12.2.2 Prediction of Imaginary Flowfields

It has been demonstrated that the external wall velocities computed by the recently developed TSWT TSP code are reliable over a wide range of test conditions. The code may be used with confidence not only at conditions where the imaginary flowfields contain mixed flow, but also at reference speeds as low as Mach 0.4. The upper limit of the reference speed has yet to be defined, but it is expected to be just below Mach 1.0. The only significant disadvantage associated with the code when compared with other subsonic methods is run-time. However, current TSWT TSP code run-times of 3-6 minutes per flowfield for the present test section/computer combination have proved to be more than adequate for development purposes.

12.2.3 Boundary Layer Growth Along the Flexible Walls

It has been demonstrated that in routine two-dimensional tests† the changes in δ^* along the flexible walls have a negligible effect on the streamlining process. In such circumstances, the effective aerodynamic contour may be taken as the physical wall shape referenced to the appropriate aerodynamically straight contour. However, at conditions which result in shock-boundary layer interactions at the flexible walls the imaginary flowfield computations should account for the effects of the wall pressure gradients on δ^*. It is believed that the thinning of δ^* due to the general pressure field prior to the shock-boundary layer interaction is more significant than any thickening of δ^* at the interaction. The quantity of data presently in hand is

† Routine two-dimensional tests are defined as model tests at any set of conditions up to those which result in the flow at both flexible walls just remaining subsonic.

limited and before any firm conclusions can be drawn further investigations are required. Initially these investigations should concentrate on determining the adequacy of the TSWT and lag-entrainment boundary layer codes in coping with shock-boundary layer interactions.

12.3 Other Findings

12.3.1 New Flexible Walls

The new flexible walls, which have been installed recently, have an improved jack/wall link mechanism designed to eliminate some weaknesses which had become apparent in the flexure design used by the original walls. Subsequent tests have demonstrated that the objectives of the new design have been fulfilled and that the new flexible walls exhibit no operational difficulties of a mechanical nature.

12.3.2 Aerodynamically Straight Wall Contours

The reference speed at which satisfactory aerodynamically straight contours were obtained using the original flexible walls was limited by the sensitivity of Mach number to flow area and by the consequences of the weaknesses in the jack/wall flexure design. However, it is believed that the new flexible walls with their jack/wall link mechanism will probably enable the determination of aerodynamically straight contours which could be used for model tests up to a reference Mach number of unity. It is expected that tests aimed at defining such contours will commence in the near future.

12.4 Concluding Remarks

A substantial body of aerodynamic data has been gathered which further illustrates the favourable effects of wall streamlining and the inherent advantages of using a shallow flexible walled test section in two-dimensional testing. Prior to this work the principle of wall streamlining had been successfully demonstrated at low speeds and up to transonic speeds where the flow at the streamlined walls remains subcritical. However, during the course of this work it has been demonstrated that the principle is still applicable and can be successfully applied in flexible walled test sections at conditions where

supercritical flow has penetrated the contoured walls and intruded into the imaginary flowfields. The procedures for wall streamlining at such conditions have been established and are relatively simple. Although there is some doubt about the adequacy of the available boundary layer codes in coping with the inevitable shock-boundary layer interactions, the procedures have enabled the demonstration of wall streamlining at conditions up to those which result in a peak Mach number of about 1.5 at the flexible walls.

The development of the adaptive flexible wall technique in two-dimensional testing is nearing maturity. An area of future development could be two-dimensional testing through the speed of sound. However, future flexible wall research will largely concentrate on three-dimensional testing since the advent of a three-dimensional wall interference-free transonic test section is eagerly awaited. Present research at the University of Southampton is aimed at the development of a technique which would utilise the two-dimensional test section of the TSWT to obtain a three-dimensional test environment in which the level of test section boundary interference can be assessed and is correctable.

13. PRINCIPAL CONCLUSIONS

1. Several transonic wall adjustment strategies have been evaluated in the TSWT by test section wall streamlining around a two-dimensional aerofoil model, with a ratio of test section height to model chord of about 1.5, over a range of test conditions in which the flow at the contoured walls remained subcritical. The applicable test regime of each strategy has been approximately defined.

2. The first documented wall adjustment strategy was proposed, developed and used by the National Physical Laboratory (NPL) in the early 1940's. TSWT data has indicated that wall streamlining according to the NPL strategy (NPL WAS) results in a *'near'* wall interference-free test environment, giving model performance indistinguishable from that obtained when using modern strategies over a wide range of test conditions.

3. The performance of the recently developed Exact wall adjustment strategy (WAS 2) compares well with the Predictive strategy (WAS 1) which has been used successfully in the TSWT for many years. The Exact strategy, however, does offer several important operational advantages over the Predictive strategy.

4. The imaginary flowfield computations which form an inherent part of the Predictive wall adjustment strategy (WAS 1) are suspect, therefore the streamlining quality of wall contours derived by the strategy is uncertain. A more detailed investigation of the problem is recommended.

5. The present version of the TSWT TSP code has proved to be a practical tool for the computation of the imaginary flowfields. The external velocity distributions predicted by the code are reliable not only at

conditions where supercritical flow and the attendant shocks extend into the imaginary flowfields, but also at reference speeds as low as Mach 0.4.

6. The principle of wall streamlining has been successfully demonstrated in a flexible walled test section at conditions where the model shocks have penetrated the streamlined walls and intruded into the imaginary flowfields. Further investigations are required before being sure of the quality of wall streamlining necessary to obtain satisfactory low levels of wall interference at such conditions. However, appropriate streamlining procedures have been developed and are relatively uncomplicated, enabling flexible walled test sections to easily cope with these high transonic flows.

14. LIST OF SYMBOLS

A1	Lift curve slope per radian
$A_{1\text{-}7}$	TSP transformation parameters
β	Prandtl-Glauert factor $(= (1 - M_\infty^2)^{\frac{1}{2}})$
C or c	Model chord
Cc	Chordwise force coefficient
C_D	Boundary layer pressure drag coefficient (Form drag coefficient)
CL or C_L	Lift coefficient
C_M	Pitching moment coefficient about the leading edge
C_N	Normal force coefficient
CP or C_p	Pressure coefficient
CP*	Sonic pressure coefficient
E	Average of the modulus of the pressure coefficient error between real and imaginary flowfields along a flexible wall
E_{av}	Average value of E from top and bottom walls
E*	Value of E when the perturbations of the imaginary flowfields are artificially set to zero
f'	Slope of aerofoil surface relative to chord line divided by δ
H or h	Test section height
h/c	Ratio of test height to model chord
K	Similarity parameter

L	$1/\Delta X$
M	Mach number
M_∞	Reference Mach number
N	$1/\Delta Z$
P	Normalised circulation
u	Velocity component in the x direction
U_∞	Reference velocity
$V_{(x)}$	Imaginary side velocity at position x
w	Velocity component in the z direction
W	Test section width
x	Co-ordinate in the reference (free stream) direction
X	Transformed co-ordinate in the reference direction
X/C or X_c	Chordwise position relative to the leading edge
y	Local wall displacement (referenced to Aerodynamically Straight)
y_{max}	Greatest positive displacement of a flexible wall
y_{min}	Greatest negative displacement of a flexible wall
Y_c	Model surface displacement from the leading edge
z	Co-ordinate normal to the reference direction
z'	Stretched co-ordinate in the z direction
Z	Transformed co-ordinate normal to the reference direction
α	Angle of incidence
γ	Ratio of specific heats

δ	Ratio of aerofoil thickness to chord
δM	Change in local wall Mach number
δy	Change in local wall displacement
δ^*	Boundary layer displacement thickness
σ	Standard deviation of wall centreline Mach number errors
σ_{av}	Average weighted standard deviation of a pair of walls
ΔX	TSP mesh size in the X direction
ΔZ	TSP mesh size in the Z direction
ϕ	Scaled perturbation potential
Φ	Velocity potential

Subscripts

T	Top wall
B	Bottom wall

15. LIST OF REFERENCES

1. Ongarato, J.R., *'Wind-Tunnel Wall Interference Studies at High Subsonic Speeds'*, Journal of Aircraft, Volume 6, No. 2, March 1969.

2. Treon, S.L., Steinle, F.W., Hagerman, J.R., Black, J.A. and Buffington, R.J., *'Further Correlation of Data from Investigations of a High-Subsonic-Speed Transport Aircraft Model in Three Major Transonic Wind Tunnels'*, AIAA Paper No. 71-291, March 1971.

3. Carter, E.C., *'Some Measurements of Porous Tunnel Wall Interference in the A.R.A. 8' x 9' Tunnel'*, Proceedings of the 35th STA Meeting, L.T.V. Corporation, Texas, March 1971.

4. Bailey, A. and Wood, S.A., *'Further Development of a High-Speed Wind Tunnel of Rectangular Cross-Section'*, British ARC R. and M. No. 1853, September 1938.

5. Lock, C.N.H. and Beavan, J.A., *'Tunnel Interference at Compressibility Speeds using the Flexible Walls of the Rectangular High-Speed Tunnel'*, British ARC R. and M. No. 2005, September 1944.

6. Hilton, W.F., *'High-Speed Aerodynamics'*, Longman Green and Co., Pages 389-391, 1951.

7. Goodyer, M.J., *'The Self Streamlining Wind Tunnel'*, NASA TM X-72699, August 1975.

8. Goodyer, M.J., *'A Low Speed Self Streamlining Wind Tunnel'*. Windtunnel Design and Testing Techniques. AGARD-CP-174, March 1976, pp. 13-1 - 13-8.

9. Wolf, S.W.D. and Goodyer, M.J., *'Self-Streamlining Wind Tunnel: Low Speed Testing and Transonic Test Section Design'*, NASA CR-145257, October 1977.

10. Wolf, S.W.D., *'Self-Streamlining Wind Tunnel Testing and Final Design Studies for the Transonic Facility'*, NASA CR-158900, June 1978.

11. Wolf, S.W.D. and Goodyer, M.J., *'Studies of Self Streamlining Wind Tunnel Real and Imaginary Flows'*, NASA CR-158831, August 1979.

12. Wolf, S.W.D., *'Turbine Blade Cascade Testing in a Flexible Walled Wind Tunnel'*, B.Sc. Honours Project, University of Southampton, April 1975.

13. Goodyer, M.J. and Wolf, S.W.D., *'The Development of a Self-Streamlining Flexible Walled Transonic Test Section'*, AIAA Paper No. 80-0440, March 1980.

14. Wolf, S.W.D., *'Selected Data from a Transonic Flexible Walled Test Section'*, NASA CR-159360, September 1980.

15. Wolf, S.W.D., *'Model and Boundary Aerodynamic Data from High Blockage Two-Dimensional Airfoil Tests in a Shallow Unstreamlined Transonic Flexible Walled Test Section'*, NASA CR-165685, April 1981.

16. Wolf, S.W.D., *'Aerodynamic Data from a Two-Dimensional Cambered Airfoil Section in a Shallow Transonic Flexible Walled Test Section'*, NASA CR-166005, October 1982.

17. Goodyer, M.J., *'Tests on a CAST 7 Two-Dimensional Airfoil in a Self-Streamlining Test Section'*, NASA CR-172291, January 1984.

18. Bailey, A. and Wood, S.A., *'The Development of a High Speed Induced Wind Tunnel of Rectangular Cross-Section'*, British ARC R. and M. No. 1791, February 1937.

19. East, R. A., *'An Investigation into the Flow over a Finite Swept Wing of Low Aspect Ratio at Low Transonic Speeds'*, B.Sc. Honours Project, University of Southampton, April 1957.

20. Beavan, J.A. and Hyde, G.A.M., *'Interim Report on the Rectangular High-Speed Tunnel including Some Pitot Traverse Measurements of Drag of the Aerofoil EC 1250'*, British ARC R. and M. No. 2067, February 1942.

21. Holder, D.W., *'The High-Speed Laboratory of the Aerodynamics Division, N.P.L. - Parts I, II and III'*, British ARC R. and M. 2560 (ARC Monograph), December 1946.

22. Preston, J.H. and Sweeting, N.E., *'Experimental Determination of the Interference on a Large Chord Symmetrical Joukowski Aerofoil Spanning a Closed Tunnel'*, British ARC R. and M. No. 1997, December 1942.

23. Preston, J.H., Sweeting, N.E. and Cox, D.K., *'The Experimental Determination of the Two-Dimensional Interference on a Large Chord Piercy 12/40 Aerofoil in a Closed Tunnel Fitted with a Flexible Roof and Floor'*, British ARC R. and M. No. 2007, September 1944.

24. Hartshorn, A.S. and Squire, H.B., *'Notes on a Visit to Southern Germany, Aug. 10-22 to Investigate German Aerodynamic Research on Cooling Ducts'*, RAE TN Aero. 1694, May 1946.

25. Smelt, R., *'A Critical Review of German Research on High-Speed Airfoil'*, The Royal Aeronautical Society, 696th Lecture, Decmeber 1946.

26. Goethert, B.H., *'Transonic Wind Tunnel Testing'*, Pergamon Press, Page 46, 1961.

27. Ferri, A. and Baronti, P., *'A Method for Transonic Wind Tunnel Conditions'*, AIAA Journal, Volume 11, No. 1, January 1973.

28. Tuttle, M.H. and Mineck, R.E., *'Adaptive Wall Wind Tunnels--A Selected, Annotated Bibliography'*, NASA TM-87639, August 1986.

29. Ganzer, U., *'Advances in Adaptive Wall Wind Tunnel Technique'*, Presented at the International Symposium on *'Recent Advances in Aerodynamics and Aeroacoustics'*, Stanford, California, August 1983.

30. Vidal, R.J. and Erickson, J.C., *'Research on Adaptive Wall Wind Tunnels'*, AEDC-TR-78-36, November 1978.

31. Erickson, J.C. and Homicz, G.F., *'Numerical Simulations of a Segmented-Plenum, Perforated, Adaptive-Wall Wind Tunnel'*, AIAA Journal, Volume 20, No. 5, May 1982.

32. Sears, W.R., *'Self-Correcting Wind Tunnels'*, 16th Lanchester Lecture (Royal Aeronautical Society), May 1973.

33. Vidal, R.J., Erickson, J.C. and Catlin, P.A., *'Experiments with a Self-Correcting Wind Tunnel'*. Wind Tunnel Design and Testing Techniques, AGARD Conference Proceedings, No. 174, March 1976, pp. 11-1 - 11-13.

34. Sears, W.R., Vidal, R.J., Erickson, J.C. and Ritter, A., *'Interference-Free Wind Tunnel Flows by Adaptive-Wall Technology'*, Journal of Aircraft, Volume 14, No. 11, November 1977.

35. Vidal, R.J. and Erickson, J.C., *'Experiments on Supercritical Flows in a Self-Correcting Wind Tunnel'*, AIAA Paper 78-788, April 1978.

36. Erickson, J.C., Wittliff, C.E. and Daughtry, D.C., *'Further Investigations of Adaptive-Wall Wind Tunnels'*, AEDC TR-80-34, October 1980.

37. Erickson, J.C., Wittliff, C.E., Padova, C. and Hamicz, C.F., *'Adaptive-Wall Wind Tunnel Investigations'*, Contract N00014-77-C-0052, Calspan Report No. RK-6040-A-2, February 1981.

38. Lo, C.F. and Kraft, E.M., *'Convergence of the Adaptive-Wall Wind Tunnel'*, AIAA Journal, Volume 16, No. 1, January 1978.

39. Kraft, E.M. and Parker, R.L., *'Experiments for the Reduction of Wind Tunnel Wall Interference by Adaptive-Wall Technology'*, AEDC TR-79-51, October 1979.

40. Parker, R.L. and Sickles, W.L., *'Two-Dimensional Adaptive-Wall Experiments'*, AEDC TR-80-63, February 1981.

41. Parker, R.L. and Sickles, W.L., *'Application of the Adaptive Wall Concept in Three Dimensions'*, Journal of Aircraft, Volume 18, No. 2, March 1981.

42. Parker, R.L. and Erickson, J.C., *'Development of Three-Dimensional Adaptive Wall Test Section with Perforated Walls'*, AGARD CP 335, Paper No. 17, May 1982.

43. Parker, R.L. and Erickson, J.C., *'Status of Three-Dimensional Adaptive-Wall Test Section Development at AEDC'*, AIAA 84-0624, March 1984.

44. McDevitt, J.B., Polek, T.E. and Hand, L.A., *'A New Facility and Technique for Two-Dimensional Aerodynamic Testing'*, Journal of Aircraft, Volume 20, No. 6, June 1983.

45. Davis, S.S., *'A Compatibility Assessment Method for Adaptive-Wall Wind Tunnels'*, AIAA Journal, Volume 20, No. 9, September 1981.

46. Schairer, E.T., *'Two-Dimensional Wind-Tunnel Interference from Measurements on Two Contours'*, Journal of Aircraft, Volume 21, No. 6, June 1984.

47. Satyanarayana, B., Schairer, E.T. and Davis, S.S., *'Adaptive-Wall Wind Tunnel Development for Transonic Testing'*, AIAA 80-0441, March 1980.

48. Bodapati, S. and Celik, Z.Z., *'Optimization Studies for the Development of an Adaptive Wall Wind Tunnel'*, Paper presented at the 11th International Congress on Instrumentation in Aerospace Simulation Facilities, Stanford, California, August 1985.

49. Schairer, E.T. and Mendoza, J.P., *'Adaptive-Wall Wind Tunnel Research at Ames Research Center'*, AGARD CP-335, May 1982.

50. Judd, M., Wolf, S.W.D. and Goodyer, M.J., *'Analytical Work in Support of the Design and Operation of Two-Dimensional Self Streamlining Test Sections'*, NASA CR-145019, July 1976.

51. Bateman, I.D., *'A Low Speed Flexible Walled Test Section for Infinite Swept Wings'*, B.Sc. Honours Project, University of Southampton, April 1986.

52. Chevallier, J.P., *'Adaptive Wall Transonic Wind Tunnels (Soufflerie Trassonique a Parois Auto-Adaptables)'*, AGARD CP-174, March 1976, pp. 12-1 - 12-8.

53. Chevallier, J.P., *'Self-Correcting Walls for a Transonic Wind Tunnel'*, NASA TT F-17254, October 1976.

54. Chevallier, J.P., Mignosi, A., Archambaud, J.P. and Seraudie, A., *'T2 Wind Tunnel Adaptive Walls - Design, Construction, and Some Typical Results'*, La Recherche Aerospatiale, No. 4, July/August 1983.

55. Archambaud, J.P. and Chevallier, J.P., *'Use of Adaptive Walls in 2-D Tests'* NASA TM-77380, February 1984.

56. Mignosi, A. and Archambaud, J.P., *'Adaptive Wall Technique of T2 Cryogenic Wind Tunnel'*, Paper presented at the Euromech Colloquium, Göttingen, October 1984.

57. Dor, J.B., *'The T2 Cryogenic Induction Tunnel in Toulouse'*, AGARD R-722, April 1985.

58. Ganzer, U., *'Adaptable Wind Tunnel Wall for 2D and 3D Model Tests'*, ICAS Paper 23-3, October 1980.

59. Ganzer, U., *'On the Use of Adaptive Walls for Transonic Wind Tunnel Testing'*, AGARD CP 335, May 1982.

60. Kilgore, R.A., *'The NASA Langley 0.3-m Transonic Cryogenic Tunnel'*, AGARD R-772, April 1985.

61. Ladson, C.L., *'A New Airfoil Capability'*. Advanced Technology Airfoil Research, Volume 1, NASA CP-2045, Part 1, March 1979.

62. Wolf, S.W.D. and Goodyer, M.J., *'Predictive Wall Adjustment Strategy for Two-Dimensional Flexible Walled Adaptive Wind Tunnel. A Detailed Description of the First One-Step Method'*, AASU Memo 85/12, January 1986.

63. Judd, M., Goodyer, M.J. and Wolf, S.W.D., *'Application of the Computer for On-Site Definition and Control of Wind Tunnel Shape for Minimum Boundary Interference'*, Presented at AGARD Specialists' Meeting on *'Numerical Methods and Windtunnel Testing'*, AGARD-CP-210, June 1976.

64. Wolf, S.W.D., *'Control Software for Two-Dimensional Airfoil Tests Using a Self-Streamlining Flexible Walled Transonic Test Section'*, NASA CR-165941, August 1982.

65. Wolf, S.W.D., *'The Design and Operational Development of Self-Streamlining Two-Dimensional Flexible Walled Test Sections'*, NASA CR-172328, March 1984.

66. Gruzdev, A.A., *'On Low-Speed Wind Tunnels with Deformable Boundaries'*, Soviet Aeronautics, Volume 23, No. 4, 1980.

67. Wedemeyer, E., Heddergott, A. and Kuczka, D., *'Deformable Adaptive Wall Test Section for Three-Dimensional Wind Tunnel Testing'*, Journal of Aircraft, Volume 22, No. 12, December 1985.

68. Ganzer, U., Igeta, Y. and Ziemann, J., *'Design and Operation of TU-Berlin Wind Tunnel with Adaptable Walls'*, ICAS Paper 84-2.1.1, September 1984.

69. Archambaud, J.P., Dor, J.B., Mignosi, A. and Lamarche, L., *'First Tests of the Two-Dimensional Automatic Wall Adaptation of the T2 Windtunnel Using Three-Dimensional Models'*, DERAT 11/5015 DN, September 1985.

70. Lamarche, L. and Wedemeyer, E., *'Minimisation of Wall Interference for Three-Dimensional Models with Two-Dimensional Wall Adaptation'*, VKI TN 149, March 1984.

71. Harney, D.J., *'Three-Dimensional Test Experience with a Transonic Adaptive-Wall Wind Tunnel'*, AFWAL-TR-83-3028, March 1983.

72. Harney, D.J., *'Three-Dimensional Testing in a Flexible-Wall Wind Tunnel'*, Presented at the AIAA 13th Aerodynamic Testing Conference, San Diego, California, March 1984.

73. Smith, J., *'A Theoretical Exploration of the Capabilities of 2D Flexible Walled Test Sections for 3D Testing'*, NLR MP 84018U, February 1984.

74. Kemp, W.B., *'Transonic Assessment of Two-Dimensional Wind Tunnel Wall Interference Using Measured Wall Pressures'*. Advanced Technology Airfoil Research--Volume I, NASA CP-2045, Part 2, March 1979, pp. 473-486.

75. Kemp, W.B., *'TWINTAN: A Program for Transonic Wall Interference Assessment in Two-Dimensional Wind Tunnels'*, NASA TM-81819, 1980.

76. Ashill, P.R. and Weeks, D.J., *'A Method for Determining Wall-Interference Corrections in Solid-Wall Tunnels from Measurements of Static Pressure at the Walls'*, RAE TR 82091, May 1982.

77. Gopinath, R., *'Wall Interference Evaluation from Pressure Measurements on Control Surfaces'*, Journal of Aircraft, Volume 19, No. 2, December 1982.

78. Kemp, W.B. and Adcock, J.B. *'Combined Four-Wall Interference Assessment in Two-Dimensional Airfoil Tests'*, AIAA Journal, Volume 21, No. 10, October 1983.

79. Mokry, M., Chan, Y.Y. and Jones, D.J., *'Two-Dimensional Wind Tunnel Wall Interference'*, AGARD AG 281, November 1983.

80. Kemp, W.B., *'TWINTN4: A Program for Transonic Four-Wall Interference Assessment in Two-Dimensional Wind Tunnels'*, NASA CR-3777, May 1984.

81. Gumbert, C.R. and Newman, P.A., *'Validation of a Wall Interference Assessment/Correction Procedure for Airfoil Tests in the Langley 0.3-m Transonic Cryogenic Tunnel'*, AIAA-84-2151, August 1984.

82. Ashill, P.R. and Keating, R.F.A., *'Calculation of Tunnel Wall Interference from Wall-Pressure Measurements'*, RAE TR 85086, October 1985.

83. Elsenaar, A. and Stanewsky, E., *'Two-Dimensional Transonic Testing Methods'*, Paper No. 5, AGARD CP 335, May 1982.

84. Smith J., *'Measured Boundary Conditions Methods for 2D Flow'*, Paper No. 9, AGARD-CP-335, May 1982.

85. Goodyer, M.J., *'Extraction of Model Performance from Wall Data in a Two-Dimensional Transonic Flexible Walled Test Section'*, NASA CR-165994, September 1982.

86. Kemp, W.B., *'Toward the Correctable-Interference Transonic Wind Tunnel'*, AIAA 9th Aerodynamic Testing Conference, June 1976.

87. Goodyer, M.J., *'Developments in Airfoil Testing at the University of Southampton'*. Advanced Technology Airfoil Research--Volume 1, NASA CP-2045, Part 1, March 1979, pp. 415-423.

88. Holder, D.W. and North, R.J., *'The 9 inch x 3 inch NPL Induced-Flow High Speed Wind Tunnel'*, ARC TP 285, June 1949.

89. Braslow, A.L. and Knox, E.C., *'Simplified Method for Determination of Critical Height of Distributed Roughness Particles for Boundary-Layer Transition at Mach Numbers from 0 to 5'*, NACA TN 4363, September 1958.

90. Lewis, M.C., *'The Status of Two-Dimensional Testing at High Transonic Speeds in the University of Southampton Transonic Self-Streamlining Wind Tunnel'*, NASA CR-3919, October 1985.

91. Lewis, M.C., *'An Evaluation in a Modern Wind Tunnel of the Transonic Adaptive Wall Adjustment Strategy Developed by NPL in the 1940's'*, AASU Memo. No. 86/11, December 1986.

92. Judd, M., *'An Exact Strategy for Flexible Wall Adjustment in Two-Dimensional Compressible Flow'*. NASA CR-181661, March 1981.

93. Judd, M., *'FLEXIWALL 3 SO: A Second Order Predictive Strategy for Rapid Wall Adjustment in Two-Dimensional Compressible Flow'*. NASA CR-181662, July 1981.

94. Norman, R.A., *'Implementation of "Rapid Wall Adjustment Strategy" to Flexible Walled Wind Tunnel'*, B.Sc Honours Project, University of Southampton, May 1983.

95. Piercy, N.A.V., *'Aerodynamics'*, English Universities Press, pp. 105-9, Revised Impression 1950.

96. Pankhurst, R.C. and Holder, D.W., *'Wind-Tunnel Technique (An Account of Experimental Methods in Low and High-Speed Wind Tunnels)'*, Sir Isaac Pitman and Sons, pp. 384-6, 1952.

97. Cobb, S.M., *'The Interference due to the Walls of a Two-Dimensional Wind Tunnel with some Attempts to Reduce it'*, M.Sc. Thesis, University of Southampton, March 1953.

98. Donovan, A.F., Lawrence, H.R., Goddard, F.E. and Gilruth, R.R., *'High Speed Problems of Aircraft and Experimental Methods'*, Volume 8 (High Speed Aerodynamics and Jet Propulsion), Princeton University Press, p. 47, 1961.

99. Mason, B.I.F., *'Development of a Program for the Flexible Wall Tunnel at Transonic Speeds'*, B.Sc Honours Project, University of Southampton, May 1980.

100. Spurr, A., *'A Computational and Experimental Study of Fully Three-Dimensional Transonic Flow in Turbomachinery'*, Ph.D. Thesis, University of Southampton, March 1980.

101. Denton, J.D., *'A Time Marching Method for Two and Three-Dimensional Blade to Blade Flows'*, British ARC R. and M. No. 3775, 1974.

102. Grossman, B. and Moretti, G., *'Time-Dependent Computation of Transonic Flows'*, AIAA Paper 70-1322, October 1970.

103. Magnus, R. and Yoshihara, H., *'Inviscid Transonic Flow over Airfoils'*, AIAA Journal, Volume 8, No. 12, December 1970.

104. Murman, E.M. and Cole, J.D., *'Calculation of Plane Steady Transonic Flows'*, AIAA Paper 70-188, January 1970.

105. Krupp, J.A., *'The Numerical Calculation of Plane Steady Transonic Flows Past Thin Lifting Aerofoils'*, Ph.D. Thesis, University of Washington, 1971.

106. Steger, J.L. and Lomax, H., *'Transonic Flow about Two-Dimensional Airfoils by Relaxation Procedures'*, AIAA Journal, Volume 10, No. 1, January 1972.

107. Krupp, J.A. and Murman, E.M., *'Computation of Transonic Flows Past Lifting Airfoils and Slender Bodies'*, AIAA Journal, Volume 10, No. 7, July 1972.

108. Murman, E.M., *'Computational Methods for Inviscid Transonic Flows with Imbedded Shock Waves'*, Boeing Scientific Research Laboratory, D1-82-1053, February 1971.

109. Emmons, H.W., *'The Numerical Solution of Compressible Fluid Flow Problems'*, NACA TN 932, 1944.

110. Emmons, H.W., *'The Theoretical Flow of a Frictionless, Adiabatic, Perfect Gas Inside of a Two-Dimensional Hyperbolic Nozzle'*, NACA TN 1003, 1946.

111. Emmons, H.W., *'Flow of a Compressible Fluid Past a Symmetrical Airfoil in a Wind Tunnel and in Free Air'*, NACA TN 1746, 1948.

112. Albone, C.M., Catherall, D., Hall, M.G. and Gaynor Joyce, *'An Improved Numerical Method for Solving the Transonic Small-Perturbation Equation for the Flow Past a Lifting Aerofoil'*, RAE TR 74056, August 1974.

113. Catherall, D., *'Solution of the Transonic Small-Perturbation Equation for Two-Dimensional Flow Past Aerofoils in Wind Tunnels'*, RAE TR 80120, October 1980.

114. Garabedian, P.R. and Korn, D.G., *'Analysis of Transonic Airfoils'*, Communications on Pure and Applied Mathematics, Volume XXIV, 1971.

115. Lewis, M.C., *'The Status of Analytical Preparation for Two-Dimensional Testing at High Transonic Speeds in the University of Southampton Transonic Self-Streamlining Wind Tunnel'*, NASA CR-3785, March 1984.

116. Keith, J.S., Ferguson, D.R. and Heck, P.H., *'Users Manual for Streamtube Curvature Analysis. Analytical Method for Predicting the Pressure Distribution about a Nacelle at Transonic Speeds'*, NASA CR-112239, Volumes 1, 2, and Appendix, 1972.

117. Goodyer, M.J., *'Computation of Imaginary-Side Pressure Distributions over the Flexible Walls of the Test Section Insert for the 0.3-m Transonic Cryogenic Tunnel'*, NASA CR-172363, June 1984.

118. Wolf, S.W.D., Goodyer, M.J. and Cook, I.D., *'Streamlining the Walls of an Empty Two-Dimensional Flexible-Walled Test Section'*, NASA CR-165936, May 1982.

119. Lewis, M.C., *'Empty Test Section Streamlining of the Transonic Self-Streamlining Wind Tunnel Fitted with New Walls'*, AASU Memo No. 86/10, June 1986.

120. Green, J.E., *'Interactions Between Shock Waves and Turbulent Boundary Layers'*, RAE TR 69098, May 1969.

121. Green, J.E., Weeks, D.J. and Brooman, J.W.F., *'Prediction of Turbulent Boundary Layers and Wakes in Compressible Flow by a Lag-Entrainment Method'*, Rept. No. ARC-R/M-3791, 1977. (Supersedes RAE TR-72231, 1973.)

122. Green, J.E., *Application of Head's Entrainment Method to the Prediction of Turbulent Boundary Layers and Wakes in Compressible Flow'*, British ARC R. and M. No. 3788, April 1972.

123. Head, M.R., *'Entrainment in the Turbulent Boundary Layer'*, British ARC R. and M. No. 3152, 1958.

124. Reshotko, E. and Tucker, M., *'Effect of a Discontinuity on Turbulent Boundary-Layer-Thickness Parameters with Application to Shock-Induced Separation'*, NACA TN 3454, 1955.

125. Ladson, C.L., *'Description and Calibration of the Langley 6-by-19-Inch Transonic Tunnel'*, NASA TN D-7182, 1973.

126. Preston, J.H., *'The Interference on a Wing Spanning a Closed Tunnel Arising from the Boundary Layers on Side Walls, with Special Reference to the Design of Two-Dimensional Tunnels'*, British ARC R. and M. 1924, 1944.

127. Bernard-Guelle, R., *'Influence of Wind Tunnel Wall Boundary Layers on Two-Dimensional Transonic Tests'*, NASA TT F-17,255, October 1976.

128. Ashill, P.R., *'Effects of Sidewall Boundary Layers on Aerofoils Mounted from Sidewalls of Wind Tunnels - Experimental Evidence and Developments of Theory'*, RAE TR-83065, August 1983.

129. Barnwell, R.W., *'A Similarity Rule for Compressibility and Sidewall Boundary Layer Effects in Two-Dimensional Wind Tunnels'*, AIAA Paper No. 79-0108, January 1979.

130. Winter, K.G. and Smith, J.H.B., *'A Comment on the Origin of Endwall Interference on Wind Tunnel Tests of Aerofoils'*, RAE TM Aero. 1816, August 1979.

131. Sewall, W.G., *'The Effects of Sidewall Boundary Layers in Two-Dimensional Subsonic and Transonic Wind Tunnels'*, AIAA 81-1297, June 1981.

132. Barnwell, R.W. and Sewall, W.G., *'Similarity Rules for Effects of Sidewall Boundary Layer in Two-Dimensional Wind Tunnels'*, Paper 3, AGARD CP-335, 1982.

133. Murthy, A.V., *'Corrections for Attached Sidewall Boundary-Layer Effects in Two-Dimensional Airfoil Testing'*, NASA CR-3873, February 1985.

134. Murthy, A.V., Johnson, C.B., Ray, E.J., Lawing, P.L. and Thibodeaux, J.J., *'Investigations of Upstream Sidewall Boundary Layer Removal Effects on a Supercritical Airfoil'*, AIAA Paper No. 83-0386, January 1983.

135. Melnik, R.E., Chow, R. and Mead, H.R., *'Theory of Viscous Transonic Flow Over Airfoils at High Reynolds Number'*, AIAA 77-680, June 1977.

136. Melnik, R.E., Mead, H.R. and Jameson, A., *'A Multi-Grid Method for the Computation of Viscid/Inviscid Interaction on Airfoils'*, AIAA 83-0234, January 1983.

137. Steinhoff, J. and Jameson, A., *'Multiple Solutions of the Transonic Potential Flow Equation'*, AIAA 81-1019, June 1981.

138. Salas, M.D., Jameson, A. and Melnik, R.E., *'A Comparative Study of the Nonuniqueness Problem of the Potential Equation'*, AIAA 83-1888, July 1983.

139. Savada, H., *'A General Correction Method of the Interference in 2-Dimensional Wind Tunnels with Ventilated Walls'*, Japan Society for Aeronautical and Space Sciences, Volume 21, No. 52, 1978.

140. Mokry, M., *'Application of the Fast Fourier Transform to Two-Dimensional Wind Tunnel Wall Interference'*, Journal of Aircraft, Volume 17, No. 6, June 1980.

141. Smith, J., *'A Method for Determining 2D Wall Interference on an Aerofoil from Measured Pressure Distributions near the Walls and on the Model'*, NLR TR-81016-U, January 1981.

142. Tuttle, M.H. and Plentovich, E.B., *'Adaptive Wall Wind Tunnels— A Selected, Annotated Bibliography'*, NASA TM-84526, November 1982.

16. LIST OF TABLES

17. LIST OF FIGURES

Fig.7.1 TSP Computing Planes (X,Z).

Fig.7.2 RAE Test Case.

Fig.7.3 The Effect of Variations in Similarity Parameter (K).

Fig.7.4 TSWT Test Case Comparison (Run 184 - $M_\infty = 0.8862$; $\alpha \simeq 4.0^o$).

Fig.7.5 Wall Representation Schemes (Run 184 - Top Wall).

Fig.7.6 Flow Diagram of TSWT TSP Code.

Fig.7.7 10% Circular Arc Aerofoil Comparison (Zero Incidence).

Fig.7.8a Imaginary Flow Predictions by Several Computational Methods (Condition 1: $M_\infty = 0.6025$; $\alpha \simeq 6.0^o$).

Fig.7.8b Imaginary Flow Predictions by Several Computational Methods (Condition 2: $M_\infty = 0.6998$; $\alpha \simeq 6.0^o$).

Fig.7.8c Imaginary Flow Predictions by Several Computational Methods (Condition 3: $M_\infty = 0.7981$; $\alpha \simeq 6.0^o$).

Fig.8.1 Distributions of Mach Number Along Centrelines of Walls Set to Aerodynamically Straight Contours (Empty Test Section). Original Walls.

Fig.8.2 Distributions of Mach Number Along Centrelines of Walls Set to Aerodynamically Straight Contours (Empty Test Section). New Walls.

Fig.8.3 Displacements of Walls from Geometrically Straight. Walls Set to Contours that Exhibit Constant Wall Mach Number ($M_\infty = 0.6$).

Fig.8.4 Wall Movements Apart from Geometrically Straight. Walls Set to Aerodynamically Straight Contour (Contour D).

Fig.9.1 Calculations of $\Delta\delta^*$ Along Top Wall of Run 184 ($M_\infty = 0.8862$; $\alpha \simeq 4.0^o$).

Fig.9.2 NACA 0012-64 Measurements (Run 235 - $M_\infty = 0.8$; $\alpha \simeq 4.0^o$). Calculations of $\Delta\delta^*$ Along Flexible Walls. Walls Streamlined by the WAS 2A Strategy.

Fig.9.3 The Effects of an Allowance for δ^* Variations on Model Pressure Distribution. Walls Streamlined by the WAS 2A Strategy.

Fig.9.4 Calculations of $\Delta\delta^*$ Along Bottom Wall of Run 184 ($M_\infty = 0.8862$; $\alpha \simeq 4.0^o$).

Fig.9.5 Imaginary Wall Mach Number Distributions Calculated by the TSWT TSP Code at Run 184 Conditions ($M_\infty = 0.8862$; $\alpha \simeq 4.0^o$).

Fig.10.1 Model Pressure Distributions ($M_\infty = 0.7$; $\alpha \simeq 4.0^o$). Walls Set to Aerodynamically Straight, Constant Pressure and Streamlined (NPL WAS) Contours.

Fig.10.2 Schlieren Pictures Illustrating the Effects of Wall Streamlining.

Fig.10.3 Model Pressure Distributions ($M_\infty = 0.7$; $\alpha \simeq 4.0^o$). Walls Set to Streamlined Contours.

Fig.10.4 NACA 0012-64 Measurements ($M_\infty = 0.7$; $\alpha \simeq 4.0^o$). Distributions of Mach Number Along Centrelines of Aerodynamically Straight and Streamlined Contours.

Fig.10.5 NACA 0012-64 Measurements ($M_\infty = 0.7$; $\alpha \simeq 4.0^o$). Displacements of Walls from Aerodynamically Straight Contours. Walls Streamlined.

Fig.10.6 NACA 0012-64 Measurements ($M_\infty = 0.7$; $\alpha \simeq 4.0^o$). Total Wall Movements Apart from Aerodynamically Straight Contours. Walls Streamlined.

Fig.10.7.1 NACA 0012-64 Section. Variation of Normal Force Coefficient with Mach Number. Walls Streamlined (WAS 1, WAS 2, NPL WAS).

Fig.10.7.2 NACA 0012-64 Section. Variation of Normal Force Coefficient with Mach Number. Walls Streamlined (WAS 1, WAS 2A, WAS 1A, WAS 1B).

Fig.10.8 Model Pressure Distributions ($M_\infty = 0.8^O$; $\alpha \simeq 6.0^O$). Walls Set to Streamlined Contours.

Fig.10.9 Model Pressure Distributions ($M_\infty = 0.8^O$; $\alpha \simeq 0.5^O$). Walls Set to Streamlined Contours.

Fig.10.10 NACA 0012-64 Measurements ($M_\infty = 0.8$; $\alpha \simeq 0.5^O$). Distributions of Mach Number Along Centrelines of Streamlined Contours.

Fig.10.11 Schlieren Pictures Illustrating the Break-Down of NPL WAS.

Fig.10.12 NACA 0012-64 Measurements ($M_\infty = 0.7$; $\alpha \simeq 6.0^O$). Wall Contours Set During a Streamlining Cycle Governed by the WAS 2 Strategy.

Fig.10.13.1 NACA 0012-64 Measurements ($\alpha \simeq 0.5^O$). Distribution of Mach Numbers Along Centrelines of Walls Set to Constant Pressure Contours.

Fig.10.13.2 NACA 0012-64 Measurements ($\alpha \simeq 2.0^O$). Distribution of Mach Numbers Along Centrelines of Walls Set to Constant Pressure Contours.

Fig.10.13.3 NACA 0012-64 Measurements ($\alpha \simeq 4.0^O$). Distribution of Mach Numbers Along Centrelines of Walls Set to Constant Pressure Contours.

Fig.10.14 NACA 0012-64 Measurements ($M_\infty = 0.7$; $\alpha \simeq 4.0^O$). Displacements of Walls Set to Aerodynamically Straight, Constant Pressure and Streamlined (NPL WAS) Contours.

Fig.10.15 Model Pressure Distributions ($M_\infty = 0.8$; $\alpha \simeq 6.0^O$). Walls Set to Wake Pinch Test Contours.

Fig.11.1 NACA 0012-64 Measurements ($M_\infty = 0.9062$; $\alpha \simeq 4.0^o$). Distributions of Real and Imaginary Mach Number Along Centrelines of Contoured Walls (Original Walls).

Fig.11.2 NACA 0012-64 Measurements ($M_\infty = 0.9543$; $\alpha \simeq 4.0^o$). Distributions of Real and Imaginary Mach Number Along Centrelines of Contoured Walls (Original Walls).

Fig.11.3 Montage of Real and Imaginary Flowfields ($M_\infty \simeq 0.89$; $\alpha \simeq 4.0^o$).

Fig.11.4 Montage of Real and Imaginary Flowfields ($M_\infty \simeq 0.87$; $\alpha \simeq 4.0^o$). B.L. Allowance.

Fig.11.5 Schlieren Picture with Wall Mach Number Distributions ($M_\infty \simeq 0.89$; $\alpha \simeq 4.0^o$).

Fig.11.6 Schlieren Picture with Wall Mach Number Distributions ($M_\infty \simeq 0.87$; $\alpha \simeq 4.0^o$). B.L. Allowance.

Fig.11.7 NACA 0012-64 Measurements ($M_\infty = 0.8726$; $\alpha \simeq 4.0^o$). Distributions of Real and Imaginary Mach Number Along Centrelines of Streamlined Walls.

Fig.11.8 NACA 0012-64 Measurements ($M_\infty = 0.8726$; $\alpha \simeq 4.0^o$). Displacements of Walls from Aerodynamically Straight Contours. Walls Streamlined.

Fig.11.9 Model Pressure Distributions ($M_\infty \simeq 0.89$; $\alpha \simeq 4.0^o$). Walls Set to Streamlined Contours to Demonstrate Repeatability of Model Data.

Fig.11.10 Model Pressure Distributions ($\alpha \simeq 4.0^o$). The Sensitivity of Model Performance to the Quality of Wall Streamlining.

Fig.11.11 Model Pressure Distributions. Comparison of TSWT Data with Reference Data.

Fig.11.12 NACA 0012-64 Measurements ($M_\infty = 0.8750$; $\alpha \simeq 4.0^o$). Distributions of Wall Mach Number Along Streamlined Walls.

Fig.11.13 Condition of NACA 0012-64 Model After Testing.

Fig.11.14 Model Pressure Distributions ($M_\infty = 0.8$; $\alpha \simeq 6.0^o$). Walls Streamlined by the WAS 1A Strategy.

Fig.11.15 Model Pressure Distributions ($\alpha \simeq 4.0^o$). The Effects of an Allowance for δ^* Variations on Model Pressure Distribution.

Fig.11.16 Imaginary Wall Mach Number Distributions Calculated by the TSWT TSP Code ($M_\infty = 0.8726$; $\alpha \simeq 4.0^o$).

TABLE 1:- ADAPTIVE WALLED TEST SECTIONS (SINCE 1970)

1.1:- 2D CAPABILITY - VENTILATED WALLS

Organisation	Tunnel	Test Section		Max Mach Number	Walls	Adaptation Control	Status
		Cross-Section (HxW)m	Length m				
AEDC (USA)	1ft Tunnel	0.305 x 0.305	0.95	>1.2	2 Perforated 2 Solid	Global + Local Porosity (Various Arrangements)	2D BER Finished
Calspan (USA)	1ft SCWT	0.305 x 0.254	1.42		2 Perforated 2 Solid	10 PCCs - Top 8 PCCs - Bottom	2D AER Finished
NASA Ames (USA)	Indraft Tunnel	0.25 x 0.13	0.736	0.8	2 Slotted 2 Solid	10 PCCs /Wall	2D/3D BER Current
	25 x 11 Tunnel	0.25 x 0.11	0.61	>0.8	2 Slotted 2 Solid	Nominally 10 PCCs/Wall	2D AER Current
	2ft TWT	0.61 x 0.61	1.53	>0.85	2 Slotted 2 Solid	16 PCCs/Wall	2D AER - Current Production - Future

Note: AER - Advanced Exploratory Research
BER - Basic Exploratory Research
PCC - Plenum Chamber Compartments

TABLE 1:- ADAPTIVE WALLED TEST SECTIONS (SINCE 1970)

1.2:- 2D CAPABILITY - FLEXIBLE IMPERMEABLE WALLS

Organisation	Tunnel	Test Section		Max Mach Number	Walls	Adaptation Control	Status
		Cross-Section (HxW)m	Length m				
Genova University (Italy)	Low Deflection Cascade	0.2 x 0.05	1.58	>0.9	2 Flexible 2 solid	33 Jacks/Wall	2D BER Current
	High Deflection Cascade	0.2 x 0.05	1.16	>0.9	2 Flexible 2 Solid	13 Jacks - Top 26 Jacks - Bottom	2D BER Current
NASA Ames (USA)	HRC-2 Tunnel	0.61 x 0.41	2.79	>0.8	2 Flexible 2 Solid	7 Jacks/Wall	2D AER Current
NASA Langley (USA)	0.3-m TCT	0.36 x 0.36	1.417	>1.1	2 Flexible 2 Solid	18 Jacks/Wall	2D Cryogenic AER - Current Production - Future
Northwestern Polytechnical University (China)	NPU 2D SSWT	0.256 x 0.150	1.3	Low speed	2 Flexible 2 Solid	19 Jacks/Wall	2D BER Current

Note: AER - Advanced Exploratory Research
BER - Basic Exploratory Research

TABLE 1:- ADAPTIVE WALLED TEST SECTIONS (SINCE 1970)

1.2:- 2D CAPABILITY - FLEXIBLE IMPERMEABLE WALLS

Organisation	Tunnel	Test Section		Max Mach Number	Walls	Adaptation Control	Status
		Cross-Section (HxW)m	Length m				
ONERA/CERT (France)	S4 LCh Tunnel	0.18 x 0.18	0.75	>1.0	2 Flexible 2 Solid	10 Jacks/Wall	2D BER Finished
	T2 Tunnel	0.37 x 0.39	1.32		2 Flexible 2 Solid	16 Jacks/Wall	2D/3D Cryogenic AER - Current
Southampton University (England)	SSWT 1	0.152 x 0.305	0.697	0.1	2 Flexible 2 Solid	18 Jacks/Wall	2D BER Finished
	SSWT 2	0.152 x 0.305	0.697	0.1	2 Flexible 2 Solid	15 Jacks/Wall	2D Sweep BER Current
	TSWT	0.15 x 0.15	1.12	>1.0	2 Flexible 2 Solid	19 Jacks/Wall	2D/3D AER Current
Technical University of Berlin (Germany)	TUB 1	0.15 x 0.15	0.69	>1.0	2 Flexible 2 Solid	8 Jacks/Wall	2D/3D AER Finished
	TUB 2	0.15 x 0.15	0.99	>1.0	2 Flexible 2 Solid	13 Jacks/Wall	2D/3D AER Current

Note: AER - Advanced Exploratory Research
BER - Basic Exploratory Research

TABLE 1:- ADAPTIVE WALLED TEST SECTIONS (SINCE 1970)

1.3:- 3D CAPABILITY

Organisation	Tunnel	Test Section		Max Mach Number	Walls	Adaptation Control	Status
		Cross-Section (HxW)m	Length m				
AEDC (USA)	1T Tunnel	0.305 x 0.305	0.953	>1.2	4 Perforated	24 Segments/Wall 8 Segments/Sidewall	3D AER Current
AFWAL (USA)	FDL 9 inch SAW	0.229 x 0.229		0.95	2 Flexible (9 Rods/Wall) 2 Solid	13 Jacks/Rod	3D BER Finished
Arizona University (USA)	HLAT	0.51 x 0.51	0.914	0.2	2 Flexible (Venetian Blinds) 2 Solid	16 Panels of Vanes + Variable Angle Nozzle	3D BER Current
DFVLR(1) (Germany)	Rubber Walled Tunnel	0.8 Diameter	2.40	>0.8	Rubber Tube	64 Jacks Total	3D BER Current
Sverdrup Technology (USA)	Automotive Tunnel	0.305 x 0.61	2.44	Low Speed	3 Flexible (12 Segmented Slats/Wall) 1 Solid	17 Jacks/Slat	3D BER Finished
Technical University of Berlin (Germany)	Octagonal Tunnel	0.15 x 0.18	0.83	>1.0	8 Flexible	78 Jacks Total	3D BER Current

Note: AER - Advanced Exploratory Research
BER - Basic Exploratory Research

(1) A new 2D adaptive test section for the DFVLR Ludwieg tube is planned for 1989.

TABLE 2.1:- CO-ORDINATES OF THE NACA 0012-64 SECTION

Section Co-ordinates	
X_c	Y_c
0.0	0.0
0.005	0.0118
0.01	0.0163
0.015	0.0196
0.02	0.0223
0.025	0.0245
0.035	0.0283
0.05	0.0327
0.07	0.0372
0.085	0.04
0.1	0.0424
0.14	0.0475
0.17	0.0505
0.2	0.0529
0.25	0.0561
0.3	0.0583
0.35	0.0596
0.4	0.06
0.45	0.0596
0.5	0.0583
0.55	0.0561
0.6	0.0531
0.65	0.0494
0.7	0.0448
0.75	0.0394
0.8	0.0332
0.85	0.0263
0.9	0.0187
0.95	0.0103
1.0	0.0012

TABLE 2.2:- PRESSURE PORT CO-ORDINATES OF THE NACA 0012-64 SECTION

Pressure Port Co-ordinates			
Upper Surface		Lower Surface	
X_c	Y_c	X_c	Y_c
0.011	0.0177	0.011	0.0182
0.024	0.0235	0.025	0.024
0.048	0.0321	0.05	0.0326
0.077	0.0381	0.074	0.0375
0.098	0.0418	0.098	0.0418
0.152	0.0491	0.151	0.049
0.2	0.0534	0.2	0.0535
0.251	0.0563	0.25	0.0562
0.299	0.0579	0.299	0.0579
0.35	0.0595	0.35	0.0595
0.398	0.06	0.402	0.06
0.448	0.0596	0.449	0.0595
0.499	0.0583	0.5	0.0582
0.549	0.0562	0.552	0.0561
0.599	0.0532	0.601	0.0531
0.649	0.0494	0.649	0.0495
0.698	0.0449	0.702	0.0445
0.749	0.0395	0.751	0.0393
0.799	0.0334	0.801	0.0311
0.848	0.0266	0.85	0.0263
0.902	0.0184	0.9	0.0187
0.949	0.0105	0.95	0.0102

TABLE 3:- QUALITY OF 'AERODYNAMICALLY STRAIGHT' WALL CONTOURS

3.1:- ORIGINAL FLEXIBLE WALLS

Contour	Approx. Mach Number (M_∞)	Designated Mach Number Band	Standard Deviation of Local Mach Number (Wall Centreline)		Average Weighted Standard Deviation (σ_{av})
			Top Wall (σ_T)	Bottom Wall (σ_B)	
1	0.58	up to 0.6	0.0030	0.0028	0.0050
2	0.8	0.6 - 0.85	0.0031	0.0048	0.0049
3	0.89	0.85 - 0.895	0.0048	0.0058	0.0059
4	0.93	0.895 - 0.935	0.0044	0.0066	0.0056
5	0.95	above 0.935	0.0176	0.0200	0.0198

3.2:- NEW FLEXIBLE WALLS

Contour	Approx. Mach Number (M_∞)	Designated Mach Number Band	Standard Deviation of Local Mach Number (Wall Centreline)		Average Weighted Standard Deviation (σ_{av})
			Top Wall (σ_T)	Bottom Wall (σ_B)	
A	0.3	up to 0.35	0.0007	0.0017	0.0040
B	0.4	0.35 - 0.45	0.0014	0.0015	0.0036
C	0.5	0.45 - 0.55	0.0012	0.0020	0.0032
D	0.6	0.55 - 0.65	0.0014	0.0024	0.0032
E	0.7	0.65 - 0.75	0.0023	0.0029	0.0037
F	0.8	above 0.75	0.0029	0.0031	0.0037

TABLE 4:- OFF-CENTRE 'AERODYNAMICALLY STRAIGHT' PERFORMANCE

4.1:- ORIGINAL FLEXIBLE WALLS

Contour	Approx. Mach Number (M_∞)	Standard Deviation of Local Mach Number	
		Top Wall (σ_T)	
		Off-Centre (Orifice 1)	Centreline (Orifice 2)
1	0.58	0.0058	0.0030
2	0.8	0.0086	0.0031
3	0.89	0.0112	0.0048
4	0.93	0.0137	0.0044
5	0.95	0.0289	0.0176

4.2:- NEW FLEXIBLE WALLS

Contour	Approx. Mach Number (M_∞)	Standard Deviation of Local Mach Number					
		Top Wall (σ_T)			Bottom Wall (σ_B)		
		Off-Centre		Centreline	Off-Centre		Centreline
		Orifice 1	Orifice 2	Orifice 3	Orifice 1	Orifice 2	Orifice 3
A	0.3	0.0057	0.0028	0.0007	0.0036	0.0041	0.0017
B	0.4	0.0069	0.0033	0.0014	0.0039	0.0044	0.0015
C	0.5	0.0091	0.0046	0.0012	0.0050	0.0056	0.0020
D	0.6	0.0141	0.0060	0.0014	0.0093	0.0101	0.0024
E	0.7	0.0159	0.0078	0.0023	0.0097	0.0097	0.0029
F	0.8	0.0173	0.0099	0.0029	0.0092	0.0083	0.0031

TABLE 5.1:- SUMMARY OF 'STREAMLINED' DATA (WAS 1)

Reference Number	Model Incidence (Deg)	Reference Mach Number (M_∞)	Model Performance			Residual Interferences(1)			Wall Loadings	
			C_L	C_D	C_M	α Error (Deg)	Camber Error (Deg)	C_p Error	E_T	E_B
1	0.5	0.4024	0.0326	-0.0126	-0.0083	0.0034	-0.0081	-0.0026	0.0040	0.0045
2	0.5	0.4985	0.0330	-0.0127	-0.0068	0.0135	0.0001	0.0022	0.0052	0.0055
3	0.5	0.6006	0.0344	-0.0124	-0.0071	0.0089	-0.0092	-0.0035	0.0096	0.0085
4	0.5	0.7035	0.0363	-0.0117	-0.0066	0.0104	0.0047	-0.0019	0.0034	0.0040
5	0.5	0.8052	0.0444	-0.0098	-0.0073	0.0014	0.0071	0.0026	0.0038	0.0034
6	2.0	0.4040	0.1577	-0.0121	-0.0359	0.0059	0.0049	-0.0042	0.0083	0.0091
7	2.0	0.5041	0.1655	-0.0122	-0.0362	0.0069	0.0035	-0.0066	0.0088	0.0082
8	2.0	0.6047	0.1688	-0.0120	-0.0352	0.0094	0.0124	-0.0041	0.0066	0.0068
9	2.0	0.7011	0.1802	-0.0112	-0.0336	0.0020	-0.0053	-0.0018	0.0047	0.0044
10	2.0	0.8040	0.2128	-0.0048	-0.0394	-0.0041	0.0093	-0.0066	0.0085	0.0077
11	4.0	0.4010	0.3392	-0.0080	-0.0766	0.0078	0.0083	-0.0012	0.0043	0.0053
12	4.0	0.5026	0.3534	-0.0088	-0.0778	0.0003	0.0189	-0.0034	0.0076	0.0076
13	4.0	0.6022	0.3719	-0.0100	-0.0778	-0.0059	0.0031	-0.0035	0.0068	0.0078

Note: (1) Residual Interferences

α Error:- Wall-induced angle of incidence at the aerofoil leading edge.

Camber Error:- Wall-induced camber over the aerofoil chord.

C_p Error:- Streamwise velocity error at the quarter chord point of the aerofoil expressed as an error in pressure coefficient.

TABLE 5.1:- SUMMARY OF 'STREAMLINED' DATA (WAS 1)

Reference Number	Model Incidence (Deg)	Reference Mach Number (M_∞)	Model Performance			Residual Interferences			Wall Loadings	
			C_L	C_D	C_M	α Error (Deg)	Camber Error (Deg)	C_p Error	E_T	E_B
14	4.0	0.7019	0.4333	-0.0074	-0.0829	0.0026	0.0022	-0.0026	0.0072	0.0067
15	4.0	0.8022	0.3417	0.0127	-0.0613	-0.0115	-0.0227	-0.0003	0.0077	0.0059
16	6.0	0.4049	0.5120	0.0009	-0.1138	-0.0032	0.0110	-0.0049	0.0066	0.0049
17	6.0	0.5054	0.5323	-0.0034	-0.1140	0.0064	0.0230	-0.0027	0.0053	0.0061
18	6.0	0.6052	0.5697	-0.0003	-0.1132	-0.0003	0.0209	-0.0031	0.0058	0.0063
19	6.0	0.6998	0.6521	0.0153	-0.1309	0.0112	0.0307	0.0027	0.0042	0.0061
20	6.0	0.7981	0.3851	0.0379	-0.0720	-0.0047	-0.0018	-0.0044	0.0047	0.0050

TABLE 5.2:- SUMMARY OF 'STREAMLINED' DATA (WAS 2)

Reference Number	Model Incidence (Deg)	Reference Mach Number (M_∞)	Model Performance			Residual Interferences			Wall Loadings	
			C_L	C_D	C_M	α Error (Deg)	Camber Error (Deg)	C_p Error	E_T	E_B
1	0.5	0.4019	0.0275	-0.0134	-0.0057	0.0071	-0.0017	-0.0058	0.0046	0.0060
2	0.5	0.5022	0.0324	-0.0130	-0.0066	0.0067	-0.0033	0.0008	0.0026	0.0034
3	0.5	0.6024	0.0331	-0.0127	-0.0066	0.0070	-0.0116	-0.0065	0.0050	0.0075
4	0.5	0.7031	0.0339	-0.0114	-0.0058	0.0138	0.0081	-0.0058	0.0042	0.0064
5	0.5	0.8041	0.0402	-0.0092	-0.0068	-0.0052	-0.0085	0.0016	0.0040	0.0022
6	2.0	0.4029	0.1603	-0.0119	-0.0370	-0.0115	-0.0050	-0.0022	0.0041	0.0028
7	2.0	0.5038	0.1610	-0.0122	-0.0350	0.0129	0.0133	-0.0004	0.0035	0.0044
8	2.0	0.5974	0.1688	-0.0120	-0.0346	0.0048	0.0101	-0.0008	0.0041	0.0044
9	2.0	0.6981	0.1731	-0.0118	-0.0312	-0.0049	0.0031	0.0033	0.0030	0.0045
10	2.0	0.8025	0.2062	-0.0054	-0.0373	-0.0046	0.0061	0.0003	0.0037	0.0031
11	4.0	0.4054	0.3360	-0.0076	-0.0750	-0.0138	-0.0042	0.0037	0.0054	0.0087
12	4.0	0.4983	0.3536	-0.0088	-0.0771	-0.0365	-0.0366	-0.0042	0.0078	0.0057
13	4.0	0.6021	0.3673	-0.0097	-0.0759	-0.0186	0.0004	-0.0005	0.0042	0.0039
14	4.0	0.6966	0.4052	-0.0077	-0.0761	-0.0083	0.0178	0.0007	0.0028	0.0058
15	4.0	0.8017	0.3182	0.0130	-0.0525	-0.0139	0.0040	0.0027	0.0045	0.0072
16	6.0	0.4069	0.5068	0.0005	-0.1107	-0.0282	-0.0041	-0.0020	0.0066	0.0074
17	6.0	0.5044	0.5287	-0.0037	-0.1113	-0.0417	-0.0188	0.0015	0.0069	0.0080

TABLE 5.2:- SUMMARY OF 'STREAMLINED' DATA (WAS 2)

Reference Number	Model Incidence (Deg)	Reference Mach Number (M_∞)	Model Performance			Residual Interferences			Wall Loadings	
			C_L	C_D	C_M	α Error (Deg)	Camber Error (Deg)	C_p Error	E_T	E_B
18	6.0	0.6033	0.5642	-0.0005	-0.1106	-0.0362	-0.0097	-0.0009	0.0072	0.0066
19	6.0	0.7027	0.6423	0.0172	-0.1266	-0.0342	-0.0005	-0.0003	0.0082	0.0063
20	6.0	0.8038	0.3424	0.0385	-0.0553	-0.0155	-0.0201	0.0010	0.0080	0.0046

TABLE 5.3:- SUMMARY OF 'STREAMLINED' DATA (WAS 1A)

Reference Number	Model Incidence (Deg)	Reference Mach Number (M_∞)	Model Performance			Residual Interferences			Wall Loadings	
			C_L	C_D	C_M	α Error (Deg)	Camber Error (Deg)	C_p Error	E_T	E_B
1	0.5	0.4040	0.0296	-0.0131	-0.0066	0.0027	-0.0019	-0.0010	0.0051	0.0072
2	0.5	0.4989	0.0339	-0.0129	-0.0080	0.0077	0.0146	-0.0024	0.0048	0.0061
3	0.5	0.6027	0.0354	-0.0123	-0.0084	0.0074	0.0076	-0.0027	0.0038	0.0051
4	0.5	0.7019	0.0377	-0.0111	-0.0082	0.0140	0.0019	-0.0020	0.0040	0.0044
5	0.5	0.8007	0.0404	-0.0092	-0.0059	0.0078	-0.0118	0.0021	0.0073	0.0061
6	2.0	0.4035	0.1586	-0.0118	-0.0366	-0.0119	-0.0032	-0.0025	0.0037	0.0027
7	2.0	0.5011	0.1570	-0.0123	-0.0330	-0.0097	0.0037	-0.0018	0.0054	0.0067
8	2.0	0.5974	0.1672	-0.0118	-0.0338	-0.0123	0.0062	0.0005	0.0042	0.0052
9	2.0	0.7004	0.1750	-0.0110	-0.0310	0.0057	0.0120	-0.0012	0.0035	0.0042
10	2.0	0.7999	0.2110	-0.0064	-0.0366	0.0000	-0.0043	0.0015	0.0018	0.0021
11	4.0	0.4034	0.3386	-0.0083	-0.0755	-0.0324	-0.0052	0.0001	0.0057	0.0047
12	4.0	0.5036	0.3525	-0.0092	-0.0769	-0.0215	-0.0078	-0.0008	0.0055	0.0061
13	4.0	0.6032	0.3702	-0.0091	-0.0773	-0.0250	-0.0172	0.0013	0.0043	0.0076
14	4.0	0.7010	0.4161	-0.0074	-0.0771	-0.0285	-0.0053	-0.0008	0.0040	0.0049
15	4.0	0.8008	0.3001	0.0150	-0.0477	-0.0031	0.0349	-0.0021	0.0030	0.0044
16	6.0	0.3979	0.5026	0.0009	-0.1109	-0.0456	-0.0247	0.0019	0.0098	0.0092
17	6.0	0.4989	0.5247	-0.0033	-0.1110	-0.0460	-0.0006	0.0019	0.0067	0.0094

TABLE 5.3:- SUMMARY OF 'STREAMLINED' DATA (WAS 1A)

Reference Number	Model Incidence (Deg)	Reference Mach Number (M_∞)	Model Performance			Residual Interferences			Wall Loadings	
			C_L	C_D	C_M	α Error (Deg)	Camber Error (Deg)	C_p Error	E_T	E_B
18	6.0	0.6054	0.5625	-0.0002	-0.1107	-0.0578	-0.0119	0.0009	0.0087	0.0076
19	6.0	0.7004	0.6540	0.0170	-0.1289	-0.0301	0.0007	0.0019	0.0060	0.0095
20	6.0	0.7998	0.3557	0.0386	-0.0588	-0.0479	-0.0109	0.0003	0.0032	0.0030

TABLE 5.4:- SUMMARY OF 'STREAMLINED' DATA (WAS 1B)

Reference Number	Model Incidence (Deg)	Reference Mach Number (M_∞)	Model Performance			Residual Interferences			Wall Loadings	
			C_L	C_D	C_M	α Error (Deg)	Camber Error (Deg)	C_p Error	E_T	E_B
1	0.5	0.3991	0.0278	-0.0131	-0.0063	-0.0002	-0.0016	-0.0008	0.0079	0.0060
2	0.5	0.5013	0.0330	-0.0130	-0.0074	-0.0012	-0.0042	-0.0027	0.0059	0.0059
3	0.5	0.6018	0.0356	-0.0123	-0.0073	0.0017	0.0076	-0.0004	0.0046	0.0040
4	0.5	0.7008	0.0330	-0.0115	-0.0054	0.0084	-0.0002	-0.0002	0.0052	0.0047
5	0.5	0.8008	0.0410	-0.0097	-0.0067	-0.0055	-0.0149	0.0041	0.0032	0.0040
6	2.0	0.4023	0.1592	-0.0119	-0.0370	0.0140	0.0059	-0.0041	0.0052	0.0057
7	2.0	0.5029	0.1676	-0.0117	-0.0380	-0.0017	-0.0087	-0.0028	0.0068	0.0076
8	2.0	0.6042	0.1703	-0.0122	-0.0352	-0.0047	-0.0012	-0.0019	0.0039	0.0028
9	2.0	0.6987	0.1724	-0.0113	-0.0301	0.0068	0.0146	-0.0006	0.0045	0.0052
10	2.0	0.8016	0.2074	-0.0065	-0.0362	-0.0056	-0.0066	0.0027	0.0031	0.0038
11	4.0	0.4035	0.3446	-0.0070	-0.0786	-0.0079	0.0130	0.0021	0.0049	0.0071
12	4.0	0.5030	0.3560	-0.0088	-0.0786	-0.0127	-0.0092	0.0006	0.0046	0.0037
13	4.0	0.6010	0.3701	-0.0099	-0.0769	-0.0132	0.0059	0.0027	0.0024	0.0045
14	4.0	0.6990	0.4194	-0.0075	-0.0778	-0.0050	-0.0222	-0.0058	0.0071	0.0036
15	4.0	0.7997	0.3074	0.0137	-0.0479	-0.0026	-0.0085	-0.0020	0.0023	0.0039
16	6.0	0.4048	0.5069	-0.0001	-0.1106	-0.0386	-0.0130	0.0011	0.0062	0.0079
17	6.0	0.5044	0.5330	-0.0044	-0.1116	-0.0214	-0.0060	0.0000	0.0040	0.0041

TABLE 5.4:- SUMMARY OF 'STREAMLINED' DATA (WAS 1B)

Reference Number	Model Incidence (Deg)	Reference Mach Number (M_∞)	Model Performance			Residual Interferences			Wall Loadings	
			C_L	C_D	C_M	α Error (Deg)	Camber Error (Deg)	C_p Error	E_T	E_B
18	6.0	0.6009	0.5679	-0.0012	-0.1112	-0.0072	0.0033	0.0013	0.0040	0.0053
19	6.0	0.7000	0.6523	0.0176	-0.1290	-0.0050	0.0007	-0.0040	0.0037	0.0054
20	6.0	0.8002	0.3453	0.0386	-0.0531	0.0111	0.0303	0.0011	0.0061	0.0035

TABLE 5.5:- SUMMARY OF 'STREAMLINED' DATA (WAS 2A)

Reference Number	Model Incidence (Deg)	Reference Mach Number (M_∞)	Model Performance			Residual Interferences			Wall Loadings	
			C_L	C_D	C_M	α Error (Deg)	Camber Error (Deg)	C_p Error	E_T	E_B
1	0.5	0.4026	0.0295	-0.0133	-0.0061	0.0037	-0.0047	0.0020	0.0043	0.0019
2	0.5	0.5022	0.0319	-0.0128	-0.0072	0.0054	-0.0081	0.0007	0.0032	0.0035
3	0.5	0.6039	0.0339	-0.0127	-0.0056	0.0036	0.0040	-0.0005	0.0045	0.0043
4	0.5	0.6991	0.0349	-0.0120	-0.0060	-0.0025	-0.0176	-0.0045	0.0054	0.0066
5	0.5	0.8057	0.0410	-0.0089	-0.0064	0.0103	0.0070	0.0024	0.0039	0.0038
6	2.0	0.3997	0.1565	-0.0119	-0.0347	-0.0119	-0.0301	-0.0050	0.0066	0.0047
7	2.0	0.4985	0.1626	-0.0122	-0.0357	0.0113	0.0108	-0.0018	0.0038	0.0041
8	2.0	0.6026	0.1646	-0.0120	-0.0335	0.0020	0.0171	-0.0010	0.0030	0.0031
9	2.0	0.7004	0.1750	-0.0110	-0.0310	0.0132	0.0116	-0.0021	0.0030	0.0040
10	2.0	0.8016	0.2082	-0.0068	-0.0365	0.0061	-0.0049	0.0027	0.0057	0.0045
11	4.0	0.4046	0.3389	-0.0078	-0.0769	-0.0097	-0.0250	-0.0001	0.0076	0.0054
12	4.0	0.4966	0.3539	-0.0086	-0.0788	-0.0260	-0.0253	-0.0001	0.0064	0.0055
13	4.0	0.5994	0.3685	-0.0096	-0.0762	-0.0216	-0.0240	-0.0037	0.0071	0.0059
14	4.0	0.7009	0.4206	-0.0068	-0.0786	-0.0062	0.0105	-0.0010	0.0050	0.0047
15	4.0	0.8015	0.3201	0.0128	-0.0543	0.0051	0.0353	0.0036	0.0066	0.0065

TABLE 6:- SUMMARY OF 'STRAIGHT WALL' DATA

Reference Number	Model Incidence (Deg)	Reference Mach Number (M_∞)	Model Performance			Residual Interferences			Wall Loadings	
			C_L	C_D	C_M	α Error (Deg)	Camber Error (Deg)	C_p Error	E_T	E_B
1	0.5	0.4079	0.0372	-0.0131	-0.0093	-0.0096	-0.0533	-0.0458	0.0342	0.0368
2	0.5	0.5040	0.0391	-0.0130	-0.0076	-0.0080	-0.0371	-0.0493	0.0372	0.0371
3	0.5	0.6001	0.0387	-0.0118	-0.0072	-0.0124	-0.0378	-0.0548	0.0437	0.0430
4	2.0	0.4067	0.1851	-0.0122	-0.0442	-0.1103	-0.4125	-0.0494	0.0509	0.0273
5	2.0	0.5019	0.1959	-0.0117	-0.0450	-0.1150	-0.4158	-0.0480	0.0522	0.0282
6	2.0	0.6064	0.2070	-0.0117	-0.0454	-0.1179	-0.4384	-0.0581	0.0569	0.0320
7	4.0	0.4050	0.4050	-0.0076	-0.0958	-0.2692	-0.9404	-0.0555	0.0760	0.1710
8	4.0	0.4986	0.4334	-0.0082	-0.1030	-0.2766	-0.9849	-0.0578	0.0768	0.0237
9	4.0	0.6002	0.4656	-0.0086	-0.1000	-0.2981	-1.0388	-0.0681	0.0856	0.0264
10	4.0	0.7046	0.4541	0.0202	-0.0896	-0.4360	-1.0966	-0.1219	0.1251	0.0676
11	6.0	0.4044	0.6046	0.0022	-0.1395	-0.4028	-1.4520	-0.0640	0.1008	0.0226
12	6.0	0.5088	0.6580	-0.0031	-0.1470	-0.4385	-1.5397	-0.0692	0.1066	0.0249
13	6.0	0.6121	0.8327	0.0177	-0.1803	-0.6008	-1.9180	-0.1070	0.1482	0.0374
14	6.0	0.7092	0.6725	0.1334	-0.2015	-1.0695	-1.7473	-0.2929	0.3038	0.2105

TABLE 7:- SUMMARY OF LIFT CURVE SLOPES

STREAMLINED WALLS

Wall Adjustment Strategy	Lift Curve Slope per Radian (Al)		
	Mach 0.4	Mach 0.5	Mach 0.6
WAS 1	5.02	5.22	5.61
WAS 2	5.00	5.25	5.56
NPL 1 WAS	5.04	5.33	5.33
NPL 2 WAS	5.01	5.19	5.29
WAS 1A	4.95	5.17	5.53
WAS 1B	5.02	5.23	5.57
WAS 2A	5.07	5.28	5.50

STRAIGHT AND CONSTANT PRESSURE WALLS

Wall Contour	Lift Curve Slope per Radian (Al)		
	Mach 0.4	Mach 0.5	Mach 0.6
Straight	5.96 (+ 19%)	6.41 (+ 23%)	8.22 (+ 47%)
Constant Pressure	4.39 (-12%)	4.47 (-14%)	4.42 (-21%)

Note: Values in brackets are the % changes of lift curve slope when compared with the WAS 1 slope.

TABLE 8:- STREAMLINING QUALITY OF WALL CONTOURS DERIVED BY THE NPL STRATEGY

Test Condition		Quality of Wall Streamlining					
Model Incidence (Deg)	Reference Mach Number (M_∞)	Aerodynamically Straight Contours		NPL 1 WAS Contours		NPL 2 WAS Contours	
		E_T (1)	E_B (1)	E_T (2)	E_B (2)	E_T (2)	E_B (2)
0.5	0.4	0.0342	0.0368	0.0133	0.0161	0.0101	0.0126
	0.5	0.0372	0.0371	0.0135	0.0151	0.0094	0.0126
	0.6	0.0437	0.0430	0.0139	0.0160	0.0111	0.0120
	0.7	0.0437	0.0515	0.0158	0.0178	0.0111	0.0125
	0.8			0.0808	0.0853	0.0237	0.0270
2.0	0.4	0.0509	0.0273	0.0176	0.0147	0.0083	0.0098
	0.5	0.0522	0.0282	0.0155	0.0152	0.0073	0.0114
	0.6	0.0569	0.0320	0.0173	0.0151	0.0095	0.0118
	0.7			0.0194	0.0186	0.0093	0.0153
	0.8			0.0583	0.0733	0.0464	0.0645
4.0	0.4	0.0760	0.1710	0.0209	0.0072	0.0142	0.0063
	0.5	0.0768	0.0237	0.0213	0.0099	0.0113	0.0131
	0.6	0.0856	0.0264	0.0192	0.0123	0.0135	0.0128
	0.7	0.1251	0.0676	0.0264	0.0185	0.0133	0.0178

Note: (1) For aerodynamically straight contours the perturbations in the imaginary flowfields are zero.

(2) When determining wall loading values (E) for NPL contours the TSWT TSP code was used to predict the imaginary flowfields.

Table 9:- STREAMLINING QUALITY OF WALL CONTOURS ADOPTED BY THE WAS 1 STRATEGY

Reference Number	Model Incidence (Deg)	Reference Mach Number (M_∞)	Wall Loadings					
			IMAG 1(1)		TSWT TSP Code		IMAG 2(2)	
			E_T	E_B	E_T	E_B	E_T	E_B
1	0.5	0.4024	0.0040	0.0045	0.0028	0.0030	0.0037	0.0031
2	0.5	0.4985	0.0052	0.0055	0.0059	0.0044	0.0069	0.0059
3	0.5	0.6006	0.0096	0.0085	0.0062	0.0047	0.0064	0.0046
4	0.5	0.7035	0.0034	0.0040	0.0055	0.0059	0.0060	0.0065
5	0.5	0.8052	0.0038	0.0034	0.0104	0.0088	0.0110	0.0093
6	2.0	0.4040	0.0083	0.0091	0.0068	0.0054	0.0056	0.0054
7	2.0	0.5041	0.0088	0.0082	0.0060	0.0044	0.0052	0.0042
8	2.0	0.6047	0.0066	0.0068	0.0031	0.0043	0.0023	0.0044
9	2.0	0.7011	0.0047	0.0044	0.0035	0.0068	0.0039	0.0069
10	2.0	0.8040	0.0085	0.0077	0.0058	0.0047	0.0059	0.0042
11	4.0	0.4010	0.0043	0.0053	0.0098	0.0111	0.0077	0.0109
12	4.0	0.5026	0.0076	0.0076	0.0098	0.0118	0.0080	0.0112
13	4.0	0.6022	0.0068	0.0078	0.0093	0.0108	0.0070	0.0100
14	4.0	0.7019	0.0072	0.0067	0.0074	0.0128	0.0059	0.0116

Note: (1) IMAG 1 - Imaginary flowfield computations embodied in the WAS 1 strategy
(2) IMAG 2 - Imaginary flowfield computations used by the WAS 2 strategy (Equation B.2 of Appendix B)

Table 9:- STREAMLINING QUALITY OF WALL CONTOURS ADOPTED BY THE WAS 1 STRATEGY

Reference Number	Model Incidence (Deg)	Reference Mach Number (M_∞)	Wall Loadings					
			IMAG 1(1)		TSWT TSP Code		IMAG 2(2)	
			E_T	E_B	E_T	E_B	E_T	E_B
15	4.0	0.8022	0.0077	0.0059	0.0074	0.0113	0.0076	0.0121
16	6.0	0.4049	0.0066	0.0049	0.0164	0.0155	0.0143	0.0134
17	6.0	0.5054	0.0053	0.0061	0.0153	0.0178	0.0112	0.0155
18	6.0	0.6052	0.0058	0.0063	0.0151	0.0172	0.0113	0.0156
19	6.0	0.6998	0.0042	0.0061	0.0123	0.0237	0.0101	0.0225
20	6.0	0.7981	0.0047	0.0050	0.0195	0.0149	0.0153	0.0147

Note: (1) IMAG 1 - Imaginary flowfield computations embodied in the WAS 1 strategy
(2) IMAG 2 - Imaginary flowfield computations used by the WAS 2 strategy (Equation B.2 of Appendix B)

TABLE 10:- WALL STREAMLINING CONVERGENCE RATES (WAS 1 AND WAS 2 STRATEGIES)

Reference Number	Model Incidence (Deg)	Nominal Mach Number (M_∞)	Start Contours	WAS 1		WAS 2		
				Iterations	E_{av}	Iterations	Scaling Factor	E_{av}
1	0.5	0.40	Straight	4	0.0042	3	0.65	0.0053
2	0.5	0.50	Straight	2	0.0053	3	0.7	0.0030
3	0.5	0.60	Straight	2	0.0090	2	0.7	0.0062
4	0.5	0.70	$M_\infty = 0.6; \alpha \simeq 0.5^o$	1	0.0037	1	0.7	0.0053
5	0.5	0.75	$M_\infty = 0.7; \alpha \simeq 0.5^o$	1	0.0054	1	0.65	0.0026
6	2.0	0.40	Straight	2	0.0087	2	0.7	0.0069
7	2.0	0.50	Straight	2	0.0085	3	0.7	0.0039
8	2.0	0.60	Straight	3	0.0067	3	0.7	0.0042
9	2.0	0.70	$M_\infty = 0.6; \alpha \simeq 2.0^o$	1	0.0045	0		0.0037
10	2.0	0.80	$M_\infty = 0.7; \alpha \simeq 2.0^o$	1	0.0081	4	0.7	0.0034
11	4.0	0.40	Straight	3	0.0048	4	0.7	0.0070
12	4.0	0.50	Straight	4	0.0076	2	0.7	0.0067
13	4.0	0.60	Straight	4	0.0073	3	0.7	0.0041
14	4.0	0.70	$M_\infty = 0.6; \alpha \simeq 4.0^o$	2	0.0069	1	0.7	0.0038
15	4.0	0.80	$M_\infty = 0.7; \alpha \simeq 4.0^o$	3	0.0068	4	0.65	0.0058

TABLE 10:- WALL STREAMLINING CONVERGENCE RATES (WAS 1 AND WAS 2 STRATEGIES)

Reference Number	Model Incidence (Deg)	Nominal Mach Number (M_∞)	Start Contours	WAS 1		WAS 2		
				Iterations	E_{av}	Iterations	Scaling Factor	E_{av}
16	6.0	0.40	Straight	3	0.0057	5	0.75	0.0070
17	6.0	0.50	Straight	3	0.0057	3	0.7	0.0074
18	6.0	0.6	Straight	3	0.0060	3	0.7	0.0069
19	6.0	0.7	$M_\infty = 0.6$; $\alpha \simeq 6.0^o$	3	0.0051	2	0.75	0.0072
20	6.0	0.8	$M_\infty = 0.7$; $\alpha \simeq 6.0^o$	6	0.0048	5	0.75	0.0063

TABLE 11:- QUALITY OF CONSTANT PRESSURE WALL CONTOURS

Reference Mach Number (M_∞)	Contour	Model Incidence (Deg)	Standard Deviation of Local Mach Number (Wall Centreline)		Average Weighted Standard Deviation (σ_{av})	Artificial Wall Loading	
			Top Wall (σ_T)	Bottom Wall (σ_B)		E_T*(1)	E_B*(1)
0.4	A.1	0.5	0.0021	0.0022	0.0054	0.0070	0.0066
	A.2	2.0	0.0016	0.0015	0.0041	0.0061	0.0042
	A.3	4.0	0.0032	0.0032	0.0080	0.0148	0.0120
0.5	B.1	0.5	0.0019	0.0024	0.0043	0.0049	0.0056
	B.2	2.0	0.0018	0.0013	0.0031	0.0053	0.0036
	B.3	4.0	0.0034	0.0040	0.0074	0.0124	0.0096
0.6	C.1	0.5	0.0021	0.0025	0.0038	0.0043	0.0043
	C.2	2.0	0.0029	0.0021	0.0042	0.0050	0.0042
	C.3	4.0	0.0040	0.0040	0.0067	0.0097	0.0089
0.7	D.1	0.5	0.0020	0.0021	0.0029	0.0029	0.0030
	D.2	2.0	0.0028	0.0020	0.0034	0.0031	0.0028
	D.3	4.0	0.0046	0.0052	0.0070	0.0074	0.0086
0.8	E.1	0.5	0.0028	0.0020	0.0030	0.0040	0.0022
	E.2	2.0	0.0035	0.0034	0.0043	0.0034	0.0035

Note: (1) When determining values for E* the perturbations of the imaginary flowfields were artificially set to zero.

TABLE 12:- STREAMLINING QUALITY AND INTERFERENCE EFFECTS OF CONSTANT PRESSURE WALL CONTOURS

Test Condition		Quality of Wall Streamlining		Interference Effects		
Model Incidence (Deg)	Reference Mach Number (M_∞)	E_T	E_B	α Error (Deg)	Camber Error (Deg)	C_p Error
0.5	0.4	0.0104	0.0088	0.0070	0.0388	0.0094
	0.5	0.0158	0.0144	0.0071	0.0335	0.0144
	0.6	0.0197	0.0181	0.0035	0.0389	0.0153
	0.7	0.0251	0.0230	0.0045	0.0393	0.0205
	0.8	0.0354	0.0314	0.0278	0.0742	0.0262
2.0	0.4	0.0246	0.0079	0.0605	0.3250	0.0148
	0.5	0.0310	0.0120	0.0510	0.3642	0.0165
	0.6	0.0299	0.0122	0.0555	0.3704	0.0157
	0.7	0.0375	0.0169	0.0613	0.4012	0.0181
	0.8	0.0470	0.0216	0.1045	0.530	0.0244
4.0	0.4	0.0494	0.0138	0.1251	0.6842	0.0158
	0.5	0.0493	0.0165	0.1397	0.7692	0.0162
	0.6	0.0603	0.0214	0.1361	0.8609	0.0190
	0.7	0.0640	0.0249	0.1498	0.9289	0.0209

Note: The interference effects at the model due to the existence of wall loading are calculated using linearised theory. The wall loading, measured in terms of E, was determined from the TSWT TSP code (to predict the imaginary flowfields) and wall pressure measurements.

TABLE 13:- RESIDUAL INTERFERENCE EFFECTS OF WALL CONTOURS DERIVED BY THE NPL STRATEGY

Test Conditions		Residual Interference Effects					
		NPL 1 WAS Contours			NPL 2 WAS Contours		
Model Incidence (Deg)	Reference Mach Number (M_∞)	α Error (Deg)	Camber Error (Deg)	C_p Error	α Error (Deg)	Camber Error (Deg)	C_p Error
0.5	0.4	0.0200	0.0088	-0.0160	0.0109	0.0269	-0.0127
	0.5	0.0041	-0.0063	-0.0159	0.0108	0.0166	-0.0119
	0.6	0.0078	0.0080	-0.0182	0.0032	0.0106	-0.0121
	0.7	0.0100	0.0044	-0.0192	0.0044	0.0151	-0.0124
	0.8	0.0328	0.0659	-0.0962	0.0218	0.0411	-0.0288
2.0	0.4	-0.0044	-0.0091	-0.0180	0.0079	0.0598	-0.0091
	0.5	0.0008	0.0131	-0.0171	0.0058	0.0690	-0.0099
	0.6	-0.0016	-0.0029	-0.0193	0.0055	0.0701	-0.0117
	0.7	-0.0054	0.0026	-0.0233	0.0068	0.1031	-0.0134
	0.8	0.0626	0.2106	-0.0771	0.0871	0.3088	-0.0623
4.0	0.4	-0.0244	-0.0780	-0.0115	0.0063	0.0811	-0.0076
	0.5	-0.0252	-0.0452	-0.0165	0.0134	0.1274	-0.0111
	0.6	-0.0161	0.0069	-0.0161	0.0287	0.1924	-0.0080
	0.7	-0.0281	-0.0569	-0.0247	0.0199	0.1651	-0.0149

Note: The residual interference effects at the model due to the existence of wall loading are calculated using linearised theory. The wall loading, measured in terms of E, was determined from the TSWT TSP code (to predict the imaginary flowfields) and wall pressure measurements.

TABLE 14:- SUMMARY OF TSWT 'STREAMLINED' DATA. MIXED FLOW IN IMAGINARY FLOWFIELDS

14.1:- ORIGINAL FLEXIBLE WALLS (SEPT. 1984)

Reference Number	Nominal Mach Number	Model Incidence (Deg)	Reference Mach Number (M_∞)	Model Performance			Wall Loadings		
				C_N	C_C	C_M	E_T	E_B	E_{av}
1	0.87	4.0	0.8658	0.1159	0.0379	0.0461	0.0083	0.0155	0.0119
2	0.90	4.0	0.8997	0.1761	0.0535	0.0185	0.0155	0.0117	0.0136
3(1)	0.90	4.0	0.9062	0.1953	0.0549	0.0052	0.0139	0.0082	0.0110
4	0.92	4.0	0.9257	0.3987	0.0785	-0.1635	0.0161	0.0069	0.0115
5(1)	0.92	4.0	0.9228	0.3788	0.0759	-0.1420	0.0120	0.0055	0.0087
6	0.94	4.0	0.9434	0.3617	0.0752	-0.1388	0.0190	0.0172	0.0181
7(1)	0.94	4.0	0.9417	0.3815	0.0759	-0.1511	0.0136	0.0123	0.0129
8(1)	0.95	4.0	0.9543	0.3882	0.0777	-0.1640	0.0152	0.0129	0.0140
9(1)	0.96	4.0	0.9638	0.3617	0.0740	-0.1387	0.0170	0.0170	0.0170
10(1)	0.97	4.0	0.9721	0.3828	0.0761	-0.1630	0.0166	0.0153	0.0159

Note: (1) The effective aerodynamic contour used in the imaginary flowfield computations includes an allowance for the variations of δ^* caused by the presence of the model.

TABLE 14:- SUMMARY OF TSWT 'STREAMLINED' DATA. MIXED FLOW IN IMAGINARY FLOWFIELDS

14.2:- NEW FLEXIBLE WALLS (MARCH 1986)

Reference Number	Nominal Mach Number	Model Incidence (Deg)	Reference Mach Number (M_∞)	Model Performance			Wall Loadings		
				C_N	C_C	C_M	E_T	E_B	E_{av}
1	0.85	4.0	0.8498	0.1075	0.0142	0.0399	0.0089	0.0071	0.0080
2	0.87	4.0	0.8750	0.1142	0.0308	0.0420	0.0079	0.0060	0.0069
3(1)	0.87	4.0	0.8726	0.1283	0.0334	0.0351	0.0072	0.0051	0.0061
4	0.89	4.0	0.8874	0.1514	0.0440	0.0284	0.0084	0.0076	0.0080
5	0.87	6.0	0.8700	0.2624	0.0375	0.0026	0.0125	0.0063	0.0094

Note: (1) The effective aerodynamic contour used in the imaginary flowfield computations includes an allowance for the variations of δ^* caused by the presence of the model.

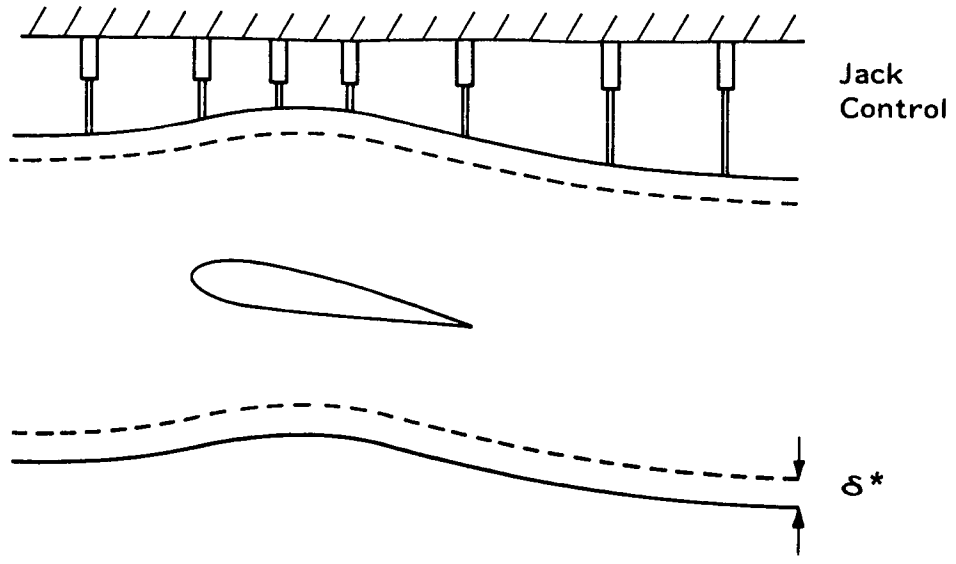

Flexible Walls

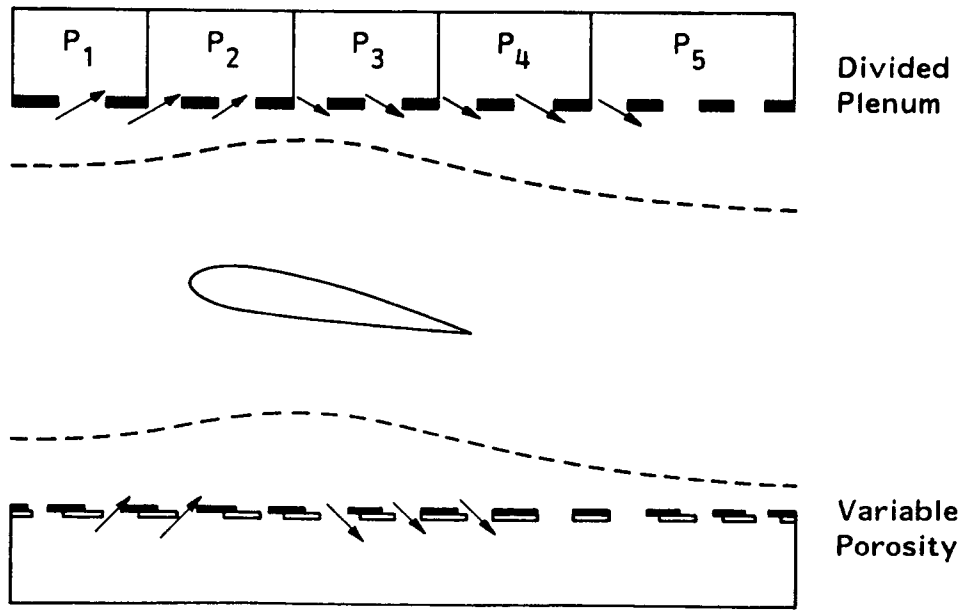

Ventilated Walls

FIG. 1.1 THE DIFFERENT TYPES OF ADAPTIVE WALLS

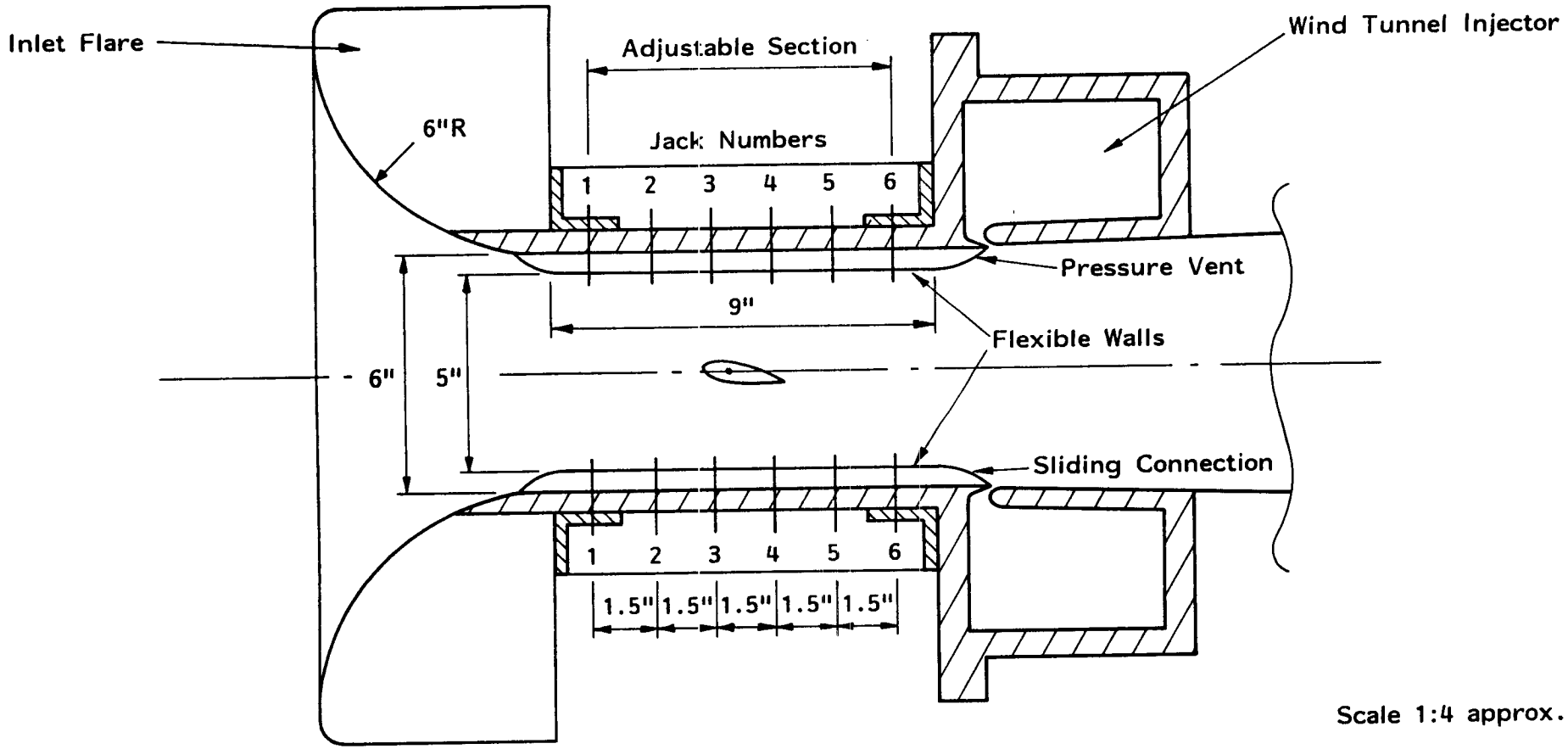

FIG. 2.1 SCHEMATIC LAYOUT OF NPL 5 inch x 2 inch TRANSONIC ADAPTIVE WALL WIND TUNNEL (1938)

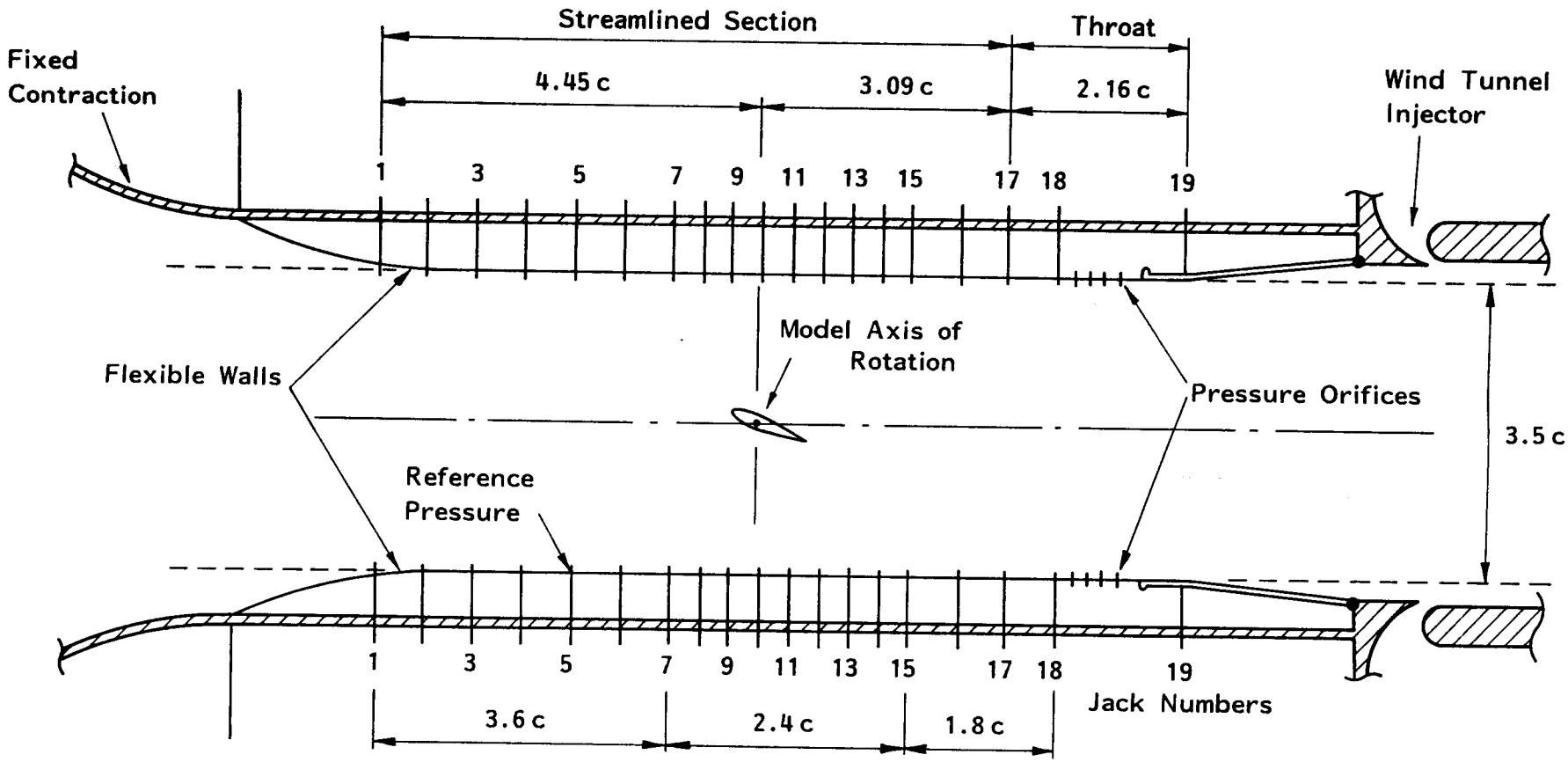

FIG. 2.2 SCHEMATIC LAYOUT OF NPL 20 inch x 8 inch RECTANGULAR TRANSONIC WIND TUNNEL (1941)

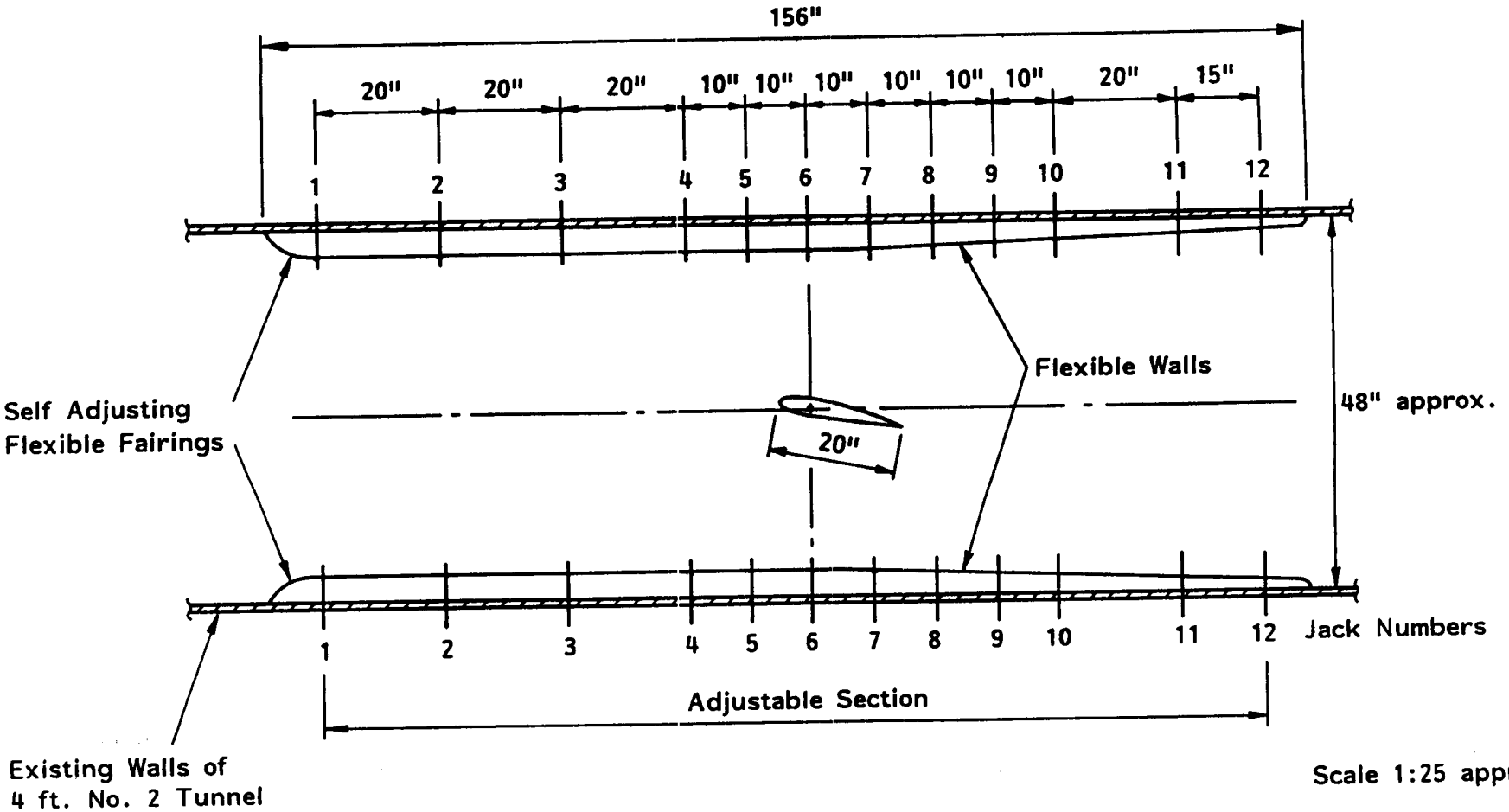

FIG. 2.3 SCHEMATIC LAYOUT OF NPL 4 ft. NO. 2 TUNNEL FITTED WITH FLEXIBLE WALLS (1944)

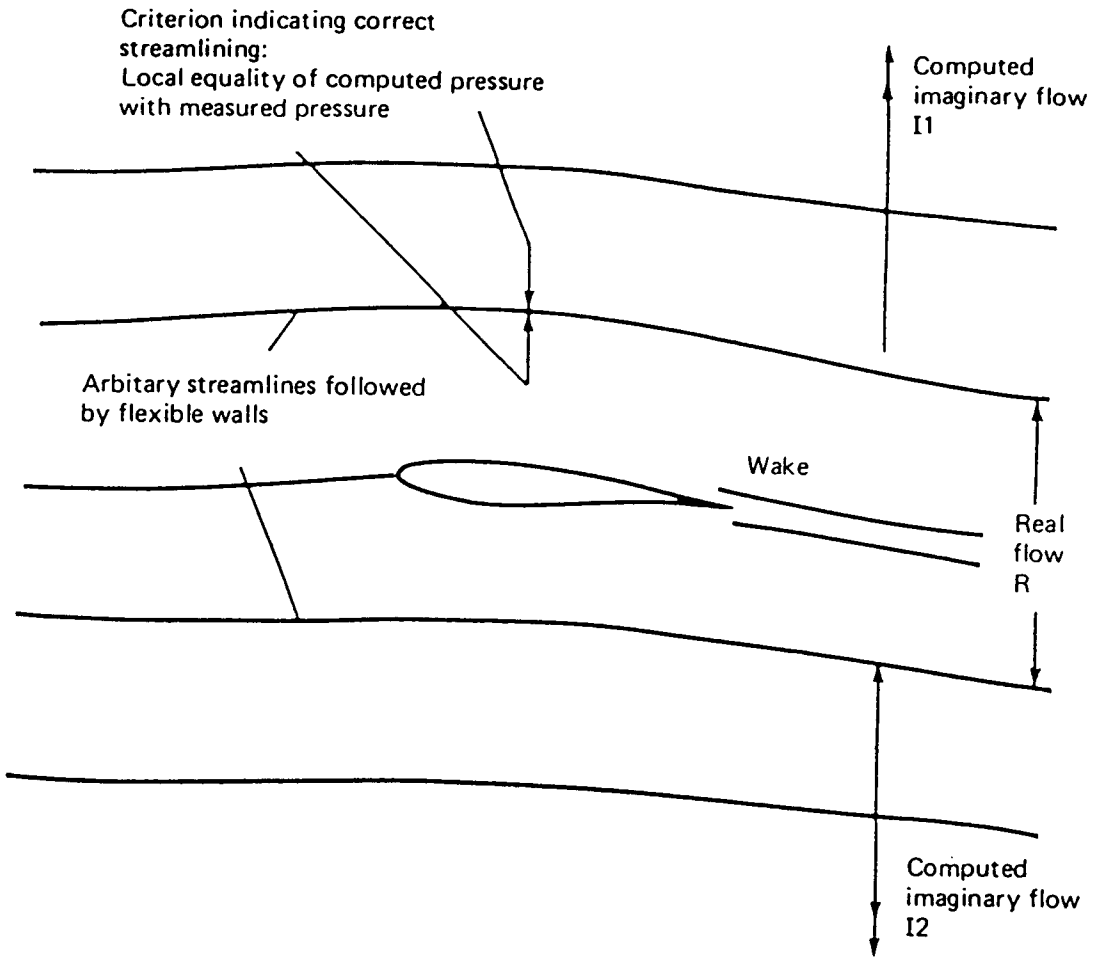

FIG. 3.1 A TWO-DIMENSIONAL FLOWFIELD ILLUSTRATING THE PRINCIPLE OF TEST SECTION STREAMLINING

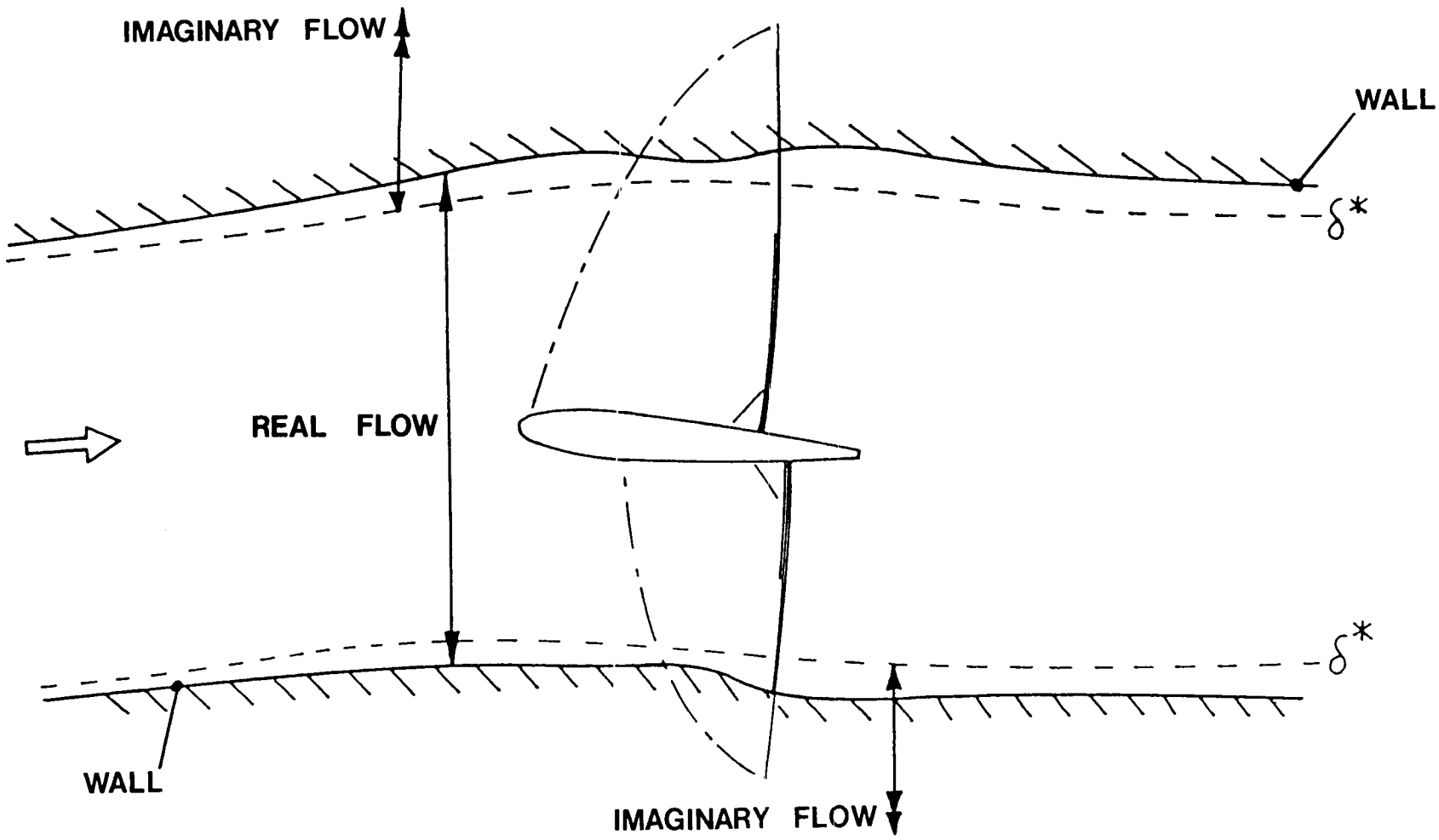

FIG. 3.2 FLOWFIELD DIVISIONS IN TWO-DIMENSIONAL TESTING

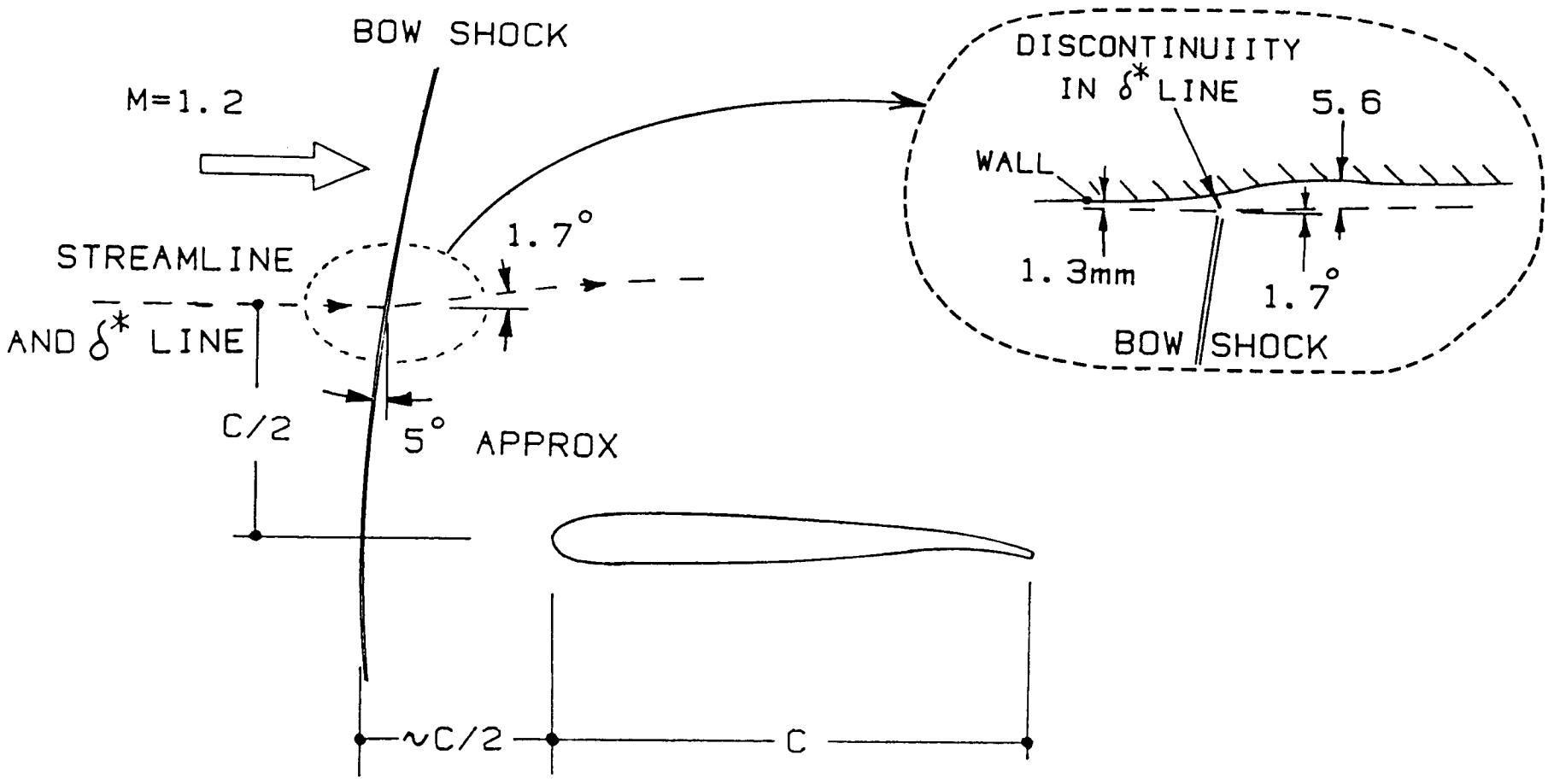

FIG. 3.3 CALCULATED WALL CONTOUR FOR STREAMLINING AT BOW SHOCK

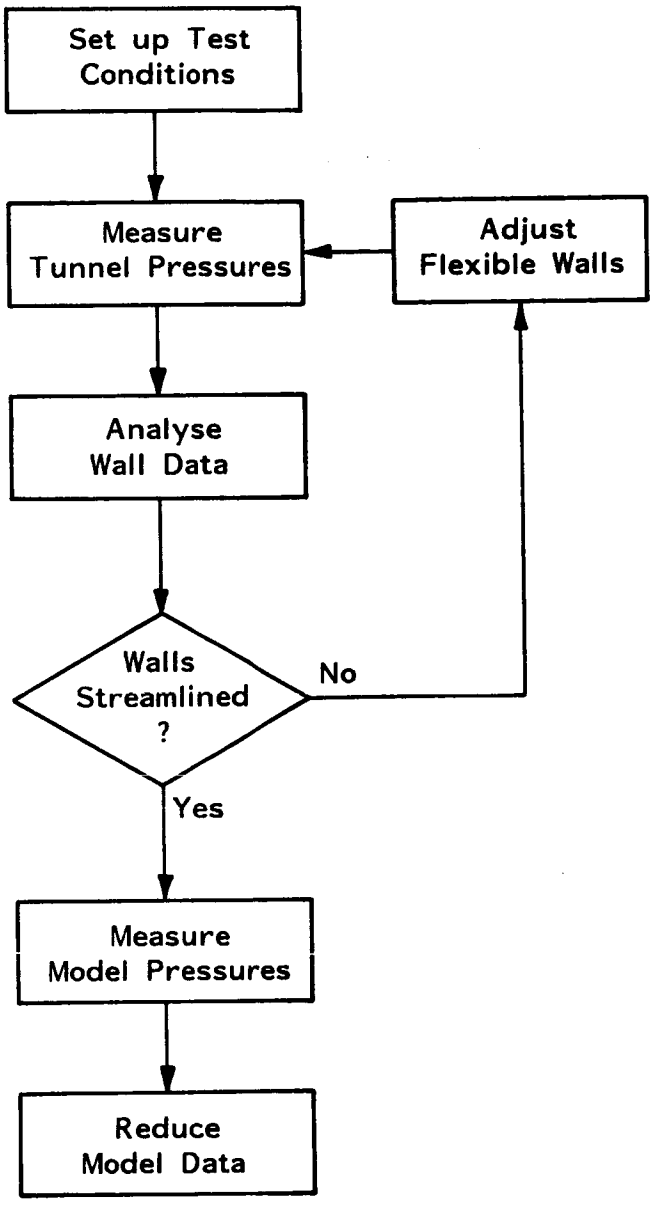

FIG. 3.4 SELF - STREAMLINING OPERATING PROCEDURE

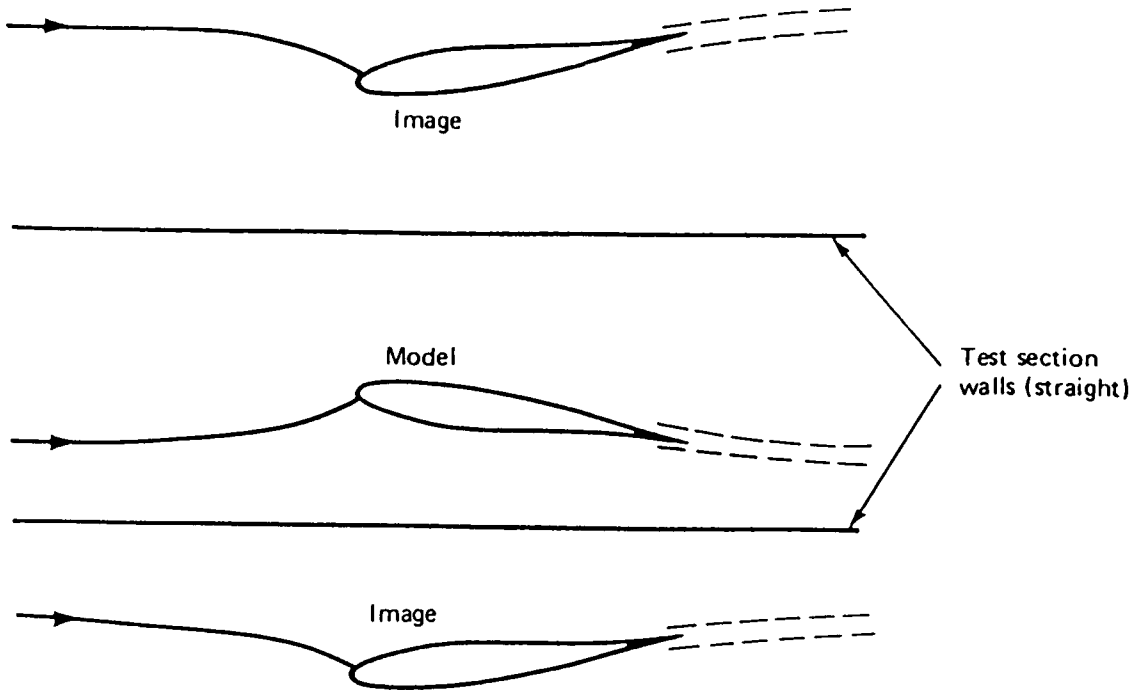

(a) Closed tunnel mode

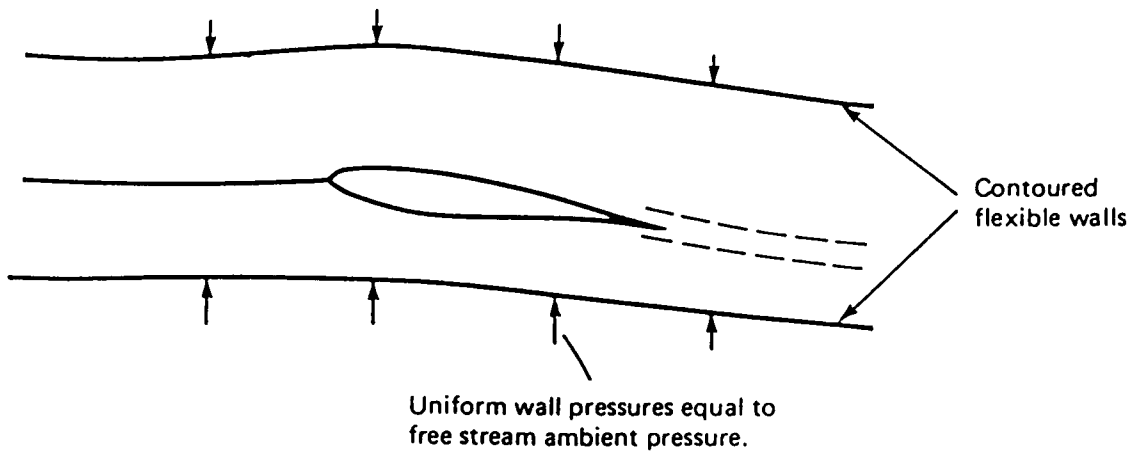

(b) Open jet mode.

FIG. 4.1 ILLUSTRATIONS OF SIX OPERATIONAL MODES OF A SELF-STREAMLINING WIND TUNNEL

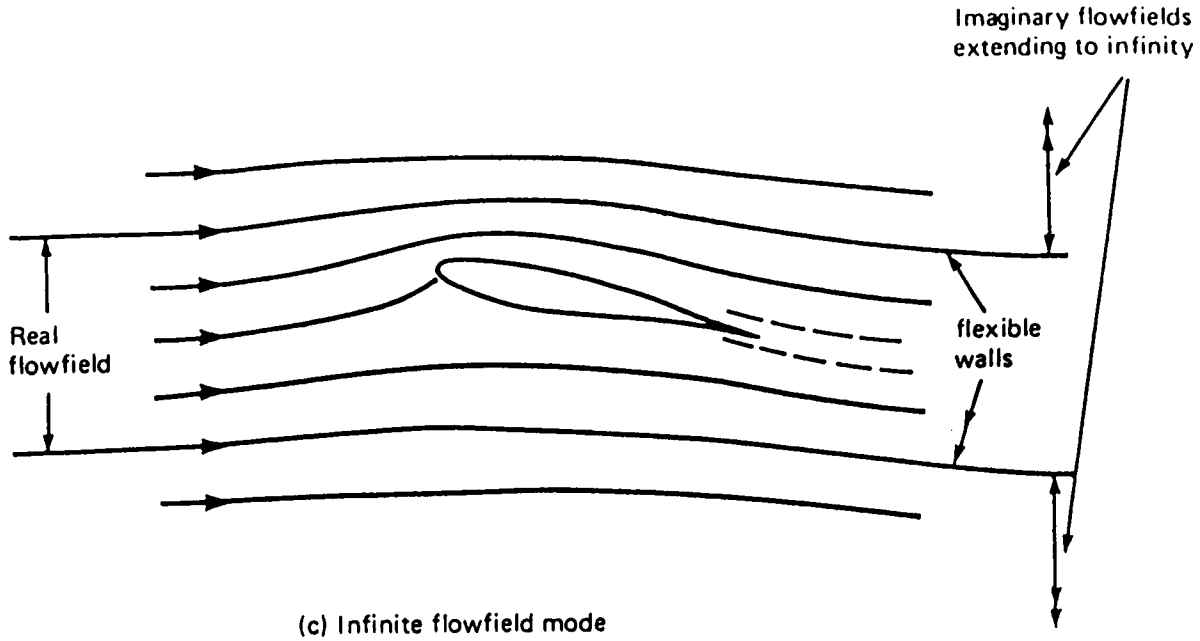

(c) Infinite flowfield mode

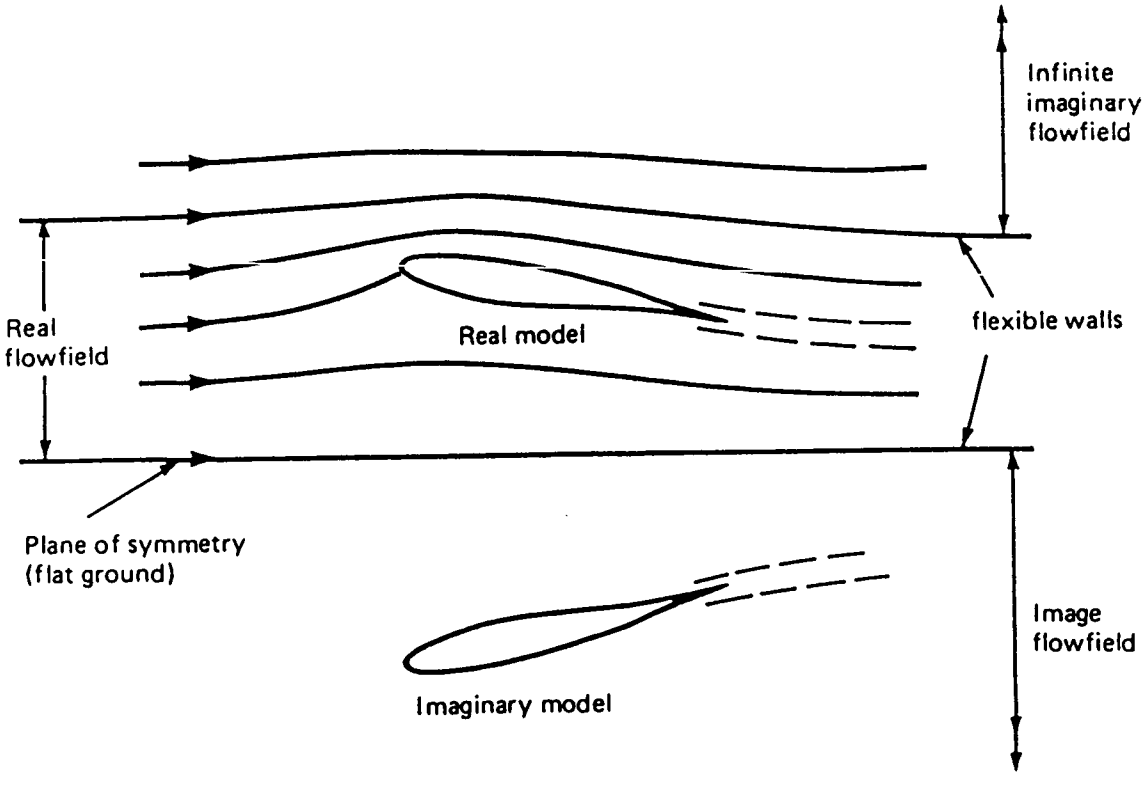

(d) Ground effect mode

FIG. 4.1 ILLUSTRATIONS OF SIX OPERATIONAL MODES OF A SELF-STREAMLINING WIND TUNNEL (CONTINUED)

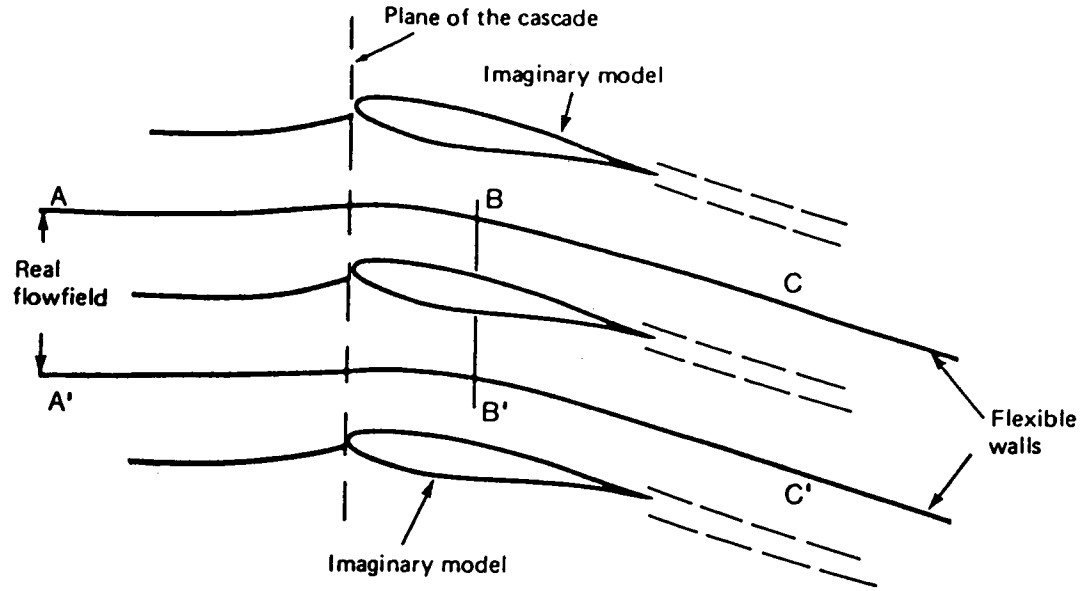

(e) Cascade mode.

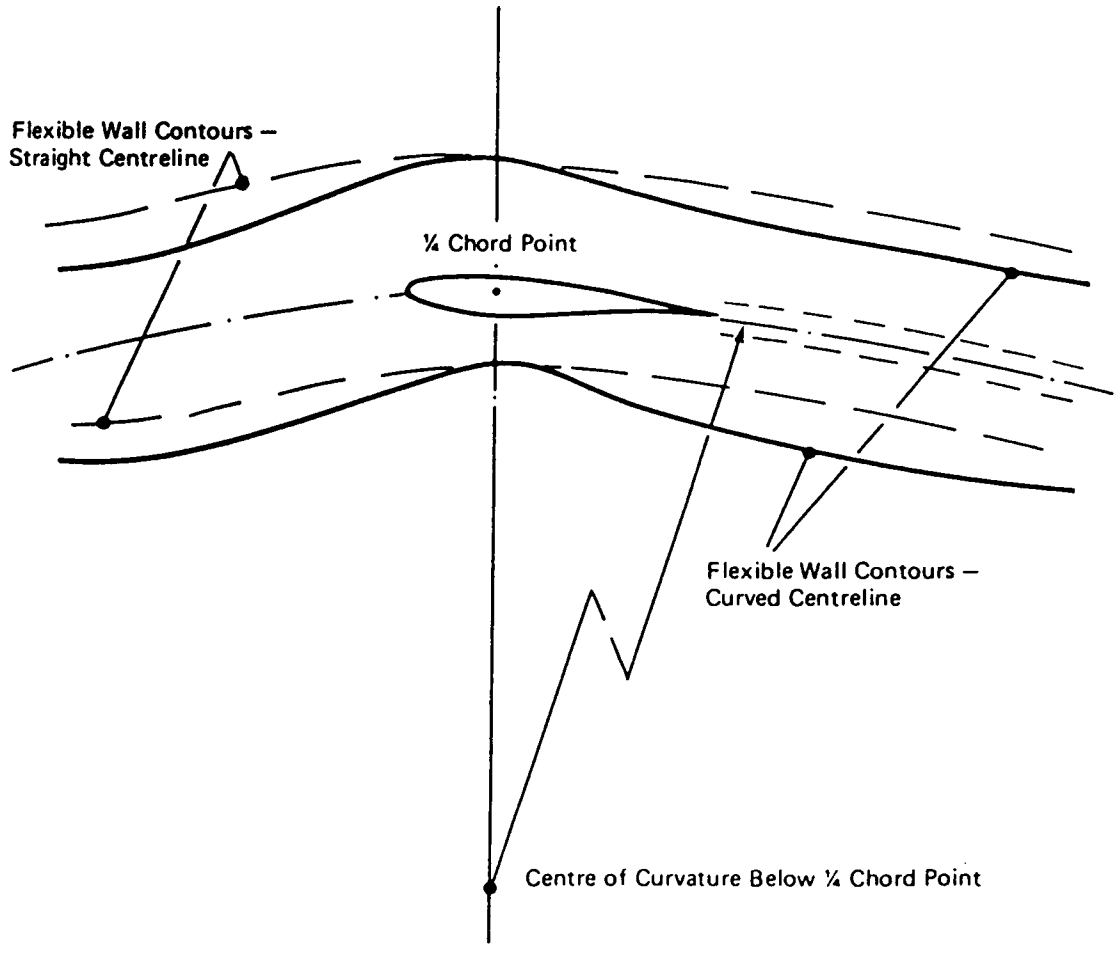

(f) Steady pitching mode

FIG 4.1 ILLUSTRATIONS OF SIX OPERATIONAL MODES OF A SELF-STREAMLINING WIND TUNNEL (CONCLUDED)

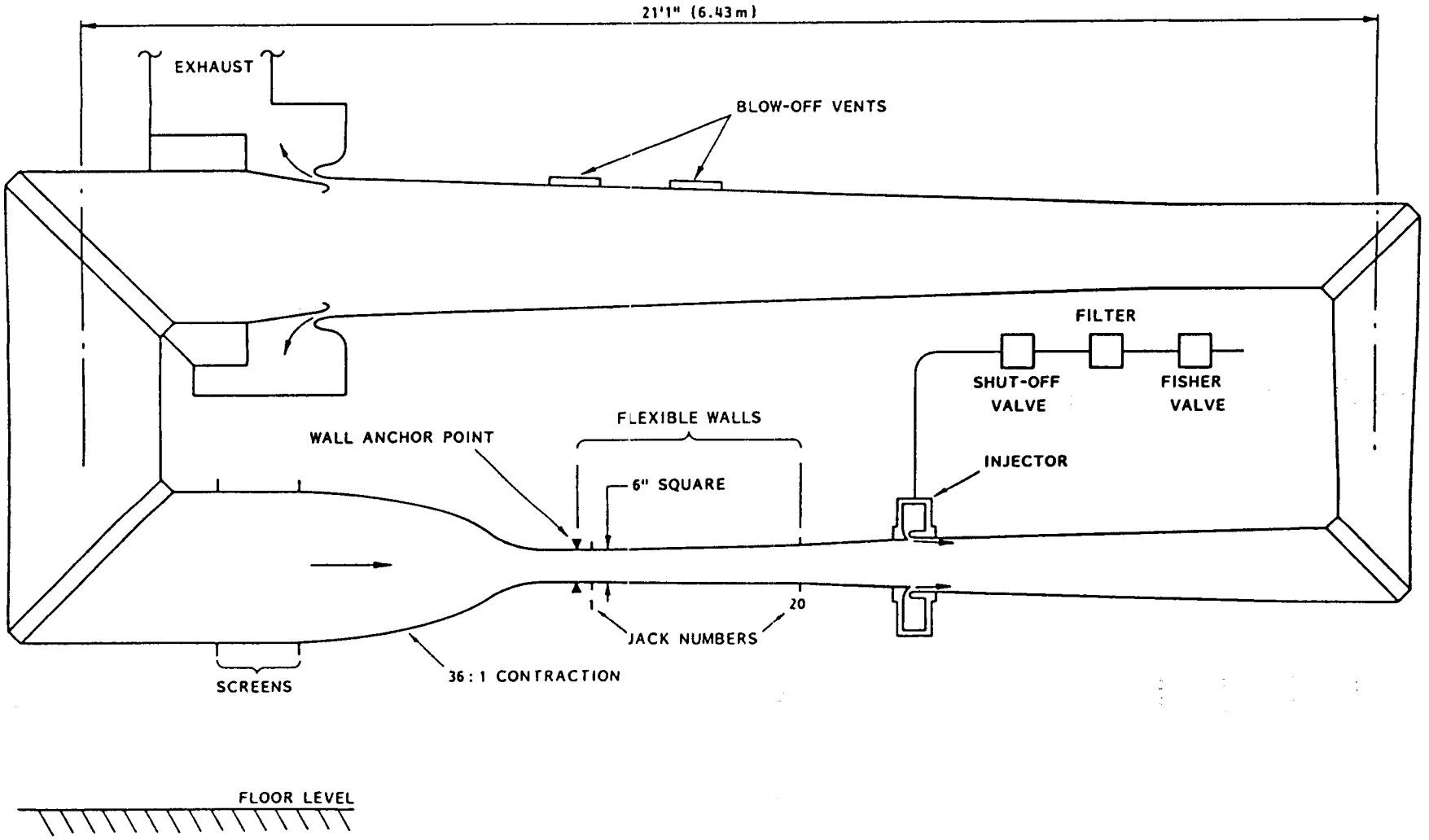

FIG. 5.1 AERODYNAMIC LINES OF THE TRANSONIC SELF-STREAMLINING WIND TUNNEL

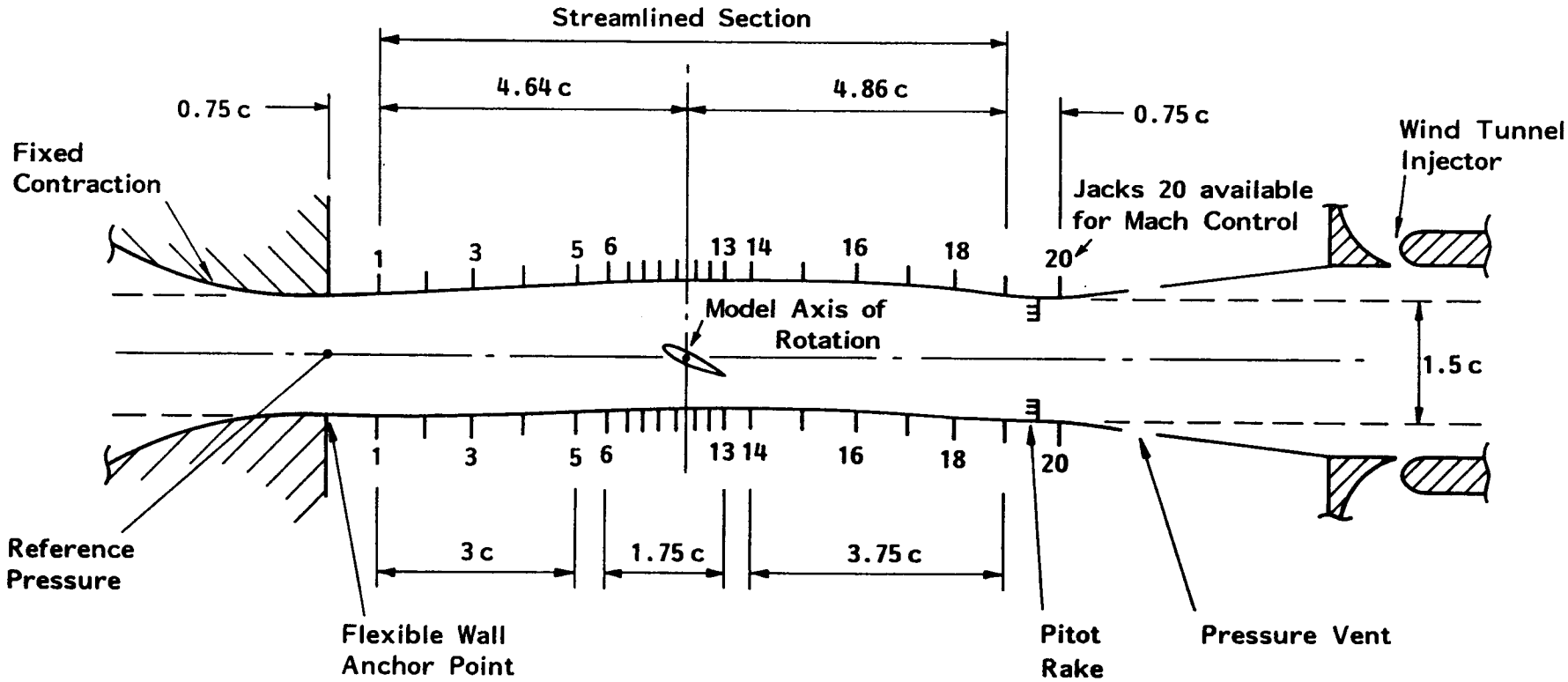

c = Aerofoil chord (= 4.0 inches)

Scale 1:10 approx.

FIG. 5.2 SCHEMATIC LAYOUT OF TRANSONIC SELF - STREAMLINING WIND TUNNEL

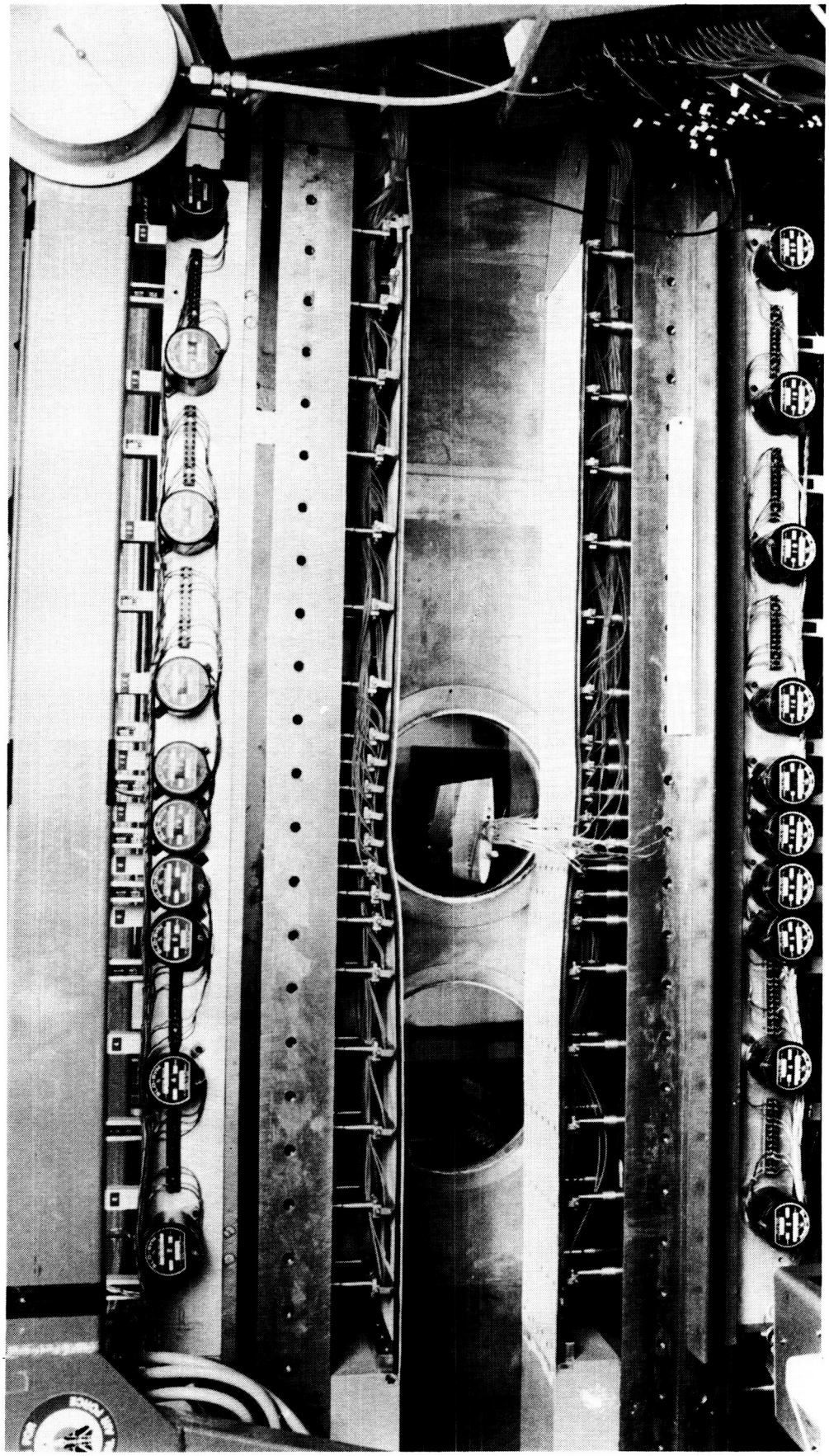

FIG. 5.3 TRANSONIC SELF-STREAMLINING TEST SECTION (SIDE-WALL REMOVED)

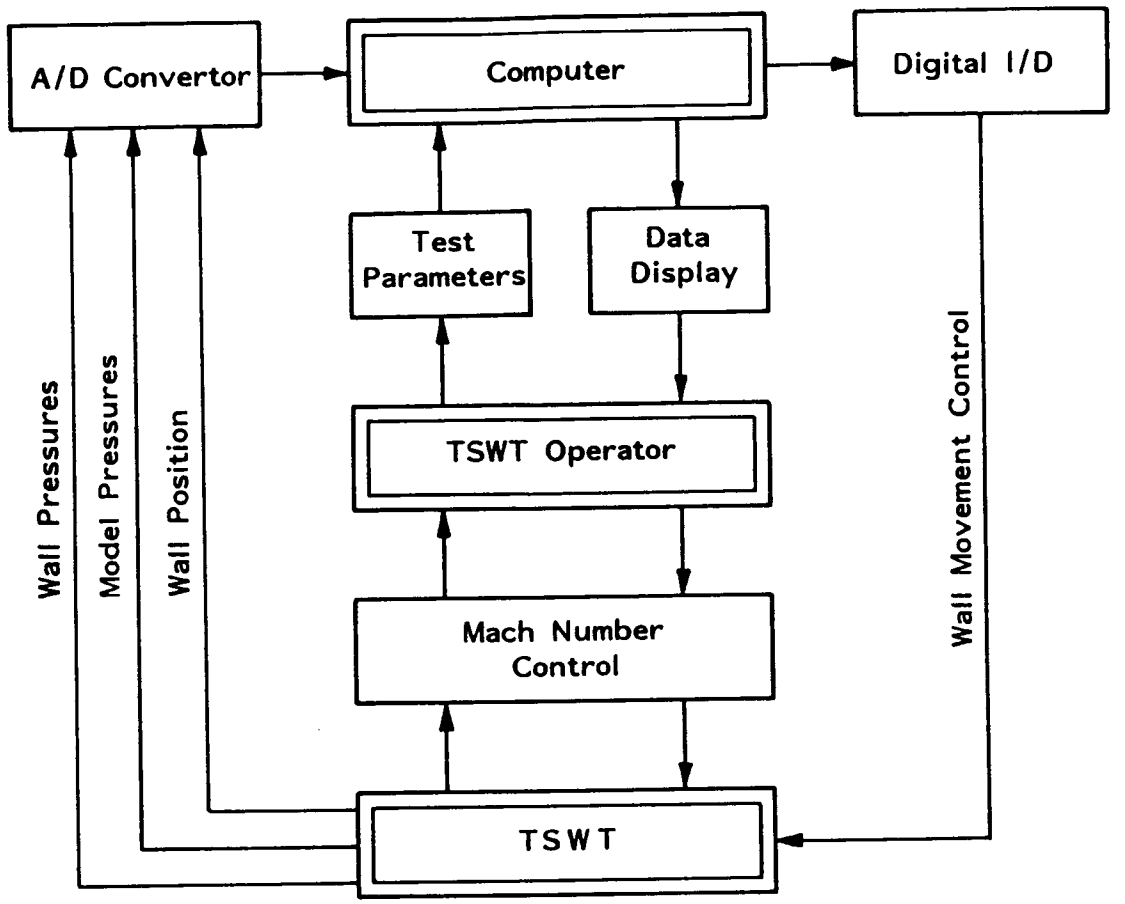

FIG. 5.4 TSWT CONTROL SYSTEM OUTLINE

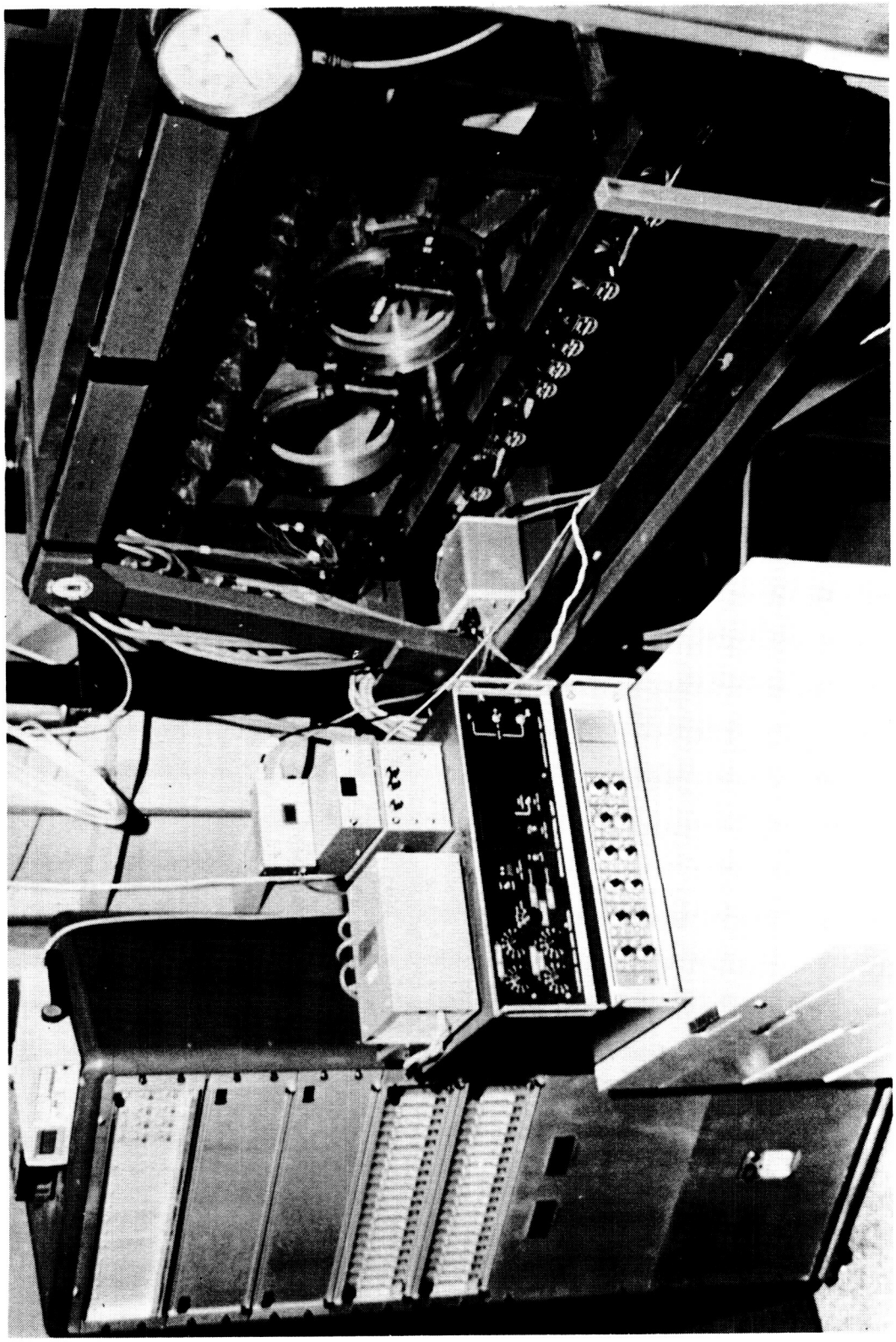

FIG. 5.5 TSWT CONTROL HARDWARE ADJACENT TO THE TSWT TEST SECTION

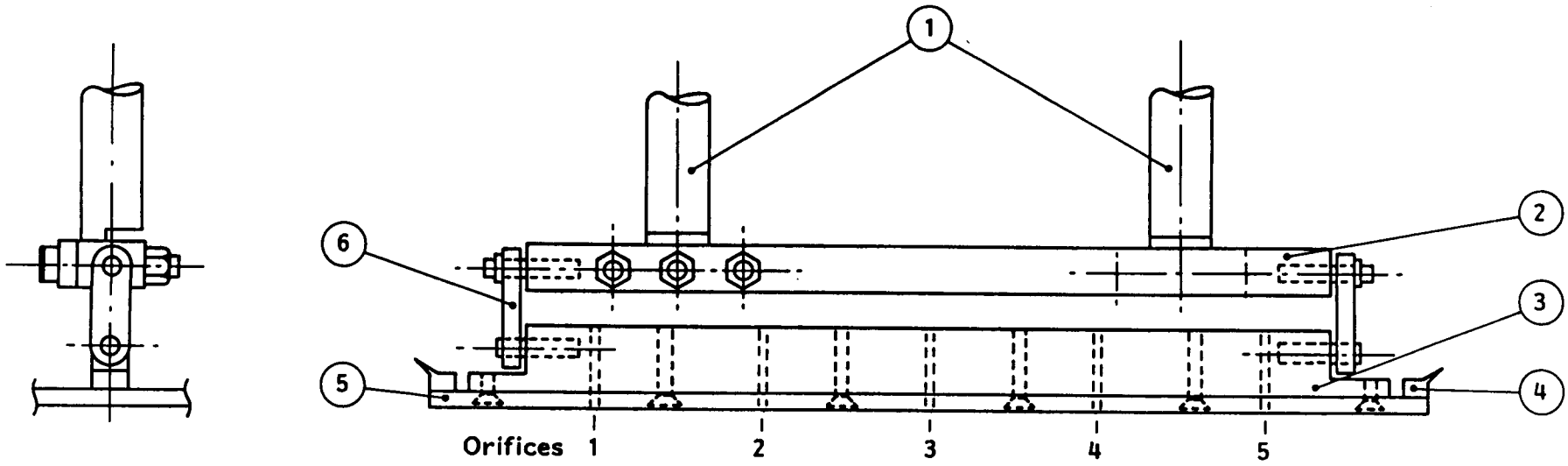

Key
(1) Jack Push Rods (2) Lifting Bar (3) Wall Stiffener Rib
(4) Rubber Seal (5) Flexible Wall (6) Swinging Link

Scale 1:1 approx.

FIG. 5.6 SCHEMATIC OF JACK/WALL LINK MECHANISM OF THE NEW FLEXIBLE WALLS

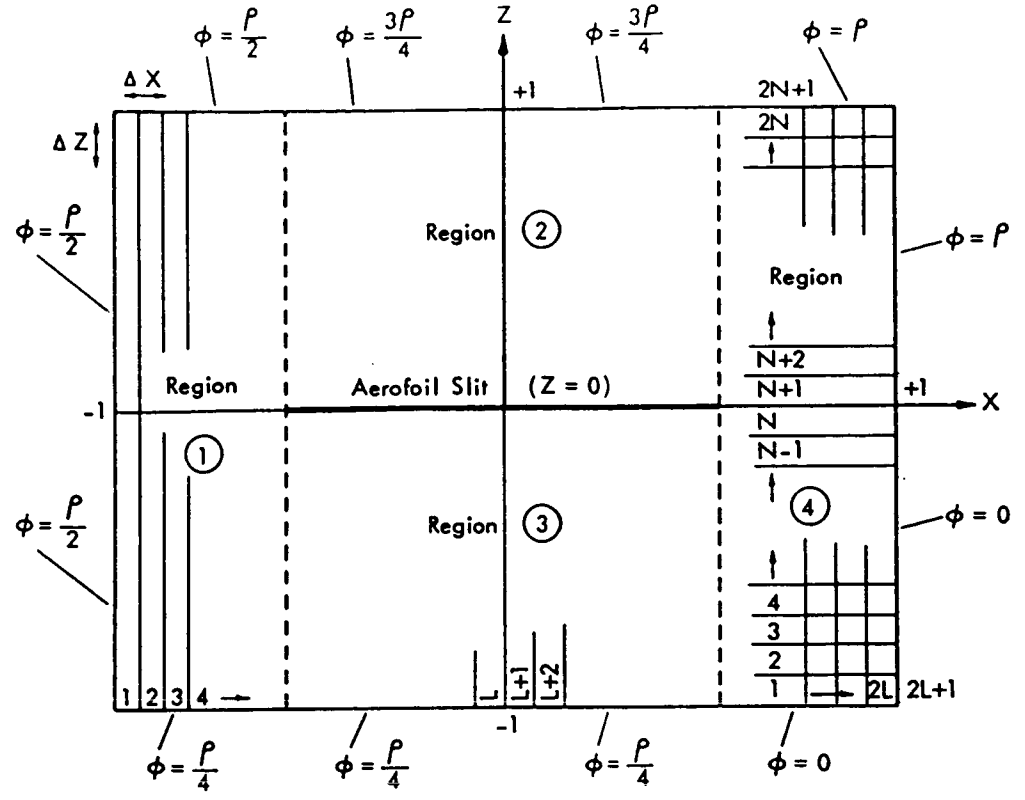

a) RAE TSP CODE

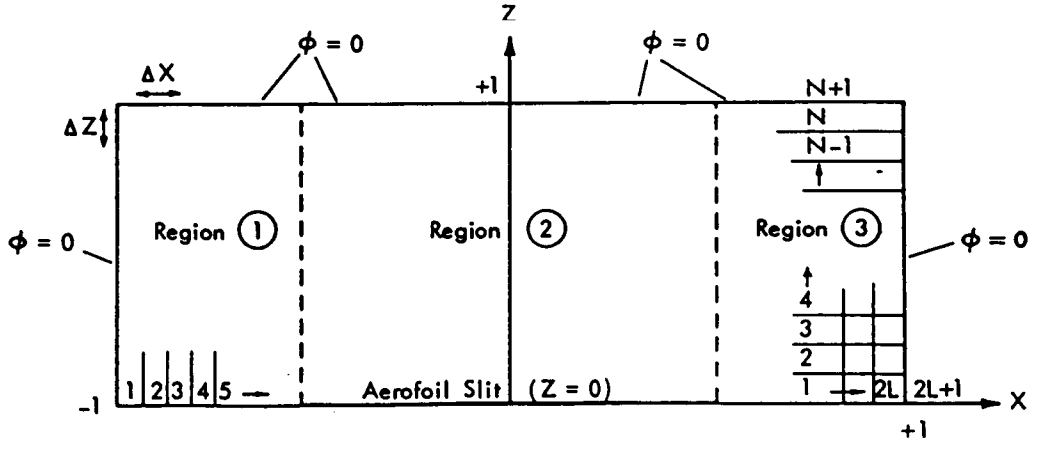

b) TSWT TSP CODE

L = 20, N = 10 } Coarse Mesh L = 40, N = 20 } Fine Mesh ϕ = Perturbation Potential

FIG. 7.1 TSP COMPUTING PLANES (X,Z)

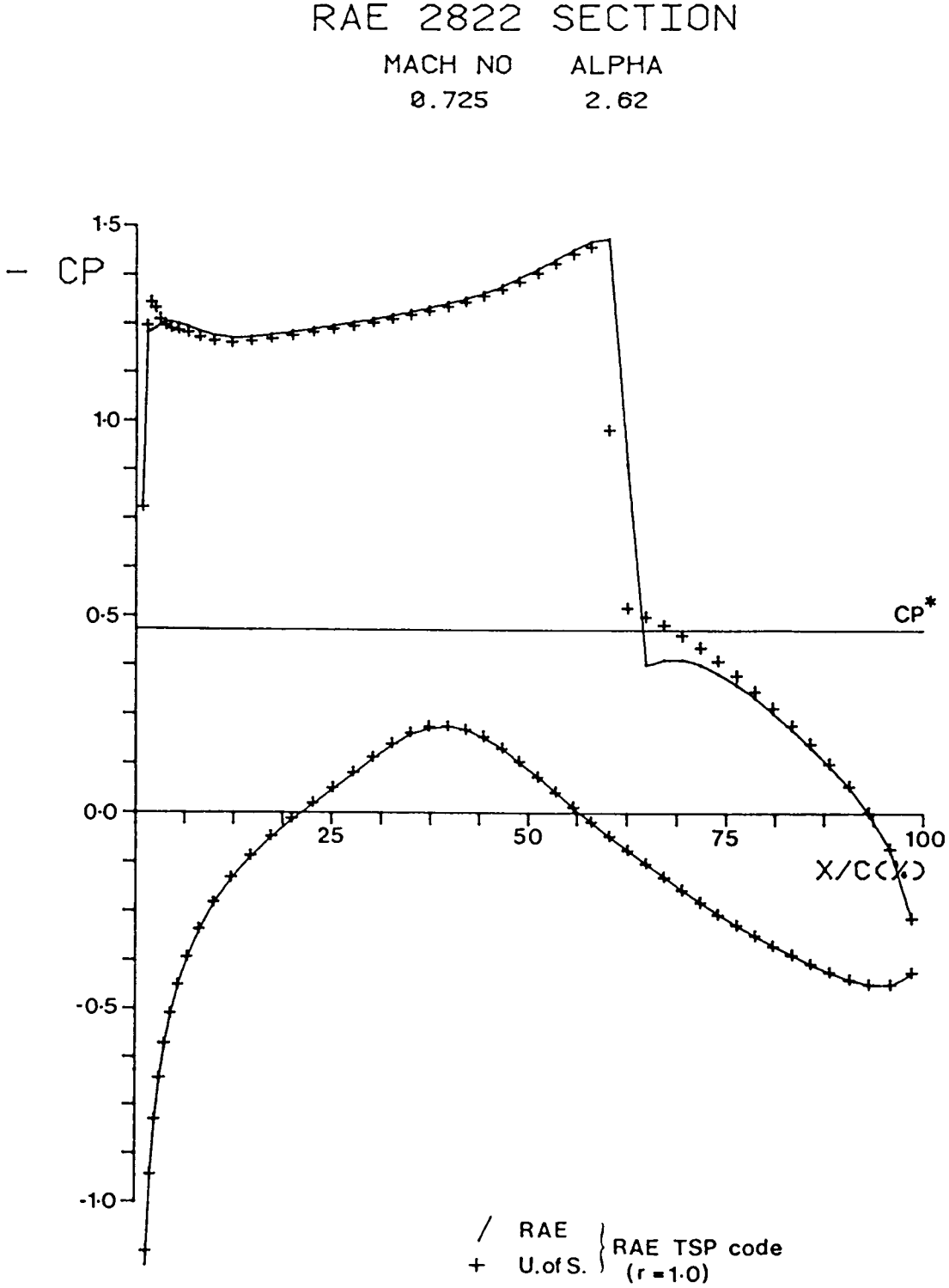

FIG. 7.2 RAE TEST CASE

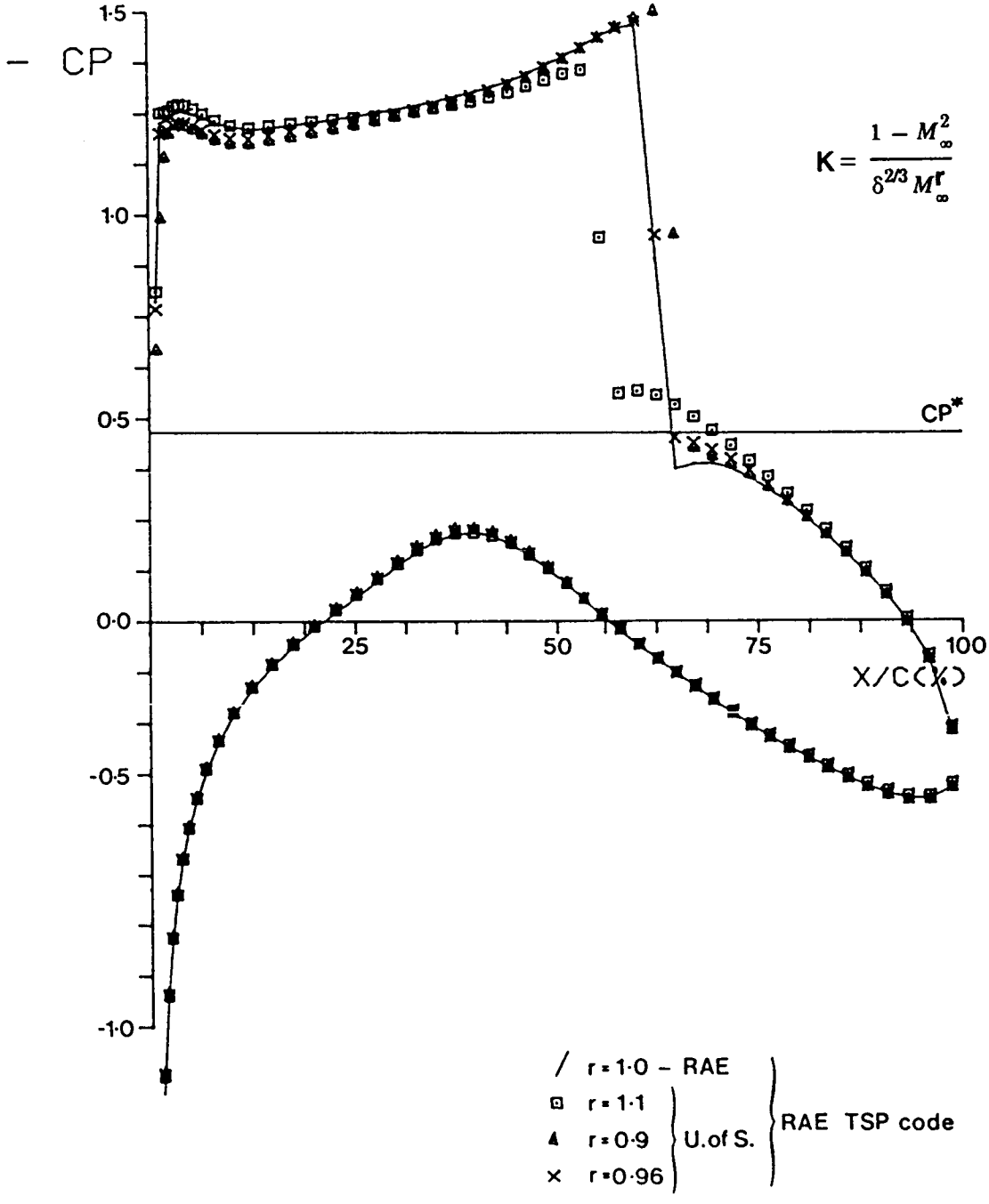

FIG. 7.3 THE EFFECT OF VARIATIONS IN SIMILARITY PARAMETER (K)

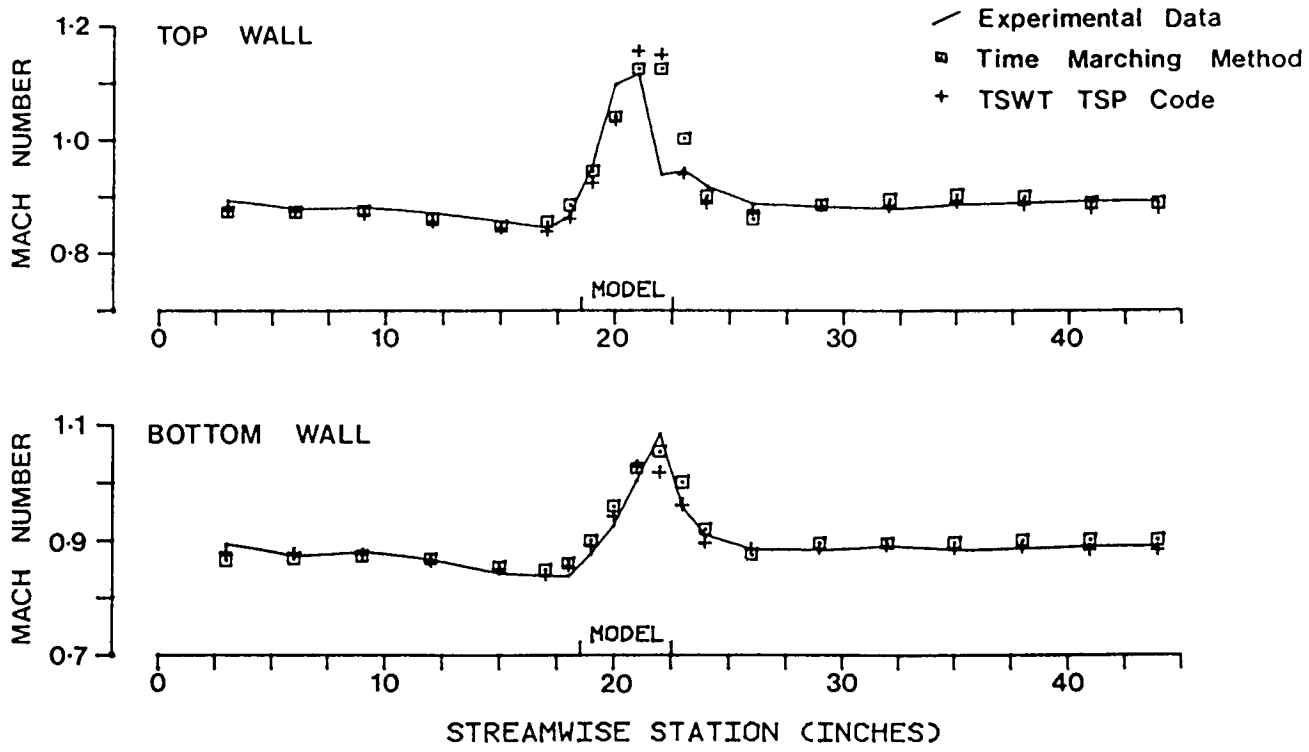

FIG. 7.4 TSWT TEST CASE COMPARISON (RUN 184 - M_∞ = 0.8862; $\alpha \simeq 4.0^o$).

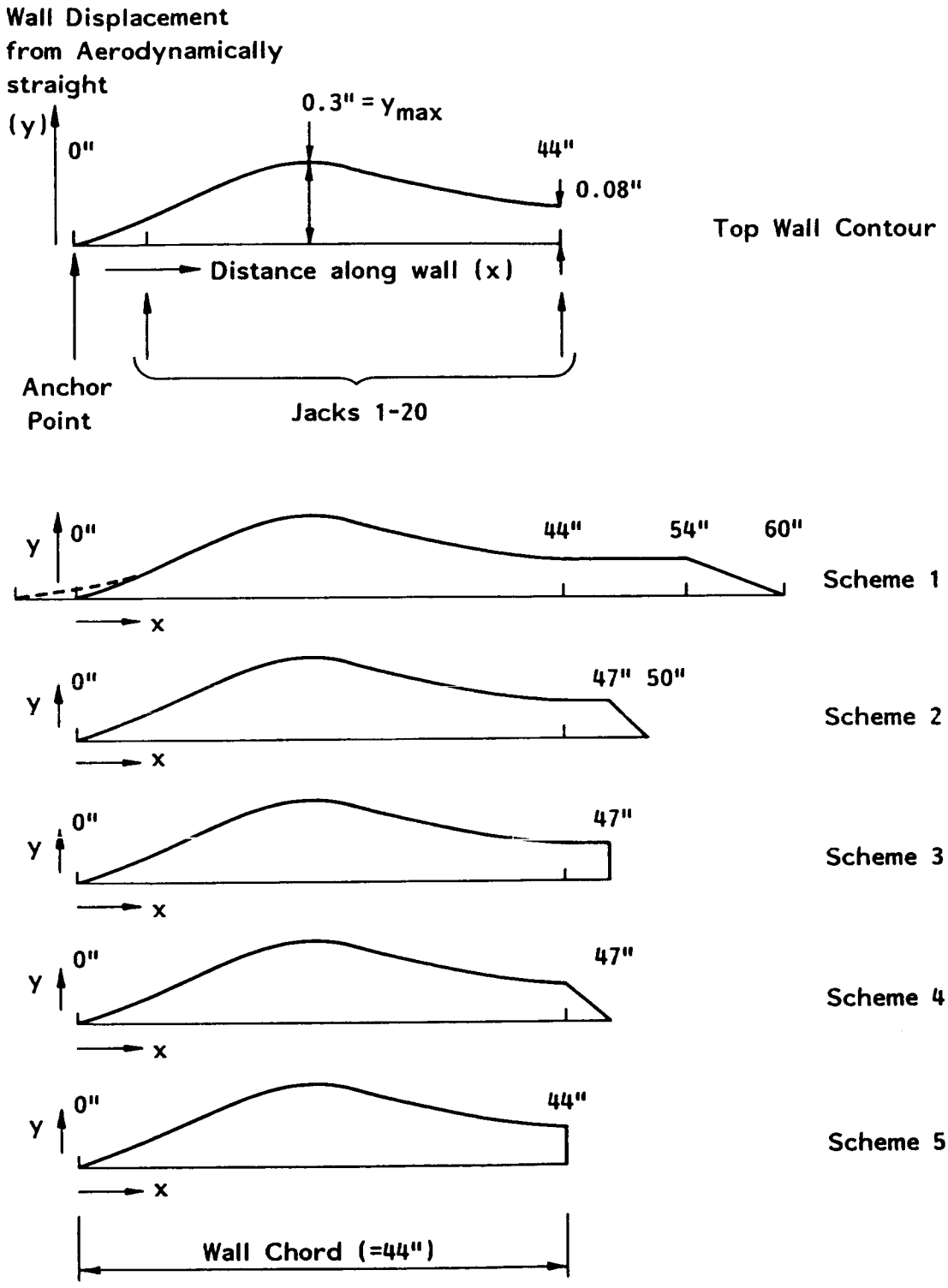

$$\delta = \frac{2\,y_{max}}{\text{Wall Chord}}$$

FIG. 7.5 WALL REPRESENTATION SCHEMES (RUN 184 - TOP WALL)

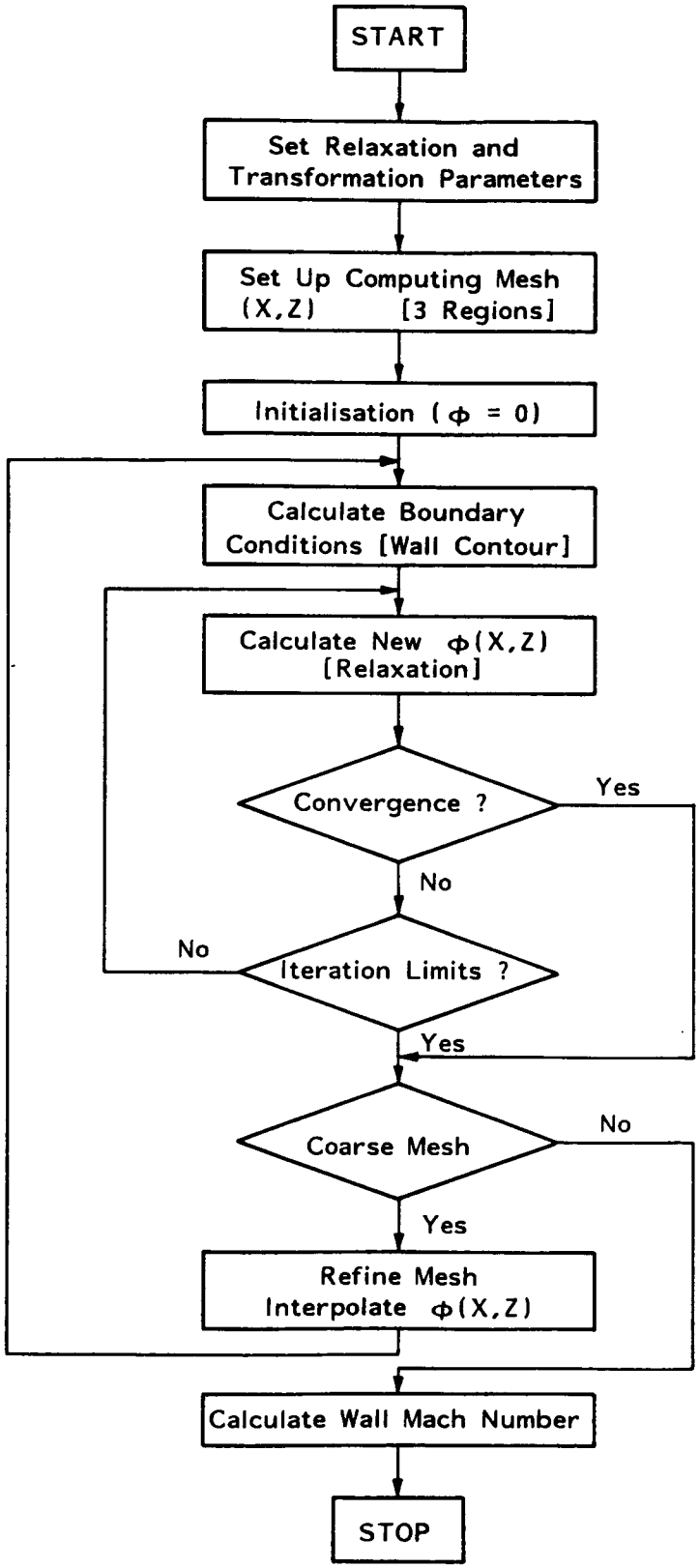

FIG. 7.6 FLOW DIAGRAM OF TSWT TSP CODE

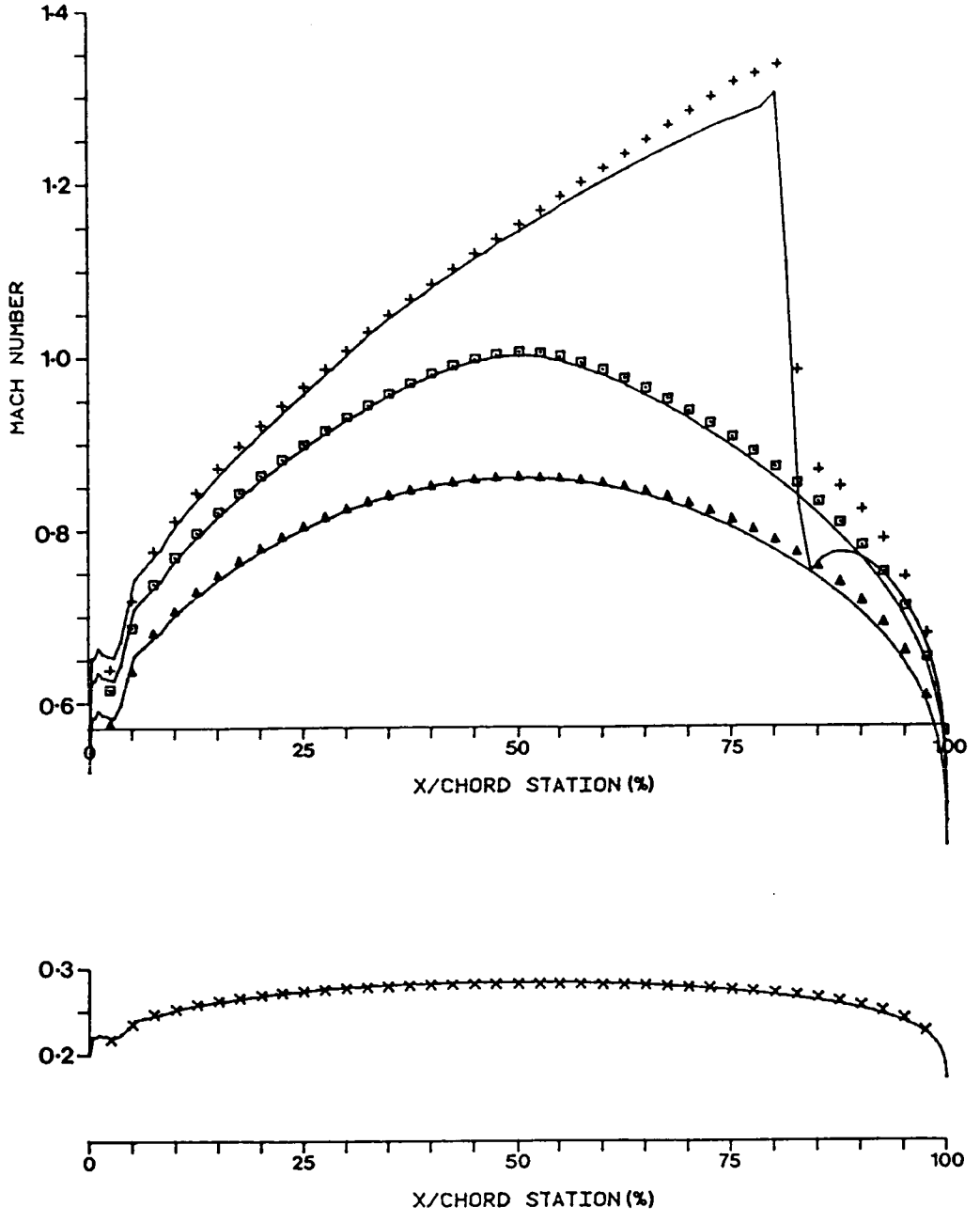

FIG. 7.7 10% CIRCULAR ARC AEROFOIL COMPARISON (ZERO INCIDENCE)

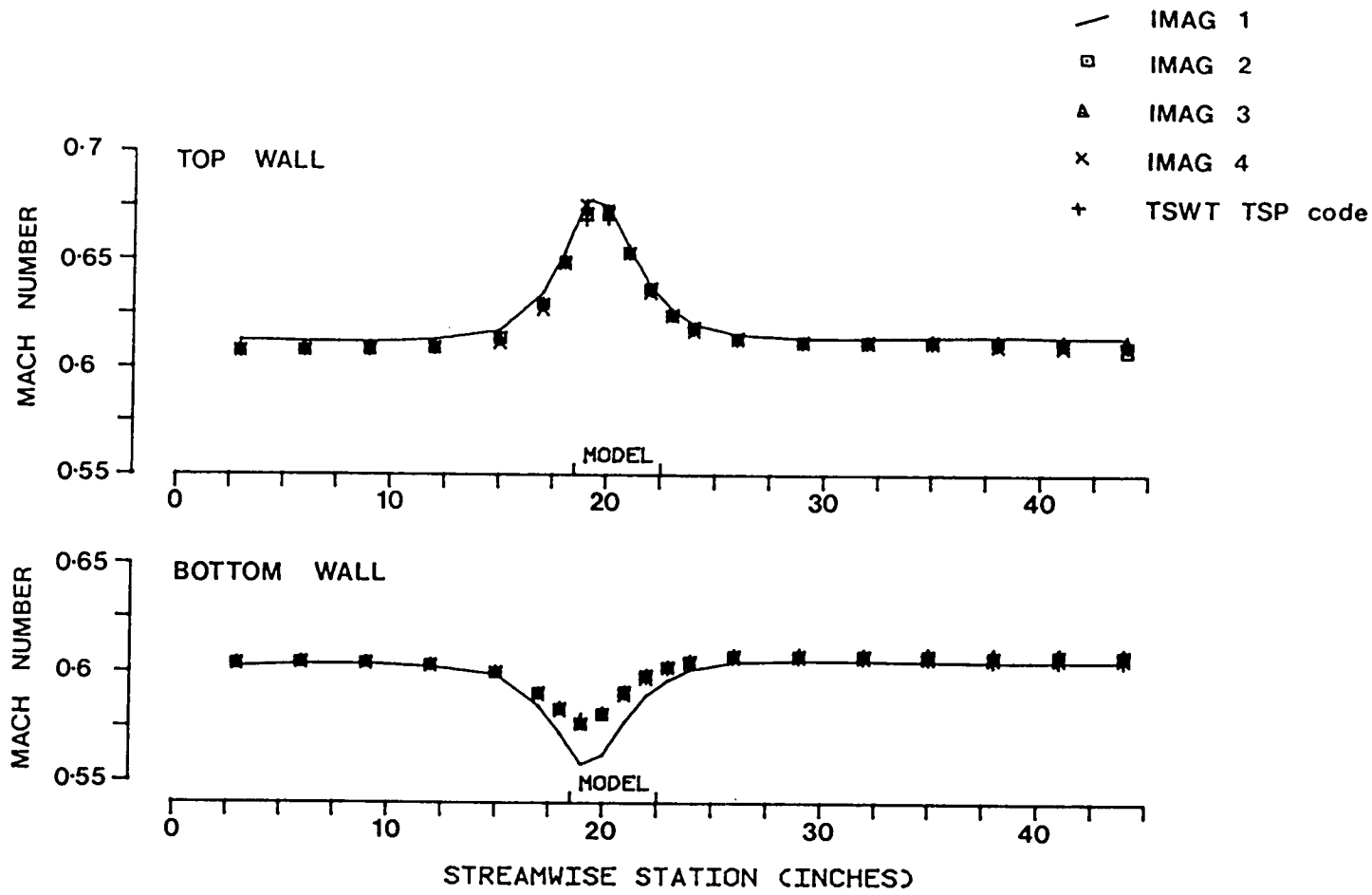

FIG. 7.8a IMAGINARY FLOW PREDICTIONS BY SEVERAL COMPUTATIONAL METHODS (CONDITION 1: $M_\infty = 0.6025$; $\alpha \simeq 6.0^o$).

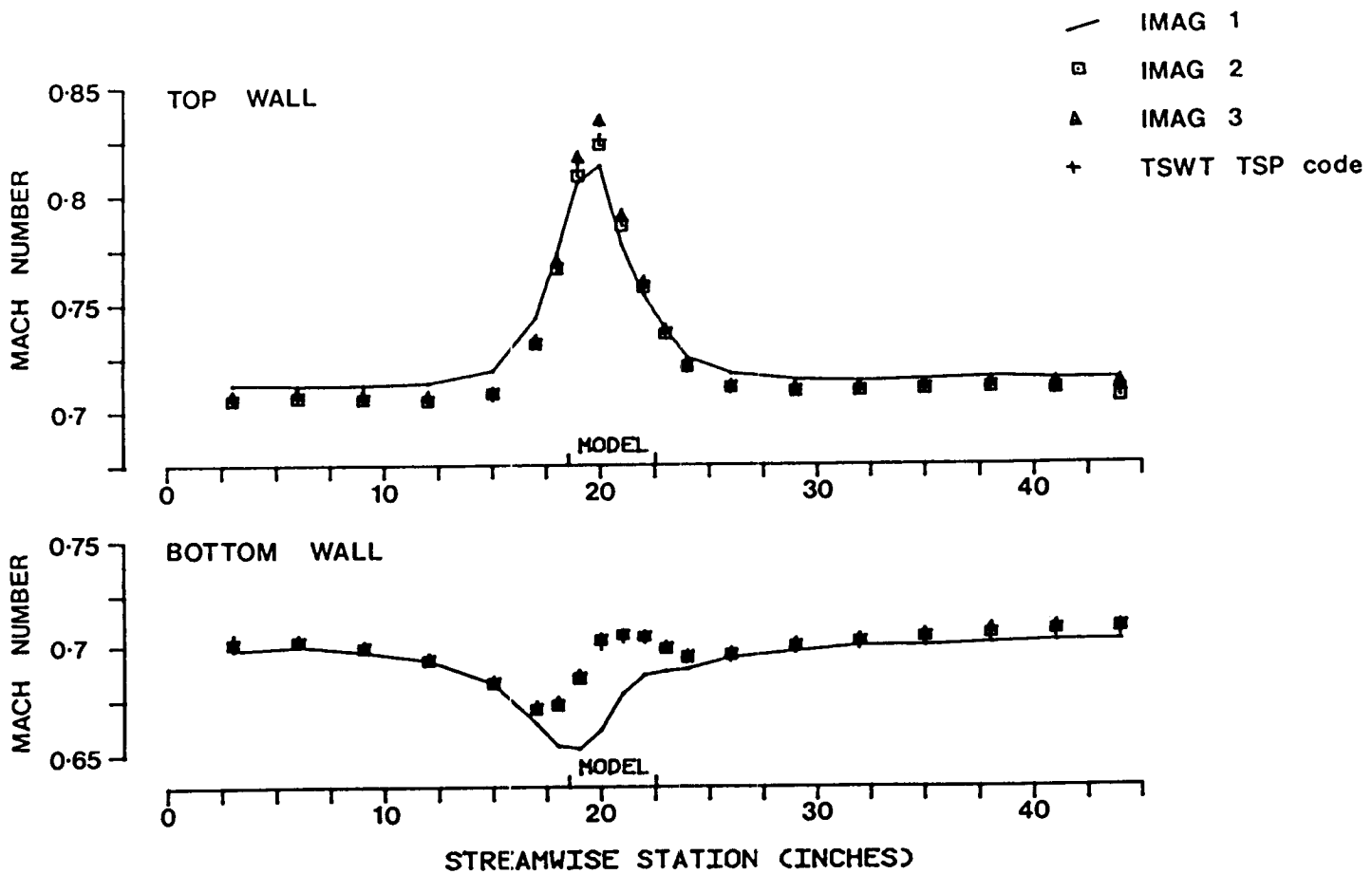

FIG. 7.8b IMAGINARY FLOW PREDICTIONS BY SEVERAL COMPUTATIONAL METHODS (CONDITION 2: $M_\infty = 0.6998$; $\alpha \simeq 6.0^o$).

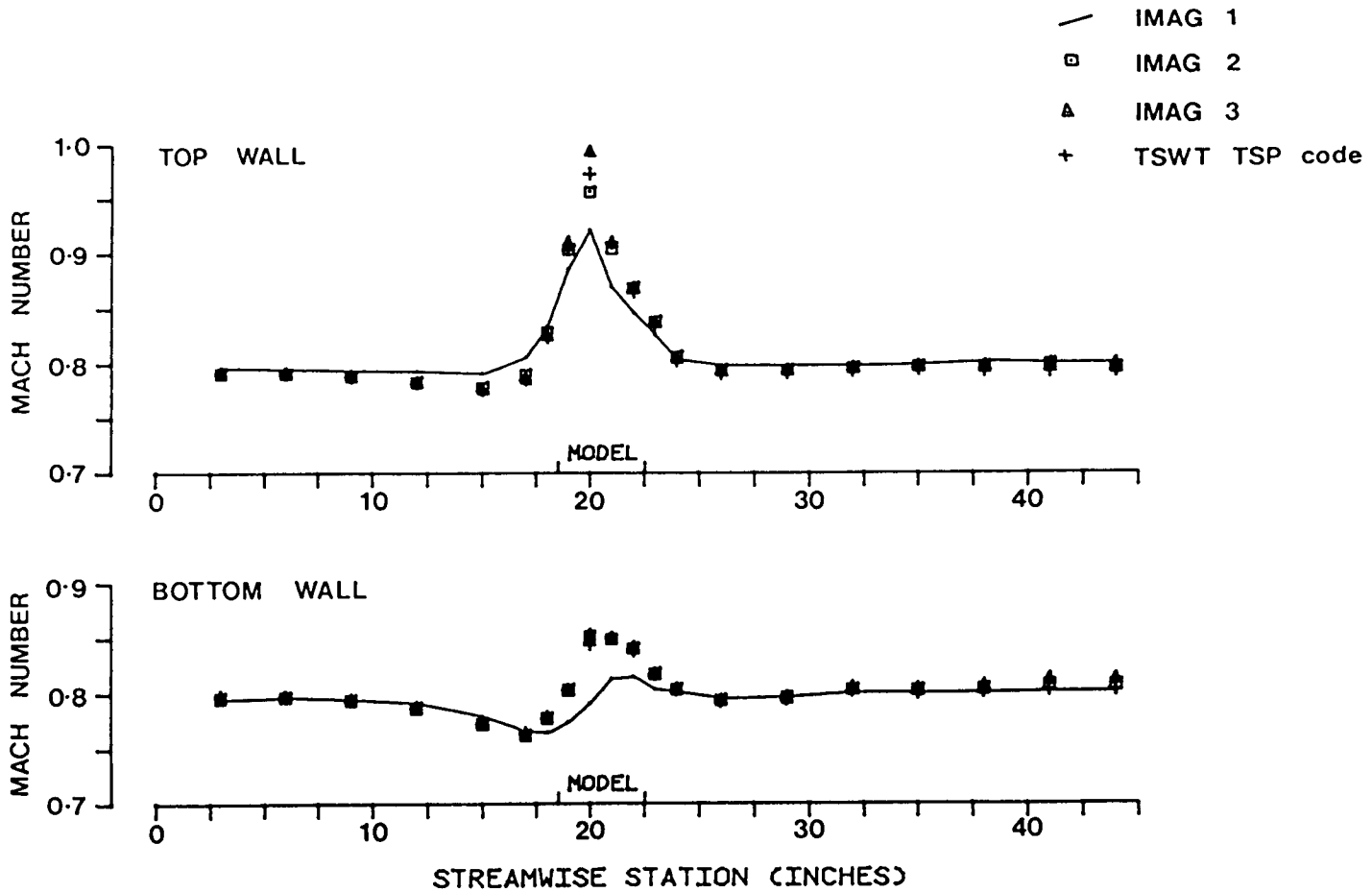

FIG. 7.8c IMAGINARY FLOW PREDICTIONS BY SEVERAL COMPUTATIONAL METHODS (CONDITION 3: $M_\infty = 0.7981$; $\alpha \simeq 6.0^o$).

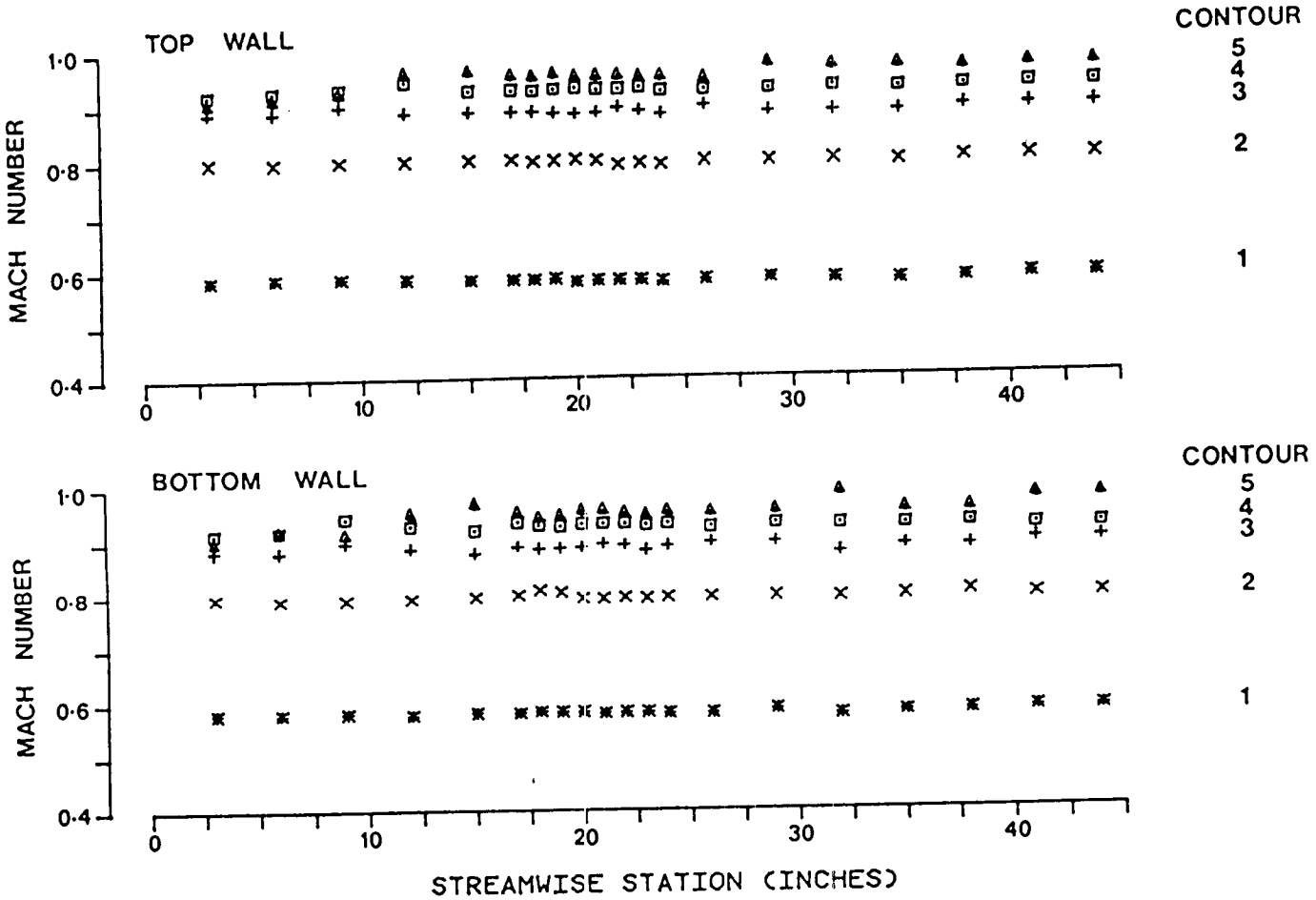

FIG. 8.1 DISTRIBUTIONS OF MACH NUMBER ALONG CENTRELINES OF WALLS SET TO AERODYNAMICALLY STRAIGHT CONTOURS (EMPTY TEST SECTION). ORIGINAL WALLS.

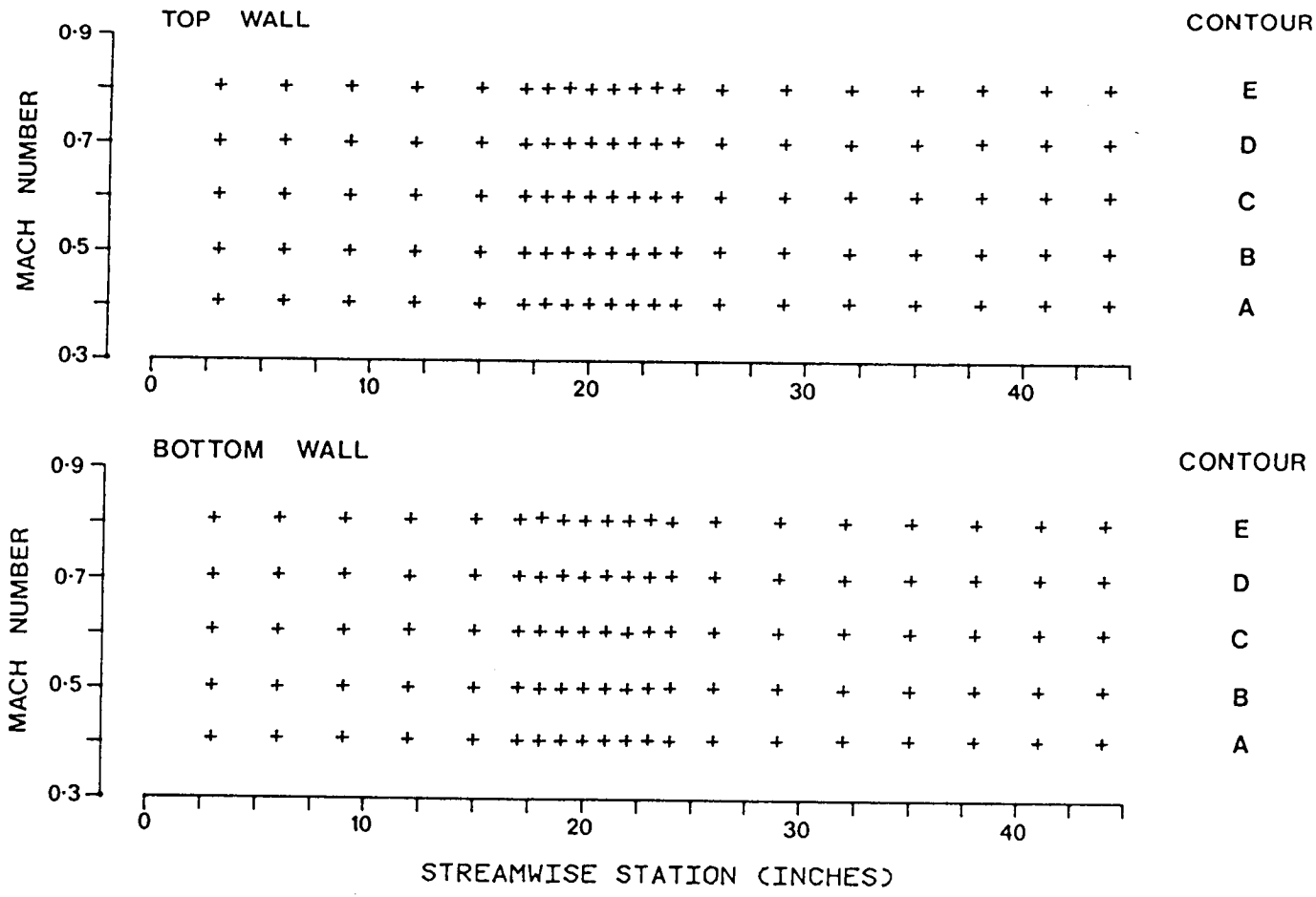

FIG. 8.2 DISTRIBUTIONS OF MACH NUMBER ALONG CENTRELINES OF WALLS SET TO AERODYNAMICALLY STRAIGHT CONTOURS (EMPTY TEST SECTION). NEW WALLS.

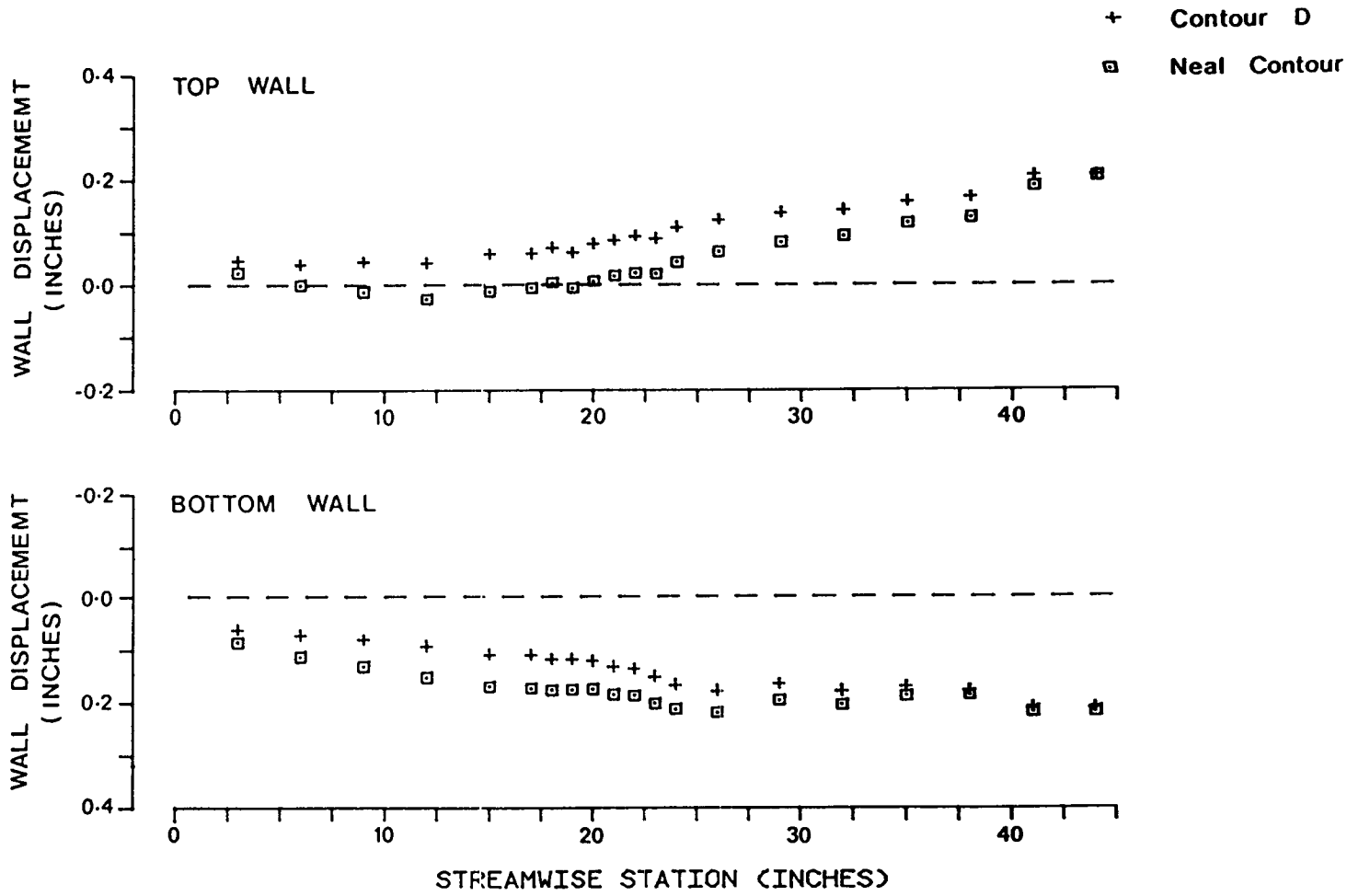

FIG. 8.3 DISPLACEMENTS OF WALLS FROM GEOMETRICALLY STRAIGHT. WALLS SET TO CONTOURS THAT EXHIBIT CONSTANT WALL MACH NUMBER (M_∞ = 0.6).

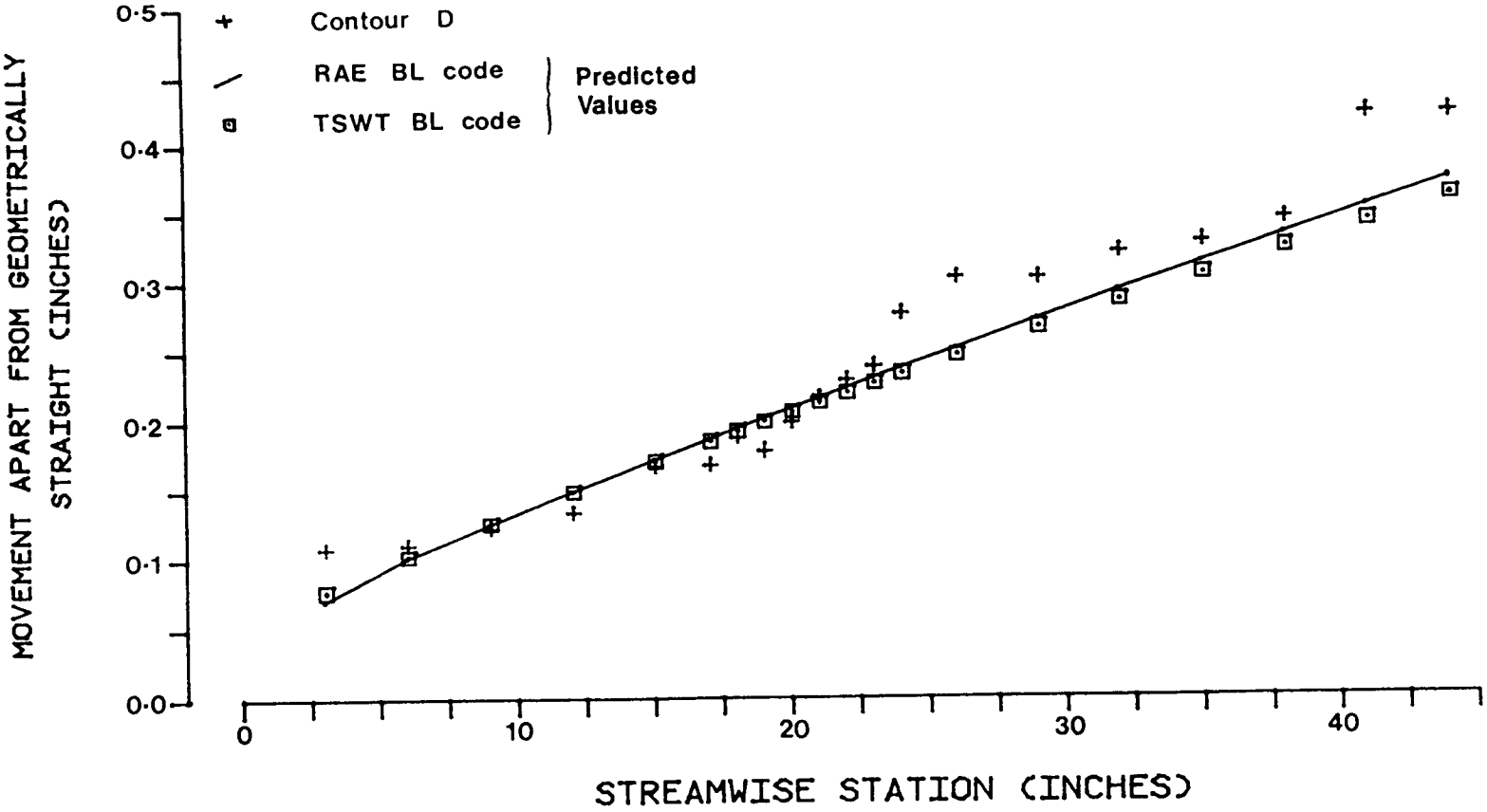

FIG. 8.4 WALL MOVEMENTS APART FROM GEOMETRICALLY STRAIGHT. WALLS SET TO AERODYNAMICALLY STRAIGHT CONTOUR (CONTOUR D).

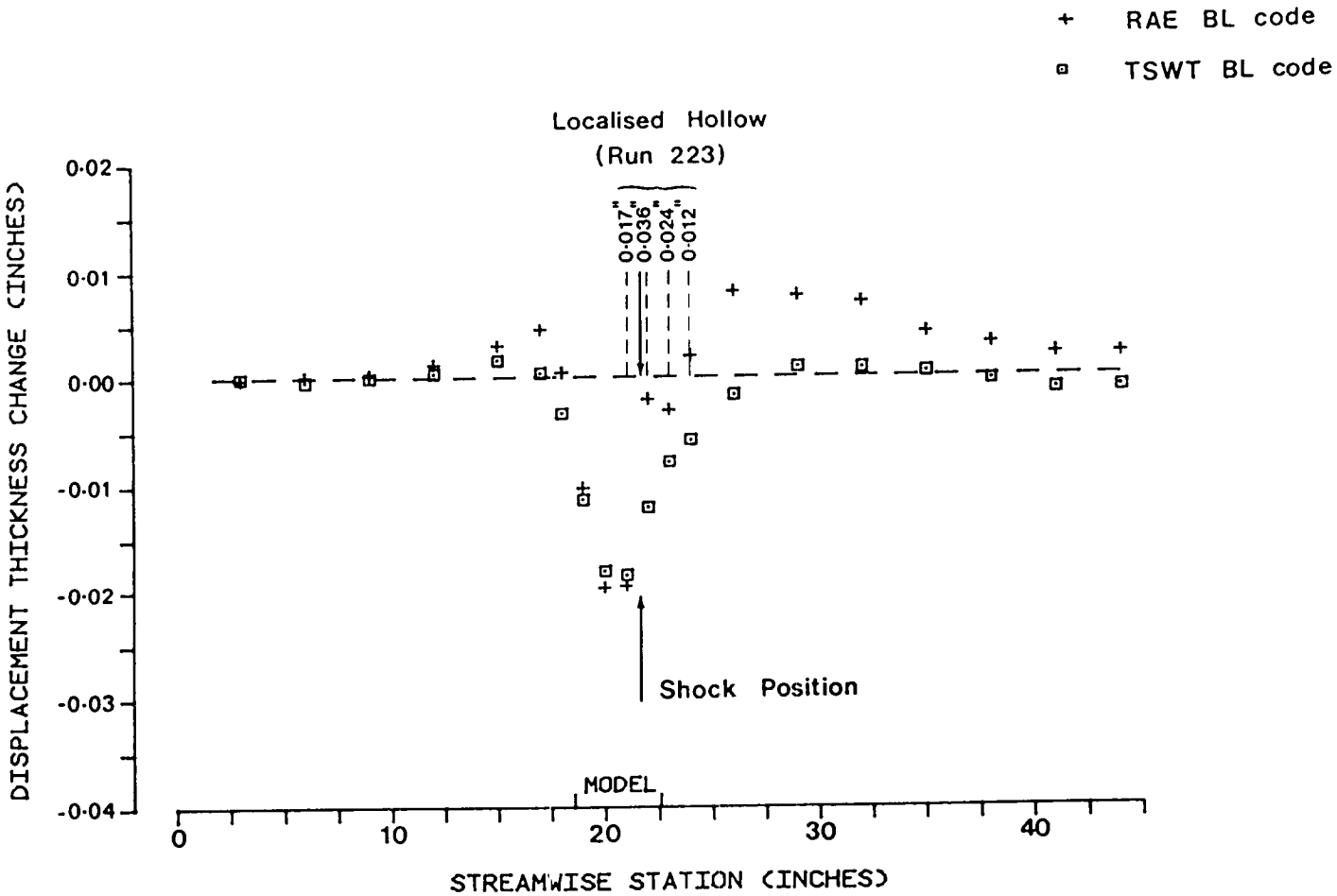

FIG. 9.1 CALCULATIONS OF $\Delta\delta^*$ ALONG TOP WALL OF RUN 184 ($M_\infty = 0.8862$; $\alpha \simeq 4.0^o$).

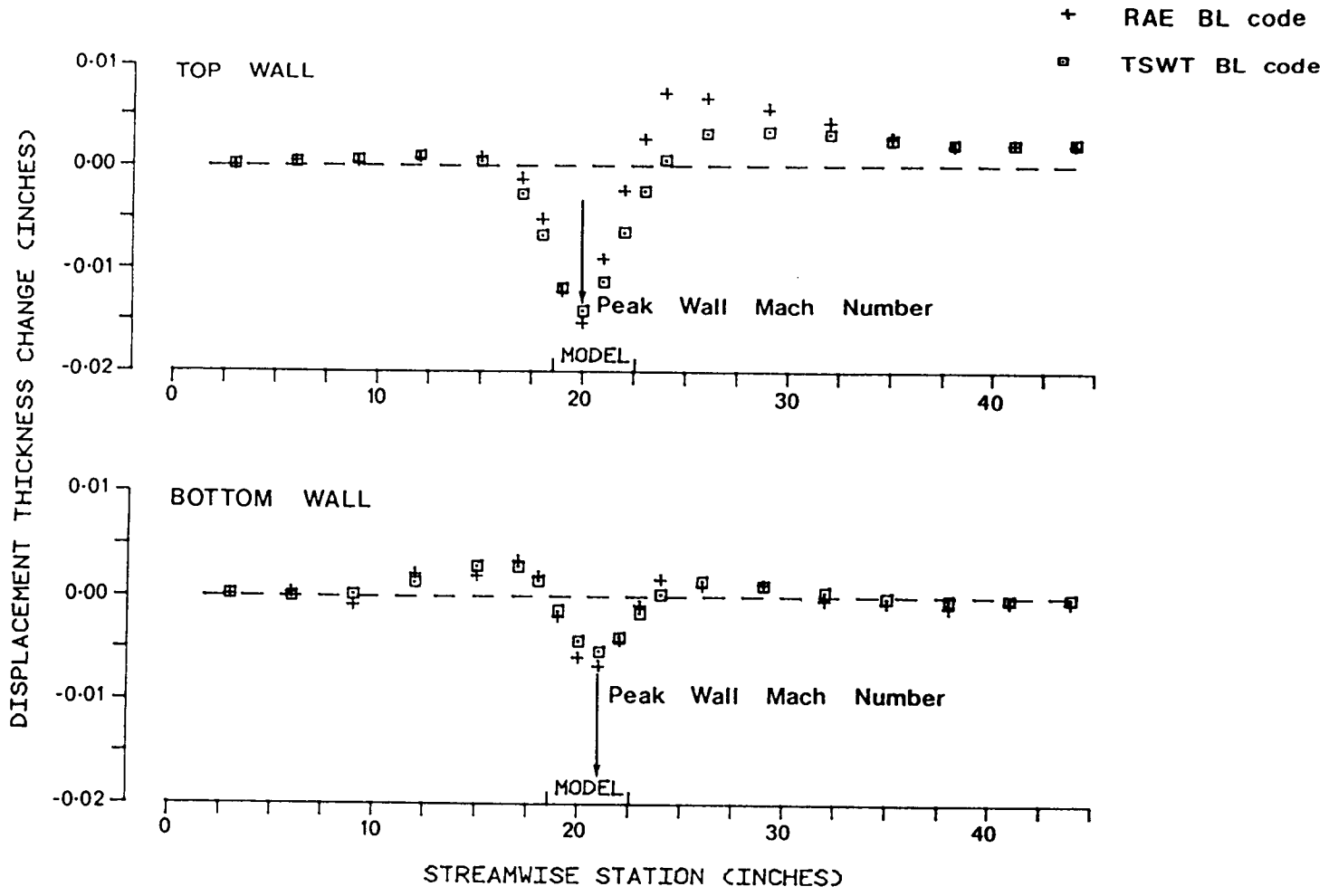

FIG. 9.2 NACA 0012-64 MEASUREMENTS (RUN 235 - $M_\infty = 0.8$; $\alpha \simeq 4.0^o$). CALCULATIONS OF $\Delta\delta^*$ ALONG FLEXIBLE WALLS. WALLS STREAMLINED BY THE WAS 2A STRATEGY.

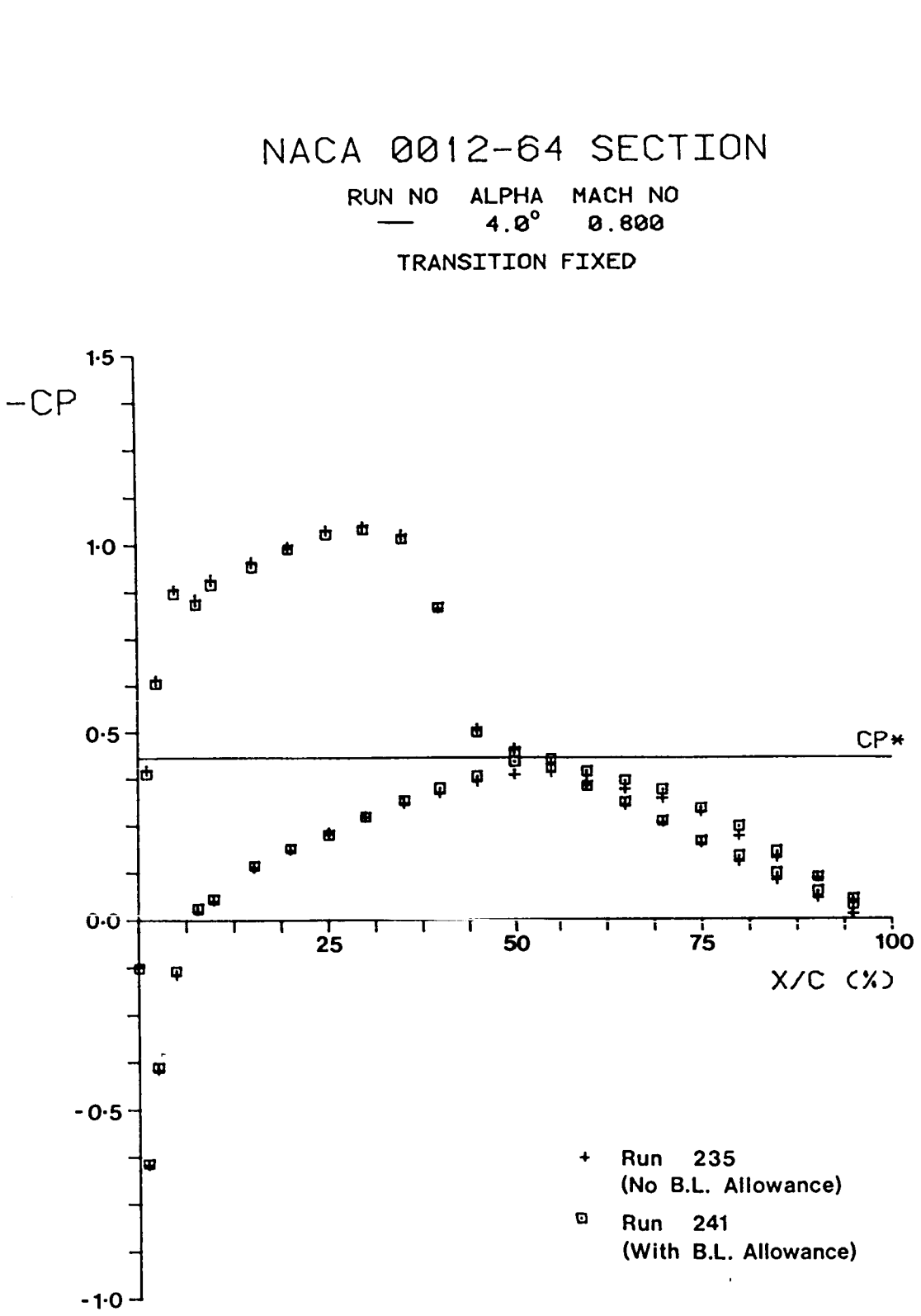

FIG. 9.3 THE EFFECTS OF AN ALLOWANCE FOR δ^* VARIATIONS ON MODEL PRESSURE DISTRIBUTION. WALLS STREAMLINED BY THE WAS 2A STRATEGY.

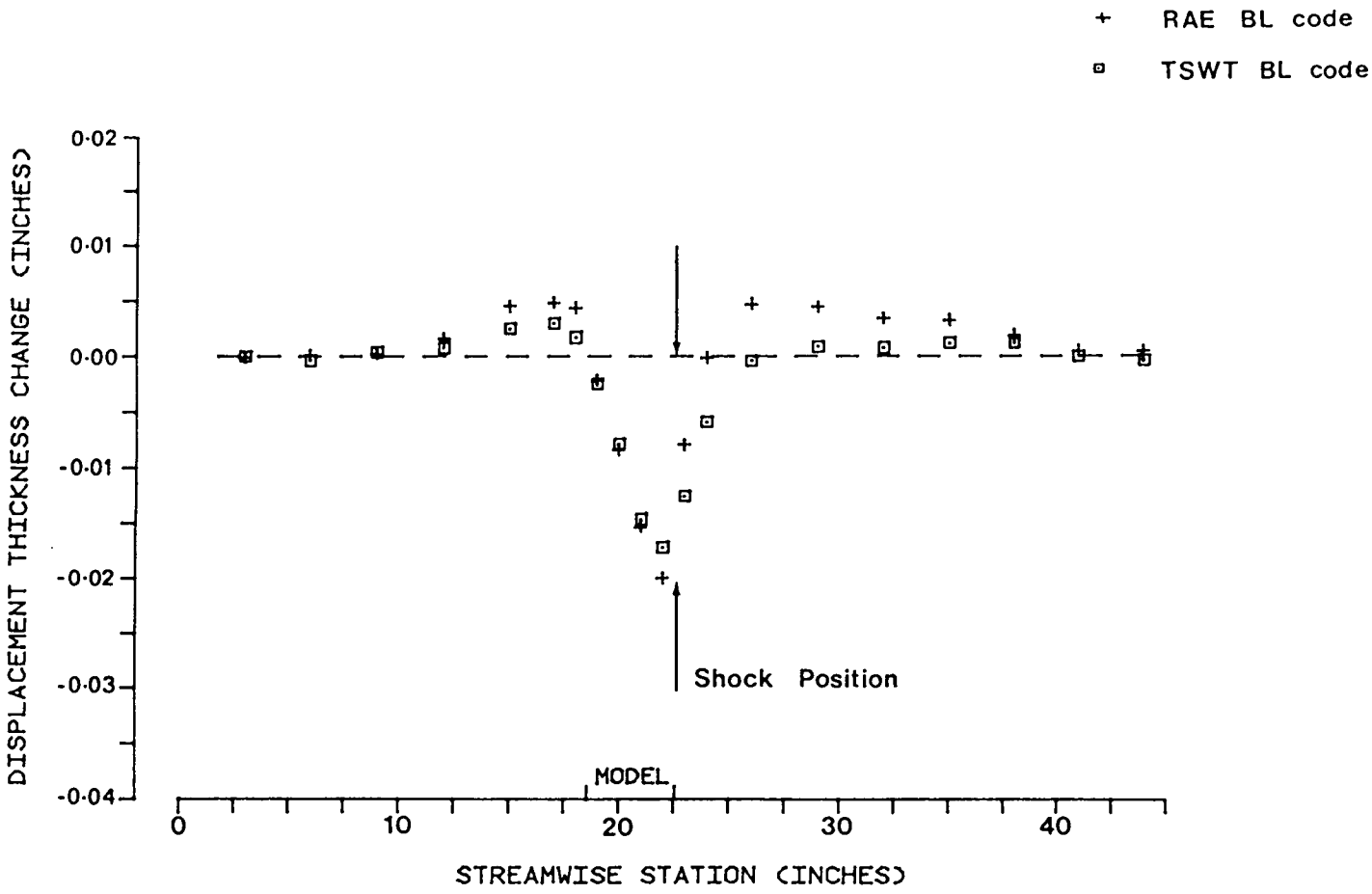

FIG. 9.4 CALCULATIONS OF $\Delta\delta^*$ ALONG BOTTOM WALL OF RUN 184 ($M_\infty = 0.8862$; $\alpha \simeq 4.0^o$).

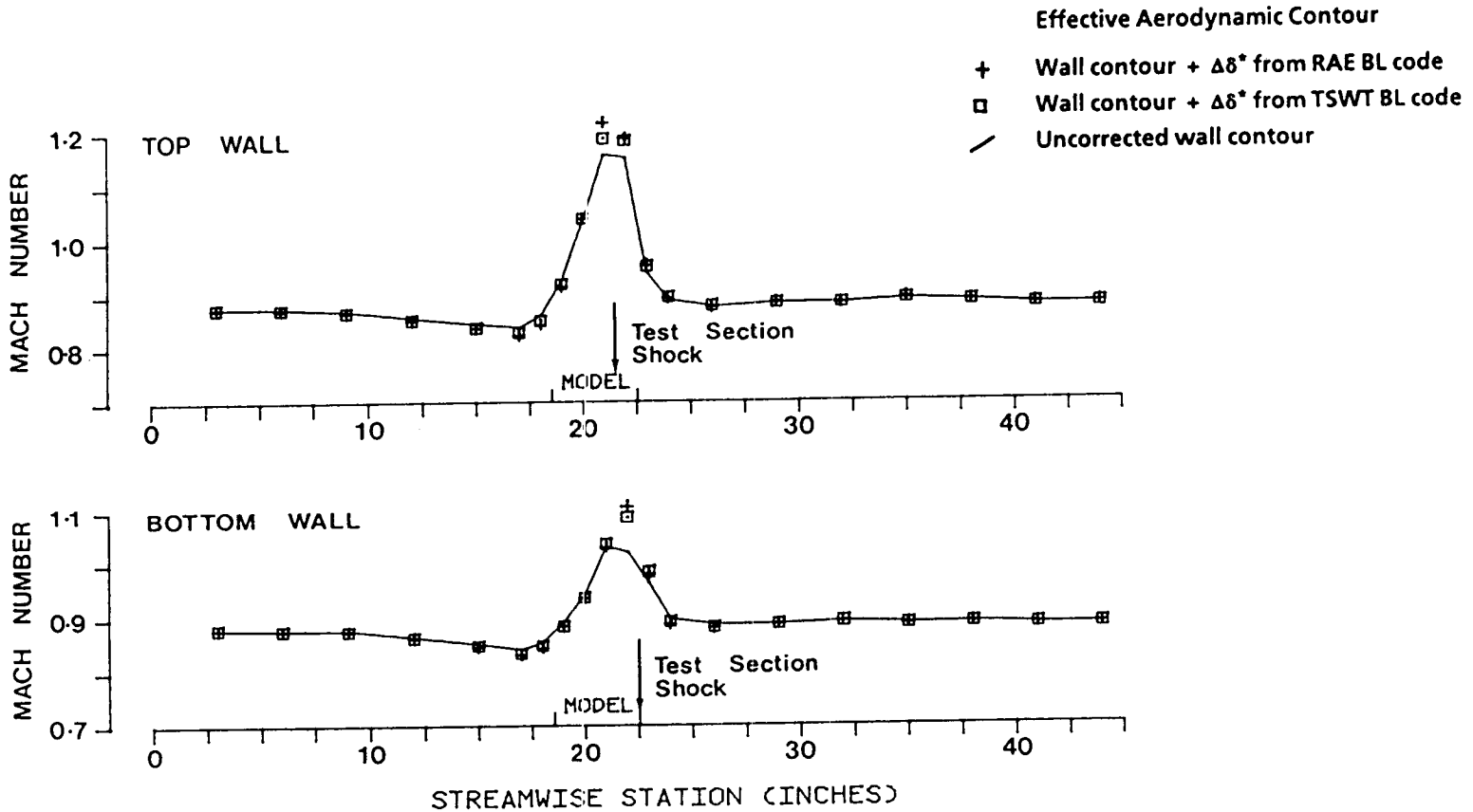

FIG. 9.5 IMAGINARY WALL MACH NUMBER DISTRIBUTIONS CALCULATED BY THE TSWT TSP CODE AT RUN 184 CONDITIONS ($M_\infty = 0.8862$; $\alpha \simeq 4.0^o$).

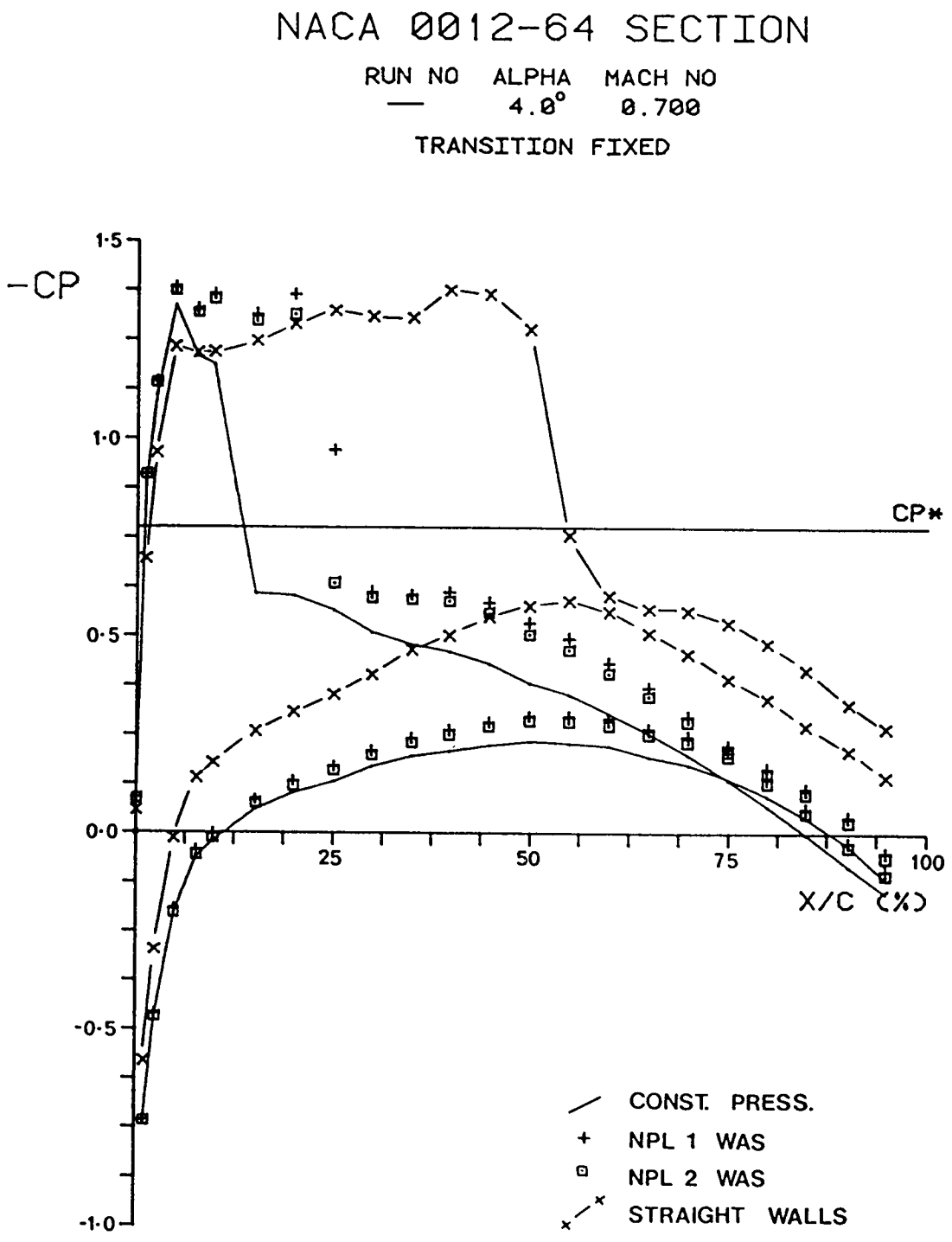

FIG. 10.1 MODEL PRESSURE DISTRIBUTIONS.
WALLS SET TO AERODYNAMICALLY STRAIGHT, CONSTANT PRESSURE AND STREAMLINED (NPL WAS) CONTOURS.

NACA 0012-64 SECTION

$M_\infty = 0.7$; $\alpha = 4.0^\circ$

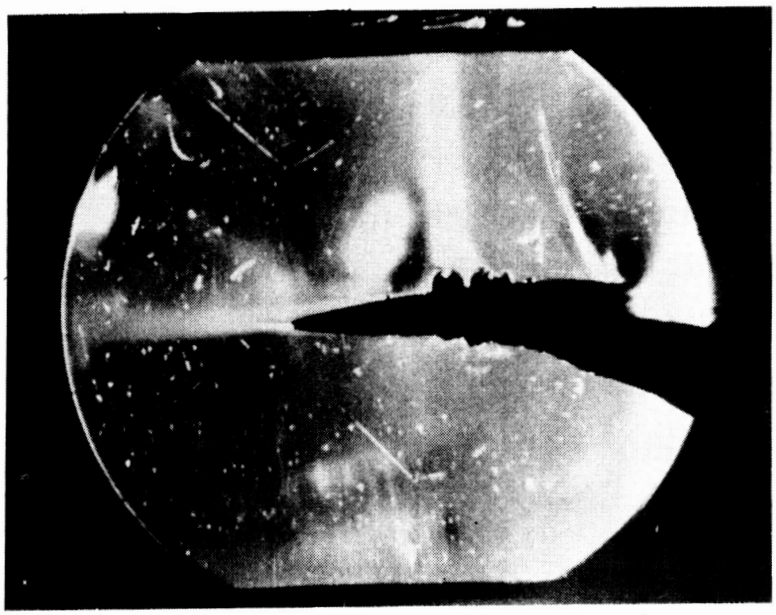

Straight Walls

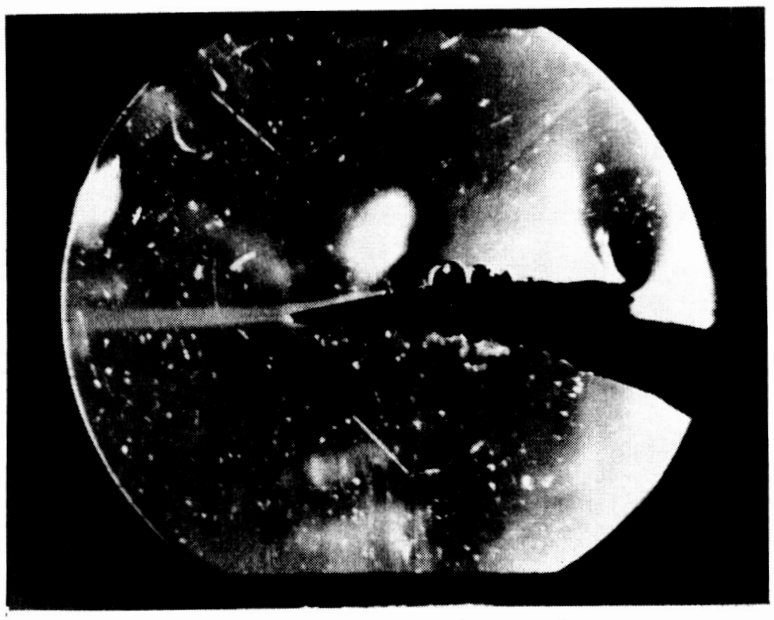

Streamlined Walls (WAS 1)

FIG.10.2 SCHLIEREN PICTURES ILLUSTRATING THE EFFECTS OF WALL STREAMLINING

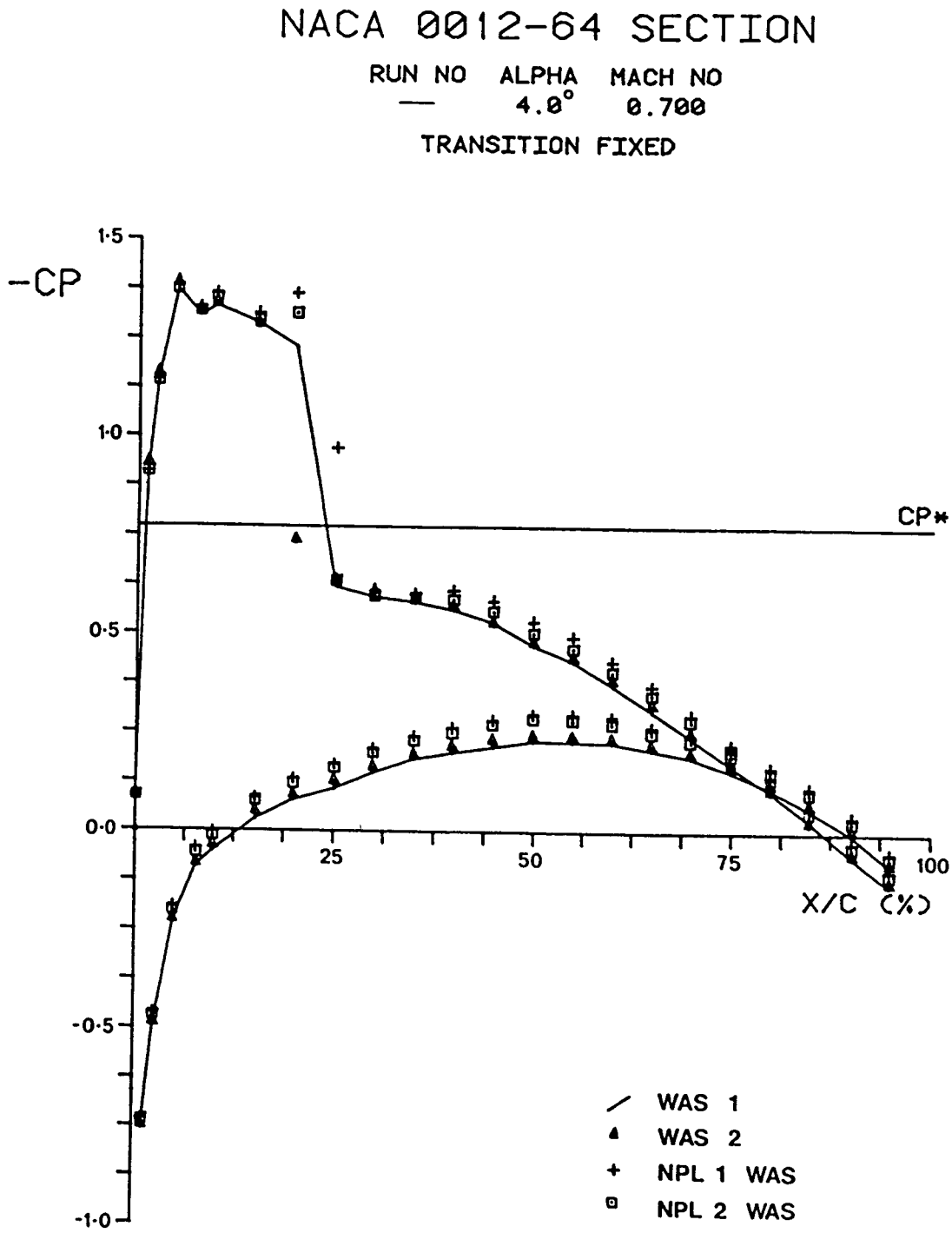

FIG. 10.3 MODEL PRESSURE DISTRIBUTIONS.
WALLS SET TO STREAMLINED CONTOURS.

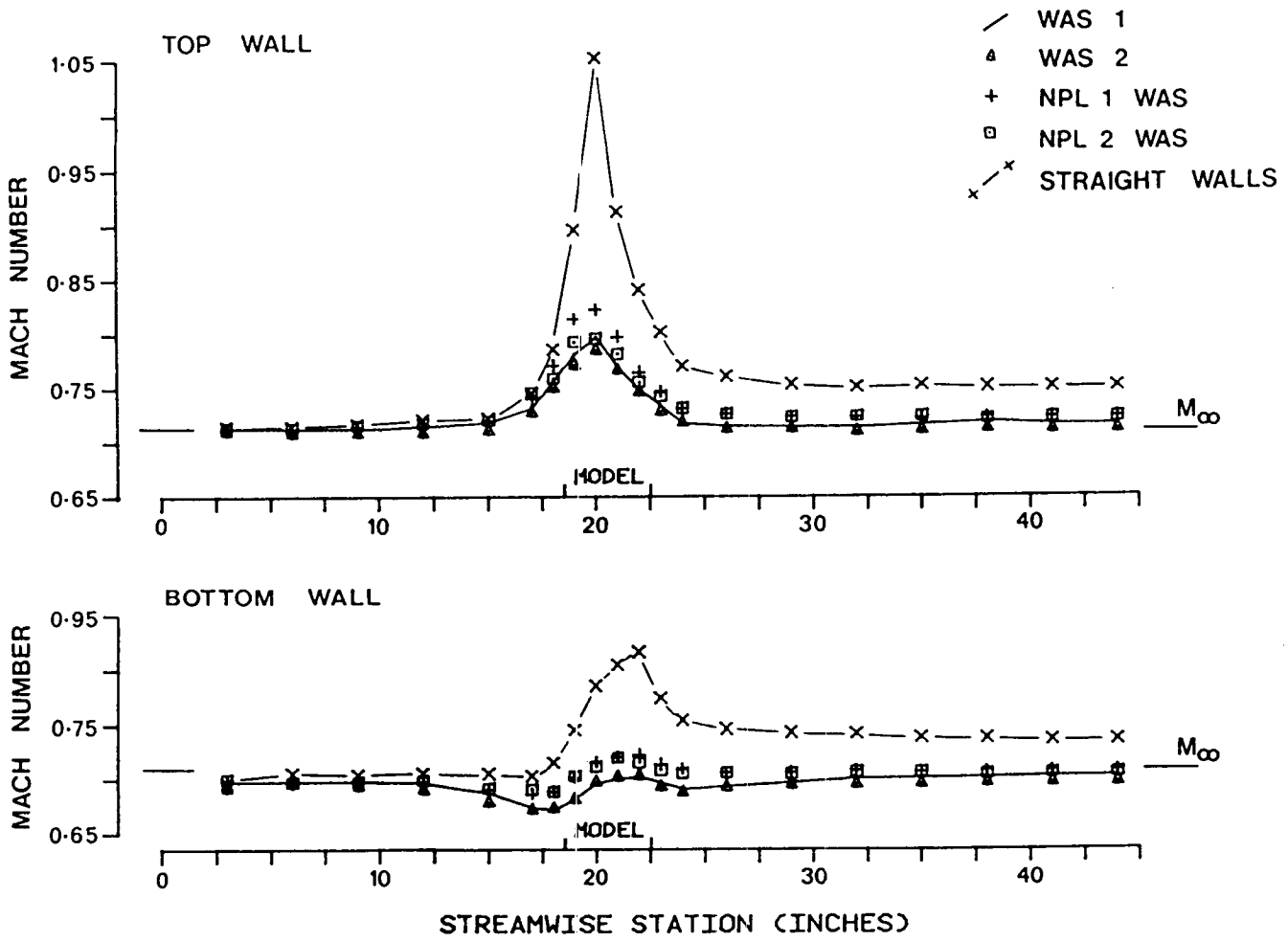

FIG. 10.4 NACA 0012-64 MEASUREMENTS ($M_\infty = 0.7$; $\alpha \simeq 4.0^o$). DISTRIBUTIONS OF MACH NUMBER ALONG CENTRELINES OF AERODYNAMICALLY STRAIGHT AND STREAMLINED CONTOURS.

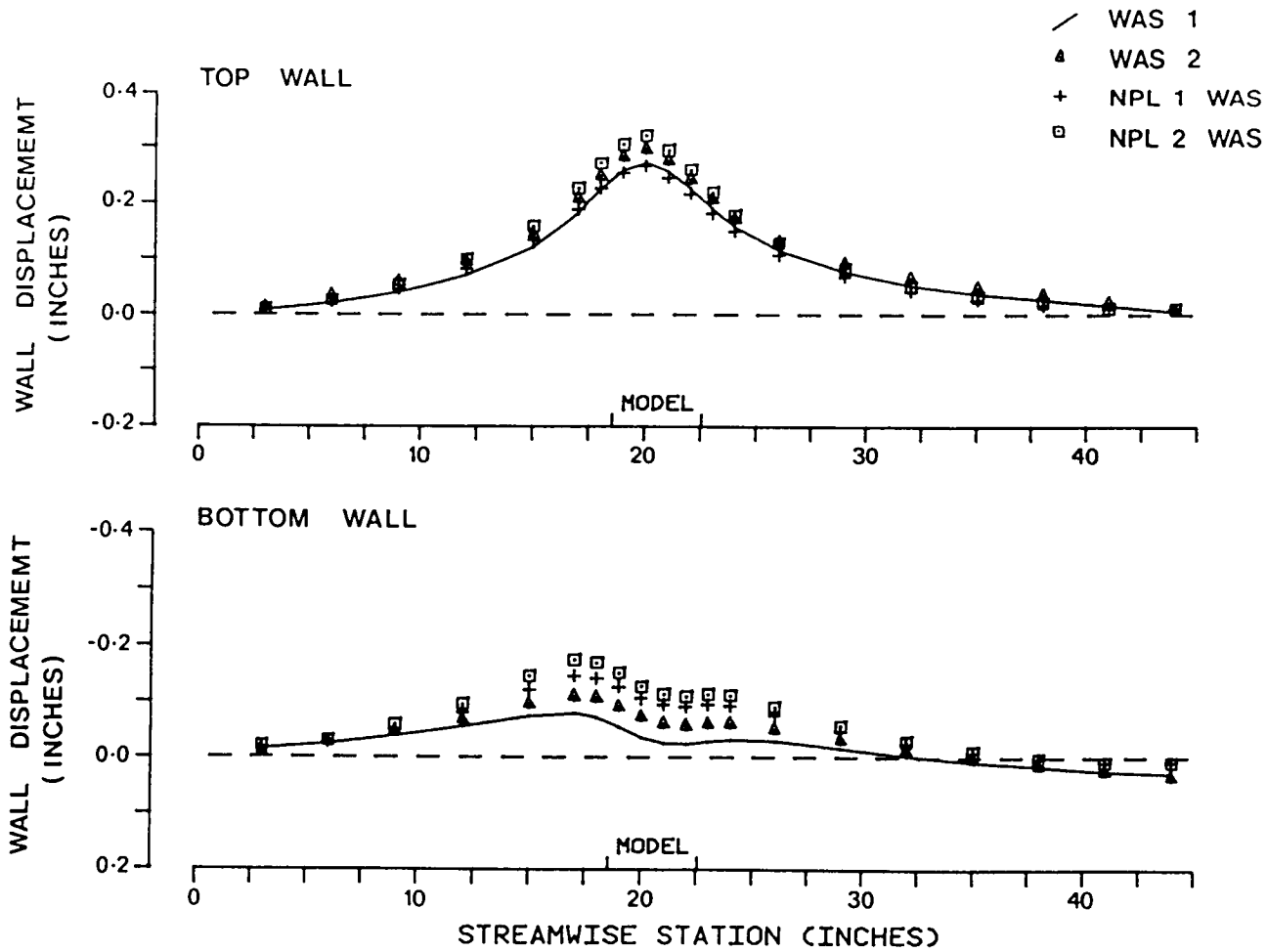

FIG. 10.5 NACA 0012-64 MEASUREMENTS (M_∞ = 0.7; $\alpha \simeq 4.0^o$). DISPLACEMENTS OF WALLS FROM AERODYNAMICALLY STRAIGHT CONTOURS. WALLS STREAMLINED.

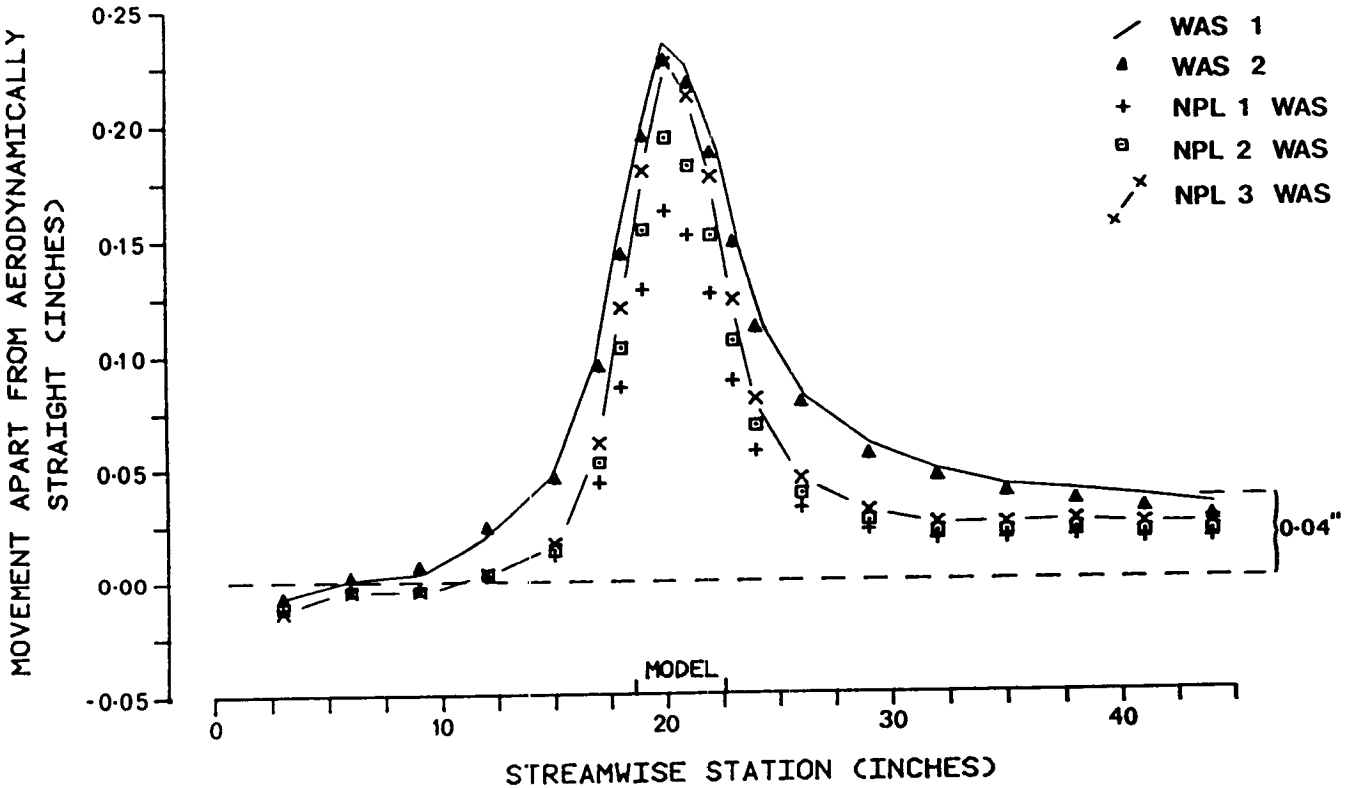

FIG. 10.6 NACA 0012-64 MEASUREMENTS ($M_\infty = 0.7$; $\alpha \simeq 4.0^o$). WALL MOVEMENTS APART FROM AERODYNAMICALLY STRAIGHT CONTOURS. WALLS STREAMLINED .

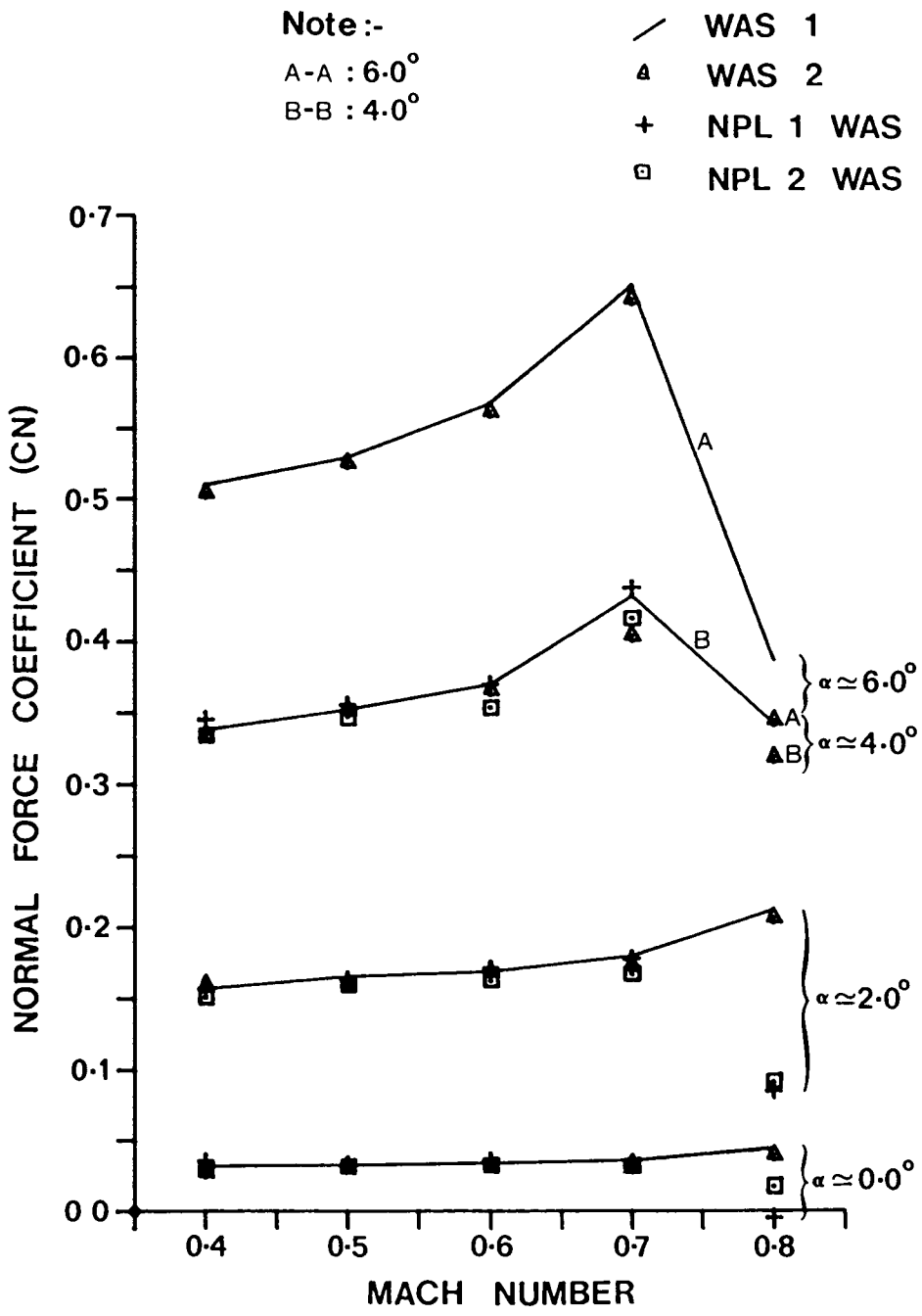

FIG. 10.7.1 NACA 0012-64 SECTION. VARIATION OF NORMAL FORCE COEFFICIENT WITH MACH NUMBER. WALLS STREAMLINED.

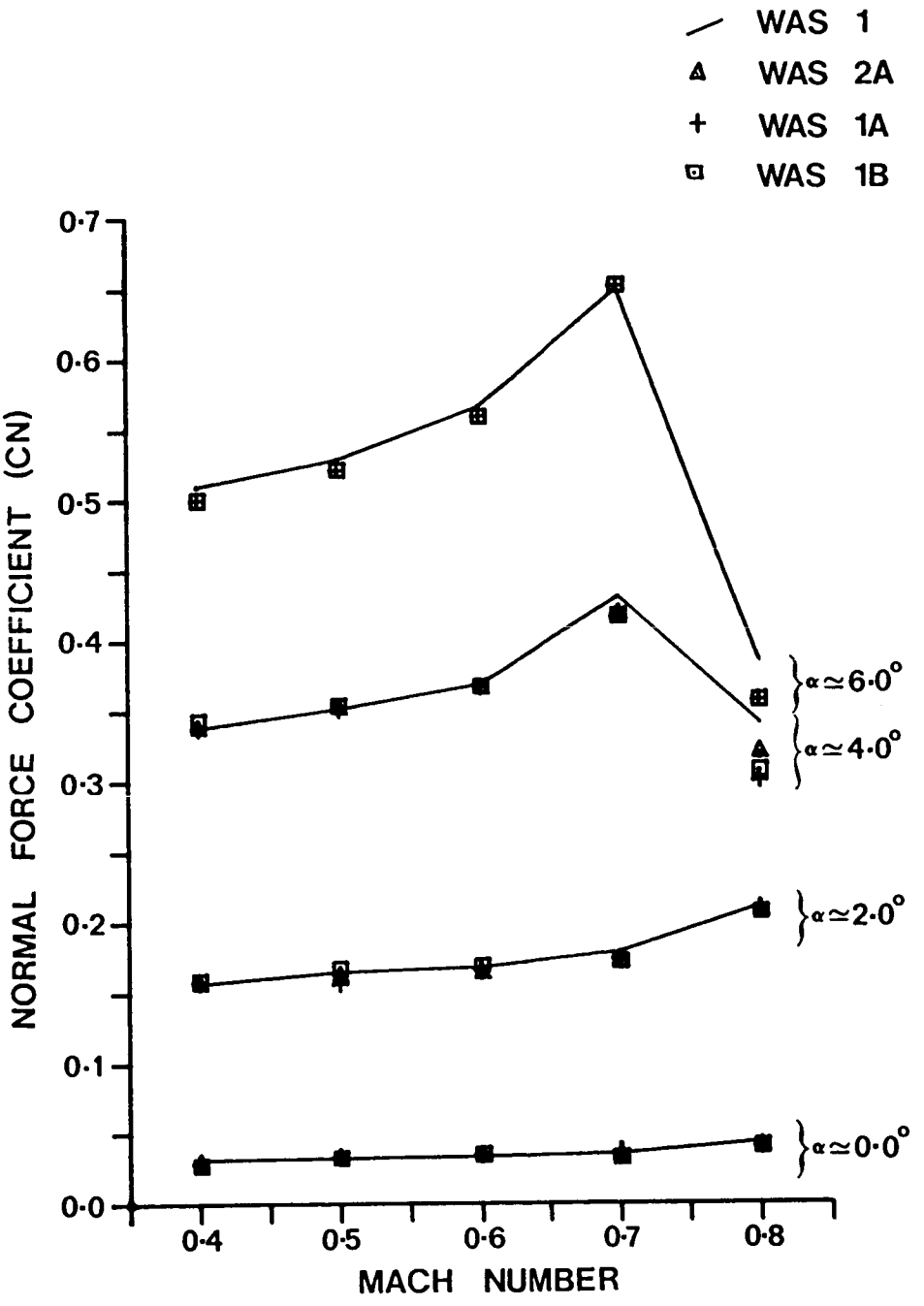

FIG. 10.7.2 NACA 0012-64 SECTION. VARIATION OF NORMAL FORCE COEFFICIENT WITH MACH NUMBER. WALLS STREAMLINED.

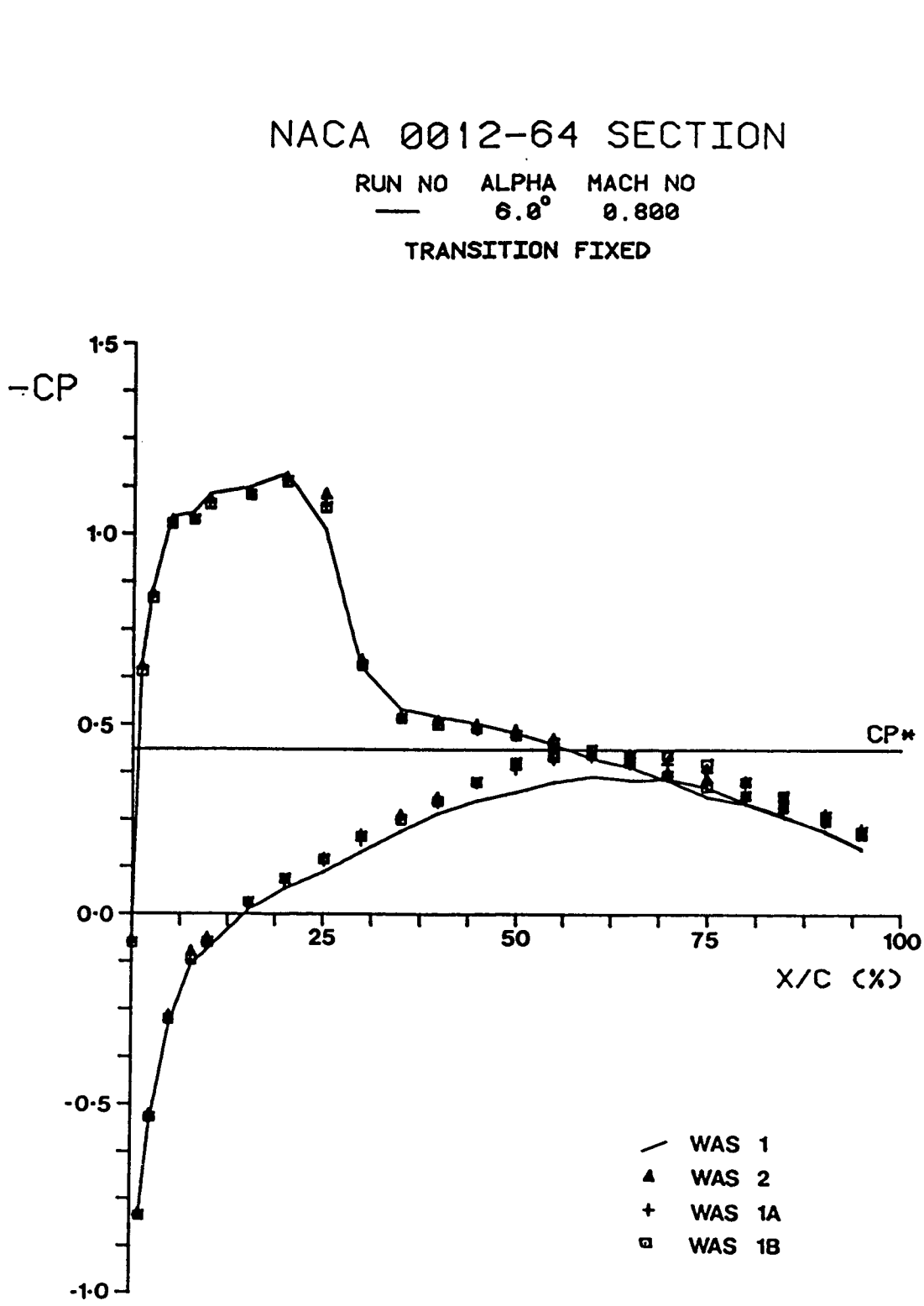

FIG. 10.8 MODEL PRESSURE DISTRIBUTIONS.
WALLS SET TO STREAMLINED CONTOURS.

★U.S. GOVERNMENT PRINTING OFFICE: 1988-526-069/86003

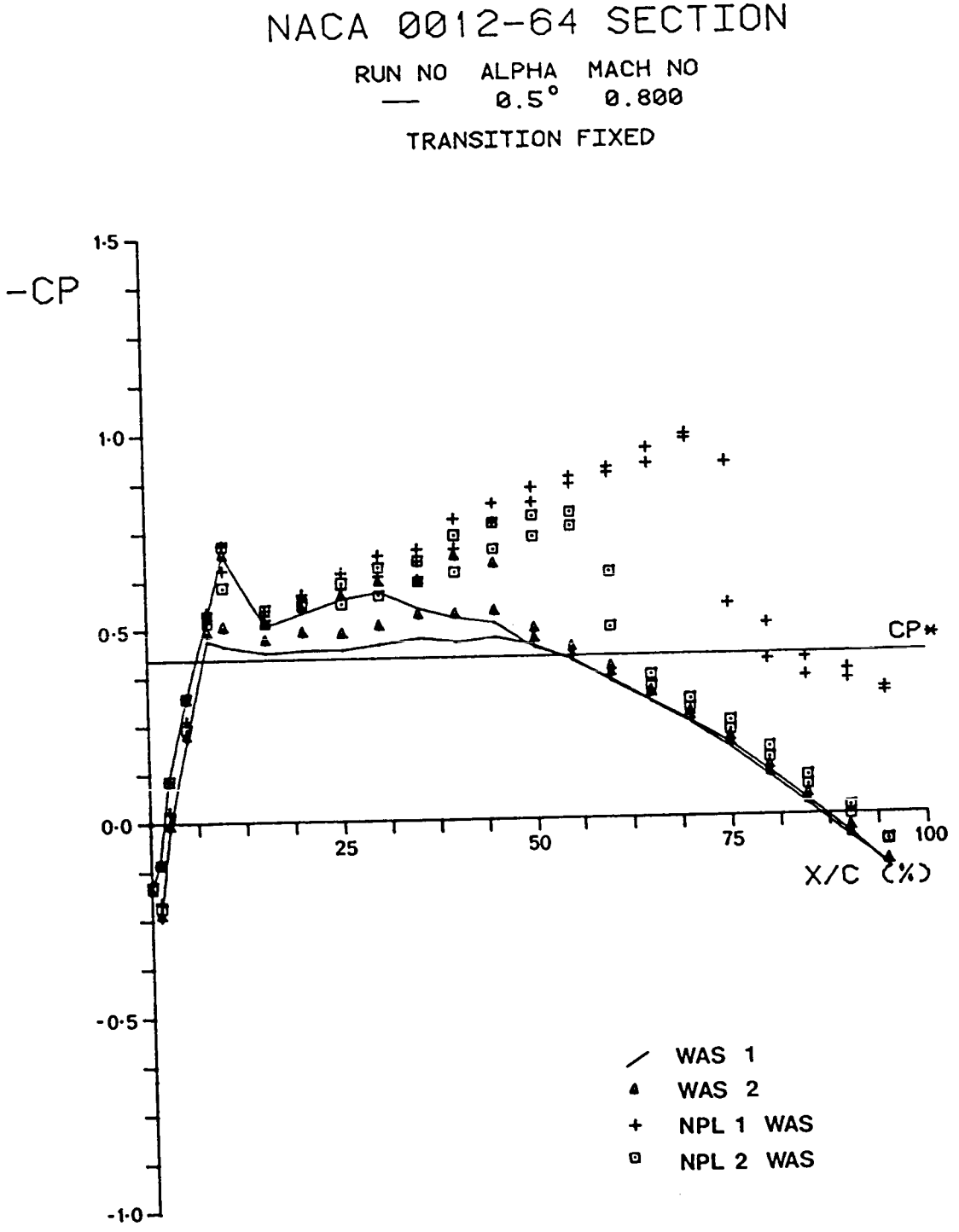

FIG. 10.9 MODEL PRESSURE DISTRIBUTIONS.
WALLS SET TO STREAMLINED CONTOURS.

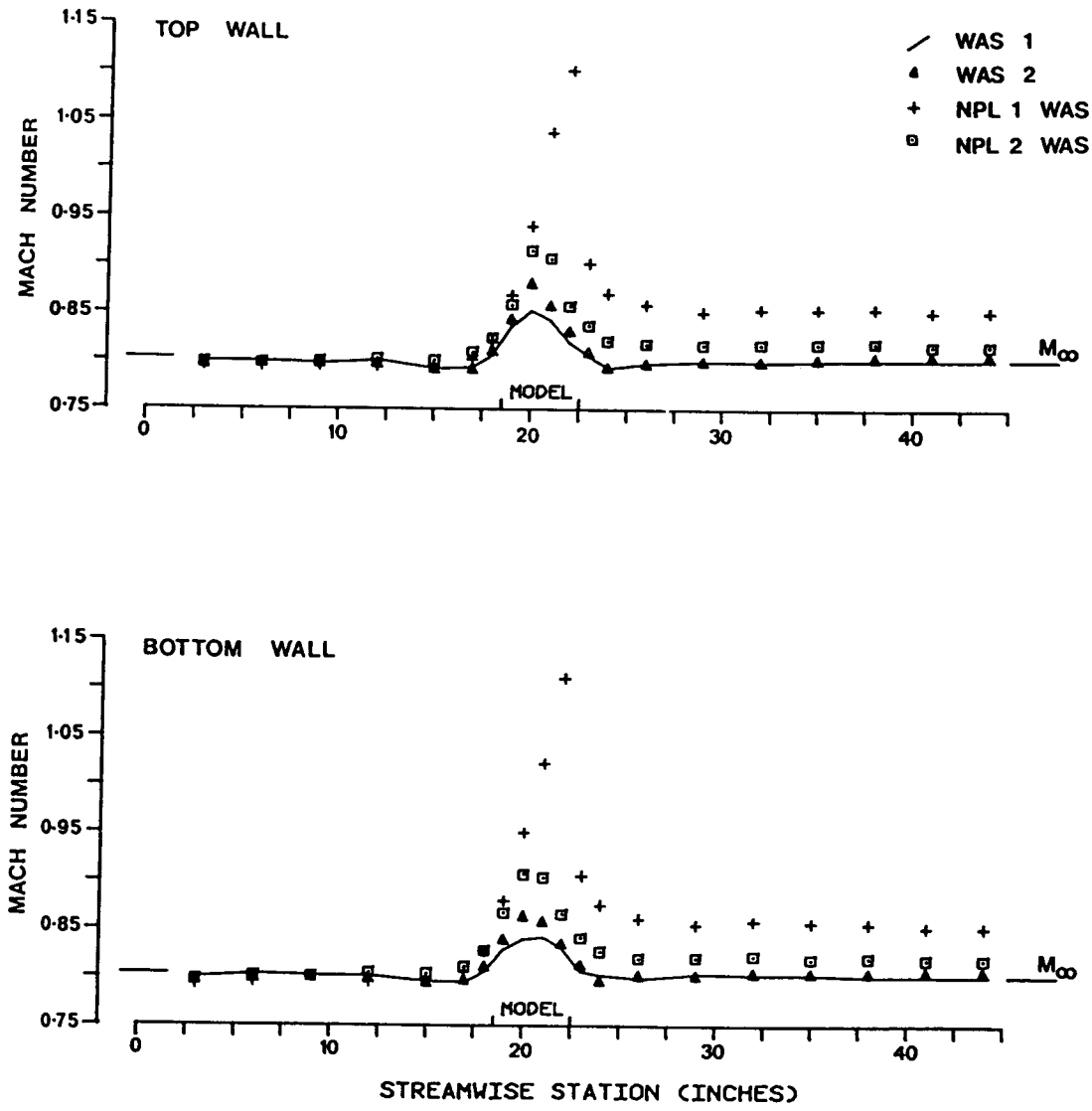

FIG. 10.10 NACA 0012-64 MEASUREMENTS ($M_\infty = 0.8$; $\alpha \simeq 0.5^O$). DISTRIBUTIONS OF MACH NUMBER ALONG CENTRELINES OF STREAMLINED CONTOURS.

NACA 0012-64 SECTION

$M_\infty = 0{\cdot}8$; $\alpha = 0{\cdot}5^\circ$

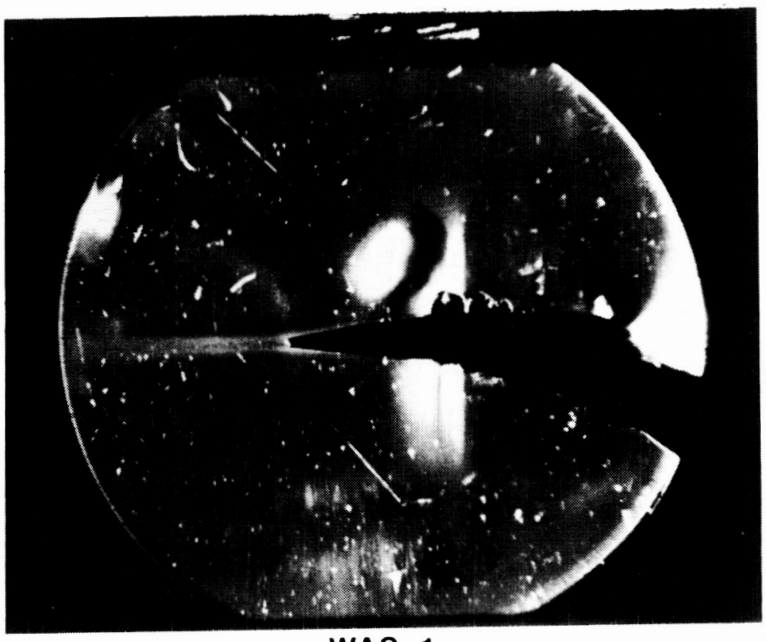

WAS 1

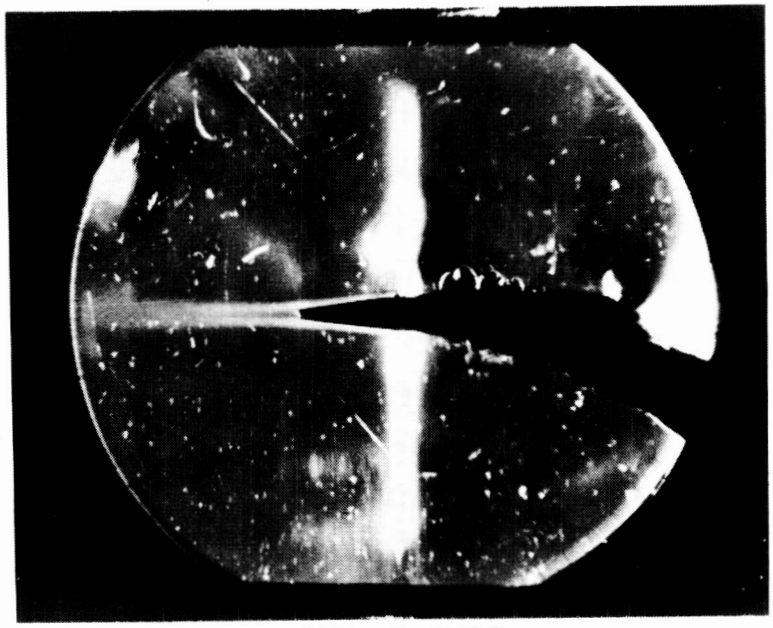

NPL 2 WAS

FIG.10.11 SCHLIEREN PICTURES ILLUSTRATING THE BREAK-DOWN OF NPL WAS

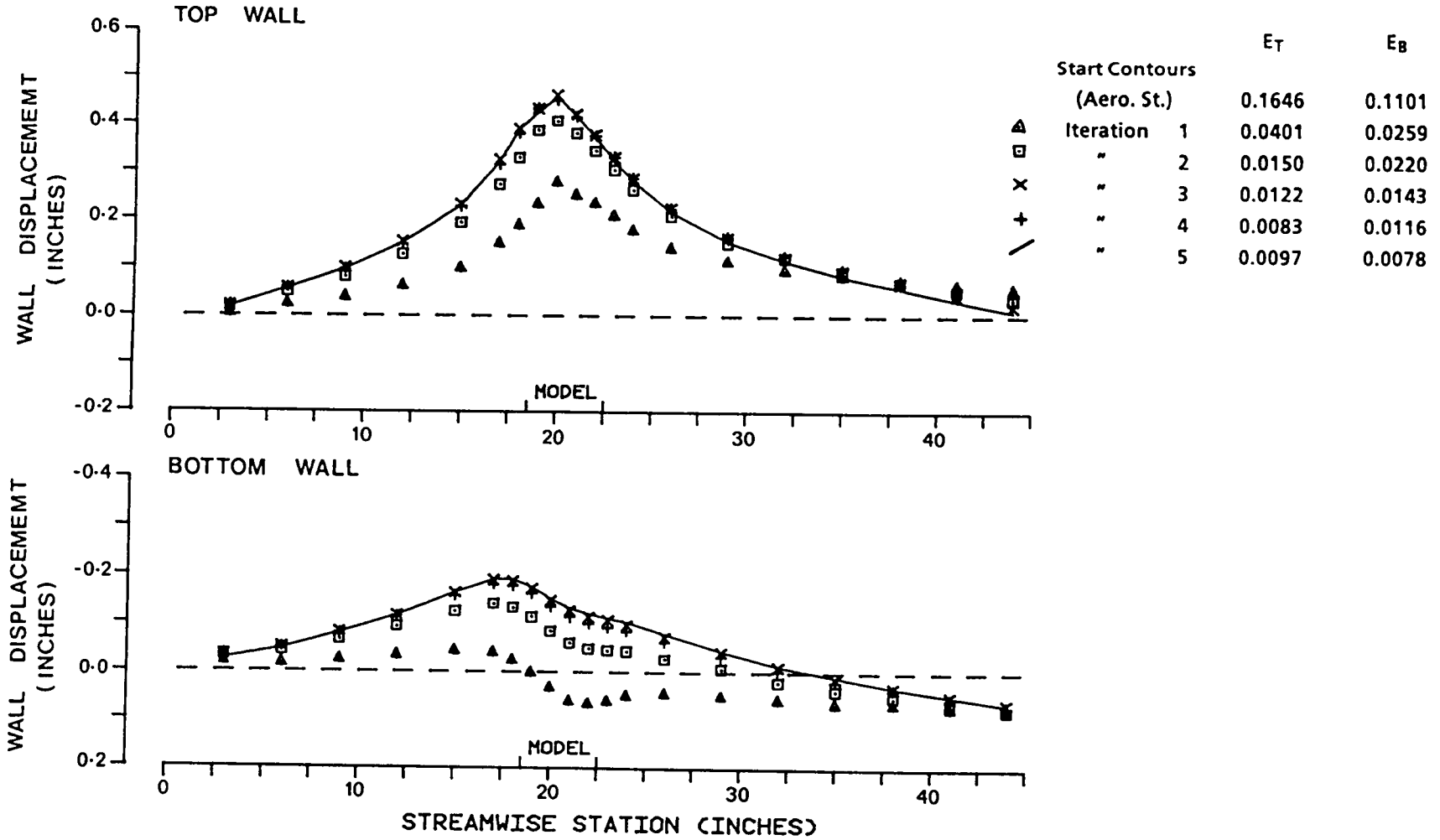

FIG. 10.12 NACA 0012-64 MEASUREMENTS ($M_\infty = 0.7$; $\alpha \simeq 6.0^o$). WALL CONTOURS SET DURING A STREAMLINING CYCLE GOVERNED BY THE WAS 2 STRATEGY.

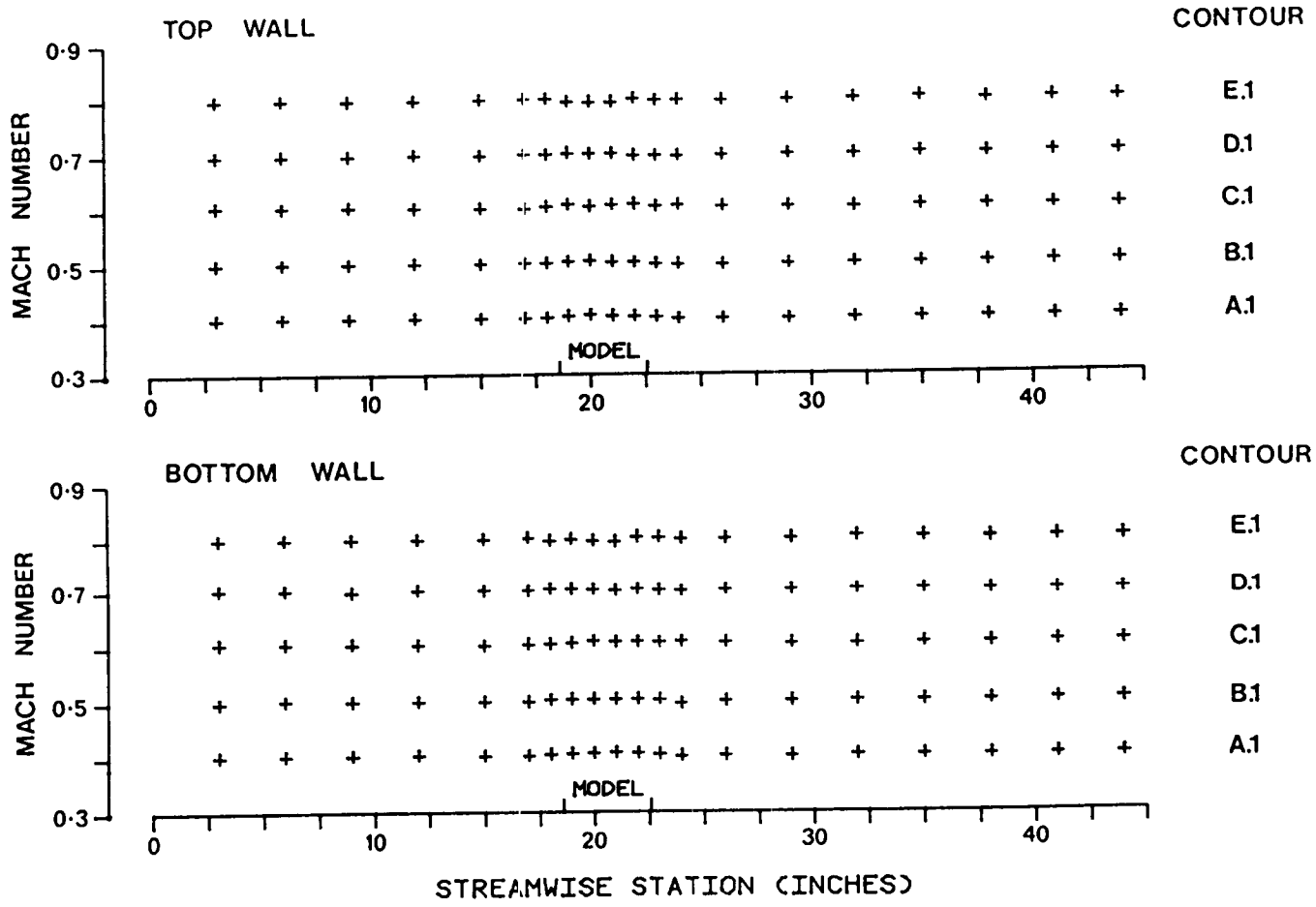

FIG. 10.13.1 NACA 0012-64 MEASUREMENTS ($\alpha \simeq 0.5^{o}$). DISTRIBUTION OF MACH NUMBERS ALONG CENTRELINES OF WALLS SET TO CONSTANT PRESSURE CONTOURS.

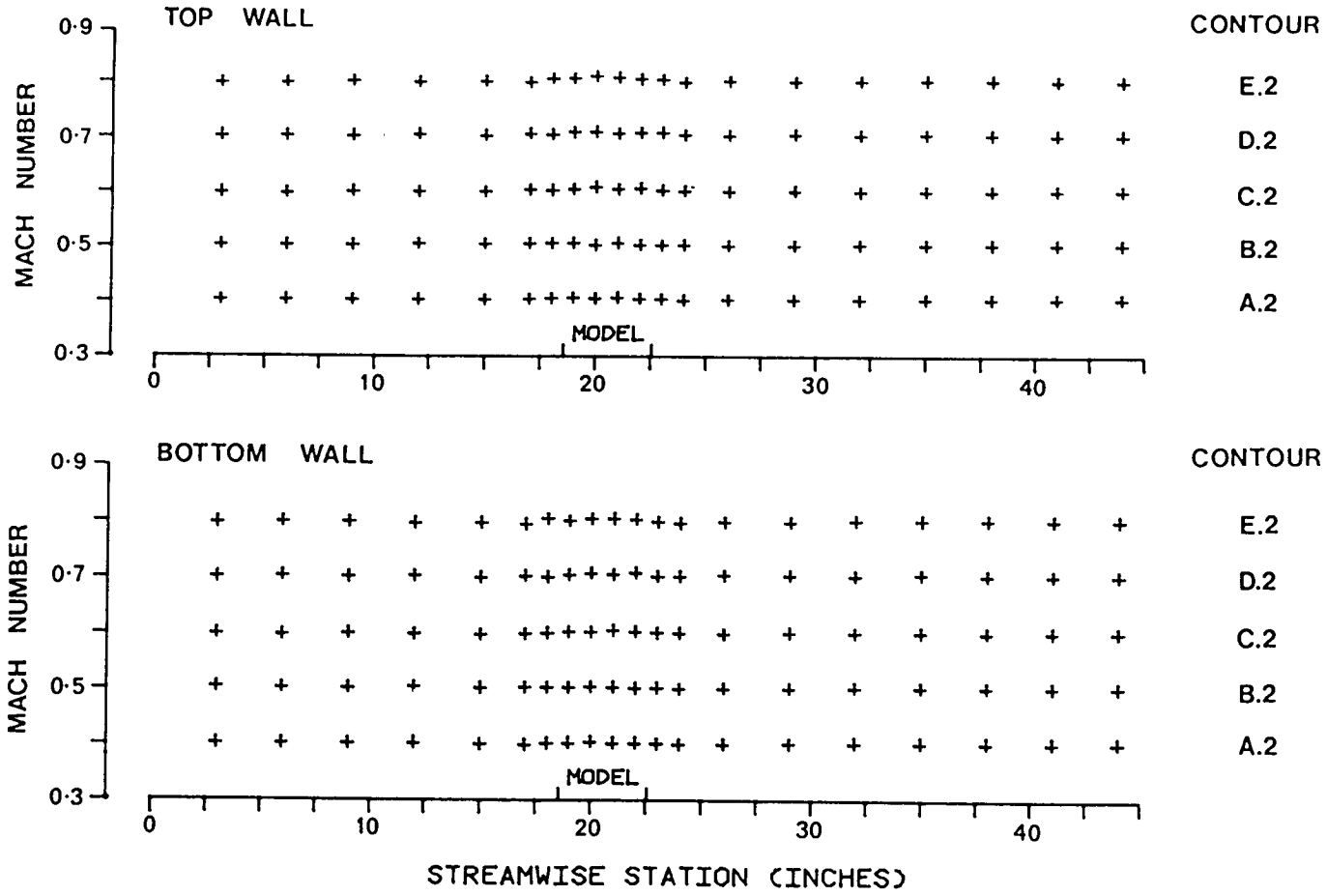

FIG. 10.13.2 NACA 0012-64 MEASUREMENTS ($\alpha \simeq 2.0^{o}$). DISTRIBUTION OF MACH NUMBERS ALONG CENTRELINES OF WALLS SET TO CONSTANT PRESSURE CONTOURS.

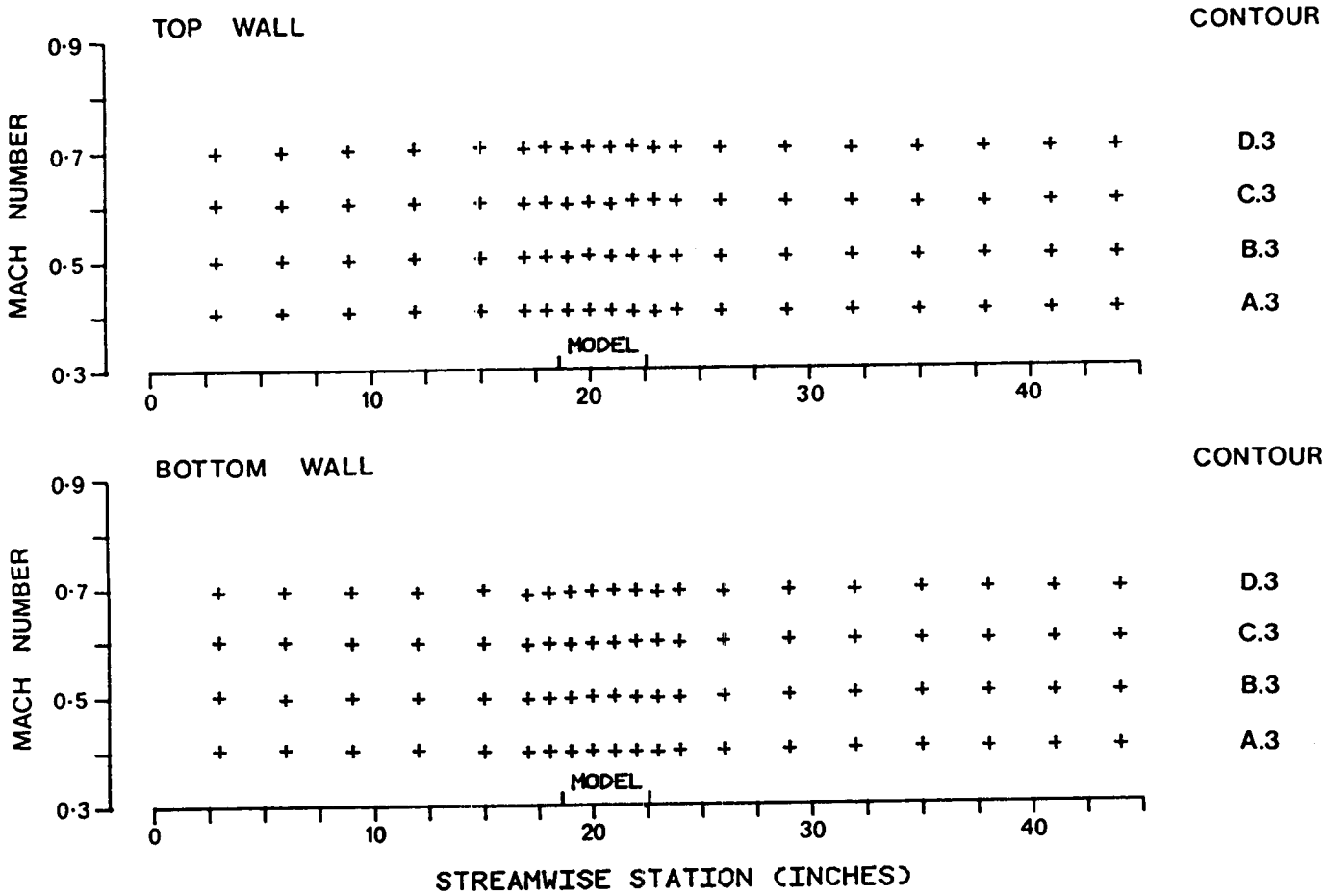

FIG. 10.13.3 NACA 0012-64 MEASUREMENTS ($\alpha \simeq 4.0^{o}$). DISTRIBUTION OF MACH NUMBERS ALONG CENTRELINES OF WALLS SET TO CONSTANT PRESSURE CONTOURS.

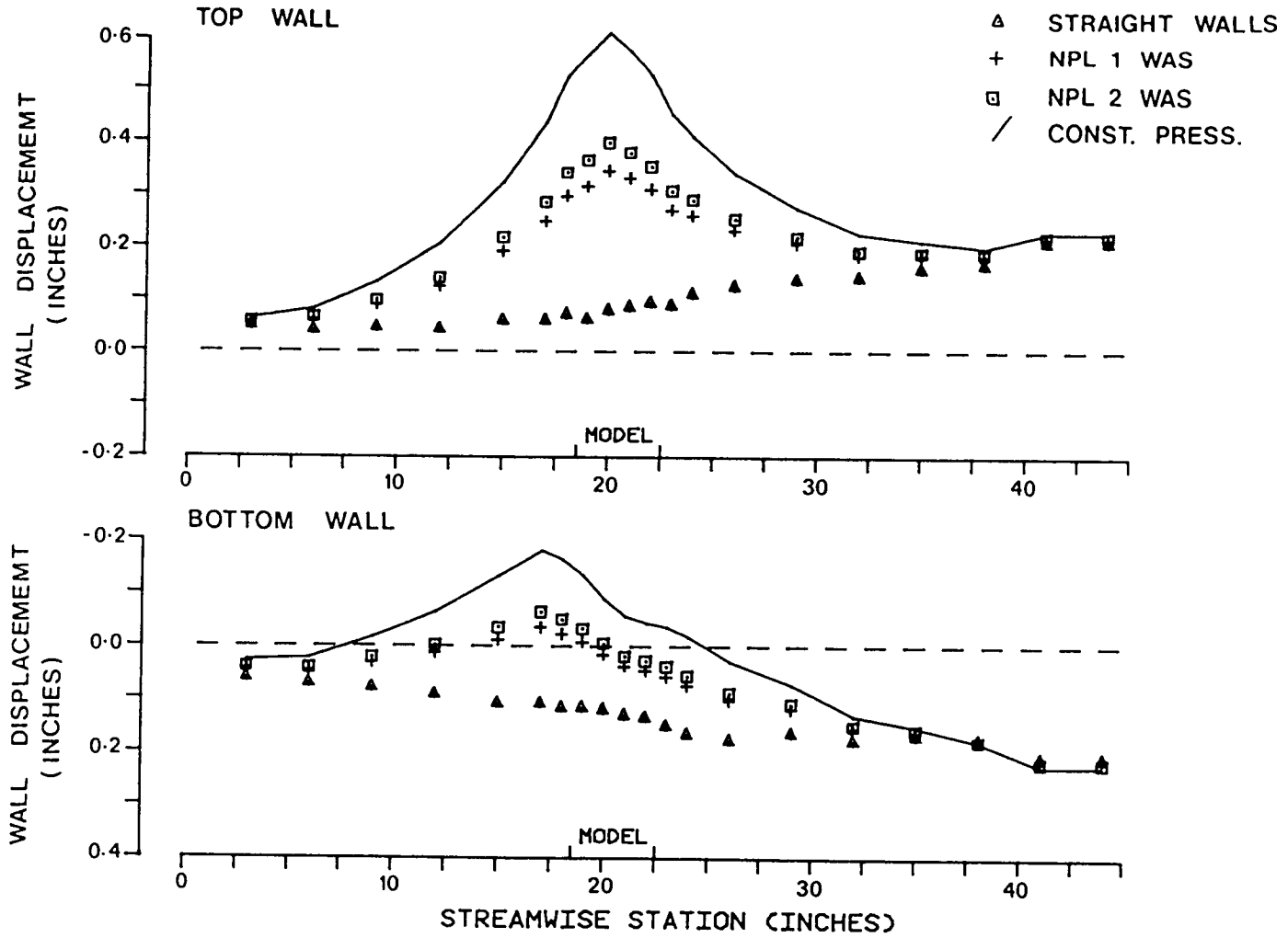

FIG. 10.14 NACA 0012-64 MEASUREMENTS ($M_\infty = 0.7$; $\alpha \simeq 4.0^o$). DISPLACEMENTS OF WALLS SET TO AERODYNAMICALLY STRAIGHT, CONSTANT PRESSURE AND STREAMLINED (NPL WAS) CONTOURS.

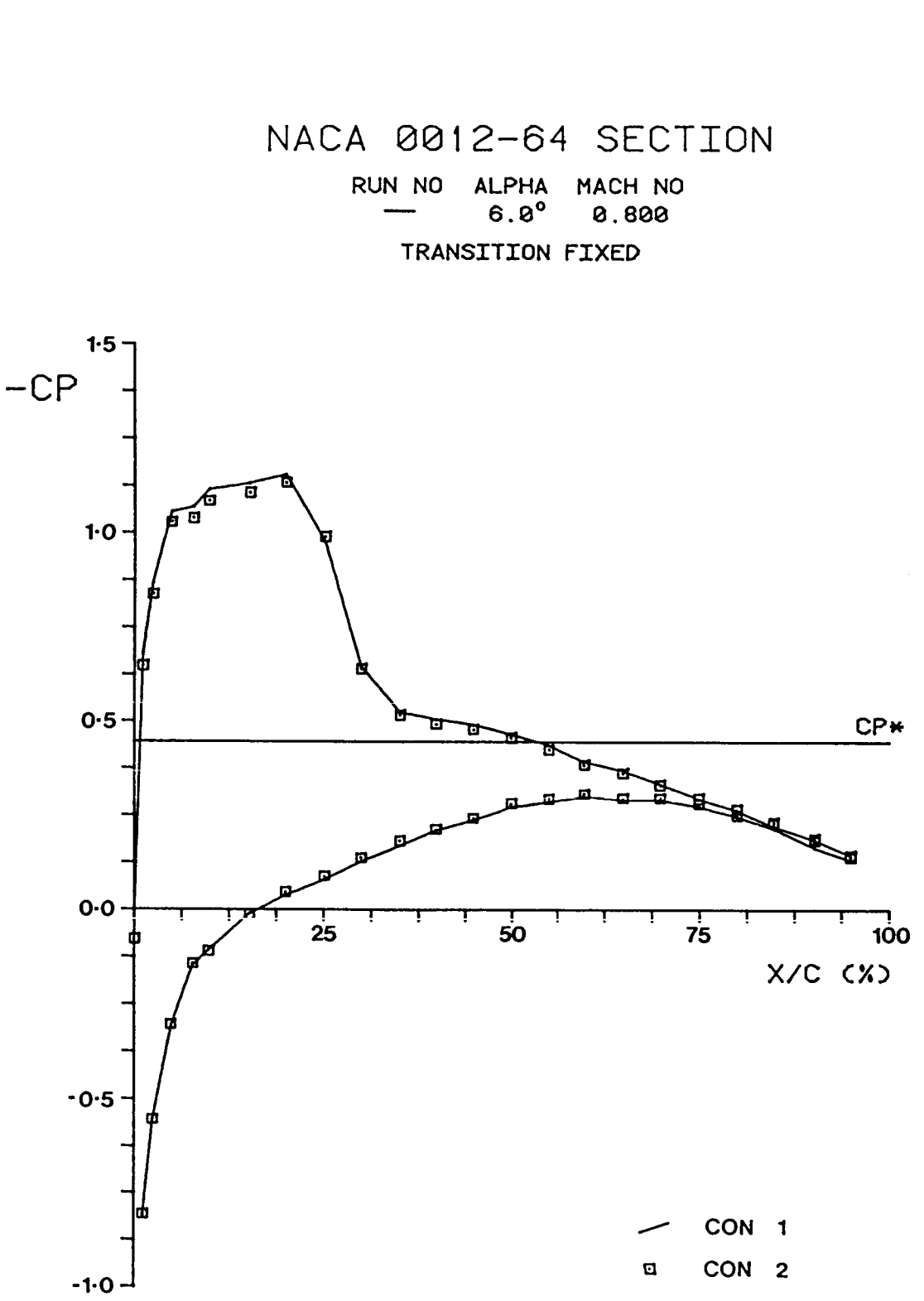

FIG. 10.15 MODEL PRESSURE DISTRIBUTIONS.
WALLS SET TO WAKE PINCH TEST CONTOURS.

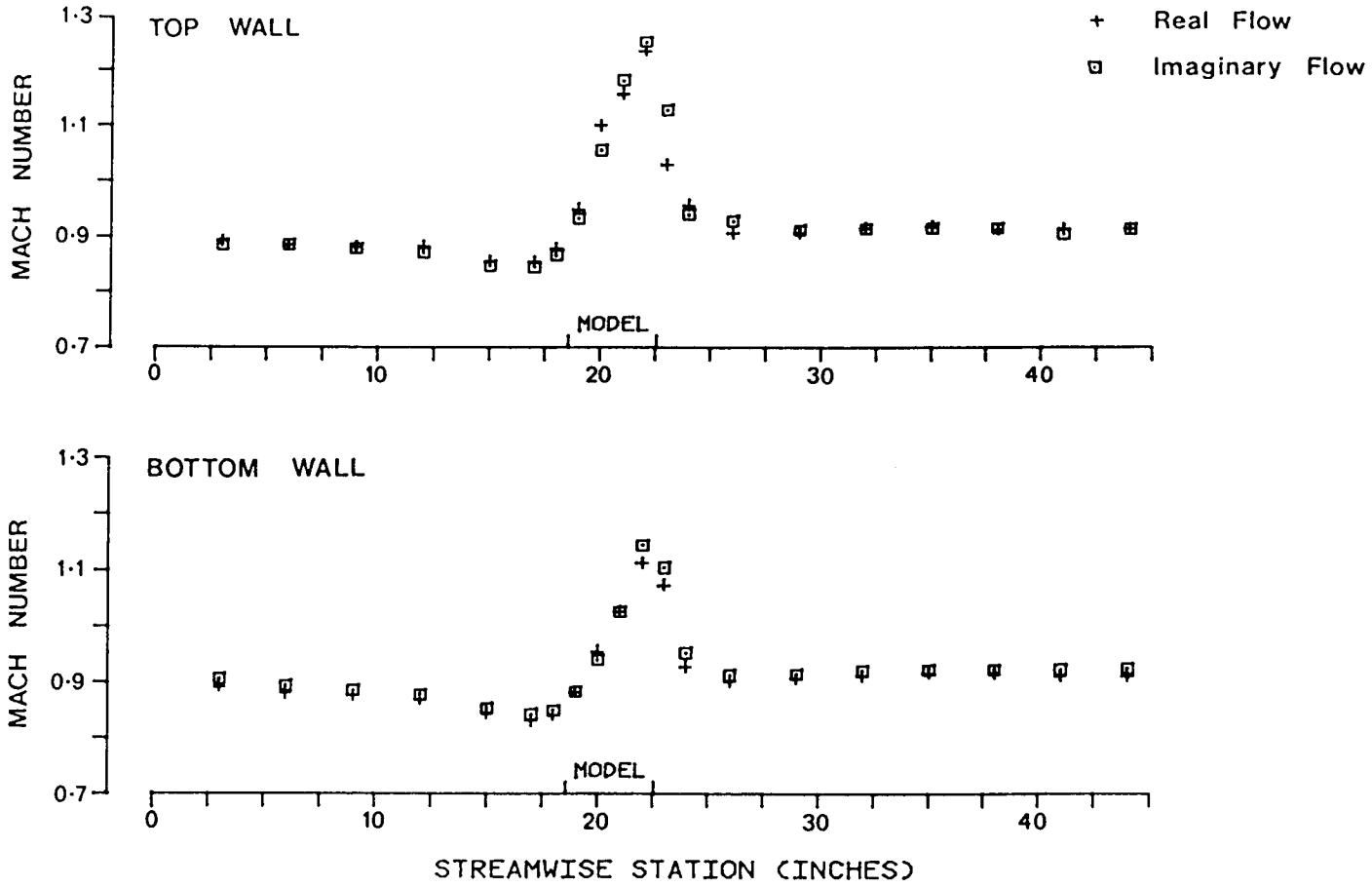

FIG. 11.1 NACA 0012-64 MEASUREMENTS (M_∞ = 0.9062; $\alpha \simeq 4.0^o$). DISTRIBUTIONS OF REAL AND IMAGINARY MACH NUMBER ALONG CENTRELINES OF CONTOURED WALLS (ORIGINAL WALLS).

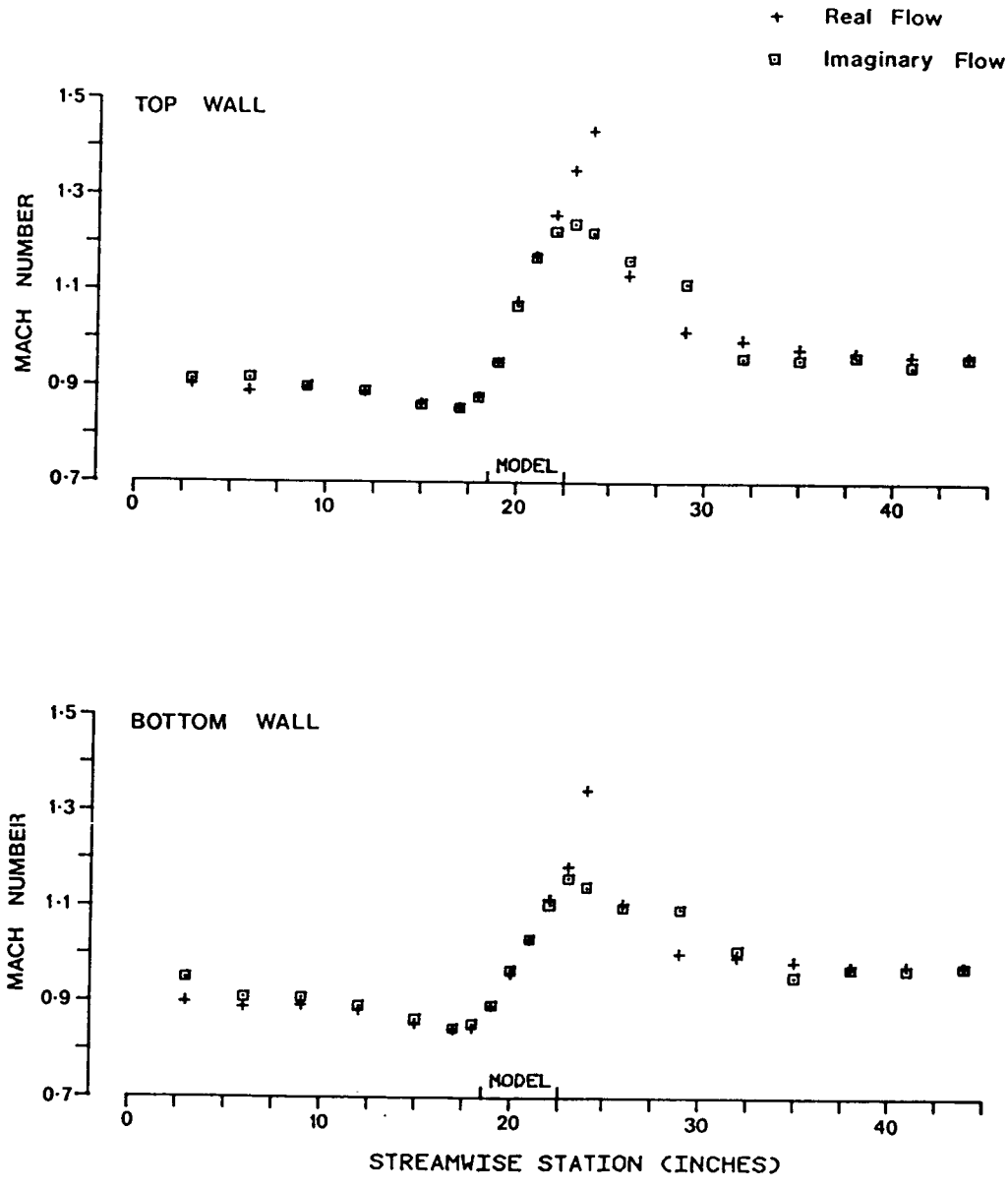

FIG. 11.2 NACA 0012-64 MEASUREMENTS ($M_\infty = 0.9543$; $\alpha \simeq 4.0^o$). DISTRIBUTIONS OF REAL AND IMAGINARY MACH NUMBER ALONG CENTRELINES OF CONTOURED WALLS (ORIGINAL WALLS).

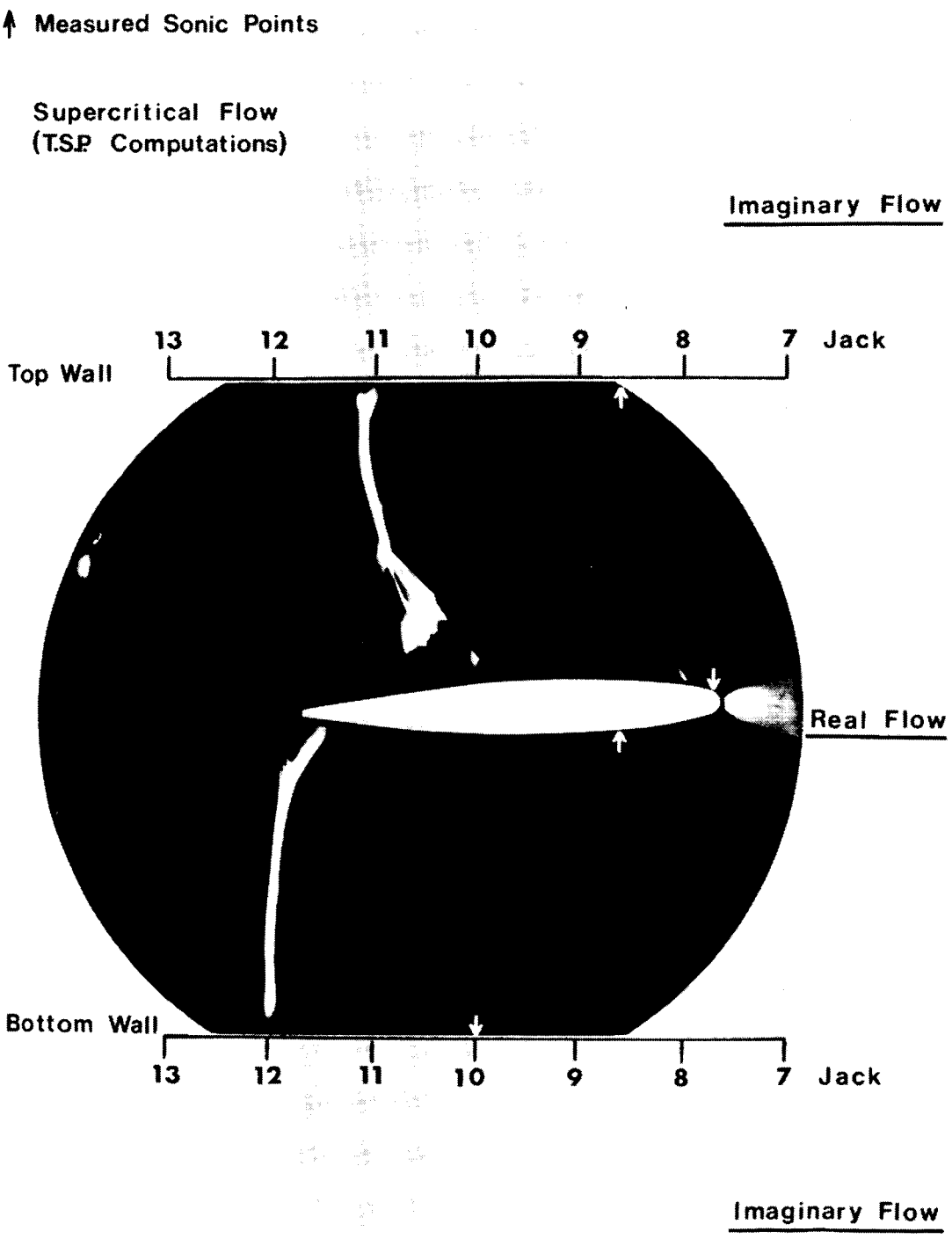

FIG. 11.3 MONTAGE OF REAL AND IMAGINARY FLOWFIELDS
$M_\infty = 0{\cdot}89$; $\alpha = 4{\cdot}0^\circ$

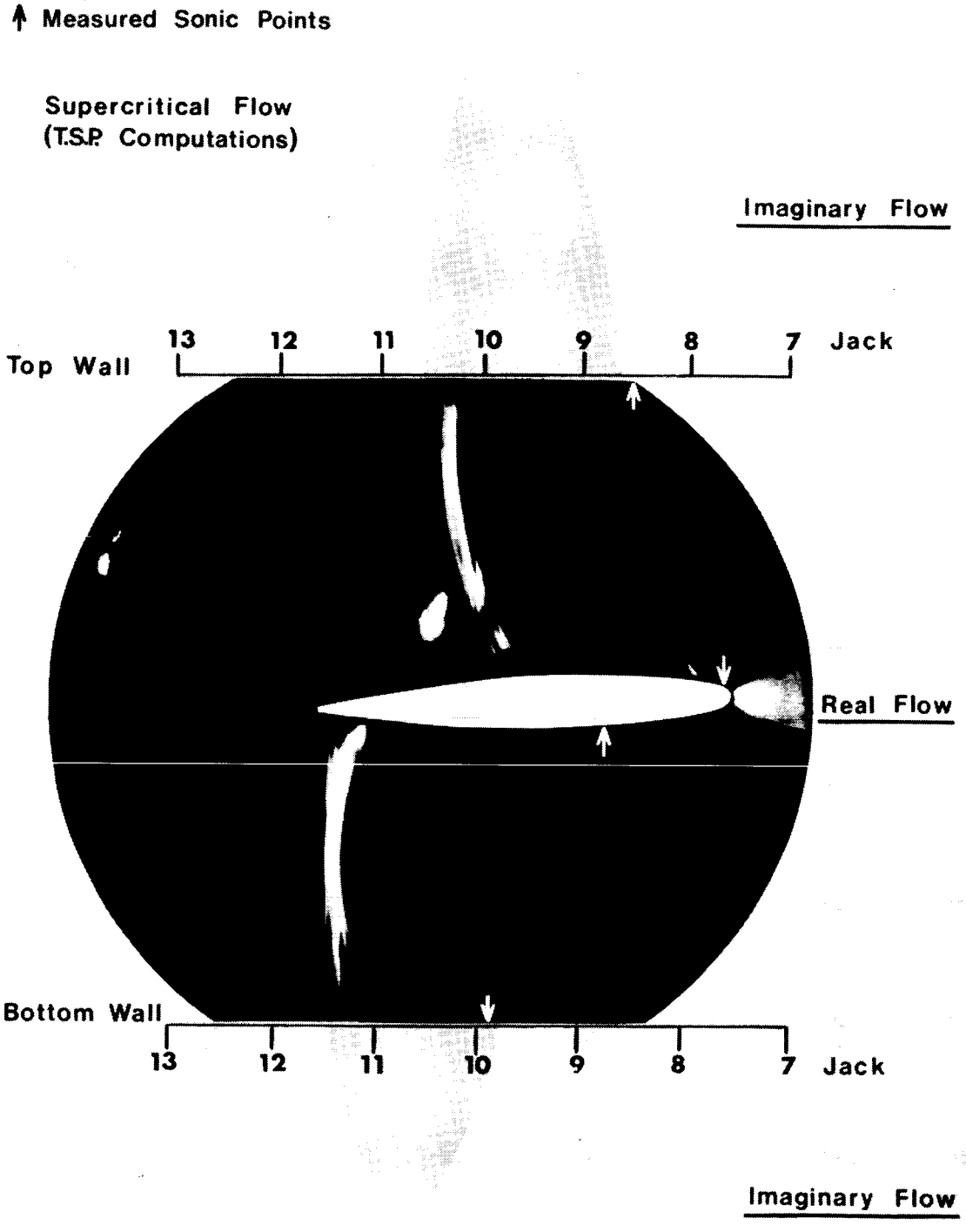

FIG. 11.4 MONTAGE OF REAL AND IMAGINARY FLOWFIELDS
$M_\infty = 0{\cdot}87$; $\alpha = 4{\cdot}0^\circ$ (B.L. ALLOWANCE)

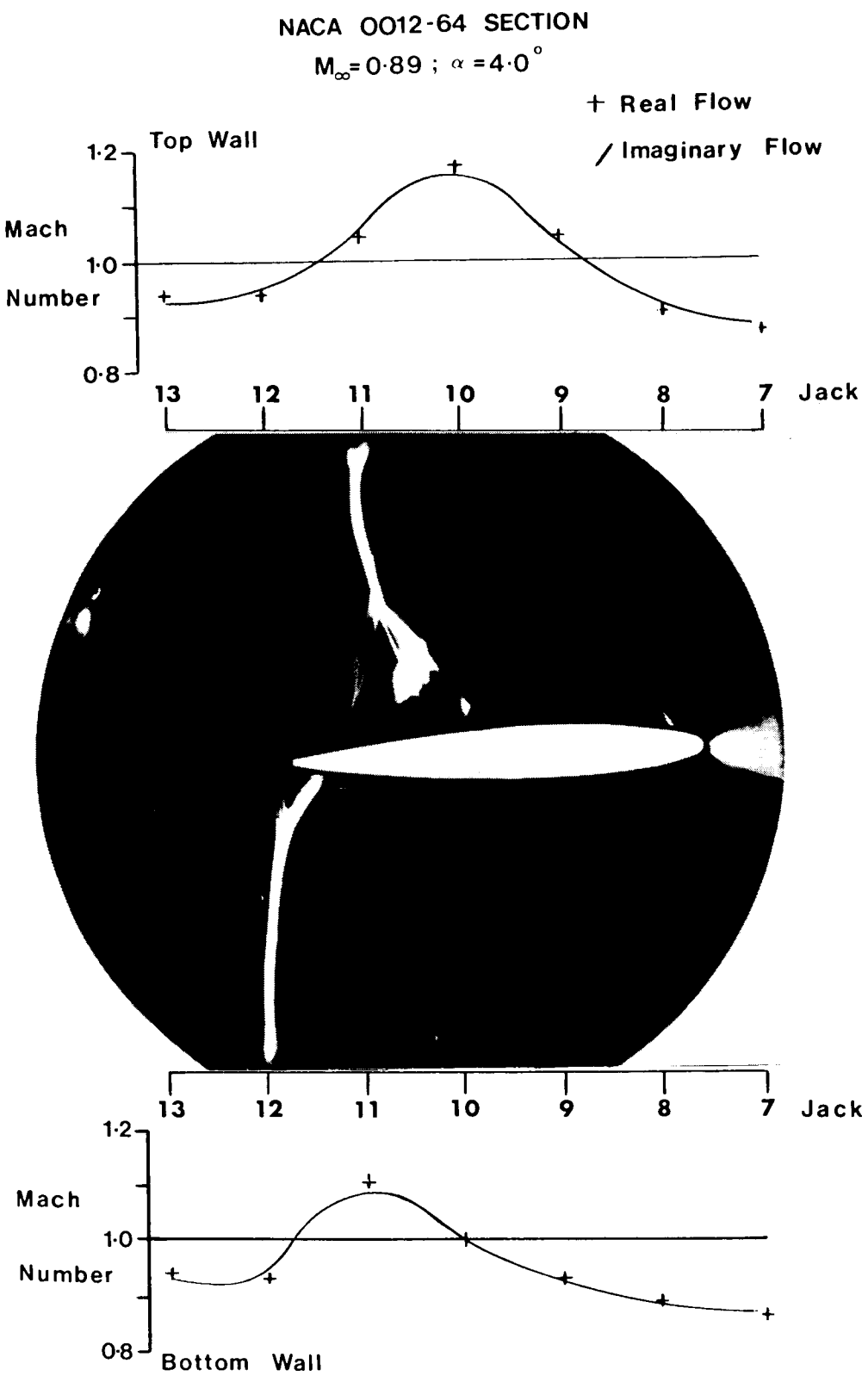

FIG. 11.5 SCHLIEREN PICTURE WITH WALL MACH NUMBER DISTRIBUTIONS

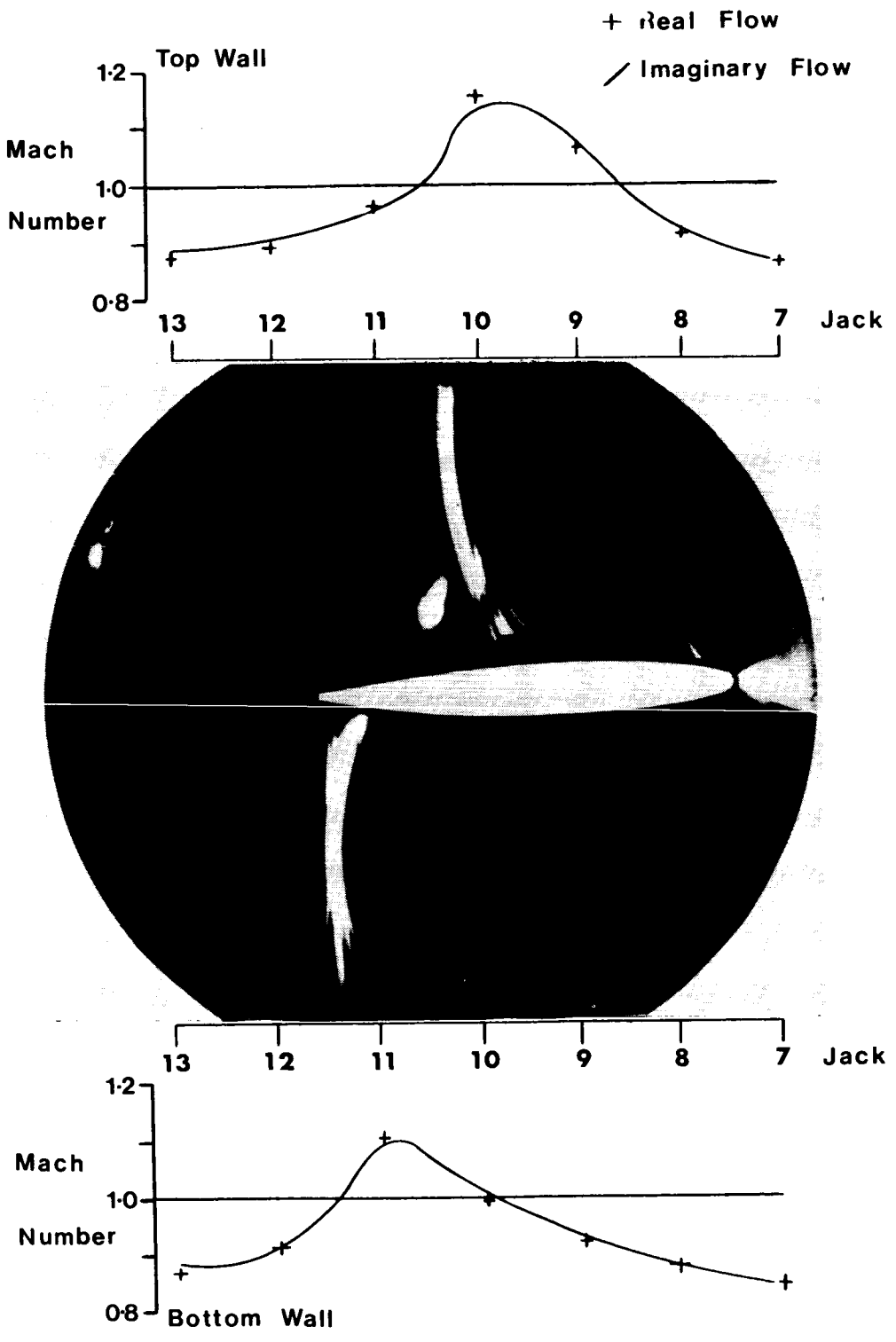

FIG. 11.6 SCHLIEREN PICTURE WITH WALL MACH NUMBER DISTRIBUTIONS (B.L. ALLOWANCE)

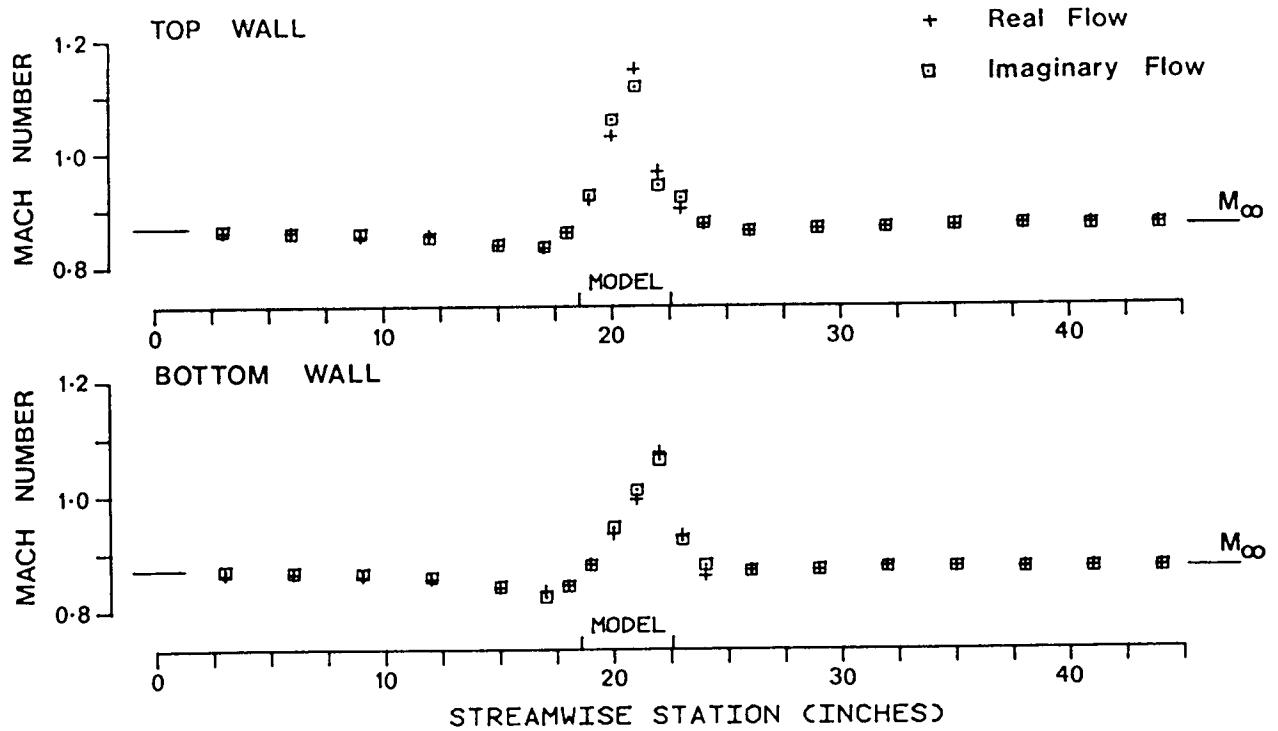

FIG. 11.7 NACA 0012-64 MEASUREMENTS (M_∞ = 0.8726; $\alpha \simeq 4.0^o$). DISTRIBUTIONS OF REAL AND IMAGINARY MACH NUMBER ALONG CENTRELINES OF STREAMLINED WALLS.

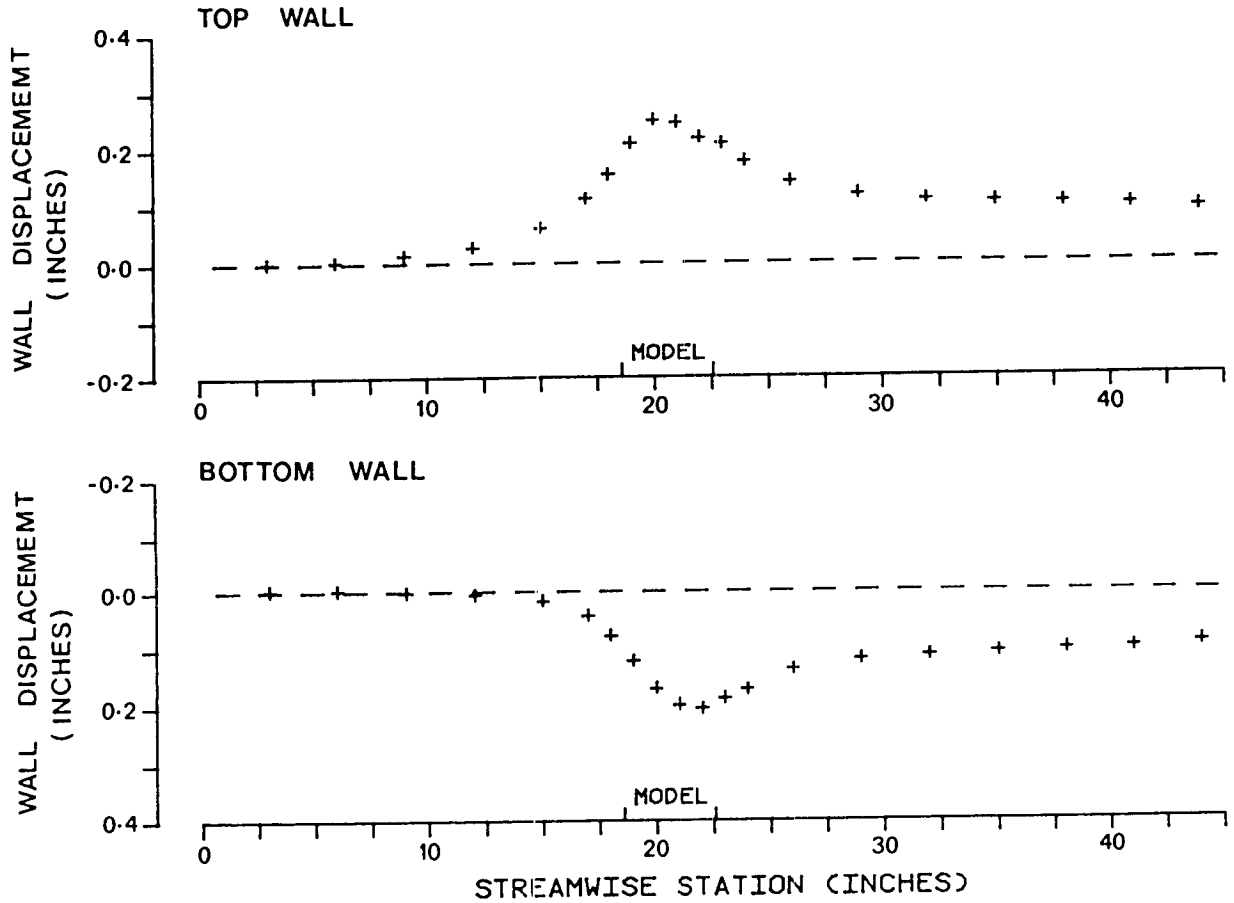

FIG. 11.8 NACA 0012-64 MEASUREMENTS (M_∞ = 0.8726; $\alpha \simeq 4.0^o$). DISPLACEMENTS OF WALLS FROM AERODYNAMICALLY STRAIGHT CONTOURS. WALLS STREAMLINED.

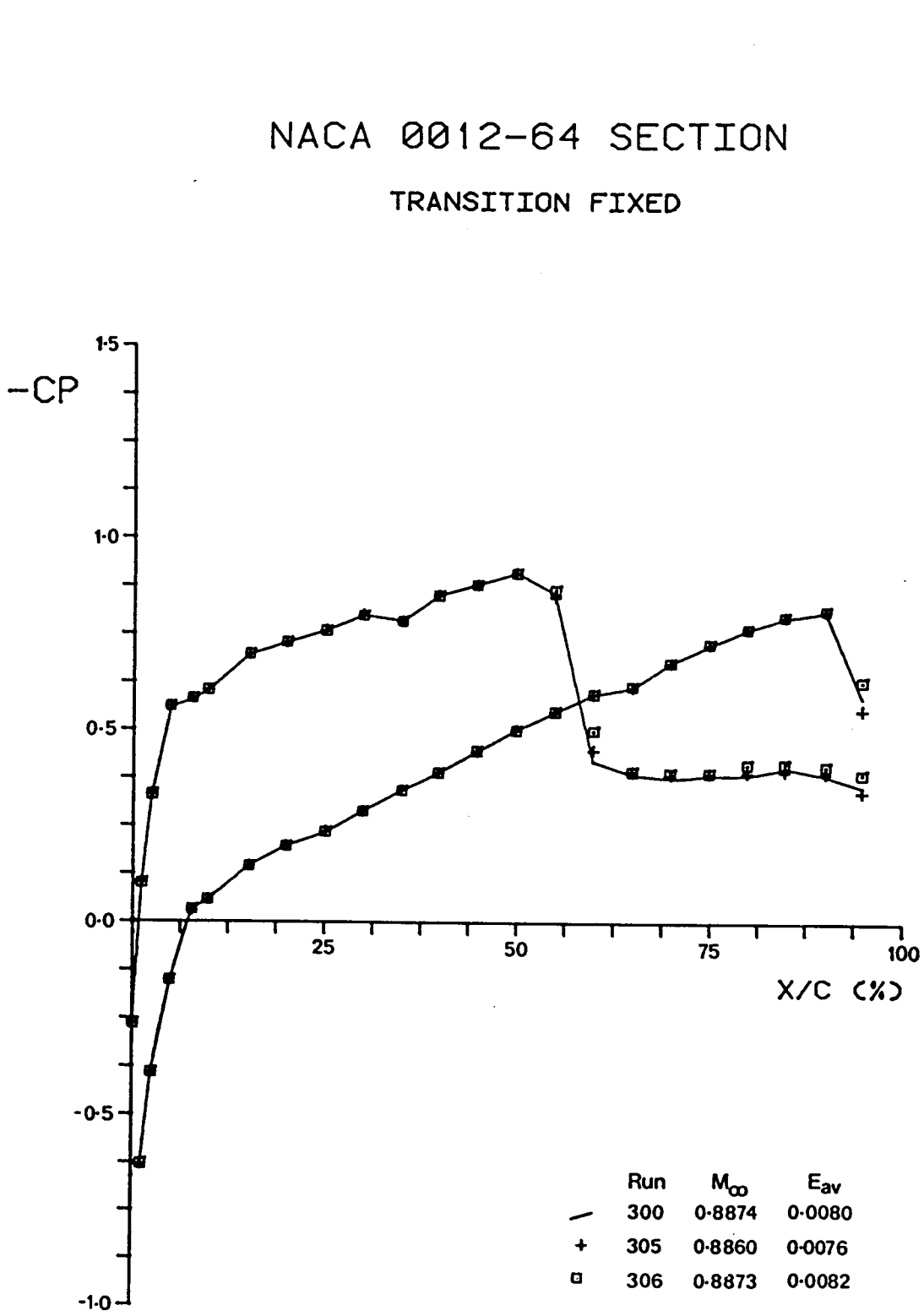

FIG. 11.9 MODEL PRESSURE DISTRIBUTIONS ($\alpha \simeq 4.0^{o}$). WALLS SET TO STREAMLINED CONTOURS TO DEMONSTRATE REPEATABILITY OF MODEL DATA.

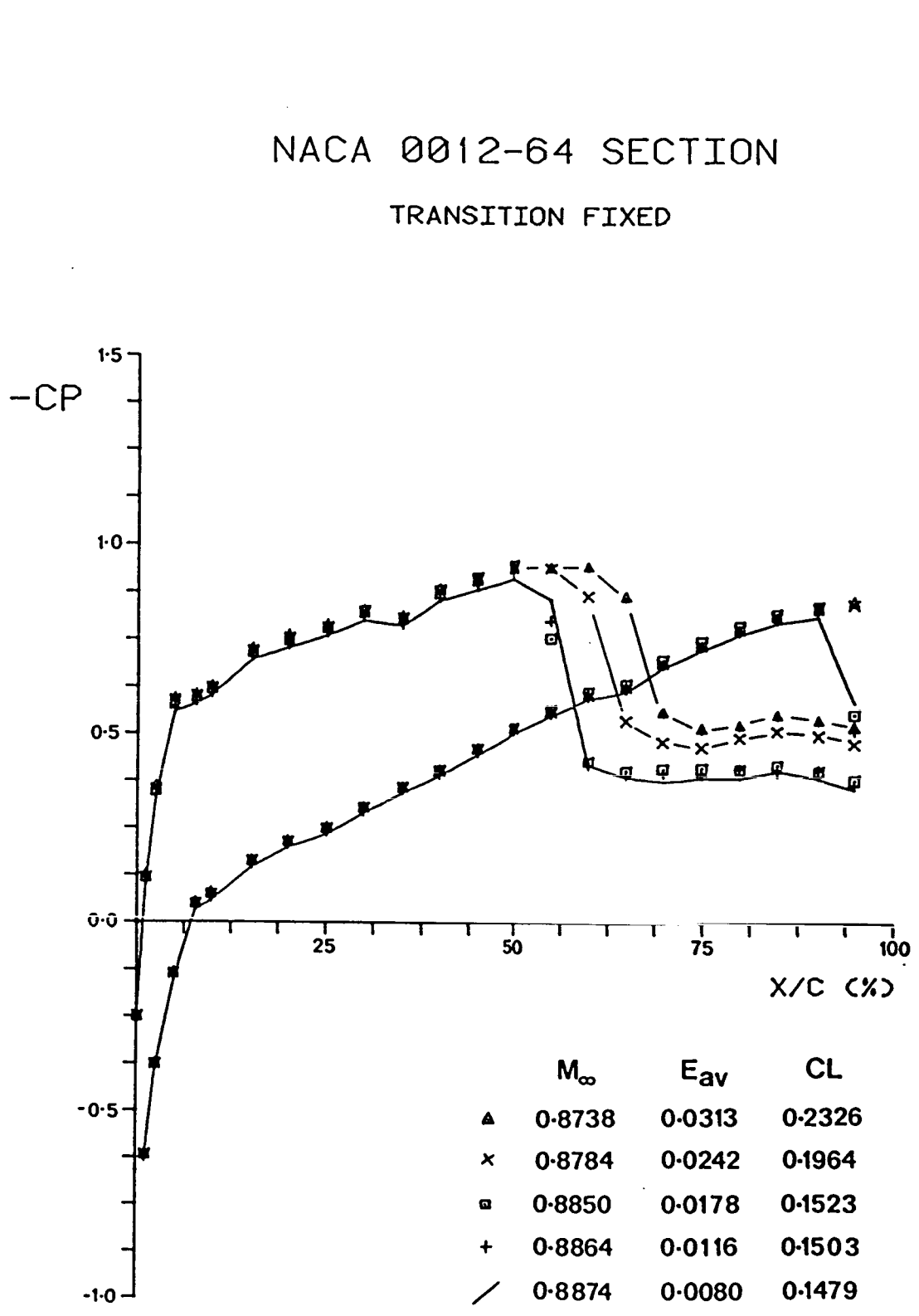

FIG. 11.10 MODEL PRESSURE DISTRIBUTIONS ($\alpha \simeq 4.0^{o}$).
THE SENSITIVITY OF MODEL PERFORMANCE TO THE QUALITY OF WALL STREAMLINING.

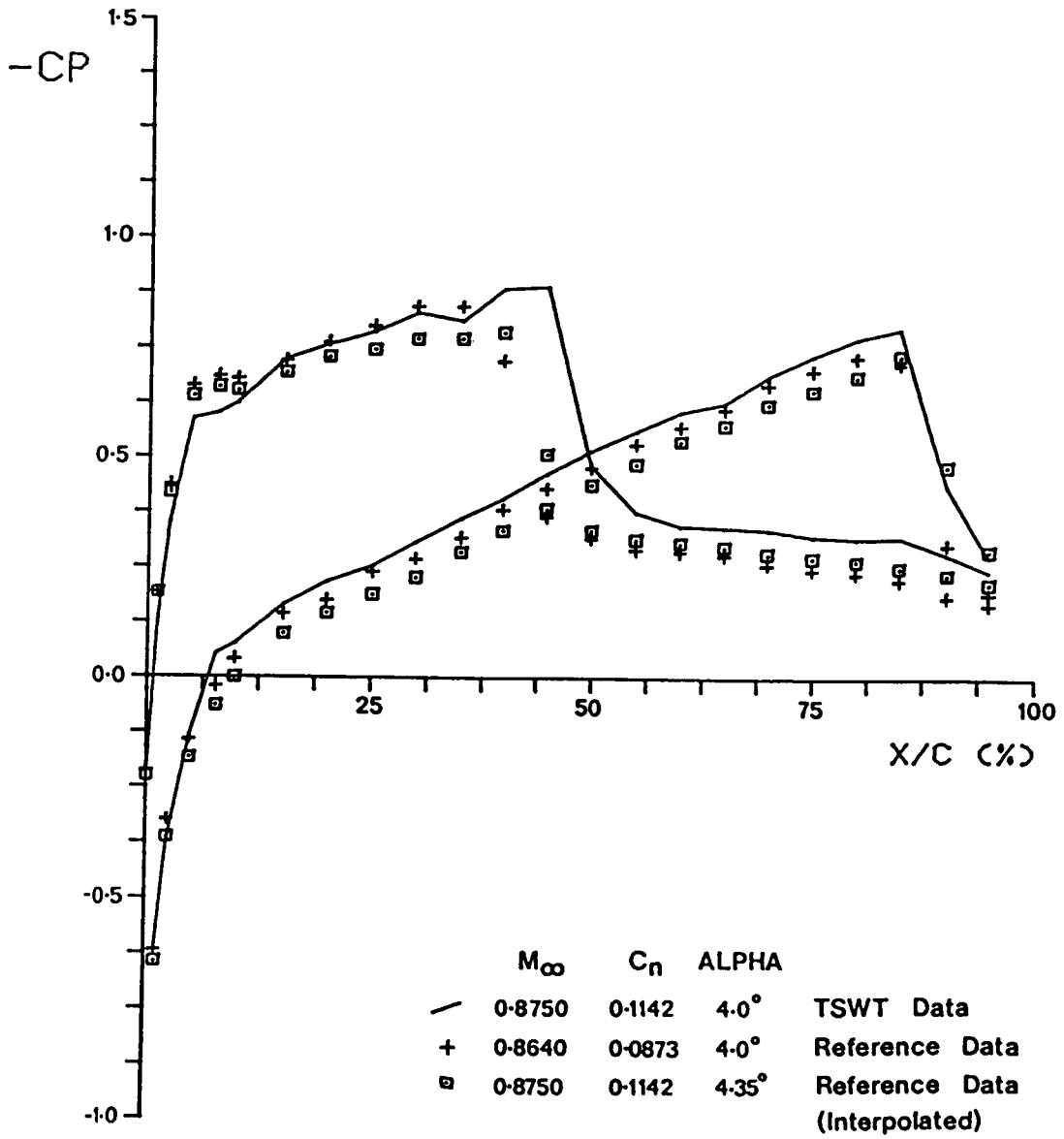

FIG. 11.11 MODEL PRESSURE DISTRIBUTIONS.
COMPARISON OF TSWT DATA WITH REFERENCE DATA.

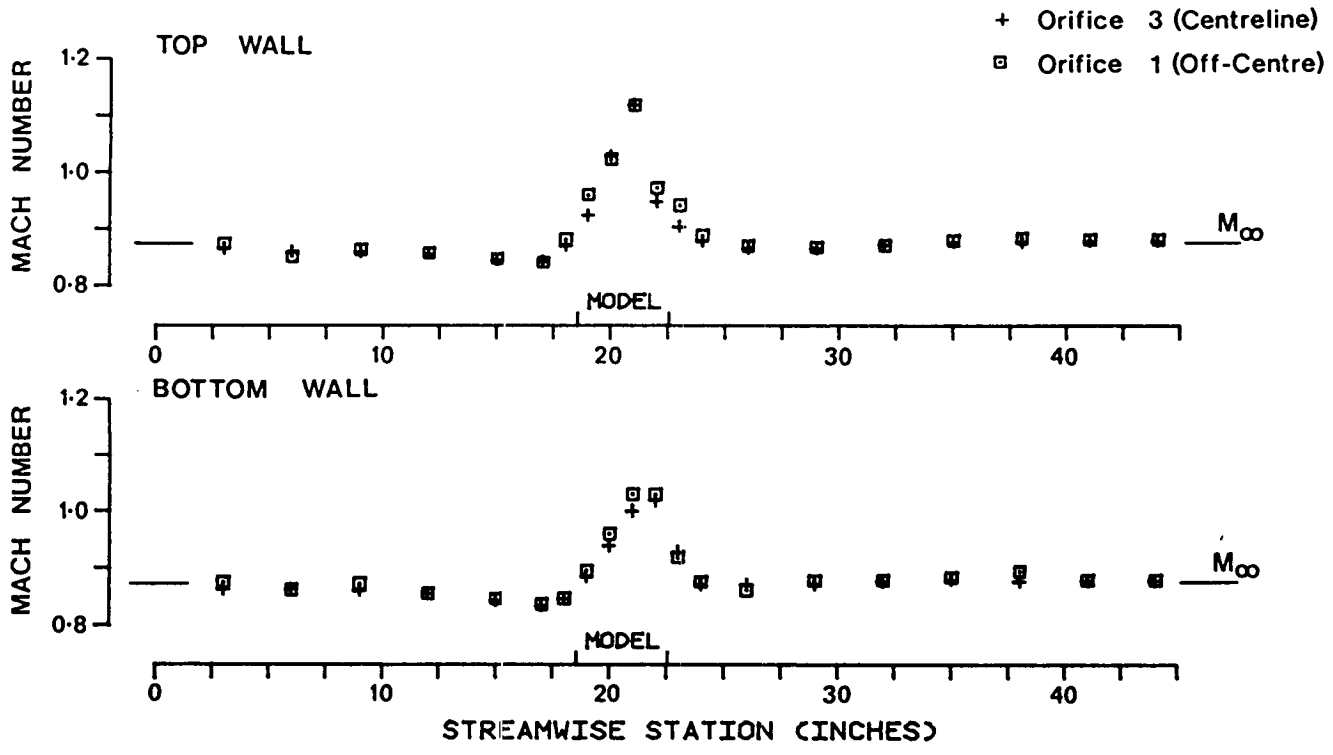

FIG. 11.12 NACA 0012-64 MEASUREMENTS (M_∞ = 0.8750; $\alpha \simeq 4.0^o$). DISTRIBUTIONS OF WALL MACH NUMBER ALONG STREAMLINED WALLS.

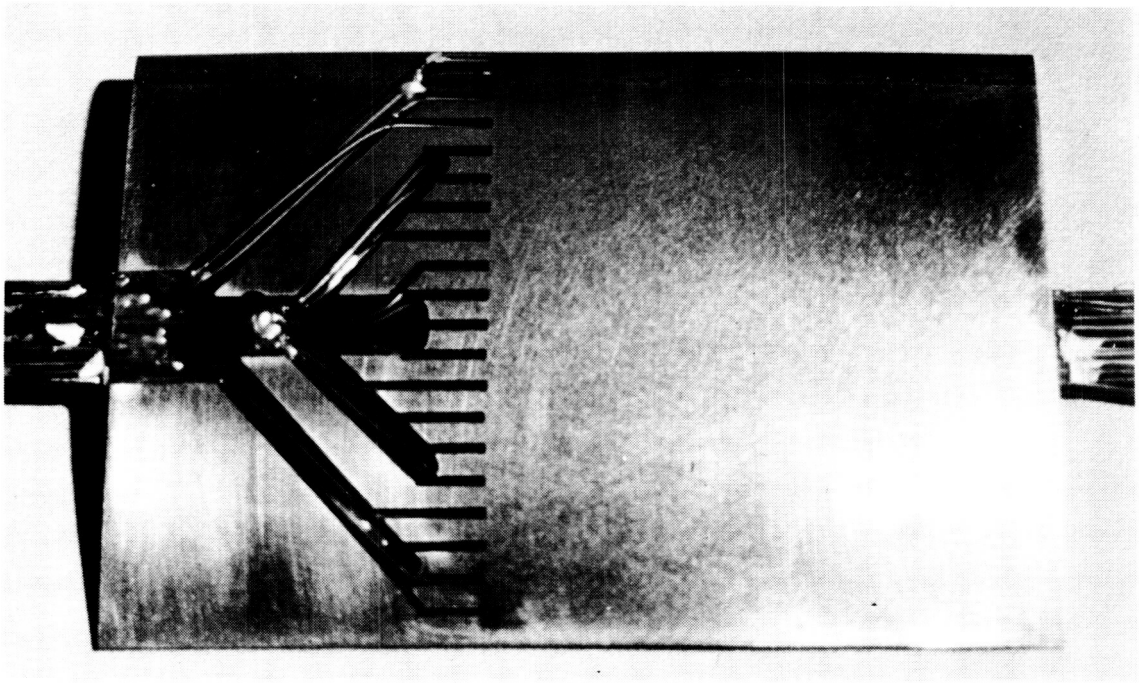

Upper Surface

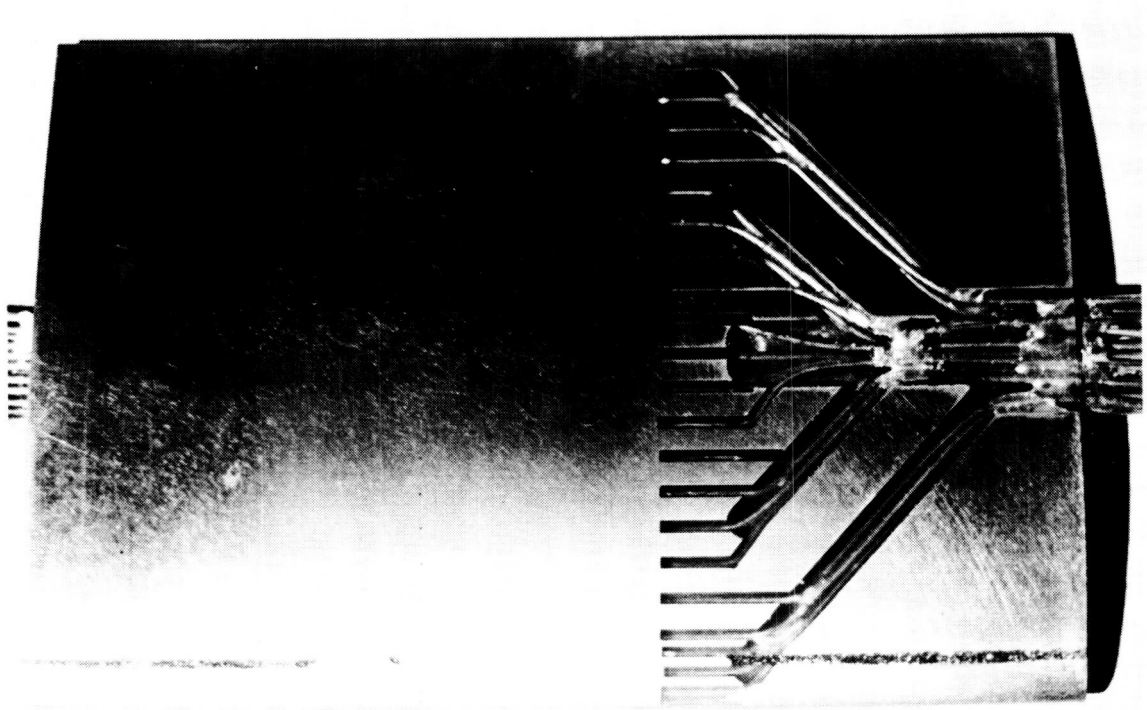

Lower Surface

FIG. 11.13 CONDITION OF NACA 0012-64 MODEL AFTER TESTING

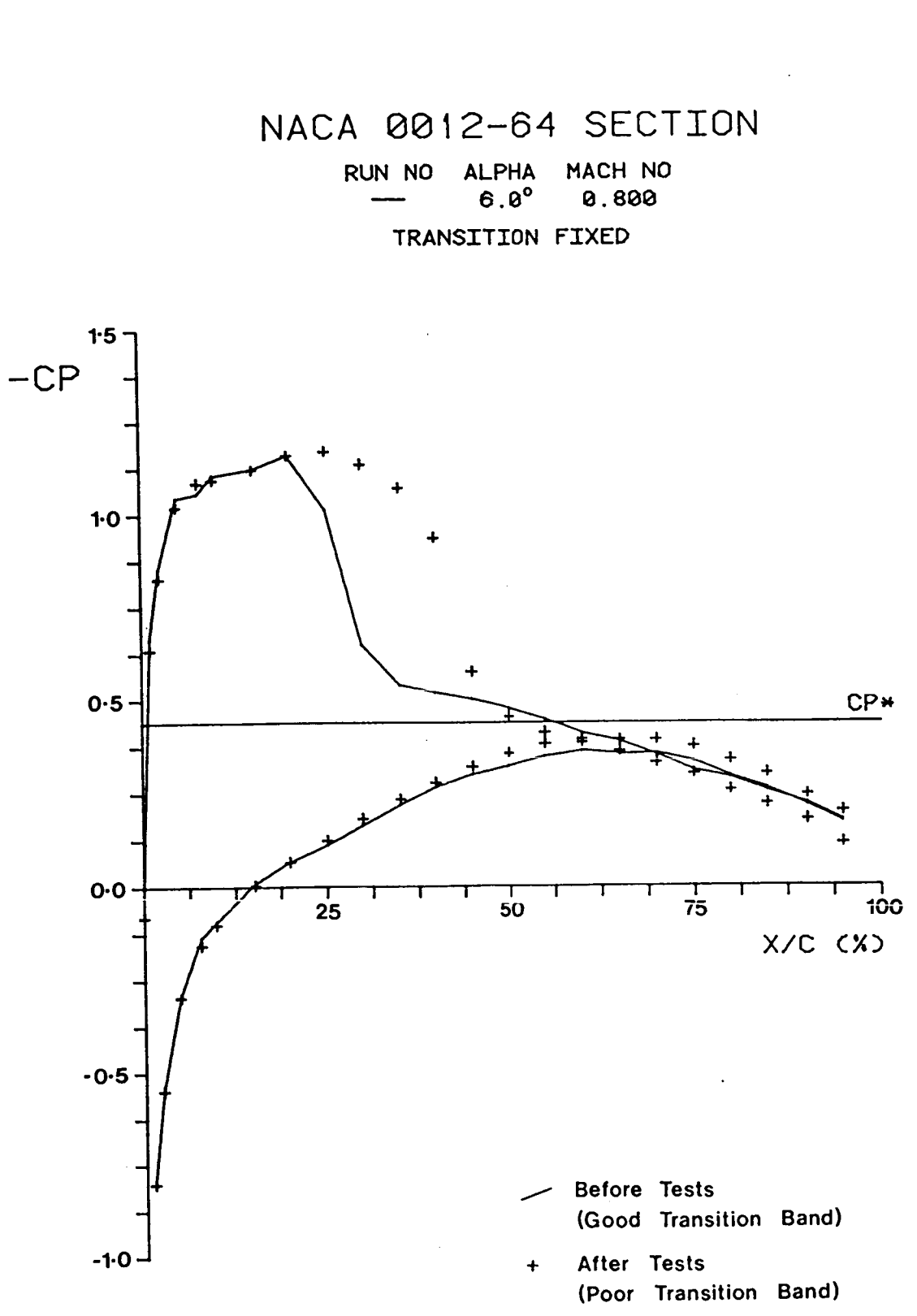

FIG. 11.14 MODEL PRESSURE DISTRIBUTIONS.
WALLS STREAMLINED BY THE WAS 1A STRATEGY.

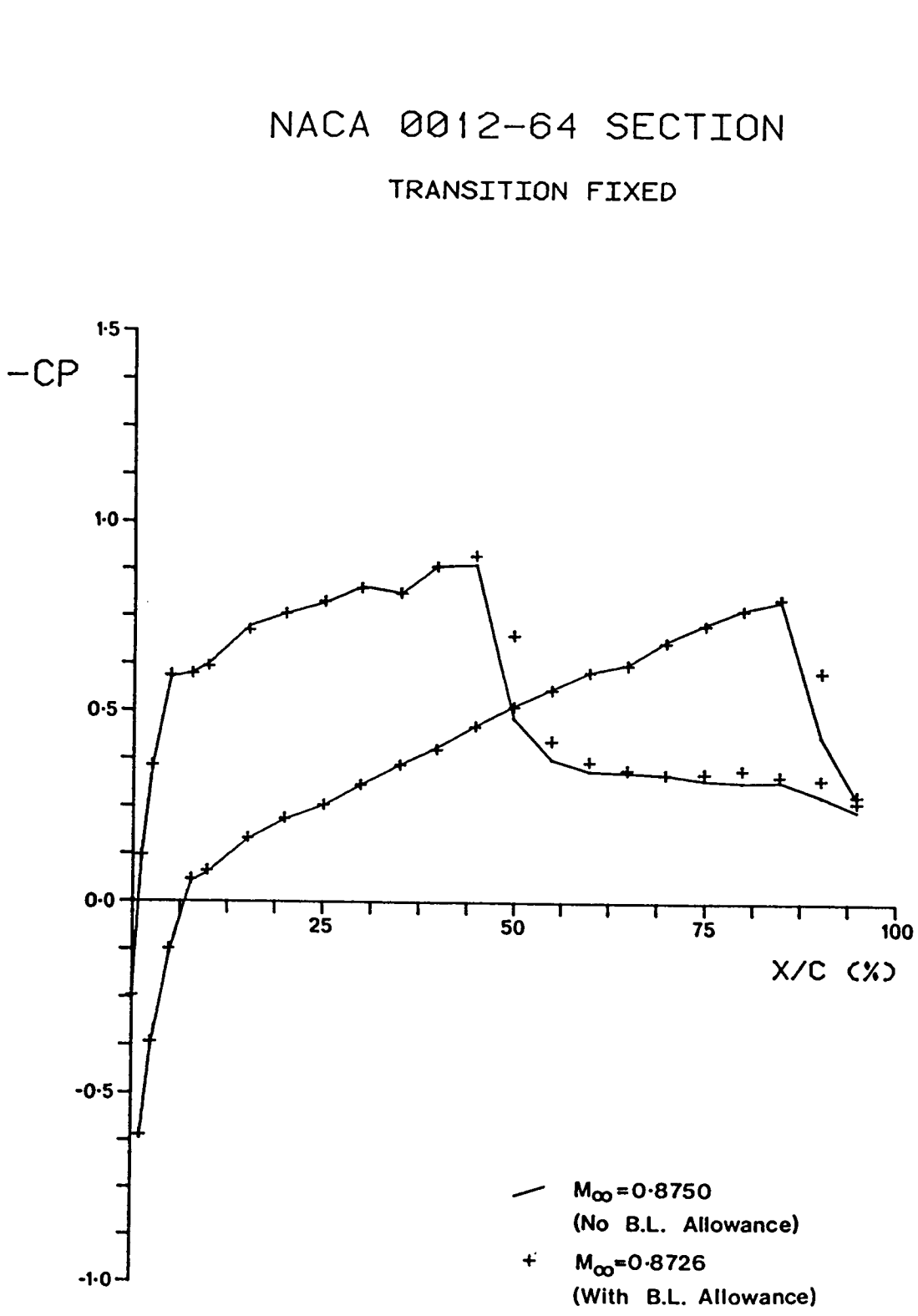

FIG. 11.15 MODEL PRESSURE DISTRIBUTIONS ($\alpha \simeq 4.0^{o}$). THE EFFECTS OF AN ALLOWANCE FOR δ^{*} VARIATIONS ON MODEL PRESSURE DISTRIBUTION.

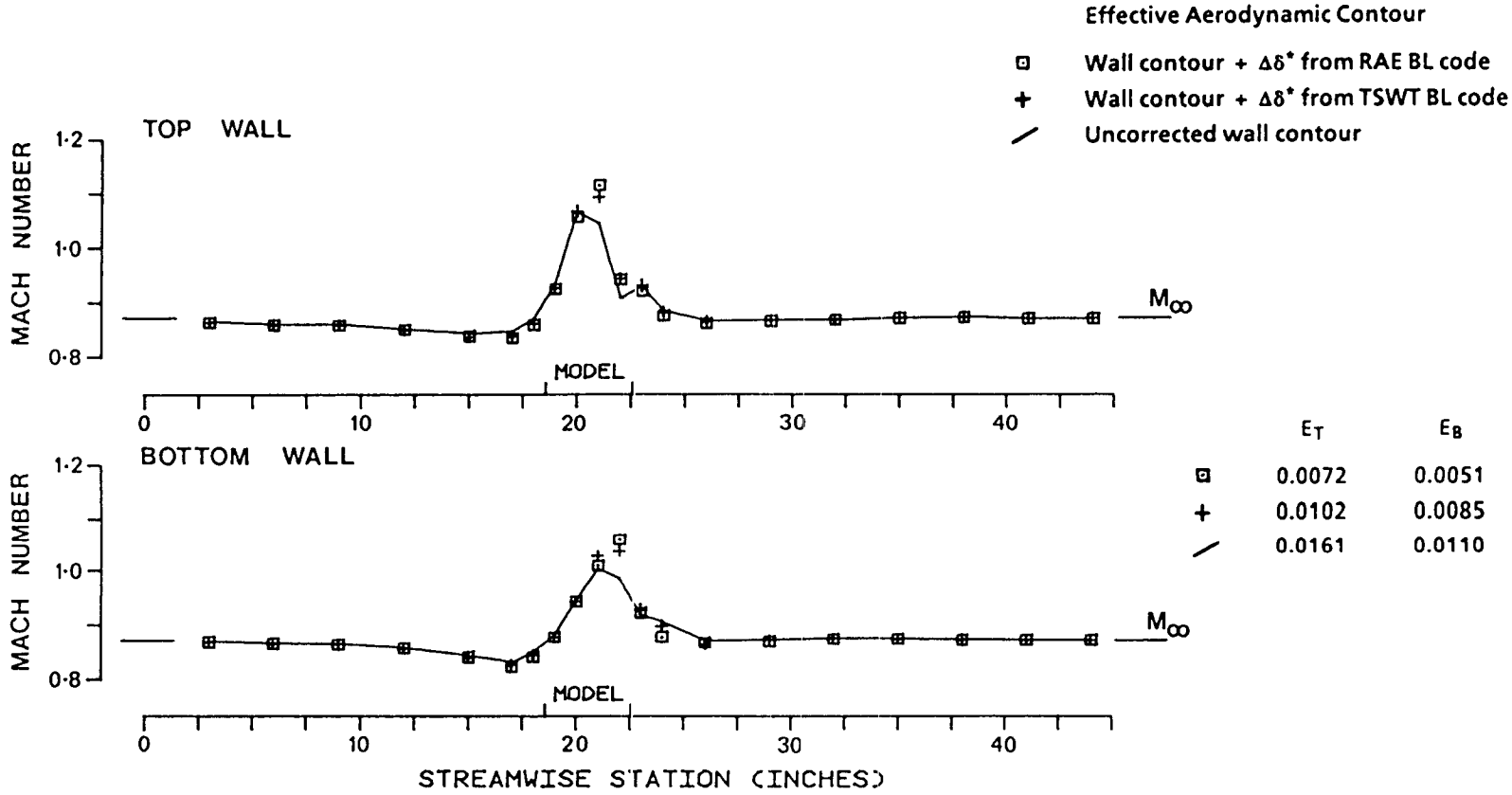

FIG. 11.16 IMAGINARY WALL MACH NUMBER DISTRIBUTIONS CALCULATED BY THE TSWT TSP CODE ($M_\infty = 0.8726$; $\alpha \simeq 4.0^o$).

APPENDIX A

OUTLINE OF THE PREDICTIVE WALL ADJUSTMENT STRATEGY

A.1. Basic Theory

The basic aerodynamic theory of the strategy applies to the case of a single flexible wall adjacent to a model. In the theory the wall slopes and changes in the wall boundary layer displacement thickness due to the presence of the model are assumed to be small.

The wall is loaded if it does not follow the desired line of a streamline in an infinite flowfield. The physical presence of the wall and the distribution of wall loading may be represented by a flat vorticity sheet, having a local vorticity strength ($\Gamma_{(x)}$) at streamwise position x given by:-

$$\Gamma_{(x)} = U_{(x)} - V_{(x)}$$

where $U_{(x)}$ = real side velocity at position x

and $V_{(x)}$ = imaginary side velocity at position x.

A velocity component $(v(\xi))$ normal to the free stream is induced at streamwise position ξ by the distribution of vorticity. This is approximately given by:-

$$v(\xi) = \frac{1}{2\pi} \int_{-\infty}^{\infty} \frac{\Gamma_{(x)}}{(\xi - x)}\, dx$$

Since a streamlined wall exhibits zero wall loading (and hence zero vorticity) the slope of the wall is adjusted by the amount which is required for a change in the normal component of the free stream velocity to oppose that due to the vorticity. This requires an increment in slope (ΔS) which is approximately given by:-

$$\Delta S = \Delta \frac{dy}{dx}(\xi) \simeq \frac{-v(\xi)}{U_\infty}$$

$$\simeq \frac{1}{2\pi U_\infty} \int \frac{\Gamma_{(x)} dx}{(x - \xi)}$$

where U_∞ = free stream velocity.

The above expression is integrated to obtain the required change in wall deflection $(\Delta y(\xi))$ to remove the vorticity and thereby eliminate the wall loading.

Following the movement of the wall to the new contour there are adjustments to the velocity either side of the wall amounting to half of the velocity imbalance before the movement. Hence the imaginary side velocity $(V_{(x)_{NEW}})$ at position x for the new wall contour is given by:-

$$V_{(x)_{NEW}} = V_{(x)} + \left[\frac{U_{(x)} - V_{(x)}}{2} \right]$$

A.2 Wall Coupling and Scaling Factors

The above described theory applies only to one flexible wall in isolation. The simultaneous application of the theory to each wall does not lead to convergence of the walls to streamlines. Allowance must be made for what may be regarded as a one-dimensional continuity effect, a strong aerodynamic coupling of the flexible walls. Convergence can be obtained by feeding a proportion of the demanded movement of one wall to the other. However the predictions of wall movement are somewhat exaggerated, therefore a scaling factor is also applied. Scaling and coupling factors are empirically determined; the values used for both walls of the TSWT are 0.7 and 0.35 respectively. For each of these modifications to the predicted wall contour there are appropriate adjustments to the calculation of the imaginary side velocity distributions.

A.3 Compressibility

Linearised compressible flow corrections are introduced in the form of the Prandtl-Glauert factor (β). The various tunnel pressure measurements, in terms of pressure coefficient (C_{p_c}), are converted to their equivalent incompressible coefficients (C_{p_I}) by:-

$$C_{p_I} = \beta C_{p_c}$$

where $\beta = \sqrt{1 - M_\infty^2}$

and M_∞ = reference Mach number

This modification to the strategy has allowed testing up to speeds just giving sonic flow at one of the streamlined walls.

APPENDIX B

EQUATIONS OF THE EXACT WALL ADJUSTMENT STRATEGY

Consider top wall only.

Symbols

β	Prandtl-Glauert factor $(= (1 - M_\infty^2)^{\frac{1}{2}})$
$F_{T(x)}$	New top wall position from straight (positive upwards)
$f_{T(x)}$	Initial top wall position from straight (positive upwards)
$f_{B(x)}$	Initial bottom wall position from straight (positive upwards)
$\Delta f_{T(x)}$	2nd order incremental change in top wall position (positive upwards)
$g_{T(x)}$	1st order incremental change in top wall position (positive upwards)
h	Nominal test section height
ℓ	Length of test section
M_∞	Reference Mach number
U_∞	Reference velocity
U_{TE}	External (imaginary) velocity increments of top wall
U_{TI}	Internal (test section) velocity increments of top wall
U_{BI}	Internal (test section) velocity increments of bottom wall
x, ξ	Co-ordinates along test section (measured from start of test section)

Equations

The new top wall position is given by:-

$$F_{T(x)} = f_{T(x)} + \Delta f_{T(x)}$$

To the 2nd order the incremental change in top wall position may be approximated to:-

$$\Delta f_{T(x)} = \left[g_{T(x)} - M_\infty^2 H_{T(x)} \right] / \left[1 + \beta^2 \Delta U_{T(x)} \right]$$

where

$$\Delta U_{T(x)} = \frac{1}{2U_\infty} \left[U_{TE(x)} + U_{TI(x)} \right]$$

and

$$H_{T(x)} = \int_o^x \Delta U_{T(\xi)} \frac{dg_{T(\xi)}}{d\xi} d\xi \qquad \text{(B.1)}$$

The external velocity increments of the top wall may be computed from the initial wall shape using the following relationship:-

$$U_{TE(x)} = \frac{U_\infty}{\beta\pi} \oint_o^\ell \frac{df_{T(\xi)}}{d\xi} \frac{d\xi}{[\xi - x]} \qquad \text{(B.2)}$$

The 1st order incremental change in top wall position is given by:-

$$g_{T(x)} = -\frac{1}{2} f_{T(x)} \qquad \text{Term A}$$

$$-\frac{\beta}{2\pi} \oint_o^{\ell} \frac{U_{TI(\xi)}}{U_\infty} ln\left[\frac{\xi - x}{\xi}\right] d\xi \qquad \text{Term B}$$

$$+\frac{\beta}{4\pi} \int_o^{\ell} \frac{U_{BI(\xi)}}{U_\infty} ln\left[\frac{(Bh)^2 + (\xi - x)^2}{(Bh)^2 + \xi^2}\right] d\xi \qquad \text{Term C}$$

$$-\frac{\beta h}{2\pi} \int_o^{\ell} f_{B(\xi)} \frac{d\xi}{\left[(Bh)^2 + (\xi - x)^2\right]} \qquad \text{Term D} \qquad \text{(B.3)}$$

Note:- 1) Term (B) has a singularity at $\xi = x$ and integration in this region must be carried out analytically with $U_{TI(x)}$ expressed locally as a polynomial. Care must also be taken to ensure that the value of $U_{TI(\xi)}$ is numerically zero as ξ tends to zero i.e. at upstream end of the test section.

2) Terms (C) and (D) are the cross-feed inputs from the lower wall velocity and wall shape.

The above equations are only applicable to the top wall, the bottom wall equations are of equivalent form.

NASA National Aeronautics and Space Administration

Report Documentation Page

1. Report No.	2. Government Accession No.	3. Recipient's Catalog No.
NASA CR-4128		

4. Title and Subtitle
Aerofoil Testing in a Self-Streamlining Flexible Walled Wind Tunnel

5. Report Date
May 1988

6. Performing Organization Code

7. Author(s)
Mark Charles Lewis

8. Performing Organization Report No.

10. Work Unit No.
505-61-01-02

9. Performing Organization Name and Address
University of Southampton
Department of Aeronautics and Astronautics
Hampshire SO9 5NH
ENGLAND

11. Contract or Grant No.
NSG-7172

13. Type of Report and Period Covered
Contractor Report

12. Sponsoring Agency Name and Address
National Aeronautics and Space Administration
Langley Research Center
Hampton, VA 23665-5225

14. Sponsoring Agency Code

15. Supplementary Notes
NASA Langley Research Center Technical Monitor: Charles L. Ladson.
The information presented in this report was offered as a thesis in partial fulfillment of the requirements for the Degree of Doctor of Philosophy, University of Southampton, Hampshire, England, July 1987.

16. Abstract

Two-dimensional self-streamlining flexible walled test sections eliminate, as far as experimentally possible, the top and bottom wall interference effects in transonic aerofoil testing. The test section sidewalls are rigid, while the impervious top and bottom walls are flexible and contoured to streamline shapes by a system of jacks, without reference to the aerofoil model. The concept of wall contouring to eliminate or minimize test section boundary interference in two-dimensional testing was first demonstrated by the National Physical Laboratory (NPL) in England during the early 1940's. The transonic streamlining strategy proposed, developed and used by NPL has been compared with several modern strategies. The NPL strategy has proved to be surprisingly good at providing a wall interference-free test environment, giving model performance indistinguishable from that obtained when using the modern strategies over a wide range of test conditions. In all previous investigations the achievement of wall streamlining in flexible walled test sections has been limited to test conditions up to those which result in the model's shock just extending to a streamlined wall. This work however, has also successfully demonstrated the feasibility of two-dimensional wall streamlining at test conditions where both model shocks have reached and penetrated through their respective flexible walls. Appropriate streamlining procedures have been established and are uncomplicated, enabling flexible walled test sections to easily cope with these high transonic flows.

17. Key Words (Suggested by Author(s))	18. Distribution Statement
Aerodynamics Airfoils Transonic Wind Tunnels Adaptive Wall Wind Tunnels	Unclassified - Unlimited Subject Category - 02

19. Security Classif. (of this report)	20. Security Classif. (of this page)	21. No. of pages	22. Price
Unclassified	Unclassified	270	A12

For sale by the National Technical Information Service, Springfield, Virginia 22161-2171